

UNITED STATES PATENT AND TRADEMARK OFFICE

BEFORE THE PATENT TRIAL AND APPEAL BOARD

APPLE INC. (“APPLE”)

Petitioner

- vs. -

COREPHOTONICS, LTD. (“COREPHOTONICS”)

Patent Owner

U.S. Patent No. 9,857,568

**DECLARATION OF INGRID HSIEH-YEE, PHD,
UNDER 37 C.F.R. § 1.68**

I, Ingrid Hsieh-Yee, Ph.D., do hereby declare as follows:

1. I have been retained as an independent expert witness on behalf of Apple Inc. (“Apple”) for an *Inter Partes* Review (“IPR”) of U.S. Patent No. 9,857,568 (“the ’568 patent”).

2. I am being compensated for my work in this matter at my accustomed hourly rate. I am also being reimbursed for reasonable and customary expenses associated with my work and testimony in this investigation. My compensation is not contingent on the results of my study, the substance of my opinions, or the outcome of this matter.

3. In the preparation of this declaration, I have reviewed the exhibits referenced below, each of these is a type of material that experts in my field would reasonably rely upon when forming their opinions:

- (1) Warren J. Smith (“Smith”), MODERN LENS DESIGN (1992), obtained from the Library of Congress, **Appendix C**;
- (2) Max Born *et al.* (“Born”), PRINCIPLES OF OPTICS, 6th Ed. (1980), obtained from the Library of Congress, **Appendix D**;
- (3) Jane Bateau *et al.* (“Bateau”), “The optics of miniature digital camera modules,” SPIE Proceedings Volume 6342, *International Optical Design Conference 2006*; 63421F (2006), obtained from the Library of Congress, **Appendix E**;
- (4) Michael P. Schaub (“Schaub”), THE DESIGN OF PLASTIC OPTICAL

- SYSTEMS (2009), obtained from the Library of Congress, **Appendix F**;
- (5) Optical Society of America (“Handbook of Optics”), HANDBOOK OF OPTICS, vol. II 2nd ed. (1995), obtained from the Library of Congress, **Appendix G**;
 - (6) MARC Record Information for HANDBOOK OF OPTICS, vol. II 2nd ed. (1995), available at the Library of Congress online catalog at <https://catalog.loc.gov/vwebv/staffView?searchId=20956&recPointer=0&recount=25&searchType=2&bibId=2068733>, accessed June 12, 2018, **Appendix H**;
 - (7) Bibliographic Record Information for HANDBOOK OF OPTICS, vol. II 2nd ed. (1995), available at the Library of Congress online catalog at <https://lcn.loc.gov/94019339>, accessed June 12, 2018, **Appendix I**;
 - (8) Copyright Registration for HANDBOOK OF OPTICS, vol. II 2nd ed. (1995), available at https://cocatalog.loc.gov/cgi-bin/Pwebrecon.cgi?v1=3&ti=1,3&Search_Arg=Handbook%20of%20optics&Search_Code=TALL&CNT=25&PID=ImyGYjD7XXbibjVvG1mOABNTznL&SEQ=20180619221237&SID=1, accessed June 19, 2018, **Appendix J**;
 - (9) William S. Beich *et al.* (“Beich”), “Polymer Optics: A manufacturer’s perspective on the factors that contribute to successful programs,” SPIE Proceedings Volume 7788, *Polymer Optics Design, Fabrication, and Materials*, obtained from the Library of Congress, **Appendix K**;
 - (10) MARC Record Information for *Polymer Optics Design, Fabrication, and Materials*, available at the Library of Congress online catalog at <https://catalog.loc.gov/vwebv/staffView?searchId=22415&recPointer>

=0&recount=25&searchType=1&bibId=16762353, accessed June 13, 2018, **Appendix L**;

(11) Bibliographic Record Information for *Polymer Optics Design, Fabrication, and Materials*, available at the Library of Congress online catalog at <https://lccn.loc.gov/2011289200>, accessed June 13, 2018, **Appendix M**;

(12) Copyright Registration for *Polymer Optics Design, Fabrication, and Materials*, available at https://cocatalog.loc.gov/cgi-bin/Pwebrecon.cgi?Search_Arg=Polymer+Optics+Design%2C+Fabrication%2C+and+Materials&Search_Code=TALL&PID=cXf7Q99L7h_q9-aeWMbj2t8gCQg&SEQ=20180619221210&CNT=25&HIST=1, accessed June 18, 2018, **Appendix N**.

4. In forming the opinions expressed within this declaration, I have considered:

- (1) The documents listed above;
- (2) The reference materials cited herein; and
- (3) My own academic background and professional experiences, as described below.

5. My complete qualifications and professional experience are described in my curriculum vitae, a copy of which is attached as **Appendix A**. The following is a brief summary of my relevant qualifications and professional experience.

6. I am currently a Professor in the Department of Library and Information Science at the Catholic University of America. I have experience working in an academic library, a medical library, and a legislative library and have been a professor for more than 25 years. I hold a Ph.D. in Library and Information Studies from the University of Wisconsin-Madison and a Masters in Library and Information Studies from the University of Wisconsin-Madison.

7. I am an expert on library cataloging and classification and have published two books on this subject, *Organizing Audiovisual and Electronic Resources for Access: A Cataloging Guide* (2000, 2006). I teach a variety of courses, including “Cataloging and Classification,” “Internet Searches and Web Design,” “Advanced Cataloging and Classification,” “Organization of Internet Resources,” “Advanced Information Retrieval and Analysis Strategies,” and “Digital Content Creation and Management.” My research interests cover cataloging and classification, information organization, metadata, information retrieval, information architecture, digital collections, scholarly communication, user interaction with information systems, and others.

8. I am fully familiar with a library cataloging encoding standard known as the “Machine-Readable Cataloging” standard, also known as “MARC,” which became the national standard for sharing bibliographic data in the United States by 1971 and the international standard by 1973. MARC is the primary

communications protocol for the transfer and storage of bibliographic metadata in libraries. Experts in my field would reasonably rely upon MARC records when forming their opinions.

9. A MARC record comprises several fields, each of which contains specific data about the work. Each field is identified by a standardized, unique, three-digit code corresponding to the type of data that follows. **Appendix B** is a true and correct copy of Parts 7 to 10 of “Understanding MARC Bibliographic” (<http://www.loc.gov/marc/umb/>) from the Library of Congress that explains commonly used MARC fields. For example, the personal author of the work is recorded in Field 100, the title is recorded in Field 245, publisher information is recorded in Field 260, and the physical volume and characteristics of a publication are recorded in Field 300, and topical subjects are recorded in the 650 fields.

10. Online Computer Library Center (OCLC) is the largest bibliographic network of the world, with more than 380 million records and more than 16,900 member institutions (many of which are libraries of some type) from 122 countries. OCLC was created “to establish, maintain and operate a computerized library network and to promote the evolution of library use, of libraries themselves, and of librarianship, and to provide processes and products for the benefit of library users and libraries, including such objectives as increasing availability of library resources to individual library patrons and reducing the rate of rise of library per-

unit costs, all for the fundamental public purpose of furthering ease of access to and use of the ever-expanding body of worldwide scientific, literary and educational knowledge and information.”¹

11. OCLC members can contribute original cataloging records in MARC to the system or derive cataloging records from existing records, an activity referred to as “copy cataloging”. When an OCLC participating institution acquires a work, it can create an original MARC record for this work in OCLC’s Connexion system (a system for catalogers to create and share MARC records), and the system will automatically generate a code for the date of record creation in the *yyymmdd* format, and the creating library’s OCLC symbol is recorded in subfield a of the 040 field. Once the MARC record is in Connexion, it becomes available to other OCLC members for adoption to their local online catalogs. The record—presented in a labeled format, not MARC—also becomes searchable and viewable on WorldCat, which is a web portal to more than 10,000 libraries worldwide.

12. Library online catalogs are based on MARC records that represent their collections and help the public understand what materials are publicly

¹ Third Article, Amended Articles of Incorporation of OCLC Online Computer Library Center, Inc. Revised May 20, 2008 (available at <https://www.oclc.org/content/dam/oclc/membership/articles-of-incorporation.pdf>)

accessible in those libraries. Most libraries with online catalogs have made their catalogs freely available on the Web. These online catalogs offer user-friendly search interfaces, often in the form of a single search box, to support searching by author, title, subject, keywords and other data elements. They also offer features for users to narrow their search results by language, year, format, and other elements. Many libraries display MARC records on their online catalogs with labels for the data elements to help the public interpret MARC records. Many libraries also offer an option to display MARC records in MARC fields. For non-serial publications such as monographs, after a MARC record is created and made searchable on a library catalog, it is customary library practice to have the physical volume processed for public access soon after, usually within a week.

13. I used authoritative information systems such as WorldCat (<http://www.worldcat.org>), the online catalog at the Library of Congress (<https://catalog.loc.gov>) and the public catalog of the United States Copyright Office (<http://cocatalog.loc.gov/cgi-bin/Pwebrecon.cgi?DB=local&PAGE=First>) to search for records. These records are identified and discussed in this declaration. Experts in the field would reasonably rely on the data described herein to form their opinions.

Appendix C

14. Appendix C is a true and correct photocopy of portions of MODERN

LENS DESIGN (“Smith”) that I made on June 15, 2018 during my personal visit to the Library of Congress. When I was originally asked to prepare this declaration, I searched WorldCat for “Modern Lens Design” and identified the Library of Congress as one of the libraries that hold this monograph. I then searched the Library of Congress online catalog to confirm the holdings information. The search results informed me that the Library of Congress provides access to Smith.

15. Appendix C is a true and correct copy of portions of Smith that I made on June 15, 2018, while the book was in my possession at the Library of Congress. I obtained **Appendix C** by personally scanning the front matter (the front cover, the title page, and the copyright page) and select content pages from Smith, specifically, pages 1-62 and 169-182 of the book, and the back cover.

Appendix D

16. Appendix D is a true and correct copy of portions of PRINCIPLES OF OPTICS (“Born”) that I made on June 20, 2018 during my personal visit to the Library of Congress. When I was originally asked to prepare this declaration, I searched WorldCat for “Principles of Optics” and identified the Library of Congress as one of the libraries that hold this monograph. I then searched the Library of Congress online catalog to confirm the holdings information. The search results informed me that the Library of Congress provides access to Born.

17. Appendix D is a true and correct copy of portions of Born that I made on June 20, 2018, while the book was in my possession at the Library of Congress. I obtained **Appendix D** by personally scanning the front matter (the front cover, the title page, and the copyright page) and select content pages from Born, specifically, pages 156-197, and the back cover of the book.

Appendix E

18. Appendix E is a true and correct copy of portions of “The optics of miniature digital camera modules” (“Bareau”) and additional pages from International Optical Design Conference 2006 that I made on June 16, 2018 during my personal visit to the Library of Congress. When I was originally asked to prepare this declaration, I accessed WorldCat for “International Optical Design Conference” because the conference proceeding is the volume that contains Bareau. The search results identified the Library of Congress as one of the libraries that hold this monograph. I then searched the Library of Congress online catalog to confirm the holdings information. The search results informed me that the Library of Congress provides access to International Optical Design Conference 2006 that contains Bareau.

19. Appendix E is a true and correct copy of portions of International Optical Design Conference 2006 that contains Bareau that I made on June 15, 2018, while the book was in my possession at the Library of Congress. I obtained

Appendix E by personally scanning the front matter (the front cover, the title page, and the copyright page) and Bateau that appears from pages 63421F-1 to 63421F-11, and the back cover of the book.

Appendix F

20. **Appendix F** is a true and correct copy of portions of THE DESIGN OF PLASTIC OPTICAL SYSTEMS (“Schaub”) that I made on June 15, 2018 during my personal visit to the Library of Congress. When I was originally asked to prepare this declaration, I searched WorldCat for “Design of Plastic Optical Systems” and identified the Library of Congress as one of the libraries that hold this monograph. I then searched the Library of Congress online catalog to confirm the holdings information. The search results informed me that the Library of Congress provides access to Schaub.

21. **Appendix F** is a true and correct copy of portions of Schaub that I made on June 15, 2018, while the book was in my possession at the Library of Congress. I obtained **Appendix F** by personally scanning the front matter (the front cover, the title page, and the copyright page) and select content pages from Schaub, specifically, the Introduction, Preface, pages 1-13 and 39-168, and the back cover of the book.

Appendix G

22. Appendix G is a true and correct copy of portions of the HANDBOOK OF OPTICS, vol. II, 2nd ed. (the “Handbook of Optics”) that I made on June 18, 2018 during my personal visit to the Library of Congress. When I was originally asked to prepare this declaration, I searched WorldCat for “Handbook of Optics” and identified the Library of Congress as one of the libraries that hold this monograph. I then searched the Library of Congress online catalog to confirm the holdings information. The search results informed me that the Library of Congress provides access to the Handbook of Optics.

23. Appendix G is a true and correct copy of portions of the Handbook of Optics that I made on June 18, 2018, while the book was in my possession at the Library of Congress. I obtained **Appendix G** by personally scanning the front matter (the front cover, the title page, and the copyright page) and select content pages from the Handbook of Optics, specifically, pages 1.3-1.41 and 34.1-34.21, and the back cover of the book.

a. Library of Congress – MARC and Bibliographic Records

24. Appendix H is a true and correct copy of the MARC record for the HANDBOOK OF OPTICS, a four volume set, whose vol. II (“Handbook of Optics”) is presented as **Appendix G**. I retrieved this record from the online catalog of the Library of Congress after searching for the book by searching “Handbook of Optics.” I personally identified and located this record, which experts in my field

would reasonably rely upon when forming their opinions.

25. **Appendix I** is a true and correct copy of the Bibliographic record for the HANDBOOK OF OPTICS, a four volume set, whose vol. II (“Handbook of Optics”) is presented as **Appendix G**. I retrieved this record from the online catalog of the Library of Congress, which experts in my field would reasonably rely upon when forming their opinions.

26. Field 245 of the MARC record (**Appendix H**) and the title field of the Bibliographic record (**Appendix I**) identify the book title as “Handbook of Optics.” Field 260 of the MARC record (**Appendix H**) and the published/created field of the Bibliographic record (**Appendix I**) show that the four volumes of the Handbook of Optics were published by McGraw-Hill in New York, NY from 1995 to 2001. Field 010 shows the Library of Congress control number (LCCN) as “94019339.” The Library of Congress has used LCCNs since 1898 to uniquely identify items in their cataloged collections. Librarians use LCCNs to locate Library of Congress cataloging records in national databases quickly. The year portion of LCCN indicates the year when a LCCN is assigned. The reason that the Handbook whose Volumes 1 and 2 were first published in 1995 was assigned the LCCN in 1994 is because of the Library of Congress Preassigned Control Number (PNC) Program. The purpose of the PNC Program is to assign control numbers in advance of publication to titles that may be added to the Library of Congress

collection. The second Field 020 in the MARC record shows the International Standard Book Number for Volume 2 as “0070479747,” which matches the ISBN on the copyright page and the back cover of **Appendix G**.

27. The first six digits of Field 008 of the MARC record (**Appendix H**) inform me that the record for the book was first created on “940520” (*i.e.*, May 20, 1994), and subfield a of Field 040 indicates “DLC” (*i.e.*, Library of Congress) was the creator. The reason a bibliographic record was created in 1994 for a publication with a copyright date of 1995 and beyond is because the record is a Cataloging in Publication (CIP) record. The Cataloging in Publication (CIP) Program of the Library of Congress is responsible for cataloging books in advance of publication to alert the library community to forthcoming publications and to facilitate acquisition. The initial CIP record is created based on information submitted by the publisher. When the CIP record is ready, it is sent to the publisher for inclusion in the publication. The Library of Congress also distributes CIP records in MARC format to large libraries, bibliographic services, and book vendors worldwide. After the book is published, the publisher is obligated to send CIP a copy, and CIP catalogers use the newly received publication to verify and update data in the original CIP record. The local note in Field 955 of the MARC record informs me of the cataloging process dates and indicates the CIP record was completed on “5-26-94” (*i.e.*, May 26, 1994) and verified on “12-01-94” (*i.e.*, Dec. 1, 1994).

28. Field 050 of the MARC Record (**Appendix H**) and the LC classification field of the Bibliographic record (**Appendix I**) show that the Handbook of Optics has a Library of Congress Classification (LCC) number of “QC369 .H35 1995,” and QC369 represents the class number for “Optics. Light,” while “H35” is the author number based on the first word of this title, “handbook.” Field 082 shows the book has a Dewey Decimal Classification (DDC) number of “535,” which represents the class number for “Light and related radiation.” Two subject headings in Field 650s indicate this book is about “Optics” and “Optical instruments,” and subfield v “Handbooks, manuals, etc.” indicates that handbook is the publication format. Field 300 shows this title consists of four volumes, and Field 505, the contents note, lists the title of each volume. Field 991 is a local note indicating that the Handbook of Optics has a call number of “QC369 .H35 1995” and is part of the General Collection. The MARC record makes the Handbook of Optics (**Appendix G**) searchable in the Library of Congress online catalog. Users interested in optics or optical instruments would be able to search for and retrieve this book by the subject areas represented by the LCC number and the DDC number, and by the subject headings in Field 650s. They could also find this book by ISBN and title.

29. Based on the information above, it is my opinion that the HANDBOOK OF OPTICS, vol. II, 2nd ed. (**Appendix G**) is a book that has been made available by

the Library of Congress, meaning that anyone who was interested in the topic would be able to search for and access the Handbook of Optics.

b. Library of Congress – Date Stamp

30. The copyright page of the Handbook of Optics in **Appendix G** bears a stamp of “LIBRARY OF CONGRESS FEB 08 1995 COPYRIGHT OFFICE” that indicates the date when the Library of Congress received the physical volume. The stamp has the appearance and distinctive characteristics of a typical check-in date stamp utilized by libraries to indicate the date a particular volume was received by the library. While the MARC record does not indicate when the Handbook of Optics was added to the Library of Congress collection, this date stamp on the copyright page shows this volume was received by the Copyright Office on “Feb 08 1995.” Because Field 955 of the MARC record shows that the cataloging record was verified on Dec. 1, 1994, adding this volume, Handbook of Optics, to the collection would not have involved the creation of a new cataloging record. Instead, the existing record would have been updated and this process would not have taken a lot of time. However, no data in the MARC or Bibliographic record indicates how soon this volume was delivered from the Copyright Office to the Cataloging Unit for cataloging and processing. Based on my understanding of the ordinary and customary cataloging and processing practices of libraries and considering the workload at the Library of Congress, my conservative estimate is

that it would not take more than one year for this volume to become available to the public, that is, the Handbook of Optics would have been available to the public by February 8, 1996.

c. United States Copyright – Copyright Registration

31. **Appendix J** is a true and accurate copy of the copyright registration record obtained from the Library of Congress. I obtained **Appendix J** by first accessing the <http://www.copyright.gov/> website, selecting the hyperlink “Search Copyright Records,” and performing a search by the title, “Handbook of optics,” to retrieve the record. I personally identified and located this record, which experts in my field would reasonably rely upon when forming their opinions. The copyright record shows that the Handbook of optics: vol. 2, devices measurements, and properties was sponsored by the Optical Society of America and Michael Bass was the Editor in Chief. The 2nd edition of vol. 2 has an imprint date of 1995.

32. The date of creation field of **Appendix J** shows “1994” as the creation date, the date of publication field shows “1994-10-04” (*i.e.*, Oct. 4, 1994) as the publication date, and the registration number/date field shows “TX0003992602/1995-02-08” as the date when the copyright registration number was assigned.

33. Based on the “Feb. 8, 1995” date stamp on the copyright page of **Appendix G**, the copyright record of **Appendix J**, and my understanding of the

ordinary and customary cataloging and processing practices of libraries, it is my opinion that the Handbook of Optics (**Appendix G**) would have been publicly available at the Library of Congress no later than Feb. 8, 1996, a year after the volume was received by the Copyright Office.

Appendix K

34. Appendix K is a true and correct copy of the portions of the book *Polymer Optics Design, Fabrication, and Materials* containing “Polymer optics: a manufacturer’s perspective on the factors that contribute to successful programs” by Beich *et al.* (“Beich”). I made this copy on June 15, 2018 during my personal visit to the Library of Congress. When I was originally asked to prepare this declaration, I searched WorldCat for “Polymer Optics Design, Fabrication, and Materials” and identified the Library of Congress as one of the libraries that hold this monograph. I then searched the Library of Congress online catalog to confirm the holdings information. The search results informed me that the Library of Congress provides access to *Polymer Optics Design, Fabrication, and Materials*, which contains Beich.

35. Appendix K is a true and correct copy of the portions of *Polymer Optics Design, Fabrication, and Materials* containing Beich. I made this copy on June 15, 2018, while the book was in my possession at the Library of Congress. I obtained **Appendix K** by personally scanning the front matter (the front cover, the

title page, the copyright page, the table of contents, and preface), the Beich article that appears from pages 778805-1 to 77805-9, and the back cover of the book.

a. Library of Congress – MARC and Bibliographic Records

36. **Appendix L** is a true and correct copy of the MARC record for *Polymer Optics Design, Fabrication, and Materials*, which contains Beich (**Appendix K**). I retrieved the MARC record from the online catalog of the Library of Congress after searching for the book title “Polymer Optics Design, Fabrication, and Materials.” I personally identified and located this record, which experts in my field would reasonably rely upon when forming their opinions.

37. **Appendix M** is a true and correct copy of the Bibliographic record for *Polymer Optics Design, Fabrication, and Materials*, which contains Beich (**Appendix K**). I retrieved the Bibliographic record from the online catalog of the Library of Congress, which experts in my field would reasonably rely upon when forming their opinions.

38. Field 245 of the MARC record (**Appendix L**) and the title of the Bibliographic record (**Appendix M**) identify the book title as “Polymer optics design, fabrication, and materials.” Field 260 of the MARC record (**Appendix L**) and the published/created field of Bibliographic record (**Appendix M**) show that *Polymer Optics Design, Fabrication, and Materials*, which contains Beich, was

published by SPIE in Bellingham, WA in 2010. Field 010 shows the Library of Congress control number as “2011289200,” which matches the label bearing the same number on the copyright page of **Appendix K**. Field 490 shows that the book belongs to the series, “Proceedings of SPIE,” whose International Standard Serial Number (ISSN) is presented in subfield x as “0277-786X,” which matches the ISSN on the copyright page of **Appendix K**.

39. Field 042 informs me that this record is a “lccopycat,” meaning it is a copy cataloging record based on a record first created by another library. Field 040 subfield a indicates the record originated from “CAI” which is the OCLC symbol for the National Research Council of Canada, according to the Directory of OCLC members (<https://www.oclc.org/en/contacts/libraries.html>). The first six digits of Field 008 and the dates in Field 955 of the MARC record (**Appendix L**) inform me that this LC record for the book was created on “110504” (*i.e.*, May 4, 2011).

While academic libraries typically make newly cataloged items available to the public soon after the cataloging work is completed, usually within a week, processing of a newly cataloged item may take longer at the Library of Congress because of the large volume of materials for processing. My estimate is that the processing may take no more than three months, meaning *Polymer Optics Design, Fabrication, and Materials*, which contains Beich, would have been available to the public at the Library of Congress no later than August 2011, three months after

the cataloging record was completed.

40. Field 050 of the MARC Record (**Appendix L**) shows that this book has a Library of Congress Classification number of “QD381.9.O66 P6483 2010,” and QD381.9.O66 represents the class number for “Optical properties.” Four subject headings in Field 650s indicate this book is about “Polymers \$x Optical properties,” “Optical materials \$x Design and construction,” “Optical films,” and “Optical coatings,” with subfield v “Congresses” indicating these topics were presented at a conference. This MARC record makes the book that contains Beich (**Appendix K**) searchable in the Library of Congress online catalog. Interested users would be able to search for and retrieve this book by the subject areas represented by the LC classification number and by the subject headings in Field 650s. They could also find the book by its title, ISBN, editors, and SPIE, the Society of Photo-Optical Instrumentation Engineers.

41. Based on the information above, it is my opinion that *Polymer Optics Design, Fabrication, and Materials*, which contains Beich (**Appendix K**), is a book that has been made available by the Library of Congress, meaning that anyone who was interested in the topic would be able to search for this book and access the Beich article at the Library of Congress.

b. Library of Congress – Bindery Date Indication

42. The back cover of *Polymer Optics Design, Fabrication, and Materials* (p.20 in **Appendix K**) bears a sticker with a date “8/30/2011” that indicates the bindery date of this volume. It supports my opinion that this publication would have been available to the public in August 2011 at the Library of Congress.

c. United States Copyright – Copyright Registration

43. **Appendix N** is a true and accurate copy of the copyright registration record obtained from the Library of Congress that confirms the publication of *Polymer Optics Design, Fabrication, and Materials*, which contains Beich. I obtained **Appendix N** by first accessing the <http://www.copyright.gov/> website, selecting the hyperlink “Search Copyright Records,” and performing a search by the title, “Polymer optics design, fabrication, and materials,” to retrieve the record. I personally identified and located this record, which experts in my field would reasonably rely upon when forming their opinions. The title field includes a note “Published: 2010-08-12. Issue: vol. 7788, 01-02 August 2010” and the registration number/date shows “TX0007236151/ 2010-10-12,” meaning the copyright registration number was assigned on Oct. 12, 2010.

44. Based on the record creation date in the MARC record (**Appendix L**), the LCCN sticker on the copyright page of **Appendix K**, the bindery date sticker on the back cover of **Appendix K**, the date information on the copyright record of **Appendix N**, and my understanding of the ordinary and customary cataloging and

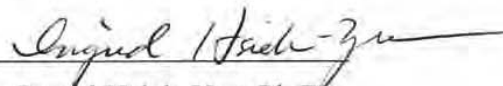
processing practices of libraries, it is my opinion that *Polymer Optics Design, Fabrication, and Materials*, which contains Beich (**Appendix K**), was publicly available at the Library of Congress no later than August 2011, three months after the cataloging work was completed.

CONCLUSION

45. In signing this declaration, I recognize that the declaration will be filed as evidence in a contested case before the Patent Trial and Appeal Board of the United States Patent and Trademark Office. I also recognize that I may be subject to cross-examination in the case. If cross-examination is required of me, I will appear.

46. I hereby declare that all statements made herein on my own knowledge are true and that all statements made on information and belief are believed to be true, and further, that these statements were made with the knowledge that willful false statements and the like so made are punishable by fine or imprisonment, or both, under Section 1001 of Title 18 of the United States Code.

Date: 6-23-2018.

Executed: 
Ingrid Hsieh-Yee, Ph.D.

APPENDIX A

Ingrid Hsieh-Yee

Professor

Dept. of Library and Information Science

Catholic University of America

Washington, D.C. 20064

E-mail: hsiehyee@cua.edu

Phone: (202) 319-5085

Fax: (202) 319-5574

Education

Ph.D. Library and Information Studies, University of Wisconsin-Madison
Minors: Sociology and Psychology

M.A. Library and Information Studies, University of Wisconsin-Madison.

M.A. Comparative Literature, University of Wisconsin-Madison.

B.A. Foreign Languages and Literature, National Taiwan University.

Work Experience

Professor, School/Dept. of Library and Information Science, Catholic University of America,
2004- (Assistant Professor, 1990-1996; Associate Professor, 1997-2004)

Co-Chair, Dept. of Library and Information Science, Catholic University of America, June 2015-
August 2016.

Acting Dean, School of Library and Information Science, Catholic University of America,
January 2010-June 2012.

Cataloger, Dept. of Legislative Reference Library, Annapolis, Maryland, 1989-1990.

Lecturer, School of Library and Information Studies, University of Wisconsin-Madison, 1988.

Teaching Assistant, School of Library and Information Studies, University of Wisconsin-
Madison, 1986-1988.

Cataloger, Health Sciences Library, University of Wisconsin-Madison, 1984-1986.

Areas of Teaching and Research Interests

Information Organization and Access; Metadata; Cataloging & Classification; Information
Architecture; Information Retrieval; Digital Collections; Scholarly Communication; Information

Behavior; Health Informatics; Human Computer Interaction; Usability Studies

Grants & Honors

Cultural Heritage Information Management Project. IMLS grant. Amount: \$498,741. Period: Aug. 2012 to July 2015. Co-PI with Dr. Youngok Choi.

D.C. Health Information Technology (HIT4): Building Capacity & Providing Access in Our Nation's Capital. Dept. of Labor H2B Training Grant. Grant amount: \$4,175,500. Grant period: Nov. 2011 to Dec. 2015. Partner with the Metropolitan School of Professional Studies of the Catholic University of America, Children's National Medical Center, D.C. Department of Employment Services, Holy Cross Hospital, Howard University, Center for Urban Progress, Providence Hospital, and Sibley Memorial Hospital.

Capital Health Careers Project. Department of Labor Healthcare Sector and Other High Growth and Emerging Industries Grant. Grant amount: \$4,953,999. Grant period: March 2010 – February 2013. Awarded to a group of healthcare organizations and educational institutions in Washington, D.C. Providence Health Foundation of Providence Hospital (Lead institution). Part of the grant supported the development of a Master's degree program in Information Technology with a concentration in Health Information Technology offered by the School of Library and Information Science.

The Washington D.C. School Librarians Project. IMLS grant. Grant amount: \$412,660. Grant period: Aug. 2007 – June 2011. The School partnered with the District of Columbia Public Schools (DCPS) and the District of Columbia Library Association to educate and mentor school media specialists for the DCPS system. PI, Jan. 2010 to June 2011.

SIG Member of the Year, American Society for Information Science and Technology (2009).

Most Outstanding Paper of *OCLC Systems & Services* (2001).

ALISE Research Grant (2001).

Most Outstanding Paper of *OCLC Systems & Services* (2000).

Research Grant from ERIC (1999-2000).

Best Research Paper Award; Association for Library and Information Science Education (1998).

Research Grants, Catholic University of America. 1991, 1992, 1993, 1996, 1998, 1999, 2004, 2005, 2006, 2007, 2013-14.

Cooperative Faculty Research Grant, Consortium of Universities in the Washington Metropolitan Area (1993-1994).

Cooperative Research Grant, Council on Library Resources (1993-1994).

Journal of the American Society for Information Science Best Paper Award (1993).

ASIS/ISI Information Science Doctoral Dissertation Scholarship (1989).

HEA Title IIB Fellowship (Dept. of Education) (1989)

Chinese-American Librarians Association Scholarship (1987).

Beta Phi Mu (1985).

Vilas Fellowship, University of Wisconsin-Madison. 1984

Publications

Choi, Y., and Hsieh-Yee, I. (2010). Finding Images in an OPAC: Analysis of User Queries, Subject Headings, and Description Notes. *Canadian Journal of Information and Library Science*, 34(3): 271 – 295.

Hsieh-Yee, I. (2008). Educating Cataloging Professionals in a Changing Information Environment. *Journal of Education for Library and Information Science*, 46(2): 93-106.

Vellucci, S. L., Hsieh-Yee, I., and Moen, W.E. (2007). The Metadata Education and Research Information Commons (MERIC): A Collaborative Teaching and Research Initiative. *Education for Information*, 25(3&4): 169-178.

NISO Framework for Guidelines for Building Good Digital Collections. 3rd ed. Baltimore, MD: National Information Standards Organization, 2007. Also available online: <http://www.niso.org/framework/framework3.pdf> (NISO Working Group members: Priscilla Caplan (chair), Grace Agnew, Murtha Baca, Tony Gill, Carl Fleischhauer, Ingrid Hsieh-Yee, Jill Koelling, and Christie Stephenson.)

Choi, Y., Hsieh-Yee, I., and Kules, B. (2007). Retrieval Effectiveness of TOC and LCSH. *Proceedings of the Joint Conference on Digital Libraries*, pp. 233-234.

Vellucci, S., and Hsieh-Yee, I. (2007). They Didn't Teach Me That in Library School! Building a Digital Teaching Commons to Enhance Metadata Teaching, Learning and Research. *Proceedings of the National Conference of the Association of College and Research Libraries, Baltimore, MD*, pp. 26-31.

Mitchell, Vanessa, and Ingrid Hsieh-Yee. (2007). Converting Ulrich's Subject Headings to FAST Headings: A Feasibility Study. *Cataloging & Classification Quarterly*, 45(1): 59-85.

- Hsieh-Yee, I., Tang, R., and Zhang, S. (2007). User Perceptions of a Federated Search System. *IEEE Technical Committee on Digital Libraries Bulletin*, Summer 3(2) (URL = <http://www.ieee-tcdl.org>).
- Tang, R., Hsieh-Yee, I., and Zhang, S. (2007). User Perceptions of MetaLib Combined Search: An Investigation of How Users Make Sense of Federated Searching." *Internet Reference Services Quarterly*, 12(12): 211-236.
- Hsieh-Yee, I., Tang, R., and Zhang, S. (2006). User Perceptions of a Federated Search System. *Proceedings of the Joint Conference on Digital Libraries, June 11-15, 2006, Chapel Hill*, p. 338.
- Hsieh-Yee, I. (2006). *Organizing Audiovisual and Electronic Resources for Access: A Cataloging Guide*. 2nd ed. Westport, Conn.: Libraries Unlimited.
- NISO A Framework of Guidance for Building Good Digital Collections*. 2nd ed. Bethesda, MD: National Information Standards Organization, 2004. Framework Advisory Group: Grace Agnew, Liz Bishoff, Priscilla Caplan (Chair), Rebecca Gunther and Ingrid Hsieh-Yee.
- Hsieh-Yee, I. (2004). Cataloging and Metadata Education in North American LIS Programs. *Library Resources & Technical Services*, 48(1): 59-68.
- Hsieh-Yee, I. (2004). Cataloging and Metadata Education. In Gary E. Gorman (Ed.), *International Yearbook of Library and Information Management 2003: Metadata Applications and Management*, (pp.204-234). London: Facet Publishing.
- Yee, P. L., Hsieh-Yee, I., Pierce, G.R., Grome, R., and Schantz, L. (2004). Self-Evaluative Intrusive Thoughts Impede Successful Searching on the Internet. *Computers in Human Behavior*, 20(1): 85-101.
- Hsieh-Yee, I. (2003). Cataloging and Metadata Education: A Proposal for Preparing Cataloging Professionals of the 21st Century. A report submitted to the ALCTS-Education Task Force in response to Action Item 5.1 of the *Bibliographic control of Web Resources: A Library of Congress Action Plan*. Approved by the Association for Library Collections and Technical Services. Web version available since April 2003 at <http://lcweb.loc.gov/catdir/bibcontrol/CatalogingandMetadataEducation.pdf>.
- Hsieh-Yee, I. (2002). Cataloging and Metadata Education: Asserting a Central Role in Information Organization. *Cataloging & Classification Quarterly* 34(½): 203-222.
- Hsieh-Yee, I., and Smith, M. (2001). The CORC Experience: Survey of Founding Libraries, Part I. *OCLC Systems & Services*, 17: 133-140. (Received "The Most Outstanding Paper of OCLC Systems & Services in 2001" award.)

- Hsieh-Yee, I., and Smith, M. (2001). The CORC Experience: Survey of Founding Libraries, Part II, Automated Tools and Usage. *OCLC Systems & Services*, 17: 166-177. (Received "The Most Outstanding Paper of OCLC Systems & Services in 2001" award.)
- Hsieh-Yee, I. (2001). ERIC User Services: Changes and Evaluation for the Future. *Government Information Quarterly*, 18: 31-42.
- Hsieh-Yee, Ingrid. (2001). Research on Web Search Behavior. *Library and Information Science Research*, 23: 167-185.
- Logan, E., and Hsieh-Yee, I. (2001). Library and Information Science Education in the Nineties. *Annual Review of Information Science and Technology*, 35: 425-477.
- Hsieh-Yee, I. (Ed.) (2001). *Library and Information Science Research*, 23 (2). A special issue in honor of the retirement of Douglas L. Zweizig.
- Hsieh-Yee, I. (2000). *ERIC User Services: Evaluation in a Decentralized Environment*. Washington, D.C.: Dept. of Education.
- Hsieh-Yee, Ingrid. (2000). *Organizing Audiovisual and Electronic Resources for Access: A Cataloging Guide*. Littleton, CO: Libraries Unlimited.
- Hsieh-Yee, I. (2000). Organizing Internet Resources: Teaching Cataloging Standards and Beyond. *OCLC Systems & Services*, 16: 130-143. (Received "The Most Outstanding Paper of OCLC Systems & Services in 2000" award.)
- Hsieh-Yee, I. (1998). The Retrieval Power of Selected Search Engines: How Well Do They Address General Reference Questions and Subject Questions? *Reference Librarian*, 60: 27-47.
- Hsieh-Yee, I. (1998). Search Tactics of Web Users in Searching for Texts, Graphics, Known Items and Subjects: A Search Simulation Study. *Reference Librarian*, 60: 61-85. (Received the 1997 Best ALISE Research Paper Award.)
- Hsieh-Yee, I. (1997). Access to OCLC and Internet Resources: LIS Educators' Views and Teaching Practices. *RQ*, 36: 569-86.
- Hsieh-Yee, I. (1997). Teaching Online and CD-ROM Resources: LIS Educators' Views and Practices. *Journal of Education for Library and Information Science*, 38: 14-34.
- Hsieh-Yee, I. (1996). The Cataloging Practices of Special Libraries and Their Relationship with OCLC. *Special Libraries*, 87: 10-20.

- Hsieh-Yee, I. (1996). Modifying Cataloging Practice and OCLC Infrastructure for Effective Organization of Internet Resources. In *Proceedings of the OCLC Internet Cataloging Colloquium*. [Online]. Available: <http://www.oclc.org/oclc/man/colloq/hsieh.htm>
- Hsieh-Yee, I. (1996). Student Use of Online Catalogs and Other Information Channels. *College & Research Libraries*, 57: 161-175.
- Hsieh-Yee, I. (1995). Ten entries in James S. C. Hu (Ed.), *Encyclopedia of Library & Information Science*, 913, 1028-29, 1036, 1037, 1145-46, 1514, 1575, 1763-64, 2216-27, 2378-79. Taipei, Taiwan: Sino-American Publishing. (Topics include "Advanced Technology/Libraries," "Information Ethics," "Instruction on Cataloging and Classification," "Instruction on Reference Services.")
- Hsieh-Yee, I. (1993). Effects of Search Experience and Subject Knowledge on Online Search Behavior: Measuring the Search Tactics of Novice and Experienced Searchers. *Journal of the American Society for Information Science*, 44: 161-174. (Received the 1993 Best JASIS Paper Award.)

Presentations

- Hsieh-Yee, I. (February, 2017) *Research Data Management: New Competencies and Opportunities for Information Professionals*. Selected for presentation at the 9th Bridging the Spectrum Symposium, Washington, D.C.
- Hsieh-Yee, I. and Lawton, P. (February, 2017) *Enhancing Catholic Portal Searches with User Terms and LCSH*. Selected for presentation at the 9th Bridging the Spectrum Symposium, Washington, D.C.
- Hsieh-Yee, I. (2016, October) *Visualizing Data for Information*. Presented at the 2016 Virginia Library Association Conference, Hot Springs, VA.
- Hsieh-Yee, I. (2016, August) *Religious Materials Toolbox for Archivists: Solutions to Problems Facing the Profession*. Presented at Archives * Records 2016, Atlanta, GA.
- Hsieh-Yee, I. and Lawton, P. (2016, March) *Enhancing Retrieval of Catholic Materials with LCSH Knowledge Structure*. Presented at the 2016 Catholic Library Association Conference, San Diego, CA.
- Fagan-Fry, J. and Hsieh-Yee, I. (2016, February) *Approaches to Digital Scholarship at Top Universities around the World: Scholarly Publishing in the Digital Age*. Presented at the 8th Bridging the Spectrum Symposium, Washington, D.C.

- Hsieh-Yee and Fagan-Fry, J. (2016, January) *Innovative Services for Digital Scholarship at Top 100 Research Libraries of the World*. Poster presented at the 2016 Annual Conference of the Association for Library and Information Science Education, Boston, Mass.
- Hsieh-Yee, I. and Lawton, P. (2015, June). *Crowdsourcing terms for CRRA portal themes*. Poster presented at the third CRRA symposium and annual meeting, Bringing the created toward the Creator: Liturgical art and design since Vatican II. Catholic Theological Union, Chicago, Illinois.
- Hsieh-Yee, I. and Lawton, P. (2015, February). *Crowdsourcing terms for thematic exploration in the Catholic Portal*. Poster presented at the 7th Annual Bridging the Spectrum Symposium, Washington, D.C.
- Hsieh-Yee, I., James, R., and Fagan-Fry, J. (2015, February). *Support for digital scholarship at top university libraries of the world*. Poster presented at the 7th Annual Bridging the Spectrum Symposium, Washington, D.C.
- Hsieh-Yee, I., Zhang, S., Lin, K., and Cherry, S. (2015, February). *Thus said the end users: Summon experience and support for research workflows*. Poster presented at the 7th Annual Bridging the Spectrum Symposium, Washington, D.C.
- Yontz, E., Hsieh-Yee, I., & Houston, S. (2015, February). *Healthy Heroes Summer Reading Club: Developing healthy youth at public libraries*. 11th Annual Jean Mills Health Symposium, Greenville, North Carolina.
- Yontz, E., Hsieh-Yee, I., and Houston, S. (2015, January). *Healthy youth and libraries: A pilot study*. Association for Library & Information Science Education (ALISE) Annual Conference, Chicago, Illinois.
- Hsieh-Yee, I. (2014, May). *Linking CRRA resources to portal themes via authority files*. Presented at the Catholic Research Resources Alliance 2014 Membership Meeting, Marquette, WI.
- Hsieh-Yee, I. (2014, April). *Enhancing subject access to CRRA resources*. Presented at the 2014 Catholic Library Association Conference, Pittsburgh, PA.
- Hsieh-Yee, I. (2014, January). *Health Information Technology Program: Educational entrepreneurship in action*. Presented at the 2014 annual Conference of the Association for Library and Information Science Education, Philadelphia, PA.
- Hsieh-Yee, I., Zhang, S., Lin, K., and Cherry, S. (2014, January). *Discovering information through Summon: An analysis of user search strategies and search success*. Paper presented at the 6th Bridging the Spectrum Symposium, Washington, D.C.

- Hsieh-Yee, I. (2012, December). *National Digital Stewardship Alliance and SLIS at CUA: An Educational Partnership*. Paper presented at Best Practices Exchange: Acquiring, Preserving, and Providing Access to Government Information in the Digital Era, Annapolis, MD
- Choi, Y. and Hsieh-Yee, I. (2010, January). *Finding Images in an OPAC: Analysis of User Queries, Subject Headings, and Description Notes*. Paper presented at 2nd Annual Bridging the Spectrum Symposium, Catholic University of America, Washington, D.C.
- Hsieh-Yee, I. and Coogan, J. (2010, January). *Google Scholar vs. Academic Search Premier: What Libraries and Searchers Need to Know*. Paper presented at 2nd Annual Bridging the Spectrum Symposium, Catholic University of America, Washington, D.C.
- Hsieh-Yee, I. (2009, November). *Information Science Education: An LIS School's Perspective*. Paper presented at Annual Meeting of the American Society for Information Science and Technology, Vancouver, British Columbia, Canada.
- Hsieh-Yee, I., Menard, E., Ya-Ning Chen, A., Shu-Jiun Chen, S., Kalfatovic, M. R., Wisser, K. M. (2009, November). *Information Organization in Libraries, Archives and Museums: Converging Practices and Collaboration Opportunities*. Presented at Annual Meeting of the American Society for Information Science and Technology, Vancouver, British Columbia, Canada. (Organizer and moderator of this panel.)
- Hsieh-Yee, I. and Coogan, J. (2009, July). *Catching up to Google Scholar: The Retrieval Power of Academic Search Premier and Google Scholar*. Poster presented at American Library Association Conference, Chicago, Illinois.
- Hsieh-Yee, I., with the CUA Scholarly Communications Project Team. (2009, January). *Digital Scholarship@CUA: Developing an Institutional Repository for CUA*. Poster presented at 1st Annual Bridging the Spectrum Symposium, Catholic University of America, Washington, D.C.
- Wise, M., Cylke, K., and Hsieh-Yee, I. (2009, January). *Digital Talking Books: Meeting the Needs of the Blind and the Handicapped*. Paper presented at the Bridging the Spectrum Symposium, Catholic University of America, Washington, D.C.
- Hsieh-Yee, I. (2009, January). *User Expectations of MERIC*. Presented at the Information Organization Competencies for the 21st Century Discussion Session of the 2009 Conference of the Association for Library and Information Science Education, Denver, Colorado.
- Choi, Y., and Hsieh-Yee, I. (2008, November). *Subject Access for Images in an OPAC*. Annual Meeting of the American Society for Information Science and Technology, Columbus, Ohio. (Also co-organized a panel on Retrieving and Using Visual Resources: Challenges and Opportunities for Research and Education.)

- Hsieh-Yee, I. (2008, June). *Educating Cataloging Professionals in a Changing Information Environment*. National Taiwan University, Taipei, Taiwan.
- Vellucci, S. L., Moen, W.E., Hsieh-Yee, I., Marson, B., and Wisser, K. (2008, January) *Building a Metadata Education and Research Community through MERIC (Metadata Education and Research Information Commons): Demo and Stakeholder Input*. A panel presented at the 2008 Conference of the Association for Library and Information Science Education, Philadelphia, Pennsylvania.
- Hsieh-Yee, I., Choi, Y. and Kules, B. (2007, October). *Searching for Books and Images in OPAC: Effects of LCSH, TOC and Subject Domains*. A poster presented at the American Society for Information Science and Technology Annual Meeting, Milwaukee, Wisconsin.
- Hsieh-Yee, I. and Coogan, J. (2007, August) *Google Scholar vs. Academic Search Premier: A Comparative Analysis*. Presented to the Faculty and Staff of the University of the District of Columbia.
- Hsieh-Yee, I. and Coogan, J. (2007, June). *Google Scholar vs. Academic Search Premier: A Comparative Analysis*. Presented to the Washington Research Library Consortium Community, Catholic University of America, Washington, D.C.
- Hsieh-Yee, I., Choi, Y., and Kules, B.. (2007, June). *What Users Need for Subject Access: Table of Contents or Subject Headings?* A poster presented at the 2007 American Library Association Annual Conference, Washington, D.C., June 2007.
- Choi, Y., Hsieh-Yee, I., and Kules, B. (2007, June). *Retrieval Effectiveness of TOC and LCSH*. A paper presented at the Joint Conference on Digital Libraries 2007, Vancouver, Canada.
- Vellucci, S. L., Hsieh-Yee, I., and Moen, W.E. (2007, May). *If We Build It, Will They Come? Building a Community of Practice for Metadata Stakeholders*. A poster presented at the Rutgers University Research Day, Bridgeton, New Jersey.
- Hsieh-Yee, I. (2007, May). *Federated Searching: User Experience & Perceptions*. International Conference on Information Organization & Retrieval, National Taiwan University, Taipei, Taiwan.
- Hsieh-Yee, I. (2007, May). *Search Performance of Google Scholar and Academic Search Premier*. International Conference on Information Organization & Retrieval, National Taiwan University, Taipei, Taiwan.
- Hsieh-Yee, I. (2007, May) *MERIC: Building a Digital Commons for Metadata Education & Research*. International Conference on Information Organization & Retrieval, National Taiwan University, Taipei, Taiwan.

- Hsieh-Yee, I., and Coogan, J. (2007, March/April). *A Comparative Analysis of Google Scholar and Academic Search Premier*. Poster presented at the Association of College & Research Libraries 13th National Conference, Baltimore, Maryland.
- Vellucci, S. L. and Hsieh-Yee, I. (2007, March/April) *They Didn't Teach Me That in Library School! Building a Digital Teaching Commons to Enhance Metadata Teaching, Learning and Research*. On-site presentation and Webcast by Elluminate. A contributed paper presented at the Association of College & Research Libraries 13th National Conference, Baltimore, Maryland. The acceptance rate for contributed paper was 20%. This paper was one of 10 conference papers chosen for live webcast during the conference.
- Moen, W., Hsieh-Yee, I. and Vellucci, S.L. (2007, January) *A DSpace Foundation for a Teaching & Research Commons: The Metadata Education and Research Information Commons*. A poster session presented at the Open Repositories Conference 2007, San Antonio, Texas.
- Tang, R., Hsieh-Yee, I., and Zhang, S. (2006, November) *User Perception of MetaLib Combined Search*. Paper presented at the Annual Meeting of the American Society for Information Science and Technology, Austin, Texas, Nov. 2006.
- Hsieh-Yee, I. (2006, November). *Federated Searching: User Perceptions, System Design, and Library Instructions*. Paper presented at the Annual Meeting of the American Society for Information Science and Technology, Austin, Texas. (Panel organizer, moderator, presenter).
- Hsieh-Yee, I. (2006, November). *Building a Digital Teaching Commons to Enhance Teaching and Learning: The MERIC Experience and Challenges*. Paper presented at the Annual Meeting of the American Society for Information Science and Technology, Austin, Texas. (Panel organizer, moderator, presenter)
- Hsieh-Yee, I. (2006, September). *Search Performance of Google Scholar and Academic Search Premier*. Paper presented at the ERIC Publishers Meeting, Washington, D.C.
- Hsieh-Yee, I., Zhang, S., and Rong Tang, R. (2006, June). *User Perceptions of a Federated Search System*. Poster presented at Joint Conference on Digital Libraries, Chapel Hill, North Carolina.
- Hsieh-Yee, I. and Zhang, S. (2006, June). *Preparing Users for Federated Search: Implications of a MetaLib User Perceptions Study*. Paper presented at the 2006 Ex Libris User Groups of North America Conference, Knoxville, Tennessee.
- Hsieh-Yee, I. (2006, January). *MERIC Organizations and Navigation*. Paper presented at the 2006 ALISE Annual Conference, San Antonio, Texas.

- Hsieh-Yee, I. (2006, January). *Metadata and Cataloging Education: Recommended Competencies*. Paper presented at the 2006 ALISE Annual Conference, San Antonio, Texas.
- Hsieh-Yee, I. (2005, November). *Digital Library Evaluation: Progress & Next Steps*. Presentation at the Annual Meeting of the American Society for Information Science & Technology, Charlotte, North Carolina.
- Hsieh-Yee, I. (2005, August). *Providing Access to Digital Content: Issues for DL Managers*. Presentation at MDK12 Digital Library Steering Committee Meeting, Columbia, Maryland.
- Hsieh-Yee, I. (2005, April). *Enhancing Teaching and Learning: The Role of School Library Media Specialists*. Presentation at Meeting of the Baltimore County Public School System School Media Specialists, Baltimore, Maryland.
- Hsieh-Yee, I. (2005, January). *Subject Access and Users: Insights & Inspirations from Marcia J. Bates*. Paper presented at the Historical Perspectives SIG, 2005 Conference of the Association for Library and Information Science Education, Boston, Massachusetts.
- Hsieh-Yee, I. (2005, January). *Electronic Resource Management: Practice, Employer Expectations, & CE Interests*. Paper presented at Technical Services Education SIG, 2005 Conference of the Association for Library and Information Science Education, Boston, Massachusetts.
- Hsieh-Yee, I. (2004, October). *Library Professionals for the Digital Age: Competencies & Preparation*. Paper presented at Bibliographic Access Management Team meeting, Library of Congress, Washington, D.C.
- Hsieh-Yee, I. (2004, January). *Cataloging and metadata expertise for the digital era*. Presented at Preparing 21st Century Cataloging and Metadata Professionals: A Workshop for Educators and Trainers, San Diego and sponsored by ALCTS, ALISE, LC, and OCLC.
- Hsieh-Yee, I. (2004, January). *Educating catalogers for the digital era*. Paper presented at the Technical Services SIG, 2004 Conference of the Association for Library and Information Science Education, San Diego.
- Hsieh-Yee, I. (2003, July). *Cataloging Education for the 21st Century*. A presentation at the Library of Congress, Washington, D.C.
- Hsieh-Yee, I. (2002, January) *Metadata Education and Research Priorities: A Delphi Study of Metadata Experts*. Presentation at the 2002 Conference of the Association for Library and Information Science Education, New Orleans.

- Hsieh-Yee, I. (2001, November). *A Delphi Study of Metadata: Preliminary Findings*. Poster session at the 2001 Annual Meeting of the American Society for Information Science & Technology, Washington, D.C.
- Hsieh-Yee, I. (2001, June). *Resources on Asian American Children: Analysis of Retrieval by Search Engines and WorldCat*. Presentation at the National Conference on Asian Pacific American Librarians, San Francisco.
- Hsieh-Yee, I. (2001, January). *Delphi Study on Metadata: Project Design*. Presentation at Research Awards Session, Association for Library & Information Science Education, Washington, D.C.
- Hsieh-Yee, I. (2000, May). *Web Search Behavior Research: Progress and Implications*. Presentation at the Symposium on Evaluating Library and Information Science Research, University of Wisconsin-Madison, Madison, Wisconsin.
- Hsieh-Yee, I. (2000, March). *ERIC User Services: Evaluation in a Decentralized Environment*. Presentation at the National ERIC Joint Directors/Technical Meeting, Arlington, Virginia.
- Hsieh-Yee, I. (2000, January). *Enhancing Learning with Web Technology*. Presentation at Faculty Conversations, Catholic University of America, Washington, D.C.
- Hsieh-Yee, I. (2000, January). *From Surrogates to Objects: CUA's Approaches to Organizing Electronic Resources*. Paper presentation at the Annual Conference of the Association for Library and Information Science Education, San Antonio, Texas.
- Yee, P., and Hsieh-Yee, I. (1997, November). *Individual Differences in Search Behavior on the WWW*. A poster session presented at the 38th Annual Meeting of the Psychonomic Society, Philadelphia, Pennsylvania.
- Hsieh-Yee, I. (1997, April). *Research + Marketing + Preparation = Job!* Presented at the "Workshop on Resume and Interview Techniques," Special Libraries Association, Student Chapter, Catholic University of America, Washington, D.C.
- Hsieh-Yee, I. (1997, February). *Creating CyberCatalogers: Education and Training*. Presentation at ALA's Midwinter Meeting, Washington, D.C.
- Hsieh-Yee, I. (1997, February). *Search Tactics of Web Users in Searching for Texts, Graphics, Known Items and Subjects: A Search Simulation Study*. Presented at the Conference of the Association for Library and Information Science Education, Washington, D.C.
- Hsieh-Yee, Ingrid. "Beginning Your Special Library/Information Center Career." Presented at SLA's "Career Day," Jan. 11, 1997, Catholic University of America.

Hsieh-Yee, I. (1996, September). *The Roles of Library and Information Scientists in Managing Electronic Information*. Presentation at Hamilton College, Clinton, New York.

Hsieh-Yee, I. (1996, May). *The Future of Cataloging as a Profession*. Presented at "The Cataloging Forum, Library of Congress, Washington, D.C.

Hsieh-Yee, I. (1994, October). *The Impact of the Internet on OPACs*. Presented at the Third Workshop on User Interfaces for OPACs, Library of Congress, Washington, D.C.

Reports

Hsieh-Yee, I., with Knowledge Management Competencies and Performance Action Group of the Federal Knowledge Management Initiative. "From Knowledge Management Competencies to Improved Organizational Performance." April 9, 2009.

Hsieh-Yee, I., with Knowledge Practices Action Group of the Federal Knowledge Management Initiative. "KM Practice in Government Agencies: Findings and Recommendations." April 9, 2009.

Hsieh-Yee, I. "Delphi Study on Metadata." 2001. Three quarterly reports submitted to the Association for Library and Information Science Education.

Hsieh-Yee, I. "College Students' Information Channels: Patterns of Use and Possible Factors in Channel Selection." 1995. Submitted to the Catholic University of America.

Hsieh-Yee, I. "The Information-Seeking Patterns of Scholars and Their Use of an Online Information System." 1994. Submitted to the Council on Library Resources.

Book Reviews

Review of *The Measurement and Evaluation of Library Services*, by Sharon L. Baker and F. Wilfrid Lancaster. *Information Processing and Management* 30 (1994): 450-52.

Review of *Subject Access to Films and Videos*, by Sheila S. Intner and William E. Studwell; and *Cataloging Unpublished Nonprint Materials*, by Verna Urbanski with Bao Chu Chang and Bernard L. Karon. *Information Processing and Management* 30 (1994): 449-50.

Review of *Automated Information Retrieval in Libraries: A Management Handbook*, by Vicki Anders. *Journal of Library and Information Science* 19 (1993): 98-100.

Review of *Full Text Databases*, by Carol Tenopir and Jung Soon Ro. *Information Processing and Management* 28 (1992): 667-68.

Review of *Descriptive Cataloging for the AACR2R And USMARC: A How-to-Do It Workbook*, by Larry Millsap and Terry Ellen Ferl. *Information Processing and Management* 28 (1992): 809-11.

Review of *MARC Manual: Understanding and Using MARC Records*, by Deborah J. Byrne. *Information Processing and Management* 28 (1992): 537-38.

Service

Professional Associations and Societies

- Library of Congress. RDA Training Program for the Profession. Co-authored with Tim Carlton. 2013-2014.
- 2014 Digital Preservation Outreach & Education Survey. Contributed to the design of the survey, 2014.
- National Digital Stewardship Alliance. Outreach Committee. 2011-2014.
- National Digital Stewardship Residency Program. Advisory Group, 2012-2013.
- FEDLINK Health Information Technology Advisory Council, 2011-2015.
- 2012 Joint Conference on Digital Libraries. Program Planning Committee, Pre-Conference Proposals Review Committee, 2012
- Catholic Research Resources Alliance. Five-Year Strategic Plan Task Force, 2011-2012
- Institute of Museum and Library Services. Grant reviewer. 2004, 2005, 2010.

- Association for Library and Information Science Education.
 - * ALISE Bodan Wynar Research Paper Award Committee, 2015, 2016, 2017
 - * ALISE Eugene Garfield Dissertation Award Competition, Jury, 2013, 2014
 - * ALISE Research Grant Competition Committee. Chair, 2012
 - * Pratt-Severn Faculty Innovation Award. Chair, 2009, 2010
 - * ALISE Doctoral Poster Jury, 2012
 - * “Information Organization Competencies for the 21st Century” Discussion session leader. 2009 Conference of the Association for Library and Information Science Education.
 - * Assisted Technical Services SIG Convener in organizing a program, “Building a Metadata Education and Research Community through MERIC (Metadata Education and Research Information Commons): Demo and Stakeholder Input” for the 2008 ALISE conference.
 - * Association for Library Collections and Technical Services/Association for Library and Information Science Education (ALCTS/ALISE) Metadata Education and Research Information Center (MERIC) Advisory Board, Co-Chair (with Sherry Vellucci), 2005-2007. Chair, 2008-2009 (leading the effort to build MERIC, a repository and collaborative space for metadata educators, practitioners, and researchers)
 - * Technical Services SIG, Convener, 2004-2005. Organized a program on “Electronic Resources Management: Current Practices, Employer Expectations, and Teaching Strategies” for the 2005 conference in Boston, Massachusetts.

- * Technical Services SIG, Convener, 2003-2004. Organized a program on “Organizing Information with Metadata: Desired Competencies and Teaching Innovations” for the 2004 conference.
 - * Technical Services SIG, Convener, 1999-2000. Organized a program on "Teaching the Organization of Electronic Resources" for the 2000 conference.
 - * Curriculum SIG, Co-convener (with Sibyl Moses), 1996-97. Organized a program on “Government Information Policy” for the 1997 conference.
- American Society for Information Science & Technology.
- * Reviewer, Conference program panel submissions and poster submissions, 2005, 2006, 2007, 2009, 2011, 2012, 2013, 2014, 2015, 2016, 2017
 - * Nomination Committee, 2009-2011
 - * Information Science Education Special Interest Group. American Society for Information Science and Technology. Chair-Elect, 2007-2008. Chair 2008-2009.
 - * Committee on Information Science Education. 1999-2006.
 - * Committee on Information Science Education. Organizing Committee for an orientation program for students at ASIS annual meetings, 1999-2001
 - * Committee on Information Science Education. Sub-committee on Student Welfare (focusing on issues related to master's education), 1998-2001
 - * SIG ED. Organizing Committee for the "Seminar on Research and Career Development" for junior researchers. 1995-96 (chair), 1997-2001
 - * ISI Doctoral Dissertation Proposal Scholarship Jury, 1997; 2001, 2002
 - * Pratt-Severn Best Student Research Paper Award Jury. Chair. 1997
 - * 1998 Midyear Meeting (referee of contributed papers), 1997
 - * Organizer and moderator of the ASIS Doctoral Forum and the Doctoral Research Seminar 1994-1995
 - * SIG Human Computer Interaction. Chair-Elect, Chair, 1993-1995
 - * Doctoral Forum Award Jury, 1995
 - * Best Student Paper Award Jury, 1995
- American Library Association.
- * Committee on Accreditation, External Review Panelist, 2009- (site visiting team 2013-2014; site visiting team 2016-2017)
 - * Association for Library Collections and Technical Services Task Force on Competencies and Education for a Career in Cataloging, member, 2008-2009
 - * Facilitator for “What They Don't Teach in Library School: Competencies, Education and Employer Expectations for a Career in Cataloging,” an Association for Library Collections and Technical Services Preconference, June 22, 2007 in Washington, D.C. Also a local liaison for bringing this program to the Catholic University of America.
 - * Facilitator for a discussion on "Effect of Electronic Resources on Technical Services" at ALA's Midwinter Meeting held in Feb. 1997 in Washington, D.C.
 - * International Relations Committee, Subcommittee Task Force for IFLA and China, 1994-1997

- Virginia Association of School Librarians. Scholarships and Awards Committee. 2010-2012
- Federal Knowledge Management Initiative, Knowledge Management Practices Action Group. Member. 2009 (leading the effort to build a knowledge management repository)
- Federal Knowledge Management Initiative, Knowledge Management Competencies & Learning Action Group. Member. 2009 (developing an action plan for helping government knowledge workers and government agencies to develop knowledge management competencies)
- National Center for Education Statistics. Technical Review Panel. 2008.
- External evaluator for a case of promotion to full professorship. University of Tennessee. 2008.
- National Information Standards Organization (NISO). Advisory Board, Revision of “IMLS Framework of Guidance for Building Good Digital Collections,” 2004, 2007.
- Library of Congress, Bibliographic Control of Web Resources: A Library of Congress Action Plan. Principal Investigator of Action Item 5.1, focusing on cataloging and metadata education for students and new librarians, 2002-2003. (worked with the Association for Library Collections and Technical Services, Education Task Force)
- Chinese American Librarians Association
 - * Chinese American Librarians Association Outstanding Library Leadership Award in Memory of Dr. Margaret Chang Fung, Award Committee, 2016-
 - * Achievement Award Jury, 2000-2001
 - * CALA Goal 2000 Task Force, 1997
 - * Scholarship Committee, 1995, 1996-1997 (chair)
 - * Board of Directors, 1994-1997
 - * Publication Committee, 1993-1995
 - * International Relations Committee, 1993-1996
- SailorSM Assessment Advisory Group (An impact study of Sailor, Maryland's Public Information Network), 1995
- Editorial boards
 - Journal of Library and Information Science. Editorial Board, 2012-
 - Chinese American Librarians Association, *Occasional Papers Series*. Editorial Board, 2009-2016.
 - Library Quarterly*. Editorial Board, 2003-2008
 - Bulletin of the Medical Library Association*, 1994-97
 - Newsletter editor for the Chinese American Librarians Association, 1989-92
- Referee for the following journals
 - Information Processing and Management*
 - Journal of Digital Information*
 - Journal of Education for Library and Information Science*
 - Journal of Information Science*

Journal of Library & Information Science
Journal of Library Metadata
Journal of the American Society for Information Science & Technology
Library and Information Science Research
Library Quarterly

- Expert reviewer, “Digital Library” course, Evaluation module, University of North Carolina, Chapel Hill, 2007-2008.
- Expert reviewer, “Information Organization” course, University of Michigan, Ann Arbor. 2007.

Catholic University of America

- School of Arts & Sciences, Committee on Appointments and Promotions, 2015-2019
- School of Arts & Sciences, Academic Council, 2015-2016.
- School of Arts & Sciences, Ordinary Professor Group, 2013-
- President’s Administrative Council, 2010-2012
- Deans’ Council, 2010-2012
- Academic Leadership Group, 2010-2012
- Academic Senate, 2003-2012
- Academic Senate, Committee on Committees and Rules, 2009-2012
- Academic Senate, Committee on Appointments and Promotions, 2005-2008
- Graduate Board, 2010-2012
- CUA Scholarly Communication Project Team, Member (2007), Chair, 2008-2009
- Academic Senate Library Committee, Interim Chair (2007), Member, 2008-2012
- Doctoral Dissertation Defense Committee, Chair, Dept. of Education, 2014, 2015
- Doctoral Dissertation Defense Committee, Chair, School of Nursing, 2006, 2008
- Dean Search Committee, 1992-1994, 1998-1999, 2002-2003, 2006-2007
- Fulbright Review Panel, 2006
- Academic Senate Committee on Computing, 1995-2003
- CUA Service Learning Advisory Board, 2001-2002
- CUA Faculty Conversations on Enhancing Teaching and Learning through Technology, Planning Group, 1999-2001
- CUA Initiative on Technology and Teaching, 1998-2001

Dept. of Library and Information Science

- Accreditation presentation, Chair, June 2015-August 2016
- Interim Co-Chair, June 2015-August 2016.
- Appointments and Promotions Committee, 1991-
- Blended Learning Committee, spring 2016-
- Colloquium and Symposium Planning Committee, fall 2016-
- Scholarship Committee, fall 2016-

- Technology Committee, fall 2016-
- Comprehensive examination editor, 2016-2017
- LIS Advisory Board, 2015-2016 (chair); fall 2016 (member)
- Committee on Planning and Assessment, 2015-2016 (chair)
- Admissions Committee, 2007-2009, Chair 2010-2012, Member 2013-2015
- Senior Faculty Committee, 2014-2016.
- Accreditation Steering Committee, 2014-2016 (Chair, 2015-2016)
- Accreditation Students Standard Committee, co-chair, 2014-2016
- Accreditation Mission, Goals, and Objectives Standard Committee, co-chair, 2014-2016
- Accreditation Curriculum Standard, member 2014-2-16
- Accreditation Administration and Finance Standard, member 2014-2016
- Cultural Heritage Information Management Project (IMLS-funded), Co-PI, 2012-2015
- Cultural Heritage Information Management Forum (scheduled for June 2015), Co-Organizer, 2013-2015
- Health Information Technology Interim Review Committee, 2015 (chair)
- Health Sciences Librarianship Advisory Group, 2015- (chair)
- Comprehensive examination editors, 2013-2014, 2016-2017
- National Digital Stewardship Alliance liaison, 2011-2014
- Advisory Board, Chair 2010-2012
- Academic Honesty Committee, Chair, 2008-2012
- Blended Learning Committee, 2010-2012
- Colloquium Committee, 2010-2012
- Comprehensive Examination Administration, 2010-2012
- Cultural Heritage Information Management Advisory Committee, 2010-2012 (chair), 2013-
- Curriculum Committee, 1991-2003, 2007-2009, Chair 2010-2012, member 2013-
- Curriculum Subcommittee on Comprehensive Examination, Chair 2009-2012
- Health Information Technology Advisory Board, Chair 2010-2012. Member 2013-
- Health Sciences Advisory Committee, 2009, Chair 2010-2012. Member 2013-
- HIT Expert Forum, Chair 2012. Member 2013-
- Health Information Technology Student Group Advisor, 2011-2012
- State Council for Higher Education of Virginia, SLIS Representative, 2010-2012
- Symposium Planning Committee, 2010-2012
- Website Management Team, Chair, 2010-2012
- Urban School Librarianship Project (IMLS-Funded), PI, 2007-2011 (chair, 2010-11)
- Failing Grades Committee, 1995-1997 (chair), 2000-2001 (chair), 2004-2005 (chair), 2007 (chair)-2011
- Faculty Search Committee, 1994-1998, 2002-2004, 2006 (chair), Fall 2007-2009, Chair fall 2009-2012
- Recruitment Committee, Chair 2010-2012
- Strategic Planning Committee, Chair 2010-2012
- Technology Committee, 2010-2012
- Accreditation Advisory Committee, 2007-2009

- Accreditation Coordinating Committee, 2007-2009
- Accreditation Steering Committee, 2007-2009
- SLIS Advisory Group, 2007-2009
- Accreditation Curriculum Standard Committee, Co-chair, 2007-2009
- Accreditation Faculty Standard Committee, Co-chair, 2007-2009
- LSC 551 Information Organization Review Team, Co-chair, 2008-2009, 2015-2016.
- Curriculum Subcommittee on Portfolios, 2009
- LSC 555 Information Systems in Libraries and Information Centers Review Team, contributor, 2008-2009
- Redesign of LSC 730 Use and Users of Libraries and Information. 2009-
- Development of a metadata institute that was taught as LSC 715 Organization of Internet Resources in 2008. The institute is being revised and will be offered in 2010 under a new course title.
- Development of lesson plans, assignments, and evaluation rubrics for LSC 606, Cataloging and Classification, for the School's NCATE accreditation. 2008
- Howard and Mathilde Rovelstad Scholarship Committee, Chair, 2004-2007
- Assistant Dean Search Committee, Chair, Fall 2007
- Liaison to the Association for Library Collections and Technical Services to bring its preconference program, Cataloging Education and Employer Expectations, to CUA during the 2007 American Library Association Annual Meeting in Washington, D.C.
- Organizer of the colloquium presentation and reception for Tamar Sadeh of Ex Libris on PRIMO June 2007
- Practicum review and design (work with potential supervisors, such as the American Indian Museum internship description revision) 2006-
- Comprehensive examinations (edits, proctoring, and grading), 1990-
- SLIS Web site redesign: Comments and suggestions. Fall 2007
- Conducted surveys of current students and alumni in preparation for the 2005 re-accreditation, 2004-2005
- Student advisement, 1990-
- Technology Committee, 1992-1999 (chair, 1996-1998), 2002-2003 (member)
- Colloquia Committee 1997-1999, 2002-2003.
- Advisor of the CUA Student Chapter of the American Society for Information Science and Technology, 2002-2003
- Visiting Professor Search Committee, 1999, 2000, 2001
- Leader, Participation in the CORC experiment, 1999-2000
- Advisor of the Special Libraries Association Student Chapter, 1993-1999; the group was recognized for outstanding leadership by SLA in 1999.
- COA planning Committee, Task Force on Electronic Presentation of SLIS Reports (team leader) 1997-1998
- COA Planning Committee, Subcommittee on Technology 1996-1998
- NLM practicum coordinator, 1997-1998
- Computer Literacy Workshops: Assisted with the development and evaluation of the workshops, 1996-1998
- Leader, Participation in the InterCat project, 1995-1997

APPENDIX B

[Library of Congress](#) >> [MARC](#) >> [Understanding MARC](#)

MARC 21 Reference Materials

[Part VII: A Summary of Commonly Used MARC 21 Fields](#)

[Part VIII: A List of Other Fields Often Seen in MARC Records](#)

[Part IX: The Leader](#)

[Part X: Field 008 for Books](#)

Part VII:

A Summary of Commonly Used MARC 21 Fields

This is a summary of the MARC 21 tags used most frequently by libraries in entering their own bibliographic records. For full listings of all MARC 21 tags, indicators, and subfield codes, see *MARC 21 Format for Bibliographic Data*.

In the explanations on these pages:

Tags -- The tags (3-digit numbers) are followed by the names of the fields they represent. In this summary, and in the *MARC 21 Format for Bibliographic Data*, if a tag can appear more than once in one bibliographic record, it is labeled repeatable (R). If it can only be used once, it is labeled non-repeatable (NR). For example, a catalog record can have several subjects, so the tags for subject added entries (6XX) are labeled repeatable (R).

Indicators -- The use of indicators is explained in fields where they are used. Indicators are one-digit numbers. Beginning with the 010 field, in every field -- following the tag -- are two character positions, one for Indicator 1 and one for Indicator 2. The indicators are not actually defined in all fields, however. And it is possible that a 2nd indicator will be used, while the 1st indicator remains undefined (or vice versa). When an indicator is undefined, the character position will be represented by the character # (for blank space).

Subfield codes -- All the data in each field (beginning with the 010 field) is divided into subfields, each of which is preceded by a delimiter-subfield code combination. The most common subfield codes used with each tag are shown. Each subfield code is preceded by the character \$, signifying a delimiter. The name of the subfield follows the code.

In general, every field MUST have a subfield 'a' (\$a). One exception that is often seen is in Field 020 (ISBN), when the ISBN information (subfield \$a) is unavailable but the price (subfield \$c) is known. Some subfields are repeatable. In this summary, repeatability is noted for only the more common repeatable subfields.

Examples: Examples follow the explanation for each field. For clarity, one space has

been placed between the tag and the first indicator, one space has been placed between the second indicator and the first delimiter- subfield code, and one space has been inserted between the delimiter-subfield code and the subfield data.

010 Library of Congress Control Number -- (LCCN)
(NR, or Not Repeatable)

Indicators undefined.

Subfield used most often:

\$a -- Library of Congress control number

Example: 010 ## \$a ###86000988#

020 International Standard Book Number -- (ISBN)
(R, or Repeatable)

Indicators undefined.

Subfields used most often:

\$a -- International Standard Book Number

\$c -- Terms of availability (often a price)

\$z -- Cancelled/invalid ISBN (R)

Example: 020 ## \$a 0877547637

040 Cataloging source -- (NR)

Indicators undefined.

Subfields used most often:

\$a -- Original cataloging agency

\$c -- Transcribing agency

\$d -- Modifying agency (R)

Example: 040 ## \$a DLC
 \$c DLC
 \$d gwhs

100 Main entry -- Personal name -- (primary author)
(NR; there can be only one main entry)

Indicator 1: Type of personal name entry element

- 0 -- Forename
- 1 -- Surname (this is the most common form)
- 3 -- Family name

Indicator 2 undefined.

Indicator 2 became obsolete in 1990. Older records may display 0 or 1

Subfields used most often:

- \$a** -- Personal name
- \$b** -- Numeration
- \$c** -- Titles and other words associated with a name (R)
- \$q** -- Fuller form of name
- \$d** -- Dates associated with a name (generally, year of birth)

Example: 100 1# \$a Gregory, Ruth W.
 \$q (Ruth Wilhelme),
 \$d 1910-

130 Main entry -- Uniform title -- (NR)*Indicator 1:* Nonfiling characters

- 0-9 -- Number of nonfiling characters present (for initial articles, including spaces)

Indicator 2 undefined.

Indicator 2 became obsolete in 1990. (See 100 above.)

Subfields used most often:

- \$a** -- Uniform title
- \$p** -- Name of part/section of a work (R)
- \$l** -- Language of a work
- \$s** -- Version
- \$f** -- Date of a work

Example: 130 0# \$a Bible.
 \$p O.T.
 \$p Psalms.

240 Uniform title (NR)*Indicator 1:* Uniform title printed or displayed

- 0 -- Not printed or displayed
- 1 -- Printed or displayed (most common)

Indicator 2: Nonfiling characters

0-9 -- Number of nonfiling characters present (for initial articles, including spaces)

Subfields used most often:

\$a -- Uniform title
\$l -- Language of a work
\$f -- Date of a work

```
Example:    240 10 $a Ile mystérieuse.
            $l English.
            $f 1978
```

245 Title Statement (NR)

Indicator 1: Title added entry

(Should the title be indexed as a title added entry?)

0 -- No title added entry

(indicates a title main entry; i.e. no author is given)

1 -- Title added entry

(the proper indicator when an author given in 1XX; the most common situation)

Indicator 2: Nonfiling characters

0-9 -- Number of nonfiling characters present, including spaces; usually set at zero, except when the title begins with an article; e.g., for *The robe*, the second indicator would be set to 4. The letters *T*, *h*, *e*, and the space following them are then ignored in alphabetizing titles. The record will be automatically filed under "*r*" -- for *Robe*.

Subfields used most often:

\$a -- Title proper
\$h -- Medium (often used for non-book media)
\$p -- Name of part/section of a work (R)
\$b -- Reminder of title (subtitles, etc.)
\$c -- Remainder of title page transcription/Statement of responsibility

```
Example:    245 14 $a The DNA story :
            $b a documentary history of gene
            cloning /
            $c James D. Watson, John Tooze.
```

246 Varying form of title (R)

Indicator 1: Note/title added entry controller

- 1 -- Note, title added entry
- 3 -- No note, title added entry

Indicator 2: Type of title

- # -- No information provided
- 0 -- Portion of title
- 1 -- Parallel title
- 4 -- Cover title
- 8 -- Spine title

Subfield used most often:

- \$a** -- Title proper

Example: 246 3# \$a Four corners power review

250 Edition statement (NR)*Indicators undefined.**Subfield used most often:*

- \$a** -- Edition statement

Example: 250 ## \$a 6th ed.

260 Publication, distribution, etc. (Imprint) (R)*Indicator 1: Sequence of publishing statements*

- # -- No information provided

*Indicator 2: Undefined**Subfields used most often:*

- \$a** -- Place of publication, distribution, etc. (R)
- \$b** -- Name of publisher, distributor, etc. (R)
- \$c** -- Date of publication, distribution, etc. (R)

Example: 260 ## \$a New York :
 \$b Chelsea House,
 \$c 1986.

300 Physical description (R)

Indicators undefined.

Subfields used most often:

\$a -- Extent (number of pages) (R)

\$b -- Other physical details (usually illustration information)

\$c -- Dimensions (cm.) (R)

\$e -- Accompanying material (for example, "teacher's guide" or "manual")

Example: 300 ## \$a 139 p. :
 \$b ill. ;
 \$c 24 cm.

440 Series statement / Added entry--Title

This field was made obsolete in 2008 to simplify the series statement. See 490 and 830.

490 Series statement (No added entry is traced from field) (R)

Indicator 1: Specifies whether series is traced (whether an 8XX tag is also present)

0 -- Series not traced

1 -- Series traced (8XX is in record)

Indicator 2 undefined.

Subfield used most often:

\$a -- Series statement (R)

\$v -- Volume number (R)

Example: 490 1# \$a Colonial American craftsmen

500 General note (R)

Indicators undefined.

Subfield used most often:

\$a -- General note (Used when no specialized note field has been defined for the information. Examples: Notes regarding the index; the source of the title; variations in title; descriptions of the nature, form, or scope of the item.)

Example: 500 ## \$a Includes index.

504 Bibliography, etc. note (R)


```

$z Rome
$v Congresses .

```

Notice that subfields \$v, \$x, and \$z in the 600 field are repeatable. Subfields \$v, \$x, \$y, and \$z do not have to be in alphabetical order. They will be in the order prescribed by the instructions given by the subject heading system.

610 Subject added entry -- Corporate name (R)

Indicator 1: Type of corporate name entry element

- 0 -- Inverted name (not used with AACR2)
- 1 -- Jurisdiction name
- 2 -- Name in direct order

Indicator 2: Subject heading system/thesaurus.

See indicator 2 under 600

Subfields used most often:

- \$a** -- Corporate name or jurisdiction name as entry element
- \$b** -- Subordinate unit (R)
- \$v** -- Form subdivision (R)
- \$x** -- General subdivision (R)
- \$y** -- Chronological subdivision (R)
- \$z** -- Geographic subdivision (R)
- \$2** -- Source of heading or term (used with 2nd indicator of 7)

```

Example:      610 10 $a United States.
                $b Army Air Forces
                $v Biography.

```

650 Subject added entry -- Topical term (Most subject headings fit here.) (R)

Indicator 1: Level of subject

- # -- No information provided

Indicator 2: Subject heading system/thesaurus

(identifies the specific list or file which was used)

- 0 -- Library of Congress Subject Headings
- 1 -- LC subject headings for children's literature
- 2 -- Medical Subject Headings
- 3 -- National Agricultural Library subject authority file
- 4 -- Source not specified
- 5 -- Canadian Subject Headings
- 6 -- Répertoire de vedettes-matière
- 7 -- Source specified in subfield \$2

700 Added entry -- Personal name (R)*Indicator 1:* Type of personal name entry element

- 0 -- Forename
- 1 -- Surname (this is the most common form)
- 3 -- Family name

Indicator 2: Type of added entry

- # -- No information provided (most common; co-authors, editors, etc.)
- 2 -- Analytical entry (The values for Indicator 2 changed in 1994 with Format Integration, and older records may display additional values. An analytical entry involves an author/title of an item contained in a work.)

Subfields used most often:

- \$a** -- Personal name
- \$b** -- Numeration
- \$c** -- Titles and other words associated with a name (R)
- \$q** -- Fuller form of name
- \$d** -- Dates associated with a name (generally, year of birth)
- \$e** -- Relator term (such as ill.) (R)
- \$4** -- Relator code (R)

Example: 700 1# \$a Baldridge, Letitia.

710 Added entry -- Corporate name (R)*Indicator 1:* Type of corporate name entry element

- 0 -- Inverted name (not used with AACR2)
- 1 -- Jurisdiction name
- 2 -- Name in direct order

Indicator 2: Type of added entry.

- See Indicator 2 under 700
- # -- No information provided
- 2 -- Analytical entry

Subfields used most often:

- \$a** -- Corporate name or jurisdiction name as entry element
- \$b** -- Subordinate unit (R)

Example: 710 2# \$a Sunburst Communications (Firm)

740 Added entry -- Uncontrolled related/analytical title (R)*Indicator 1:* Nonfiling characters

\$v -- Volume number

Example: 830 #0 \$a Railroads of America (Macmillan)

[[Back to Top of Page](#)]

Part VIII:

A List of Other Fields Often Seen in MARC Records

001	Control number
003	Control number identifier
005	Date and time of latest transaction
006	Fixed-length data elements -- additional material characteristics
007	Physical description fixed field
008	Fixed length data elements (See Part X)
022	International Standard Serial Number (ISSN)
037	Source of acquisition
041	Language code
043	Geographic area code
050	Library of Congress call number
060	National Library of Medicine call number
082	Dewey Decimal classification number (the one recommended by the Library of Congress; locally-assigned call numbers may appear elsewhere)
110	Main entry -- Corporate name (less frequent under AACR2 rules)
256	Computer file characteristics
263	Projected publication date (indicates a CIP -- Cataloging in Publication -- record)
306	Playing time
508	Creation/production credits note
510	Citation/references note (review sources)
511	Participant or performer note
521	Target audience note (first indicator: 0 = reading grade level, 1 = interest age level, 2 = interest grade level, 3 = special audience characteristics, 4 = motivation interest level)
530	Additional physical form available note
538	System details note
586	Awards note
656	Index term -- Occupation
730	Added entry -- Uniform title
852	Location

- 856 Electronic location and access
 9XX Reserved for local use. (They are used by vendors, systems, or individual libraries to exchange additional data)

[[Back to Top of Page](#)]

Part IX:

The Leader

There are 24 positions in the Leader, numbered from 00 to 23. For fuller explanation, see the *MARC 21 Format for Bibliographic Data*.

- 00-04 Record length (calculated by the computer for each record)
 05 Record status
 a = increase in encoding level
 c = corrected or revised
 d = deleted
 n = new
 p = increase in encoding from prepublication (previous CIP)
 06 Type of record
 a = language material
 c = printed music
 d = manuscript music
 e = cartographic material
 f = manuscript cartographic material
 g = projected medium
 i = nonmusical sound recording
 j = musical sound recording
 k = 2-dimensional nonprojectable graphic
 m = computer file
 o = kit
 p = mixed materials
 r = 3-dimensional artifact or naturally occurring object
 t = manuscript language material
 07 Bibliographic level
 a = monographic component part
 b = serial component part
 c = collection
 d = subunit
 i = integrating resource
 m = monograph/item
 s = serial
 08 Type of control
 # = no specified type
 a = archival

- 09 Character coding scheme
 - # = MARC-8
 - a = UCS/Unicode
- 10 Indicator count (always "2")
- 11 Subfield code count (always "2")
- 12-16 Base address of data (calculated by the computer for each record)
- 17 Encoding level
 - # = full level
 - 1 = full level, material not examined
 - 2 = less-than-full level, material not examined
 - 3 = abbreviated level
 - 4 = core level
 - 5 = partial (preliminary) level
 - 7 = minimal level
 - 8 = prepublication level (CIP)
 - u = unknown
 - z = not applicable
- 18 Descriptive cataloging form
 - # = non-ISBD
 - a = AACR2
 - i = ISBD
 - u = unknown
- 19 Multipart resource record level
 - # = Not specified or not applicable
 - a = Set
 - b = Part with independent title
 - c = Part with dependent title
- 20 Length of the length-of-field portion (always "4")
- 21 Length of the starting-character-position portion (always "5")
- 22 Length of the implementation-defined portion (always "0")
- 23 Undefined (always "0")

[\[Back to Top of Page \]](#)

Part X:

Field 008 for Books

Field 008 is used for Fixed Length Data Elements ("Fixed Field Codes"). There are 40 character positions in field 008, numbered from 00-39. Undefined positions must contain either a blank (#) or a fill character (|). Positions 00-17 and 35-39 are defined the same way for all media.

The information shown here for positions 18-34 applies only to books. For explanation of all the positions below and for positions 18-34 for other media, see the *MARC 21 Format for Bibliographic Data*.

Note that field 008 has no indicators or subfield codes.

- 00-05 Date entered on file (YYMMDD),
where Y=year, M=month, and D=day
- 06 Type of date/publication status:
 b = no dates given; B.C. date involved
 e = detailed date
 s = single known date/probable date
 m = multiple dates
 r = reprint/reissue date (Date 1) and original date (Date 2)
 n = dates unknown
 q = questionable date
 t = publication date and copyright date
 | = no attempt to code
- 07-10 Date 1/beginning date of publication
- 11-14 Date 2/ending date of publication

Date fields contain the year(s) of publication. The type of date(s) in these elements are specified in fixed field element 06: Type of date/publication status. (For further details, see the field 008 description in the *MARC 21 Format for Bibliographic Data*.)

- 15-17 Place of publication, production, or execution
 For example:
 pk# = Pakistan
 cau = California (US)

(For a full list of codes used in these positions, see the [MARC Code List for Countries](#).)

- 18-21 Illustrations (up to 4 codes):
 # = no illustrations
 a = illustrations
 b = maps
 c = portraits
 d = charts
 e = plans
 f = plates
 g = music
 h = facsimiles
 i = coats of arms
 j = genealogical tables
 k = forms
 l = samples
 m = phonodisc, phonowire, etc.
 o = photographs
 p = illuminations
 | = no attempt to code
- 22 Target audience:
 # = unknown or not specified

- a = preschool
 - b = primary
 - c = pre-adolescent
 - d = adolescent
 - e = adult
 - f = specialized
 - g = general
 - j = juvenile
 - | = no attempt to code
- 23 Form of item:
- # = none of the following
 - a = microfilm
 - b = microfiche
 - c = microopaque
 - d = large print
 - f = braille
 - r = regular print reproduction
 - s = electronic
 - | = no attempt to code
- 24-27 Nature of contents (up to 4):
- # = no specified nature of contents
 - a = abstracts/summaries
 - b = bibliographies (is one or contains one)
 - c = catalogs
 - d = dictionaries
 - e = encyclopedias
 - f = handbooks
 - g = legal articles
 - i = indexes
 - j = patent document
 - k = discographies
 - l = legislation
 - m = theses
 - n = surveys of literature
 - o = reviews
 - p = programmed texts
 - q = filmographies
 - r = directories
 - s = statistics
 - t = technical reports
 - u = standards/specifications
 - v = legal cases and notes
 - w = law reports and digests
 - z = treaties
 - | = no attempt to code
- 28 Government publication:
- # = not a government publication

- i = international intergovernmental
 - f = federal/national
 - a = autonomous or semi-autonomous component
 - s = state, provincial, territorial, dependent, etc.
 - m = multistate
 - c = multilocal
 - l = local
 - z = other type of government publication
 - o = government publication -- level undetermined
 - u = unknown if item is government publication
 - | = no attempt to code
- 29 Conference publication:
- 0 = not a conference publication
 - 1 = conference publication
 - | = no attempt to code
- 30 Festschrift:
- 0 = not a festschrift
 - 1 = festschrift
 - | = no attempt to code
- 31 Index:
- 0 = no index
 - 1 = index present
 - | = no attempt to code
- 32 Undefined (since 1990) (Earlier records may contain the values 0 or 1)
- # = Undefined
 - | = no attempt to code
- 33 Literary form:
- 0 = not fiction (not further specified)
 - 1 = fiction (not further specified)
 - c = comic strips
 - d = dramas
 - e = essays
 - f = novels
 - h = humor, satires, etc.
 - i = letters
 - j = short stories
 - m = mixed forms
 - p = poetry
 - s = speeches
 - u = unknown
 - | = no attempt to code
- 34 Biography:
- # = no biographical material
 - a = autobiography
 - b = individual biography
 - c = collective biography
 - d = contains biographical information

- 35-37 | = no attempt to code
 Language:
 A three-letter code. For example: eng fre ger spa rus ita

(For a full list of codes used in these positions, see the [MARC Code List for Languages](#).)

- 38 Modified record:
 # = not modified
 x = missing characters (because of characters unavailable in MARC character set)
 s = shortened
 d = "dashed-on" information omitted
 r = completely romanized/printed cards in script
 o = completely romanized/printed cards romanized
 | = no attempt to code
- 39 Cataloging source:
 # = national bibliographic agency
 c = cooperative cataloging program
 d = other sources
 u = unknown
 | = no attempt to code

[[Back to Top of Page](#)]

[[Back to Table of Contents](#)] -- [[Continue to Part 11](#)]



Library of Congress

Library of Congress Help Desk (10/27/2009)

APPENDIX C

**OPTICAL AND ELECTRO-OPTICAL
ENGINEERING SERIES**

MODERN LENS DESIGN

A Resource Manual

WARREN J. SMITH
GENESEE OPTICS SOFTWARE, INC.

ROBERT E. FISCHER & WARREN J. SMITH, Series Editors

Optical and Electro-Optical Engineering Series
Robert E. Fischer and Warren J. Smith, Series Editors

Published

ALLARD • *Fiber Optics Handbook*
HECHT • *The Laser Guidebook*
NISHIHARA, HARUNA, SUHARA • *Optical Integrated Circuits*
RANCOURT • *Optical Thin Films Users' Handbook*
SIBLEY • *Optical Communications*
SMITH • *Modern Optical Engineering*
STOVER • *Optical Scattering*
WYATT • *Electro-Optical System Design*

Other Published Books of Interest

CSELT • *Fiber Optic Communications Handbook*
KAO • *Optical Fiber Systems*
KEISER • *Optical Fiber Communications*
MACLEOD • *Thin Film Optical Filters*
OPTICAL SOCIETY OF AMERICA • *Handbook of Optics*

To order, or to receive additional information on these or any other McGraw-Hill titles, please call 1-800-822-8158 in the United States. In other countries, please contact your local McGraw-Hill office.

MH92

Engineering Series
Smith, Series Editors

Integrated Circuits
Handbook

gn

Handbook

ms

of Optics

ation on these or
l 1-800-822-8158
please contact

MH92

Modern Lens Design

A Resource Manual

Warren J. Smith

Chief Scientist

Kaiser Electro-Optics, Inc.

Carlsbad, California

Genesee Optics Software, Inc.

Rochester, New York

McGraw-Hill, Inc.

New York St. Louis San Francisco Auckland Bogotá
Caracas Lisbon London Madrid Mexico Milan
Montreal New Delhi Paris San Juan São Paulo
Singapore Sydney Tokyo Toronto

Library of Congress Cataloging-in-Publication Data

Smith, Warren J.

Modern lens design : a resource manual / Warren J. Smith and Genesee Optics Software, Inc.

p. cm.—(Optical and electro-optical engineering series)

Includes index.

ISBN 0-07-059178-4

1. Lenses—Design and construction—Handbooks, manuals, etc.

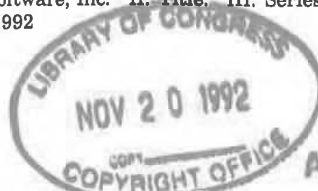
I. Genesee Optics Software, Inc. II. Title. III. Series.

QC385.2.D47S65 1992

681'.423—dc20

92-20038

CIP



Copyright © 1992 by McGraw-Hill, Inc. All rights reserved. Printed in the United States of America. Except as permitted under the United States Copyright Act of 1976, no part of this publication may be reproduced or distributed in any form or by any means, or stored in a data base or retrieval system, without the prior written permission of the publisher.

1 2 3 4 5 6 7 8 9 0 DOC/DOC 9 8 7 6 5 4 3 2

ISBN 0-07-059178-4

QC 385
.2
.D47 S65
1992
Copy 2

The sponsoring editor for this book was Daniel A. Gonneau, the editing supervisor was David E. Fogarty, and the production supervisor was Suzanne W. Babeuf. It was set in Century Schoolbook by McGraw-Hill's Professional Book Group composition unit.

Printed and bound by R. R. Donnelley & Sons Company.

OPTICS TOOLBOX is a registered trademark of Genesee Optics Software, Inc.

Information contained in this work has been obtained by McGraw-Hill, Inc., from sources believed to be reliable. However, neither McGraw-Hill nor its authors guarantee the accuracy or completeness of any information published herein, and neither McGraw-Hill nor its authors shall be responsible for any errors, omissions, or damages arising out of use of this information. This work is published with the understanding that McGraw-Hill and its authors are supplying information but are not attempting to render engineering or other professional services. If such services are required, the assistance of an appropriate professional should be sought.

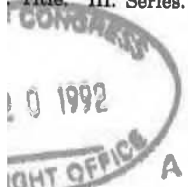
Publication Data

Manual / Warren J. Smith and

(optical engineering series)

on—Handbooks, manuals, etc.

Title III Series.



92-20038
CIP

Copyright © 1992. All rights reserved. Printed
except as permitted under the
no part of this publication may
be reproduced in any form or by any means, or stored
in a retrieval system, without the prior written
permission of Genesee Optics

8 7 6 5 4 3 2

QC 385
.2
.D47 S65
1992
Copy 2

by Daniel A. Gonneau, the
author, and the production
was set in Century Schoolbook
type composition unit.

McGraw-Hill & Sons Company.

Genesee Optics

Information obtained by McGraw-Hill is not guaranteed to be reliable. However, neither McGraw-Hill nor its authors are responsible for any errors, omissions, or inaccuracies in this work. This work is published as is. McGraw-Hill and its authors are not rendering engineering or other professional services. If such services are required, the assistance of a qualified professional should be sought.

Contents

Preface ix

Chapter 1. Introduction	1
Chapter 2. Automatic Lens Design: Managing the Lens Design Program	3
2.1 The Merit Function	3
2.2 Optimization	5
2.3 Local Minima	6
2.4 Types of Merit Functions	8
2.5 Stagnation	9
2.6 Generalized Simulated Annealing	10
2.7 Considerations about Variables for Optimization	10
2.8 How to Increase the Speed or Field of a System and Avoid Ray Failure Problems	14
2.9 Test Plate Fits, Melt Fits, and Thickness Fits	16
2.10 Spectral Weighting	18
2.11 How to Get Started	19
Chapter 3. Improving a Design	25
3.1 Standard Improvement Techniques	25
3.2 Glass Changes (Index and V Value)	25
3.3 Splitting Elements	27
3.4 Separating a Cemented Doublet	30
3.5 Compounding an Element	30
3.6 Vignetting and Its Uses	33
3.7 Eliminating a Weak Element; the Concentric Problem	34
3.8 Balancing Aberrations	35
3.9 The Symmetrical Principle	39
3.10 Aspheric Surfaces	40

v

Chapter 4. Evaluation: How Good Is This Design?	43
4.1 The Uses of a Preliminary Evaluation	43
4.2 OPD versus Measures of Performance	43
4.3 Blur Spot Size versus Certain Aberrations	47
4.4 MTF—The Modulation Transfer Function	48
Chapter 5. Lens Design Data	49
5.1 About the Sample Lenses	49
5.2 Lens Prescriptions, Drawings, and Aberration Plots	50
5.3 Estimating the Potential of a Design	54
5.4 Scaling a Design, Its Aberrations, and Its MTF	57
5.5 Notes on the Interpretation of Ray Intercept Plots	58
Chapter 6. Telescope Objectives	63
6.1 The Thin Doublet	63
6.2 Secondary Spectrum (Achromatic Systems)	72
6.3 Spherochromatism	75
6.4 Zonal Spherical Aberration	75
6.5 Induced Aberrations	79
6.6 Three-Element Objectives	79
Chapter 7. Eyepieces and Magnifiers	87
7.1 Eyepieces	87
7.2 Two Magnifier Designs	89
7.3 Simple Two- and Three-Element Eyepieces	92
7.4 Four-Element Eyepieces	92
7.5 Five-Element Eyepieces	101
7.6 Six- and Seven-Element Eyepieces	101
Chapter 8. Cooke Triplet Anastigmats	123
8.1 Airspaced Triplet Anastigmats	123
8.2 Glass Choice	125
8.3 Vertex Length and Residual Aberrations	125
8.4 Other Design Considerations	127
Chapter 9. Reverse Telephoto (Retrofocus and Fish-Eye) Lenses	147
9.1 The Reverse Telephoto Principle	147
9.2 The Basic Retrofocus Lens	148
9.3 The Fish-Eye, or Extreme Wide-Angle Reverse Telephoto, Lenses	150

How Good Is This Design?	43
Evaluation	43
Performance	43
Chromatic Aberrations	47
Transfer Function	48
	49
	49
	50
	54
	57
	58
	63
	63
	72
	75
	75
	79
	79
	87
	87
	89
	92
	92
	101
	101
	123
	123
	125
	125
	127
	147
	147
	148
	150

Chapter 10. Telephoto Lenses	169
10.1 The Basic Telephoto	169
10.2 Close-up or Macro Lenses	170
10.3 Sample Telephoto Designs	170
Chapter 11. Double-Meniscus Anastigmats	183
11.1 Meniscus Components	183
11.2 Hypergon, Topogon, and Metrogon	183
11.3 Protar, Dagor, and Convertible Lenses	185
11.4 The Split Dagor	190
11.5 The Dogmar	190
Chapter 12. The Tessar, Heliar, and Other Compounded Triplets	197
12.1 The Classic Tessar	197
12.2 The Hellar/Pentac	210
12.3 Other Compounded Triplets	210
Chapter 13. The Petzval Lens; Head-up Display Lenses	221
13.1 The Petzval Portrait Lens	221
13.2 The Petzval Projection Lens	221
13.3 The Petzval with a Field Flattenor	224
13.4 Very High Speed Petzval Lenses	228
13.5 Head-up Display (HUD) Lenses; Binocular Lenses	236
Chapter 14. Split Triplets	239
Chapter 15. Microscope Objectives	257
15.1 General Considerations	257
15.2 Classical Objective Design Forms; the Aplanatic Front	258
15.3 Flat-Field Objectives	261
15.4 Reflecting Objectives	262
15.5 The Sample Lenses	263
Chapter 16. Mirror and Catadioptric Systems	271
16.1 The Good and the Bad Points of Mirrors	271
16.2 The Classical Two-Mirror Systems	271
16.3 Catadioptric Systems	285
16.4 Confocal Paraboloids	295
16.5 Unobscured Systems	296
Chapter 17. The Biotar or Double-Gauss Lens	303
17.1 The Basic Six-Element Version	303
17.2 The Seven-Element Biotar-Split-Rear Singlet	319
17.3 The Seven-Element Biotar-Broken Contact Front Doublet	319

viii Contents

17.4	The Seven-Element Biotar—One Compounded Outer Element	340
17.5	The Eight-Element Biotar	340
17.6	Miscellaneous Biotars	340
Chapter 18. Wide-Angle Lenses with Negative Outer Elements		355
Chapter 19. Projection TV Lenses and Macro Lenses		365
19.1	Projection TV Lenses	365
19.2	Macro Lenses	367
Chapter 20. Zoom Lenses		373
Chapter 21. Infrared Systems		393
21.1	Infrared Optics	393
21.2	IR Objective Lenses	394
21.3	IR Telescopes	406
Chapter 22. Scanner/f-θ and Laser Disk/Collimator Lenses		411
22.1	Monochromatic Systems	411
22.2	Scanner Lenses	411
22.3	Laser Disk, Focusing, and Collimator Lenses	412
Chapter 23. Tolerance Budgeting		431
23.1	The Tolerance Budget	431
23.2	Additive Tolerances	434
23.3	Establishing the Tolerance Budget	438
Formulary		441
F.1	Sign Conventions, Symbols, and Definitions	441
F.2	The Cardinal Points	443
F.3	Image Equations	443
F.4	Paraxial Ray Tracing (Surface by Surface)	444
F.5	Invariants	445
F.6	Paraxial Ray Tracing (Component by Component)	445
F.7	Two-Component Relationships	446
F.8	Third-Order Aberrations—Surface Contributions	447
F.9	Third-Order Aberrations—Thin Lens Contributions	449
F.10	Stop Shift Equations	450
F.11	Third-Order Aberrations—Contributions from Aspheric Surfaces	451
F.12	Conversion of Aberrations to Wavefront Deformation (OPD, Optical Path Difference)	451
Appendix. Lens Listings		453
Index		465

Preface

Two-Element Compound Outer Element	340
with Negative Outer Elements	340
with Positive Outer Elements	340
with Negative Outer Elements	355
with Positive Outer Elements	365
with Negative Outer Elements	367
with Positive Outer Elements	373
with Negative Outer Elements	393
with Positive Outer Elements	393
with Negative Outer Elements	394
with Positive Outer Elements	406
with Negative Outer Elements	411
with Positive Outer Elements	411
with Negative Outer Elements	411
with Positive Outer Elements	412
with Negative Outer Elements	431
with Positive Outer Elements	431
with Negative Outer Elements	434
with Positive Outer Elements	438
with Negative Outer Elements	441
with Positive Outer Elements	441
with Negative Outer Elements	443
with Positive Outer Elements	443
with Negative Outer Elements	444
with Positive Outer Elements	445
with Negative Outer Elements	445
with Positive Outer Elements	446
with Negative Outer Elements	447
with Positive Outer Elements	449
with Negative Outer Elements	450
with Positive Outer Elements	451
with Negative Outer Elements	451
with Positive Outer Elements	453

This book had its inception in the early 1980s, when Bob Fischer and I, as coeditors of the then Macmillan, now McGraw-Hill, Series on Optical and Electro-Optical Engineering, were planning the sort of books we wanted in the series. The concept was outlined initially in 1982, and an extensive proposal was submitted to, and accepted by, Macmillan in 1986. At this point my proposed collaborators elected to pursue other interests, and the project was put on the shelf until it was revived by the present set of authors.

My coauthor is Genesee Optics Software, Inc. Obviously the book is the product of the work of real people, i.e., myself and the staff of Genesee. In alphabetical order, the Genesee personnel who have been involved are Charles Dubois, Henry Gintner, Robert MacIntyre, David Pixley, Lynn VanOrden, and Scott Weller. They have been responsible for the computerized lens data tables, lens drawings, and aberration plots which illustrate each lens design.

Many of the lens designs included in this book are from OPTICS TOOLBOX® (a software product of Genesee Optics Software), which was originally authored by Robert E. Hopkins and Scott W. Weller. OPTICS TOOLBOX is a collection of lens designs and design commentary within an expert-system, artificial-intelligence, relational data base.

This author's optical design experience has spanned almost five decades. In that period lens design has undergone many radical changes. It has progressed from what was a semi-intuitive art practiced by a very small number of extremely patient and dedicated lovers of detail and precision. These designers used a very limited amount of laborious computation, combined with great understanding of lens design principles and dogged perseverance to produce what are now the classic lens design forms. Most of these design forms are still the best, and as such are the basis of many modern optical systems. However, the manner in which lenses are designed today is almost completely different in both technique and philosophy. This change is, of course, the

ix

result of the vastly increased computational speed now available to the lens designer.

In essence, much modern lens design consists of the selection of a starting lens form and its subsequent optimization by an automatic lens design program, which may or may not be guided or adjusted along the way by the lens designer. Since the function of the lens design program is to drive the design form to the nearest local optimum (as defined by a *merit function*), it is obvious that the starting design form and the merit function together uniquely define which local optimum design will be the result of this process.

Thus it is apparent that, in addition to a knowledge of the principles of optical design, a knowledge of appropriate starting-point designs and of techniques for guiding the design program have become essential elements of modern lens design. The lens designs in this book have been chosen to provide a good selection of starting-point designs and to illustrate important design principles. The design techniques described are those which the author has found to be useful in designing with an optimization program. Many of the techniques have been developed or refined in the course of teaching lens design and optical system design; indeed, a few of them were initially suggested or inspired by my students.

In order to maximize their usefulness, the lens designs in this book are presented in three parts: the lens prescription, a drawing of the lens which includes a marginal ray and a full-field principal ray, and a plot of the aberrations. The inclusion of these two rays allows the user to determine the approximate path of any other ray of interest. For easy comparison, all lenses are shown at a focal length of approximately 100, regardless of their application. The performance data is shown as aberration plots; we chose this in preference to MTF plots because the MTF is valid only for the focal length for which it was calculated, and because the MTF cannot be scaled. The aberration plots *can* be scaled, and in addition they indicate what aberrations are present and show which aberrations limit the performance of the lens. We have expanded on the usual longitudinal presentation of spherical aberration and curvature of field by adding ray intercept plots in three colors for the axial, 0.7 zonal, and full-field positions. We feel that this presentation gives a much more complete, informative, and useful picture of the characteristics of a lens design.

This book is intended to build on some knowledge of both geometrical optics and the basic elements of lens design. It is thus, in a sense, a companion volume to the author's *Modern Optical Engineering*, which covers such material at some length. Presumably the user of this text will already have at least a reasonable familiarity with this material.

and computational speed now available to

lens design consists of the selection of a subsequent optimization by an automatic may or may not be guided or adjusted designer. Since the function of the lens design form to the nearest local optimum n), it is obvious that the starting design together uniquely define which local optimum of this process.

In addition to a knowledge of the principles of appropriate starting-point designs the design program have become essential design. The lens designs in this book a good selection of starting-point designs design principles. The design techniques the author has found to be useful in design program. Many of the techniques have been course of teaching lens design and optical of them were initially suggested or in-

usefulness, the lens designs in this book the lens prescription, a drawing of the axial ray and a full-field principal ray, and the inclusion of these two rays allows the approximate path of any other ray of interest. These are shown at a focal length of approximately their application. The performance data is we chose this in preference to MTF plots only for the focal length for which it was

MTF cannot be scaled. The aberration condition they indicate what aberrations are aberrations limit the performance of the lens. The usual longitudinal presentation of spherical field by adding ray intercept plots in 7 zonal, and full-field positions. We feel a much more complete, informative, and characteristics of a lens design.

It is based on some knowledge of both geometrical aspects of lens design. It is thus, in a sense, the author's *Modern Optical Engineering*, at some length. Presumably the user of at least a reasonable familiarity with this

There are really only a few well-understood and widely utilized principles of optical design. If one can master a thorough understanding of these principles, their effects, and their mechanisms, it is easy to recognize them in existing designs and also easy to apply them to one's own design work. It is our intent to promote such understanding by presenting both expositions and annotated design examples of these principles.

Readers are free to use the designs contained in this book as starting points for their own design efforts, or in any other way they see fit. Most of the designs presented have, as noted, been patented; such designs may or may not be currently subject to legal protection, although there may, of course, be differences of opinion as to the effectiveness of such protection. The reader must accept full responsibility for meeting whatever limitations are imposed on the use of these designs by any patent or copyright coverage (whether indicated herein or not).

Warren J. Smith

Introduction

Modern Lens Design is intended as an aid to lens designers who work with the many commercially available lens design computer programs. We assume that the reader understands basic optical principles and may, in fact, have a command of the fundamentals of classical optical design methods. For those who want or need information in these areas, the following books should prove helpful. This author's *Modern Optical Engineering: The Design of Optical Systems*, 2d ed., McGraw-Hill, 1990, is a comprehensive coverage of optical system design; it includes two full chapters which deal specifically with lens design in considerable detail. Rudolf Kingslake's *Optical System Design* (1983), *Fundamentals of Lens Design* (1978), and *A History of the Photographic Lens* (1989), all by Academic Press, are complete, authoritative, and very well written.

Authoritative books on lens design are rare, especially in English; there are only a few others available. The Kingslake series *Applied Optics and Optical Engineering*, Academic Press, contains several chapters of special interest to lens designers. Volume 3 (1965) has chapters on lens design, photographic objectives, and eyepieces. Volume 8 (1980) has chapters on camera lenses, aspherics, automatic design, and image quality. Volume 10 (1987) contains an extensive chapter on afocal systems. Milton Laikin's *Lens Design*, Marcel Dekker, 1991, is a volume similar to this one, with prescriptions and lens drawings. Its format differs in that no aberration plots are included; instead, modulation transfer function (MTF) data for a specific focal length and f number are given. Now out of print, Arthur Cox's *A System of Optical Design*, Focal Press, 1964, contains a complete, if unique, approach to lens design, plus prescriptions and (longitudinal) aberration plots for many lens design patents.

This book has several primary aims. It is intended as a source book

for a variety of designed lens types which can serve as suitable starting points for a lens designer's efforts. A study of the comparative characteristics of the annotated designs contained herein should also illustrate the application of many of the classic lens design principles. It is also intended as a handy, if abridged, reference to many of the equations and relationships which find frequent use in lens design. Most of these are contained in the Formulary at the end of the book. And last, but not least, the text contains extensive discussions of design techniques which are appropriate to modern optical design with an automatic lens design computer program.

The book begins with a discussion of automatic lens design programs and how to use them. The merit function, optimization, variables, and the various techniques which are useful in connection with a program are covered. Chapter 3 details many specific improvement strategies which may be applied to an existing design to improve its performance. The evaluation of a design is discussed from the standpoint of ray and wave aberrations, and integrated with such standard measures as MTF and Strehl ratio. The sample lens designs follow. Each presents the prescription data, a drawing of the lens with marginal and chief rays, and an aberration analysis consisting of ray intercept plots for three field angles, longitudinal plots of spherical aberration and field curvature, and a plot of distortion. A discussion of the salient features of each design accompanies the sample designs, and comments (in some cases quite extensive) regarding the design approach are given for each class of lens. The Formulary, intended as a convenient reference, concludes the book.

The design of the telescope objective is covered in Chap. 6, beginning with the classic forms and continuing with several possible modifications which can be used to improve the aberration correction. These are treated in considerable detail because they represent techniques which are generally applicable to all types of designs. For similar reasons, Chap. 8 deals with the basic principles of airspaced anastigmats in a rather extended treatment. The complexities of the interrelationships involved in the Cooke triplet anastigmat are important to understand, as are the (almost universal) relationships between the vertex length of an ordinary anastigmat lens and its capabilities as regards speed and angular coverage.

Automatic Lens Design: Managing the Lens Design Program

types which can serve as suitable starting points for the designer's efforts. A study of the comparative designs contained herein should also provide the designer with many of the classic lens design principles. This book, if abridged, reference to many of the designs which find frequent use in lens design. The Formulary at the end of the book. The Appendix contains extensive discussions of design methods appropriate to modern optical design with the aid of a computer program.

A discussion of automatic lens design programs.

The merit function, optimization, variables, and techniques which are useful in connection with automatic lens design. Chapter 3 details many specific improvements which can be applied to an existing design to improve its performance. The optimization of a design is discussed from the standpoint of the merit function, and integrated with such standard design techniques. The sample lens designs follow. For each design, a drawing of the lens with marginal ray analysis consisting of ray angles, longitudinal plots of spherical aberration, and a plot of distortion. A discussion of design accompanies the sample designs, and is quite extensive) regarding the design of a lens. The Formulary, intended as a reference, concludes the book.

The objective is covered in Chap. 6, beginning with several possible methods to improve the aberration correction. The details are given because they represent techniques applicable to all types of designs. For simplicity, the basic principles of airspaced lenses are given a brief treatment. The complexities of the design of the Cooke triplet anastigmat are important. The (almost universal) relationships between the design of an ordinary anastigmat lens and its capabilities are given.

2.1 The Merit Function

What is usually referred to as *automatic lens design* is, of course, nothing of the sort. The computer programs which are so described are actually optimization programs which drive an optical design to a local optimum, as defined by a *merit function* (which is not a true merit function, but actually a defect function). In spite of the preceding disclaimers, we will use these commonly accepted terms in the discussions which follow.

Broadly speaking, the merit function can be described as a combination or function of calculated characteristics, which is intended to completely describe, with a single number, the value or quality of a given lens design. This is obviously an exceedingly difficult thing to do. The typical merit function is the sum of the squares of many image defects; usually these image defects are evaluated for three locations in the field of view (unless the system covers a very large or a very small angular field). The squares of the defects are used so that a negative value of one defect does not offset a positive value of some other defect.

The defects may be of many different kinds; usually most are related to the quality of the image. However, any characteristic which can be calculated may be assigned a target value and its departure from that target regarded as a defect. Some less elaborate programs utilize the third-order (Seidel) aberrations; these provide a rapid and efficient way of adjusting a design. These cannot be regarded as optimizing the image quality, but they do work well in correcting ordinary lenses. Another type of merit function traces a large number of

rays from an object point. The radial distance of the image plane intersection of the ray from the centroid of all the ray intersections is then the image defect. Thus the merit function is effectively the sum of the root-mean-square (rms) spot sizes for several field angles. This type of merit function, while inefficient in that it requires many rays to be traced, has the advantage that it is both versatile and in some ways relatively foolproof. Some merit functions calculate the values of the classical aberrations, and convert (or weight) them into their equivalent wavefront deformations. (See Formulary Sec. F-12 for the conversion factors for several common aberrations.) This approach is very efficient as regards computing time, but requires careful design of the merit function. Still another type of merit function uses the variance of the wavefront to define the defect items. The merit function used in the various David Grey programs is of this type, and is certainly one of the best of the commercially available merit functions in producing a good balance of the aberrations.

Characteristics which do not relate to image quality can also be controlled by the lens design program. Specific construction parameters, such as radii, thicknesses, spaces, and the like, as well as focal length, working distance, magnification, numerical aperture, required clear apertures, etc., can be controlled. Some programs include such items in the merit function along with the image defects. There are two drawbacks which somewhat offset the neat simplicity of this approach. One is that if the first-order characteristics which are targeted are not initially close to the target values, the program may correct the image aberrations without controlling these first-order characteristics; the result may be, for example, a well-corrected lens with the wrong focal length or numerical aperture. The program often finds this to be a local optimum and is unable to move away from it. The other drawback is that the inclusion of these items in the merit function has the effect of slowing the process of improving the image quality. An alternative approach is to use a system of constraints outside the merit function. Note also that many of these items can be controlled by features which are included in almost all programs, namely *angle-solves* and *height-solves*. These algebraically solve for a radius or space to produce a desired ray slope or height.

In any case, the merit function is a summation of suitably weighted defect items which, it is hoped, describes in a single number the worth of the system. The smaller the value of the merit function, the better the lens. The numerical value of the merit function depends on the construction of the optical system; it is a function of the construction parameters which are designated as variables. Without getting into the details of the mathematics involved, we can realize that the merit function is an n -dimensional space, where n is the number of the vari-

he radial distance of the image plane in the centroid of all the ray intersections is the merit function is effectively the sum of the spot sizes for several field angles. This is inefficient in that it requires many rays to be traced to determine the merit function. The program is both versatile and in some cases, the merit functions calculate the values of the spot sizes and convert (or weight) them into their relative contributions. (See Formulary Sec. F-12 for the treatment of the 11 common aberrations.) This approach is computationally intensive, but requires careful design of the merit function. Another type of merit function uses the spot sizes to define the defect items. The merit function of the Grey programs is of this type, and is one of the commercially available merit functions for the optimization of the aberrations.

Another type of merit function can also be constructed to optimize a program. Specific construction parameters, such as radii of curvature, focal length, magnification, numerical aperture, required clearances, etc., are included. Some programs include such items as coma, astigmatism, and distortion with the image defects. There are two types of programs. One offsets the neat simplicity of this approach by including higher-order characteristics which are targeted for optimization. In such target values, the program may correct for distortion by controlling these first-order characteristics. For example, a well-corrected lens with the required numerical aperture. The program often finds a minimum and is unable to move away from it. The inclusion of these items in the merit function complicates the process of improving the image quality. It is to use a system of constraints outside of the merit function so that many of these items can be controlled. In almost all programs, namely in the commercial programs. These algebraically solve for a radius of curvature, slope, or height.

The merit function is a summation of suitably weighted terms. It describes in a single number the worth of the merit function, the better the value of the merit function depends on the construction parameters; it is a function of the construction parameters treated as variables. Without getting into the details of the optimization process involved, we can realize that the merit function is a function of the construction parameters, where n is the number of the vari-

able constructional parameters in the optical system. The task of the design program is to find a location in this space (i.e., a lens prescription or a solution vector) which minimizes the size of the merit function. In general, for a lens of reasonable complexity there will be many such locations in a typical merit function space. The automatic design program will simply drive the lens design to the nearest minimum in the merit function.

2.2 Optimization

The lens design program typically operates this way: Each variable parameter is changed (one at a time) by a small increment whose size is chosen as a compromise between a large value (to get good numerical accuracy) and a small value (to get the local differential). The change produced in every item in the merit function is calculated. The result is a matrix of the partial derivatives of the defect items with respect to the parameters. Since there are usually many more defect items than variable parameters, the solution is a classical least-squares solution. It is based on the assumption that the relationships between the defect items and the variable parameters are linear. Since this is usually a false assumption, an ordinary least-squares solution will often produce an unrealizable lens or one which may in fact be worse than the starting design. The *damped least-squares* solution, in effect, adds the weighted squares of the parameter changes to the merit function, heavily penalizing any large changes and thus limiting the size of the changes in the solution. The mathematics of this process are described in Spencer, "A Flexible Automatic Lens Correction Program," *Applied Optics*, vol. 2, 1963, pp. 1257-1264, and by Smith in W. Driscoll (ed.), *Handbook of Optics*, McGraw-Hill, New York, 1978.

If the changes are small, the nonlinearity will not ruin the process, and the solution, although an approximate one, will be an improvement on the starting design. Continued repetition of the process will eventually drive the design to the nearest local optimum.

One can visualize the situation by assuming that there are only two variable parameters. Then the merit function space can be compared to a landscape where latitude and longitude correspond to the variables and the elevation represents the value of the merit function. Thus the starting lens design is represented by a particular location in the landscape and the optimization routine will move the lens design downhill until a minimum elevation is found. Since there may be many depressions in the terrain of the landscape, this optimum may not be the best there is; it is a local optimum and there can be no assurance (except in very simple systems) that we have found a global

optimum in the merit function. This simple topological analogy helps to understand the dominant limitations of the optimization process: the program finds the nearest minimum in the merit function, and that minimum is uniquely determined by the design coordinates at which the process is begun. The landscape analogy is easy for the human mind to comprehend; when it is extended to a 10- or 20-dimension space, one can realize only that it is apt to be an extremely complex neighborhood.

2.3 Local Minima

Figure 2.1 shows a contour map of a hypothetical two-variable merit function, with three significant local minima at points *A*, *B*, and *C*; there are also three other minima at *D*, *E*, and *F*. It is immediately apparent that if we begin an optimization at point *Z*, the minimum at point *B* is the only one which the routine can find. A start at *Y* on the ridge at the lower left will go to the minimum at *C*. However, a start

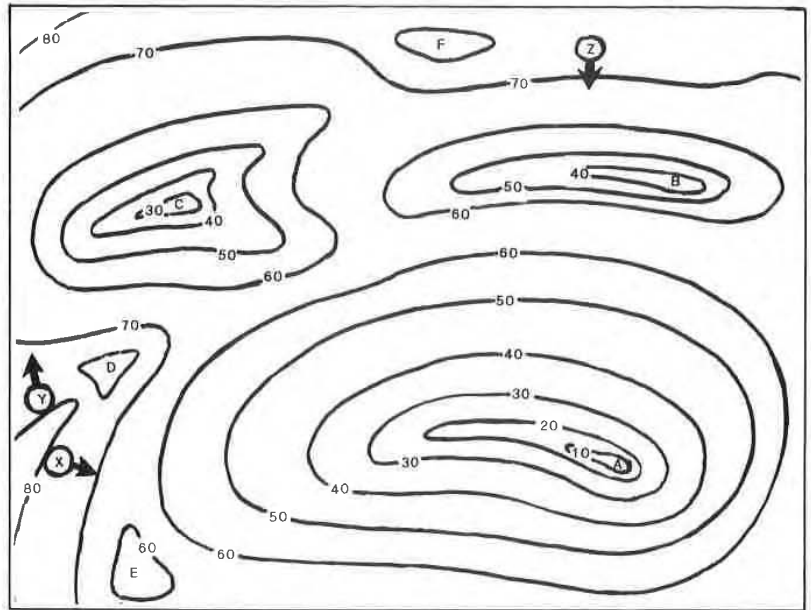
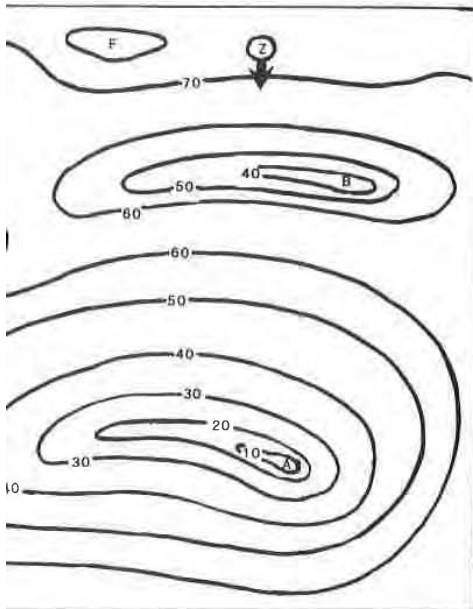


Figure 2.1 Topography of a hypothetical two-variable merit function, with three significant minima (*A*, *B*, *C*) and three trivial minima (*D*, *E*, *F*). The minimum to which a design program will go depends on the point at which the optimization process is started. Starting points *X*, *Y*, and *Z* each lead to a different design minimum; other starting points can lead to one of the trivial minima.

on. This simple topological analogy helps
 limitations of the optimization process:
 st minimum in the merit function, and
 determined by the design coordinates at
 the landscape analogy is easy for the hu-
 when it is extended to a 10- or 20-
 lize only that it is apt to be an extremely

map of a hypothetical two-variable merit
 ant local minima at points A, B, and C;
 inima at D, E, and F. It is immediately
 optimization at point Z, the minimum at
 the routine can find. A start at Y on the
 to the minimum at C. However, a start



ical two-variable merit function, with three signif-
 icant local minima (A, B, and C). The minimum to which a
 routine can find. A start at Y on the map leads to the
 minimum at C. However, a start at Z leads to the minimum
 at A. Other local minima at D, E, and F are also present,
 but they are trivial minima.

at X, which is only a short distance away from Y, will find the best
 minimum of the three, at point A. If we had even a vague knowledge
 of the topography of the merit function, we could easily choose a start-
 ing point in the lower right quadrant of the map which would guar-
 antee finding point A. Note also that a modest change in any of the
 three starting points could cause the program to stagnate in one of the
 trivial minima at D, E, or F. It is this sort of minimum from which one
 can escape by "jolting" the design, as described below.

The fact that the automatic design program is severely limited and
 can find only the nearest optimum emphasizes the need for a knowl-
 edge of lens design, in order that one can select a starting design form
 which is close to a good optimum. This is the only way that an auto-
 matic program can systematically find a good design. If the program is
 started out near a poor local optimum, the result is a poor design.

The mathematics of the damped least-squares solution involves the
 inversion of a matrix. In spite of the damping action, the process can
 be slowed or aborted by either of the following conditions: (1) A vari-
 able which does not change (or which produces only a very small
 change in) the merit function items. (2) Two variables which have the
 same, nearly the same, or scaled effects on the items of the merit func-
 tion. Fortunately, these conditions are rarely met exactly, and they
 can be easily avoided.

If the program settles into an unsatisfactory optimum (such as those
 at D, E, and F in Fig. 2.1) it can often be jolted out of it by manually
 introducing a significant change in one or more parameters. The trick
 is to make a change which is in the direction of a better design form.
 (Again, a knowledge of lens designs is virtually a necessity.) Some-
 times simply freezing a variable to a desirable form can be sufficient
 to force a move into a better neighborhood. The difficulty is that too
 big a change may cause rays to miss surfaces or to encounter total in-
 ternal reflection, and the optimization process may break down. Con-
 versely, too small a change may not be sufficient to allow the design to
 escape from a poor local optimum. Also, one should remember that if
 the program is one which adjusts (optimizes) the damping factor, the
 factor is usually made quite small near an optimum, because the pro-
 gram is taking small steps and the situation looks quite linear; after
 the system is jolted, it is probably in a highly nonlinear region and a
 big damping factor may be needed to prevent a breakdown. A manual
 increase of the damping factor can often avoid this problem.

Another often-encountered problem is a design which persists in
 moving to an obviously undesirable form (when you *know* that there is
 a much better, very different one—the one that you want). Freezing
 the form of one part of the lens for a few cycles of optimization will
 often allow the rest of the lens to settle into the neighborhood of the

desired optimum. For example, if one were to try to convert a Cooke triplet into a split front crown form, the process might produce either a form which is like the original triplet with a narrow airspaced crack in the front crown, or a form with rather wild meniscus elements. A technique which will usually avoid these unfortunate local optima in this case is to freeze the front element to a plano-convex form by fixing the second surface to a plane for a few cycles of optimization. Again, one must know which lens forms are the good ones.

2.4 Types of Merit Functions

Many programs allow the user to define the merit function. This can be a valuable feature because it is almost impossible to design a truly *universal* merit function. As an example, consider the design of a simple Fraunhofer telescope objective: a merit function which controls the spherical and chromatic aberrations of the axial marginal ray and the coma of the oblique ray bundle (plus the focal length) is all that is necessary. If the design complexity is increased by allowing the airspace to vary and/or adding another element, the merit function may then profitably include entries which will control zonal spherical, spherochromatism, and/or fifth-order coma. But as long as the lens is thin and in contact with the aperture stop, it would be foolish to include in the merit function entries to control field curvature and astigmatism. There is simply no way that a thin stop-in-contact lens can have any control over the inherent large negative astigmatism; the presence of a target for this aberration in the merit function will simply slow down the solution process. It would be ridiculous to use a merit function of the type required for a photographic objective to design an ordinary telescope objective. (Indeed, an attempt to correct the field curvature may lead to a compromise design with a severely undercorrected axial spherical aberration which, in combination with coma, may fool the computer program into thinking that it has found a useful optimum.)

There are many design tasks in this category, where the requirements are effectively limited in number and a simple, equally limited merit function is clearly the best choice. In such cases, it is usually obvious that some specific state of correction will yield the best results; there is no need to *balance* the correction of one aberration against another.

More often, however, the situation is not so simple; compromises and balances are required and a more complex, suitably weighted merit function is necessary. This can be a delicate and somewhat tricky matter. For example, in the design of a lens with a significant aperture and field, there is almost always a (poor) local optimum in

le, if one were to try to convert a Cooke
n form, the process might produce either
nal triplet with a narrow airspaced crack
r with rather wild meniscus elements. A
r avoid these unfortunate local optima in
element to a plano-convex form by fixing
e for a few cycles of optimization. Again,
rms are the good ones.

ns

er to define the merit function. This can
it is almost impossible to design a truly
an example, consider the design of a sim-
ctive: a merit function which controls the
rations of the axial marginal ray and the
le (plus the focal length) is all that is nec-
ity is increased by allowing the airspace
er element, the merit function may then
which will control zonal spherical,
th-order coma. But as long as the lens is
aperture stop, it would be foolish to in-
tries to control field curvature and astig-
way that a thin stop-in-contact lens can
herent large negative astigmatism; the
beration in the merit function will sim-
process. It would be ridiculous to use a
quired for a photographic objective to de-
fective. (Indeed, an attempt to correct the
a compromise design with a severely
al aberration which, in combination with
program into thinking that it has found

isks in this category, where the require-
in number and a simple, equally limited
best choice. In such cases, it is usually
ate of correction will yield the best re-
alance the correction of one aberration

situation is not so simple; compromises
nd a more complex, suitably weighted
This can be a delicate and somewhat
n the design of a lens with a significant
almost always a (poor) local optimum in

which (1) the spherical aberration is left quite undercorrected, (2) a
compromise focus is chosen well inside the paraxial focus, (3) the
Petzval field is made inward-curving, and (4) overcorrected oblique
spherical aberration is introduced to "balance" the design. A program
which relies on the rms spot radius for its merit function is very likely
to fall into this trap. A better design usually results if the spherical
(both axial and oblique) aberrations are corrected, the Petzval curva-
ture is reduced, and a small amount of overcorrected astigmatism is
introduced. When one recognizes this sort of situation, it is a simple
matter to adjust the weighting of the appropriate targets in the merit
function to force the design into a form with the type of aberration bal-
ance which is desired. Another way to avoid this problem is to force
the system to be evaluated/optimized at the paraxial focus rather than
at a compromise focus, i.e., to not allow defocusing. As can be seen, the
design of a general-purpose merit function which will optimally bal-
ance a wide variety of applications is not a simple matter.

Although it is not always necessary, there are occasions when it is
helpful to begin the design process by controlling only the first-order
properties (image size, image location, spatial limitations, etc.). Then
one proceeds to control the chromatic and perhaps the Petzval aberrat-
ions. (Things may even go better if the first-order and the chromatic
are fairly completely worked out by hand before submitting the sys-
tem to an automatic design process.) The next step in the sequence is
to correct the primary aberrations (spherical, coma, astigmatism, and
distortion), either directly or by using the Seidel coefficients, and fi-
nally proceed to balancing and correcting the higher-order residuals.
This sort of ordered approach is sometimes useful (or even necessary)
when one is exploring terra incognita, and, of course, it requires a
user-defined merit function if it is to be implemented.

2.5 Stagnation

Sometimes the automatic design process will stagnate and the conver-
gence toward a solution will become so slow as to be imperceptible.
This can result from being in a very flat and broad optimum in the
merit function. It can also result from an ill-designed merit function.
Often first-order properties which are specified in the merit function
are the cause of the problem. It is only too easy to require contradic-
tory or redundant characteristics. This is especially true for zoom
lenses or multiconfiguration systems, which can be confusingly com-
plex. When stagnation occurs, or convergence is slower than you know
it should be, it is wise to stop and examine the merit function for prob-
lems. Look critically at every item in the merit function and consider
what it is intended to be doing and what it *actually* does. Eliminate

redundancies and try to make each entry in the merit function explicitly control its intended characteristic. Stagnation may also result from a starting design which is so far from a solution that differential changes to the variables have a negligible effect.

2.6 Generalized Simulated Annealing

The discussions above have centered on the standard damped least-squares program, or its equivalent. There have been several versions of *random search* programs proposed in the past. The most recent of these is quite sophisticated and is called *generalized simulated annealing*. In this, the computer randomly selects the lens dimensions (within a limited range and according to some probability distribution) and evaluates the resulting lens prescription. If the new version is better than the old, it is unconditionally accepted. If it is worse, it *may* be accepted, on the basis of random chance, weighted by a probability function which reduces the chance of acceptance in proportion to the amount that the lens is worse than the original form. This sort of approach obviously allows the program an easy escape from the local minima described with Fig. 2.1, but it equally obviously requires a very large number of trials before a random chance can find a good combination of dimensions for the lens. Nonetheless, it does work, but not rapidly. Perhaps as computers increase in speed, a program of this sort will displace or supplement the damped least-squares as the routine of choice for automatic lens design.

2.7 Considerations about Variables for Optimization

The potential variables for use in optimization include: the surface curvatures, conic constants, and asphericities; the surface spacings; and the refractive characteristics of the materials involved. Occasionally tilts and decentrations are also included as variables.

Materials

Although the material characteristics are not continuous variables, for optical glasses at least, the index and dispersion (or V value) can be varied within the boundaries of the glass map (Fig. 2.2) as if they were. The real glass nearest the optimized values can be substituted for the optimized glass to achieve nearly the same resultant design after another cycle or two of optimization with the real glass. Note that this is *not* true for partial dispersions, since there are relatively few glasses with partial dispersions unusual enough to be useful in the

each entry in the merit function explicit characteristic. Stagnation may also result is so far from a solution that differential a negligible effect.

Annealing

centered on the standard damped least-squares algorithm. There have been several versions proposed in the past. The most recent of them is called *generalized simulated annealing* and randomly selects the lens dimensions according to some probability distributing lens prescription. If the new version is unconditionally accepted. If it is worse, it is accepted with a probability of random chance, weighted by a probability that the chance of acceptance is proportionally worse than the original form. This sort of algorithm gives the program an easy escape from the local minima of Fig. 2.1, but it equally obviously requires a long time before a random chance can find a good design for the lens. Nonetheless, it does work, but as computers increase in speed, a program of this sort will eventually outpace the damped least-squares as the routine design.

Variables for

Variables in optimization include: the surface curvatures and asphericities; the surface spacings; the refractive indices of the materials involved. Occasionally, the material type is also included as variables.

Characteristics are not continuous variables, but the refractive index and dispersion (or V value) can be treated as if they were. The glass map (Fig. 2.2) as if they were continuous. The optimized values can be substituted into the design nearly the same resultant design as if the real glass were used. Note that the refractive indices and dispersions, since there are relatively few unusual enough to be useful in the

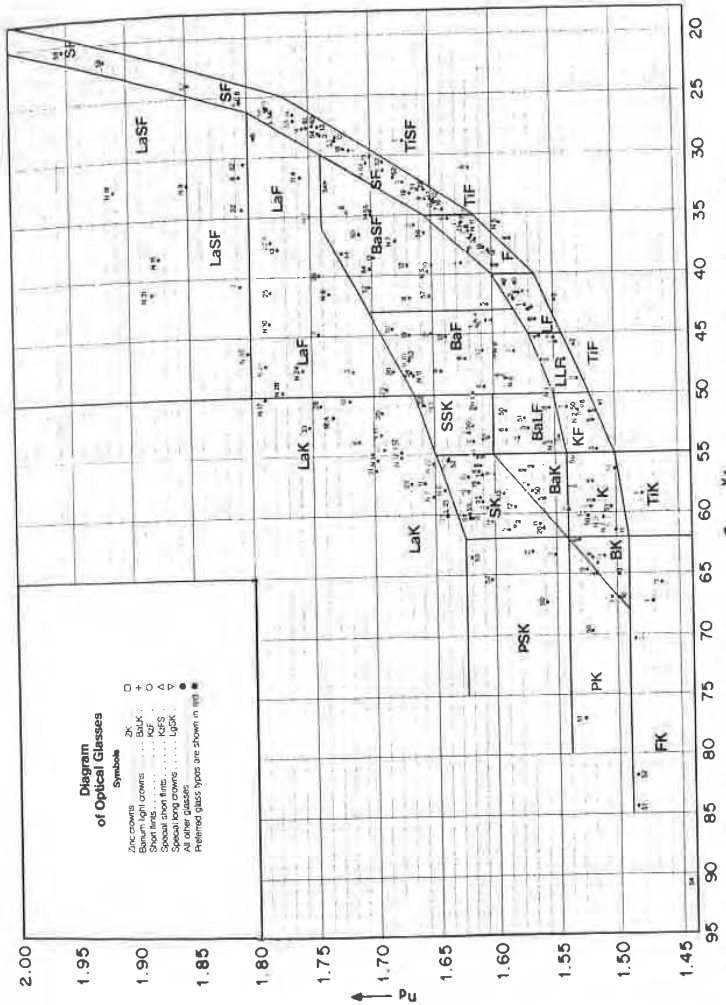


Figure 2.2 The glass map or "glass veil." Index (n_d) plotted against reciprocal relative dispersion (Abbe V value). The glass types are indicated by the letters in each area. The glass line is made up of the glasses of types K, KF, LLF, F, and SF, which are strung along the bottom of the veil. (Note that K stands for *kron*, German for crown, and S stands for *schwer*, or heavy or dense.) (Courtesy of Schott Glass Technologies, Inc., Duryea, Pa.)

correction of secondary spectrum. Obviously, for applications outside the spectral regions where optical glass is usable, one cannot treat the refractive characteristics as variables, since the available materials tend to be few and far between.

In many of the simpler types of designs it is essential to allow the glass characteristics to vary. In the Cooke triplet for example, the relationship between the V values of the crown and flint elements determines the overall length of the lens. As described in Sec. 8.3, the length of a triplet (and that of most anastigmats) determines the amount of higher-order spherical aberration and astigmatism; these in turn determine the aperture and field coverage capabilities of the lens. If these types of lenses are to be optimized to suit the application at hand, the glass characteristics *must* be allowed to vary.

Some optimization programs have difficulty with the bounds of the glass map; if this is a problem, the optimization process is often facilitated by starting the variable glass well away from the boundary, so that it can find its best value before encountering the boundary problem.

It is often better to vary the flint glasses than to vary the crowns. This is because the crowns usually tend to go to the upper left corner (high index, high V value) of the glass map. Flints head for the lower right corner, and are then, of course, constrained to lie on the glass line. The glasses along the glass line are numerous, inexpensive, and almost universally well behaved. On the other hand, the crown glasses in the upper left corner include in their number many which are expensive and/or easily attacked by the environment. Thus one might be willing to accept the computer's choice of a glass along the glass line, but would prefer to make a more discriminating selection from among the others.

Curvatures

In general, one would expect to want to make use of every available variable. This is almost always true regarding the curvatures, all of which, unless there is a reason to constrain the shape of an element, are usually allowed to vary.

Airspaces

Ordinarily, airspaces may be regarded in the same light as curvatures, since they are continuously variable and are very effective variables.

Defocusing

Although the distance by which the design image plane departs from the paraxial focus is usually an airspace, and can be regarded as a variable,

trum. Obviously, for applications outside optical glass is usable, one cannot treat the variables, since the available materials are limited.

In the Cooke triplet for example, the relative values of the crown and flint elements determine the spherical aberration and astigmatism; these values and field coverage capabilities of the lens are to be optimized to suit the application. Distortions *must* be allowed to vary.

Designers have difficulty with the bounds of the optimization process is often facilitated by the use of glass well away from the boundary, and the value before encountering the boundary.

Flint glasses than to vary the crowns. Designers usually tend to go to the upper left corner of the glass map. Flints head for the lower right of course, constrained to lie on the glass map line are numerous, inexpensive, and readily available. On the other hand, the crown glasses often include in their number many which are attacked by the environment. Thus one must be a computer's choice of a glass along the boundary to make a more discriminating selection.

It is not to want to make use of every available glass. It is true regarding the curvatures, all of the elements tend to constrain the shape of an element,

which are regarded in the same light as curvatures. Thicknesses are usually variable and are very effective variables.

When the design image plane departs from the paraxial focus, it can be regarded as a variable,

its effects can be insidious. If the image surface is allowed to depart from the paraxial focus from the beginning of the optimization process, an unfortunate lens may result. In some lenses, and with some optimization merit functions, the tendency is to produce a lens with:

1. The image plane well inside the paraxial focus
2. A large undercorrected spherical aberration
3. A strongly inward-curving field
4. A heavy overcorrecting oblique spherical aberration

Although this combination occupies a local optimum in the merit function, this is usually not the best state of correction. It fools the optimization program because the undercorrected spherical causes the best axial focus to lie to the left of the paraxial focus and the overcorrected oblique spherical causes the best off-axis focus to lie to the right of the inward-curving field; the net result is that, to the optimization program, the field seems flat. One can usually avoid this pitfall by not allowing any defocus in the early stages of the optimization and/or putting a heavy penalty on the defocusing. Note that for *some* lenses, such as non-diffraction-limited systems used with detectors, the correction described above may in fact be a good one. See the comments on aberration balance in Sec. 3.8.

Thickness

Element thicknesses must be regarded quite differently than airspaces. They must of course be bounded by the necessity for a practical edge thickness for the positive elements and a reasonable center thickness for the negative elements. In many designs, element thickness is an insignificant and ineffective variable (and one whose effects are easily duplicated by an adjacent airspace). In this circumstance one can arbitrarily select a thickness on the basis of economy or ease of fabrication. The elements in such designs are typically quite thin; see, for example, a telescope objective or an ordinary Cooke triplet.

There are, however, many systems in which the element thickness is not only an effective variable, but one which is essential to the success of the design type. The older meniscus lenses (Protar, Dagor, etc.) and the double-Gauss forms depend on the separation of the concave and convex surfaces of their thick meniscus components to control the Petzval curvature and, in many instances, the higher-order aberrations. In lenses of this type it is absolutely essential that these glass thicknesses be allowed to vary.

One must be wary of and skeptical toward a thickness variable which is very weakly effective. Occasionally an optimization program will produce a design with an overly thick element, where the large

thickness produces only a very small improvement (which is not worth the added cost of producing the thick element). This occurs because the optimization routine will seek out any improvement that it can get, no matter how small, and without concern as to the cost. It is wise to test the value of a thick element if there is any doubt about its utility. This is readily accomplished with another optimization run which fixes the thickness in question to a smaller value. Very often the performance of the thin version will not be noticeably different from that of the "optimum" thicker version. Although most significant with respect to lens thickness, this same rationale obviously applies to air-spaces as well.

Aspheric surfaces

Surface asphericity can be an extremely effective (if sometimes expensive) variable, but it is one that often requires a bit of finesse. On occasion, one may be ill-advised to begin an optimization with the conic constant and all the aspheric deformation coefficients used simultaneously as variables. The conic constant and the fourth-order deformation coefficient both affect the third-order aberrations in exactly the same way. Thus they are at least partially redundant, but more significantly, identical variables have an undesirable effect on the mathematics of the optimization process. It is often advisable to vary one or the other, but not both. A safe practice is to vary only the conic constant (or the fourth-order term) at first, and then add the higher-order terms (sixth, eighth, tenth) one at a time, as necessary. The tenth-order term is, in many systems, totally unnecessary, adding little or nothing to the quality of the system; in fact, the eighth-order term is often something that can be done without.

A surface defined by a tenth-order polynomial can cause the spherical aberration to be corrected exactly to zero at four ray heights. If there are only four axial rays in the merit function, their ray intercept errors may all be brought to zero; the danger is that, between these rays, the residual aberration may be unacceptably large. A tenth-order surface can be a rather extreme shape. Thus the use of an aspheric surface sometimes calls for more rays in the merit function than one might otherwise expect to need. With a program which allows wavefront deformation or optical path difference (OPD) targets in the merit function, the severity of this problem can be lessened.

2.8 How to Increase the Speed or Field of a System and Avoid Ray Failure Problems

Very often, the lens designer is faced with the necessity of increasing the speed (i.e., relative aperture, numerical aperture, etc.) and/or the

ry small improvement (which is not worth the thick element). This occurs because all seek out any improvement that it can find without concern as to the cost. It is wise to proceed if there is any doubt about its utility. Proceed with another optimization run which converges to a smaller value. Very often the performance will not be noticeably different from that of the previous version. Although most significant with re-entrance, the same rationale obviously applies to air-

extremely effective (if sometimes expensive) that often requires a bit of finesse. On occasion to begin an optimization with the conic deformation coefficients used simultaneously constant and the fourth-order deformation correct the third-order aberrations in exactly the same way at least partially redundant, but more often the higher order aberrations have an undesirable effect on the optimization process. It is often advisable to vary the conic constant (the first term) at first, and then add the higher-order terms one at a time, as necessary. The optimization systems, totally unnecessary, adding little to the merit of the system; in fact, the eighth-order optimization can be done without.

Fourth-order polynomial can cause the spheroidal aberration to be zero at four ray heights. If the aberration is zero in the merit function, their ray intercepts are zero; the danger is that, between these heights the aberration may be unacceptably large. A tenth-order polynomial may be unacceptably large. Thus the use of an optimization program calls for more rays in the merit function than expected to need. With a program which allows for optical path difference (OPD) targets the severity of this problem can be lessened.

Speed or Field of a Lens or Lens Problems

One is faced with the necessity of increasing the field of view, numerical aperture, etc.) and/or the

field of view of an existing optical system. There are two common reasons why this may be desirable. One may want to adapt an existing design (such as those in this book) to an application which requires a larger aperture or wider field than that for which the original lens has been configured. The other common situation is simply the creation of an entirely new system with a relatively large aperture and/or field. In either case, the difficulty which can arise is that the rays which are needed to design the system may not be able to get through the initial lens prescription.

There are two reasons that a ray may not be able to get through. One reason is that the height of the ray at a surface may be greater than the radius of the surface; the ray simply misses the surface entirely and its path obviously cannot be calculated any further. The second reason is that the ray may encounter total internal reflection (TIR) in passing from a higher index to a lower; again, the ray path cannot be calculated. Each of these conditions represents a boundary which, if crossed, causes failure of the ray trace. Note also that, as these boundaries are approached, the situation rapidly becomes very unstable. This is because, close to the boundary, the angle of incidence (for the case of the ray approaching the value of the radius) or the angle of refraction (for the case of the ray approaching TIR) is very near to 90°. Near this angle, Snell's law of refraction ($n \sin I = n' \sin I'$) becomes very nonlinear, producing a highly unstable situation which often explodes as the lens construction parameters are incremented in the course of the optimization.

A good way of dealing with this situation is simply to back off from the aperture and/or field requirement that is causing the problem. Many design programs have the capability to easily adjust or scale the aperture and field angle. If a change is made to smaller values of aperture or field, the rays will no longer be so near to the failure boundary. If the lens is now optimized, the program is very likely to adjust the lens parameters so as to reduce the angles of incidence, because this is usually a factor which causes the aberrations to be reduced. The optimizing changes can thus be expected to pull the problem situation in the system further away from the ray failure boundary, *if this is possible*.

After the optimization has relaxed the problem, the field and/or the aperture can usually be adjusted (scaled) to a moderately larger value without again encountering the failure boundary. Depending on just how sensitive the system is to the problem, an increase of about 10 to 50 percent may be appropriate. Now another cycle of optimization will strongly tend to again reduce the troublesome angles of incidence.

This process of adjusting (scaling) the field or the aperture to larger values and then optimizing is continued until the desired aperture or

field is attained without ray failures. This works well, *provided* that this desired result is possible for the lens configuration which is under study. It may be necessary to choose another configuration, usually one with more elements. When this is necessary, a drawing of the lens and rays (of the last design form which has successfully passed all the rays) will usually indicate which rays and which surfaces are causing the problem. One simply looks for angles of incidence or refraction which are large (and often near 90°). Then the offending element can be split into two (or more) elements which are shaped to reduce these angles. The scale-and-optimize process can now be repeated with a much improved chance of success. Note that, in general, the examination of the critical ray paths (typically those of the marginal rays) for large angles of incidence or refraction is a technique which will often indicate the source of a design problem.

2.9 Test Plate Fits, Melt Fits, and Thickness Fits

When the deleterious effects of fabrication tolerances become too large to bear, a technique commonly used to reduce these effects is to fit the lens design to the known values for the radius tooling and/or to the measured glass indices. The former is called a *test plate* (or *test glass* or *tooling*) fit; the latter is called a *melt fit*.

The *test plate fit* is begun by first obtaining a list of the available test plate radii from the shop which is scheduled to fabricate the lens. It is wise to ascertain that the radius values of the list are not just nominal values, but are based on accurate and recent measurements of the test plates, since there is often a significant difference between the two.

The fit is carried out as follows: A surface is selected at which to begin the process. This selection is based on one of the following criteria: (1) the surface most sensitive to change,* (2) the surface with the shortest radius, (3) the strongest surface [i.e., with the largest surface power $(n' - n)/r$], or (4) the surface which shows the largest curvature difference from the nearest available test plate radius. Very often all four of these criteria will indicate the same surface; if not, the choice of which one to use is almost a matter of taste. The nearest radius on the test plate list is substituted for the selected surface and the lens is reoptimized, allowing all the variable parameters to change

*Note that the relative sensitivity of any dimension of the system can be determined quite easily by making an incremental change in the dimension and noting the effect it produces on the merit function. This, of course, assumes a merit function which accurately represents the quality of the image.

failures. This works well, *provided* that for the lens configuration which is under consideration this is necessary, a drawing of the lens form which has successfully passed all the high rays and which surfaces are causing problems for angles of incidence or refraction (near 90°). Then the offending element can be replaced with elements which are shaped to reduce these effects. This process can now be repeated with access. Note that, in general, the examination (typically those of the marginal rays) for refraction is a technique which will often solve the problem.

ts, and

of fabrication tolerances become too large. One way used to reduce these effects is to fit the values for the radius tooling and/or to the former is called a *test plate* (or *test glass*) called a *melt fit*.

by first obtaining a list of the available plates which is scheduled to fabricate the lens. The radius values of the list are not just based on accurate and recent measurements. There is often a significant difference between

follows: A surface is selected at which to work. The selection is based on one of the following: (1) the surface which is most sensitive to change,* (2) the surface with the strongest surface [i.e., with the largest curvature], or (3) the surface which shows the largest curvature at the nearest available test plate radius. Very often the results will indicate the same surface; if not, the selection is almost a matter of taste. The nearest radius is substituted for the selected surface and the effect of all the variable parameters to change

any of any dimension of the system can be determined. A small change in the dimension and noting the effect it has on the image, of course, assumes a merit function which accurately predicts the image.

(except of course, the radius which has been set to the test plate value).

Another surface is then chosen and fixed to the nearest test plate radius; the lens is reoptimized again. This process is repeated until all the surfaces have been fitted to test plates. It is usually wise to avoid fitting both surfaces of a singlet (or all surfaces of a component) until all components have at least one fitted surface each. This allows the unfitted surface to vary and adjust for power, chromatic, and Petzval aberrations and the like for as long as possible.

With a reasonably complete test plate list, all radii can usually be fitted without significantly degrading the image quality (i.e., the merit function). In fact, the merit function is often slightly improved by this process, because of the additional cycles of optimization which have been performed. If the test plate list is limited or has a gap in it, it may not be possible to fit all the design radii to test plates without degrading the performance. In such a case, one must either fabricate new tooling and test plates, or seek a new vendor for the parts.

A *melt fit* reoptimizes the lens design by using measured data for the material indices instead of the nominal values from the glass catalog. This measured data comes in the form of what is called a *melt sheet* provided by the glass manufacturer or supplier. For noncritical applications, this data is usually sufficient. A worthwhile elaboration of the process is to determine the difference between the measured index values and the catalog values. These differences are then plotted against wavelength. This plot should be a smooth, relatively level line. A data point which does not plot smoothly is suspect; the measured data may well be in error. Next, a smoothly drawn curve through the points is used to determine improved values for the index differences. These differences are then applied to the catalog values to arrive at better values for the measured melt data, and the improved values are used in the melt fit reoptimization. The smoothed curve of differences can also be used to determine the index for wavelengths which are not included in the melt sheet.

An ordinary melt sheet will list the indices for the wavelengths of d, e, C, F, and g light. These are usually not individually measured. Instead, the index is measured for d light and the index difference between C and F light is measured. These two measurements are fed into a computer program which uses the known characteristics of the glass type to calculate the indices for e, C, F, and g light. This, while not ideal, is adequate for many, even most, applications. However, for some critical applications, and for all applications in which an attempt has been made to reduce or correct the secondary spectrum, it is usually quite unsatisfactory. For an additional charge, the glass manufacturer can provide what is usually called a *precision* melt sheet, for

which the indices have been measured individually, and to a greater precision. Index values for **wavelengths** specific to the application can also be measured. It is, of course, wise to subject even this data to the difference test and smoothing process described in the preceding paragraph.

We called the last of these fits a *thickness fit* in the heading for this section. This is a process which is carried out during the final assembly of the lens. In sum, one reoptimizes the lens by varying the air-spaces of the system, using accurately measured data for the radii, thicknesses, and indices of the fabricated elements. If the melt data and the test plate data are available, this just amounts to adding the measured element thicknesses and reoptimizing.

As can be seen, all of the above procedures are designed to almost completely eliminate the effects of the fabrication tolerances on the performance of the system. What is left, instead of the tolerances, is the uncertainty or inaccuracy of the various measurements on which the fits are based. The effect is usually quite modest and, therefore, acceptable. However, these uncertainties are, in fact, the exact equivalent of tolerances in determining the performance of the fabricated system.

2.10 Spectral Weighting

In any ray-tracing process, the index of refraction of the material is, of necessity, that corresponding to a single specific wavelength. Most lens *design* programs allow the use of only three wavelengths to represent the spectral bandpass for which the system is to be designed. Several *analysis* programs allow the use of five or ten suitably weighted wavelengths in calculating such things as MTF, point spread functions, radial energy distributions, and the like.

In either case, the question becomes, "What wavelengths should I use, and how should they be weighted?" For visual systems and just three wavelengths, the classical answer is to use d (or e), C, and F light, with weightings typically set at 1.0, 0.5, and 0.5 respectively. For other applications, this approximately corresponds to using the central wavelength and the wavelengths 25 percent from the extreme edges of the passband. If the results of an image analysis need not be especially precise, three wavelengths may be sufficient. For calculations done in the midst of the design process, this is often good enough to enable a judgment as to the relative merit of, or the rate of improvement between, two stages in the design process.

However, what should one do *in general*? To immediately dispose of the obvious, it is apparent that the more wavelengths that are used, the more accurate the results can be. That said, how do we select the

measured individually, and to a greater wavelength specific to the application can be made. It is wise to subject even this data to the same process described in the preceding paragraphs.

One often fits a *thickness fit* in the heading for this process which is carried out during the final assembly. This reoptimizes the lens by varying the air-glass interface using accurately measured data for the radii, thicknesses, and refractive indices of the fabricated elements. If the melt data is available, this just amounts to adding the thicknesses and reoptimizing.

The above procedures are designed to almost completely eliminate the effects of the fabrication tolerances on the system. What is left, instead of the tolerances, is the accuracy of the various measurements on which the design is based. This is usually quite modest and, therefore, the uncertainties are, in fact, the exact equivalent of determining the performance of the fabricated

lens. The index of refraction of the material is, of course, fixed to a single specific wavelength. Most designs use the use of only three wavelengths to represent the passband for which the system is to be designed. This allows the use of five or ten suitably spaced wavelengths in calculating such things as MTF, point spread function, energy distributions, and the like.

The question then becomes, "What wavelengths should I use and how should they be weighted?" For visual systems and just as a practical answer is to use d (or e), C , and F wavelengths, which are typically set at 1.0, 0.5, and 0.5 respectively. The number of wavelengths is approximately corresponds to using the extreme wavelengths 25 percent from the extreme ends of the passband. The results of an image analysis need not be used. For calculation of the design process, this is often good enough. The relative merit of, or the rate of improvement in the design process.

What do we do *in general*? To immediately dispose of the question; that the more wavelengths that are used, the better the results can be. That said, how do we select the

wavelengths to be used? There are three obvious choices. In order to assess the full effects of the chromatic aberrations, one would like to include the extreme long and short wavelengths. One would also probably like to consider dividing the spectral weighting function into increments of equal power or response, so that each wavelength would represent an equally weighted sector. But if this is done, the extremes of the spectral passband are not included. Another possible option is to choose wavelengths which are evenly distributed across the spectral band, and to weight them according to the spectral response function. One might choose an even distribution on a wavelength scale, or what might be a bit better, an even distribution on a wave number (reciprocal wavelength) scale.

From this it should be apparent that most wavelength and weighting choices are based on some sort of compromise. Often the outer two wavelengths are chosen to be fairly close to the ends of the passband and the intermediate wavelengths and weights are a compromise between an even power distribution and an even wavelength spacing. If there are peaks or bumps in the spectral response function, wavelengths are often selected to be at or near the peaks. Note that, to a limited extent, one's choices will partially control the design process: heavier weighting at the ends of the spectrum will obviously emphasize both primary and secondary chromatic aberration, spherochromatism, and the like; heavy weights on the central wavelengths will emphasize the monochromatic aberrations at the expense of the chromatic.

2.11 How to Get Started

Experienced designers are often asked questions such as "How do you know where to start?" or "How did you decide that a (name of a design type) could meet the specs?" or "Why did you shift the components around?"

The answer to these questions is almost always "Experience," which probably means that the full answer is different for every problem. It would be foolhardy to pretend to be able to give a complete, definitive answer or set of answers to such questions, but there are a few guidelines which should be reasonably dependable.

Figure 2.3 is, in effect, a compilation of some of that experience. If the system to be designed roughly corresponds to a photographic objective or to one of the other types indicated, the figure can be used as an easy guide to the selection of an appropriate form. In this plot the areas corresponding to various combinations of field and aperture are labeled to indicate the type of system which is commonly used there. Obviously the boundary of each area is fuzzy and ill-defined. In a pre-

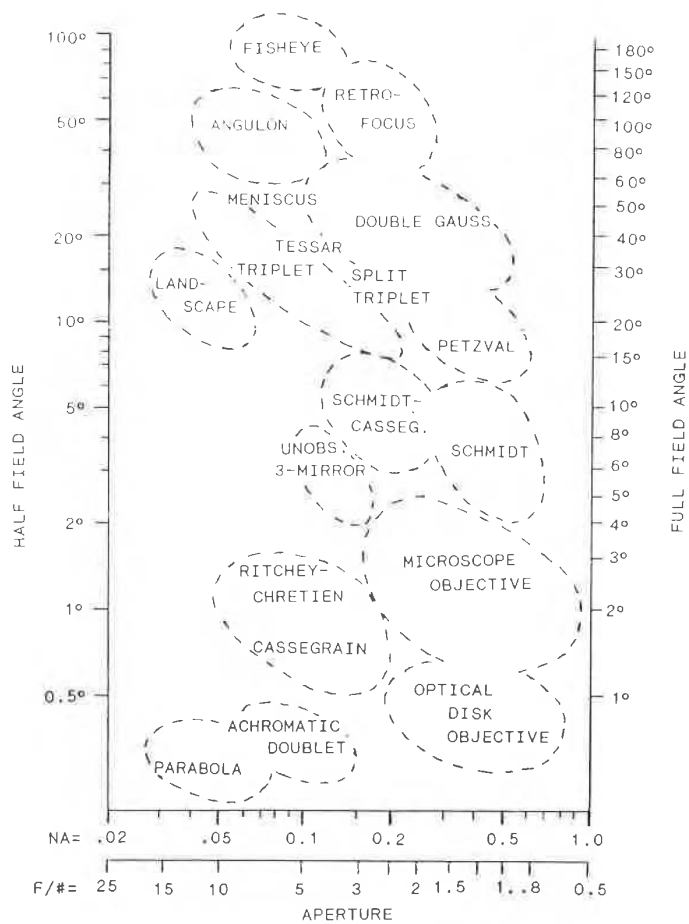


Figure 2.3 Map showing the design types which are commonly used for various combinations of aperture and field of view.

sentation of this type there is also an implied level of performance within each area, which is presumably typical of each particular lens type. In general, the performance (image quality, resolution, or whatever) is better when a given lens type is optimized for a smaller field and/or smaller aperture, that is, for a combination closer to the origin of the plot. Thus one can select the design type from Fig 2.3 corresponding to the field-aperture combination required with reasonable assurance that it is an appropriate choice. But should the performance

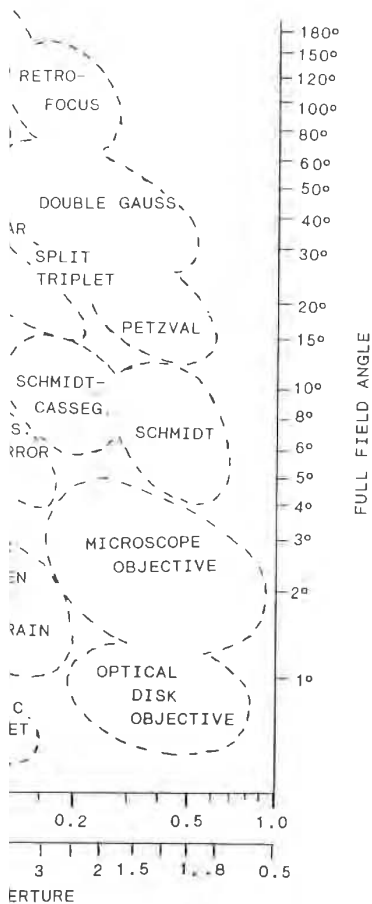


Figure 2.3 shows the performance capability of various lens types which are commonly used for a given field of view.

There is also an implied level of performance, presumably typical of each particular lens type. Each lens type is optimized for a smaller field of view, and it is, for a combination closer to the origin of the graph. To select the design type from Fig 2.3 correctly, one must make the appropriate choice. But should the performance

prove inadequate for the application at hand, one can move up to the form which is above and to the right on the plot, which should have a greater performance capability. Of course, if the required level of performance is known in advance to be relatively high, one would select the more capable type to begin with. The same selection approach can be applied to the components of a more complex system. There are many design types and applications which are not represented on this necessarily abbreviated chart. However, many of these are presented in the lens designs included in this book; the reader may wish to mark up Fig. 2.3 to add the types which are of particular interest.

For a complex system, the approach must start on a more fundamental level. The first step is to collect and tabulate the requirements to be met; these may include such things as:

- Resolution or performance (versus diffraction limit)
- Wavelength
- Fields of view
- Image size
- Aperture, numerical aperture (NA), and f number
- Vignetting or illumination uniformity
- Focal lengths or magnifications
- Space limitations

The next step is to make a first-order layout of the system which will satisfy the requirements. The first-order layout is simply an arrangement of component powers (or focal lengths) and spacings which will produce an image in the required location, in the required orientation, and of the required size. At this stage, no consideration is given to the design type of each component; one is concerned only with its power, aperture, and field as first-order, i.e., paraxial, characteristics. For systems (or portions of systems) which consist of two components, the equations of Sec. F.7 can be extremely useful. For more complex systems, the component by component ray-tracing equations of Sec. F.6 may be used. A general approach is to trace rays which will define the required characteristics. The ray-trace results (ray heights, ray slopes, intersection lengths, etc.) can be expressed as equations with the component powers and spacings as unknowns to be solved for. An important facet of this stage is that one should try to find a layout which minimizes the component powers, or minimizes (or equalizes) the "work" (ray height times component power). Doing this will almost always produce a system with less aberration residuals, one

which is less expensive to fabricate and less sensitive to fabrication and alignment errors.

Sometimes one can leap directly from the first-order layout to choosing the component design types, and thence to the optimization stage. However, if this is not the case, the next step is usually to analyze and/or correct the chromatic aberrations. Equations F.9.6 and F.10.7 can be used for the whole system, or the components can be individually achromatized. To this end, the element powers for a thin achromatic doublet are given by

$$\phi_A = \frac{V_A}{(V_A - V_B)F} \quad (2.1)$$

$$\phi_B = \frac{V_B}{(V_B - V_A)F} = \frac{1}{F} - \phi_A \quad (2.2)$$

and the element surface curvatures are determined from

$$C_1 - C_2 = \frac{\phi}{n - 1} = \frac{1}{r_1} - \frac{1}{r_2} \quad (2.3)$$

At this point a sketch of the system is often helpful. Simply make a scale drawing, showing each element as either a plano-convex or an equi-convex form (or plano-concave or equi-concave for negative elements). If the elements look too fat, they should be split into two or more elements. Be sure that the element diameters are sized properly for the rays that they must pass. At this stage the system should begin to look like a good lens.

The next step is to give some consideration to the Petzval curvature. Choosing suitable anastigmat types for the components is one way to handle this. Another is to use a field flattener in an appropriate location (i.e., near an image) in the system. And, of course, the usual device of configuring the system or component with separated positive and negative elements or surfaces to reduce the Petzval sum can always be utilized if a new design must be created from scratch.

Often many of these steps can be handled conveniently and expeditiously by the automatic design program. The first-order layout can be done with zero-thickness plano-convex or plano-concave elements, allowing the spaces and the curvatures of the curved surfaces (but not the plano surfaces) to vary. The merit function is a simple one, configured to define the required first-order characteristics. Note well the comments in Sec. 2.5 regarding stagnation and contradictory or redundant first-order entries in the merit function.

Since the chromatic aberrations and the Petzval curvature depend on element power and not on element shape, the lens design program

abricate and less sensitive to fabrication
 ectly from the first-order layout to choos-
 es, and thence to the optimization stage.
 ase, the next step is usually to analyze
 aberrations. Equations F.9.6 and F.10.7
 stem, or the components can be individu-
 nd, the element powers for a thin achro-

$$\phi = \frac{V_A}{(V_A - V_B)F} \quad (2.1)$$

$$\frac{V_B}{(V_B - V_A)F} = \frac{1}{F} - \phi_A \quad (2.2)$$

vatures are determined from

$$\phi_2 = \frac{\phi}{n-1} = \frac{1}{r_1} - \frac{1}{r_2} \quad (2.3)$$

ie system is often helpful. Simply make a
 element as either a plano-convex or an
 onconcave or equi-concave for negative ele-
 too fat, they should be split into two or
 the element diameters are sized properly
 ass. At this stage the system should begin

ne consideration to the Petzval curvature.
 at types for the components is one way to
 e a field flattener in an appropriate loca-
 the system. And, of course, the usual de-
 m or component with separated positive
 rfaces to reduce the Petzval sum can al-
 sign must be created from scratch.

can be handled conveniently and expedi-
 gn program. The first-order layout can be
 no-convex or plano-concave elements, al-
 urvatures of the curved surfaces (but not
 he merit function is a simple one, config-
 first-order characteristics. Note well the
 ding stagnation and contradictory or re-
 n the merit function.

tations and the Petzval curvature depend
 n element shape, the lens design program

can also be used to find a layout which is a preliminary solution with
 the chromatic and Petzval adjusted to desired, reasonable values,
 which typically should be small and negative.

Sometimes it is useful as a next step to allow the elements to bend,
 and to correct the third-order aberrations. This can be done by putting
 an angle-solve on the second surface of each element so that the axial
 ray slope is maintained. More often than not, however, the next step
 will skip over the third-order and go directly to a full-dress thick lens
 optimization run.

And, of course, in the best of all worlds, one simply sets up what seems
 to be a likely layout and proceeds directly to the automatic lens design
 program, which promptly turns out an excellent design. "Experience!"
 Lots of luck!



Improving a Design

3.1 Standard Improvement Techniques

There are several classic design modification techniques which can be reliably used to improve an existing lens design. They are:

1. Split an element into two (or more) elements
2. Compound a singlet into a doublet (or triplet)
3. Raise the index of the positive singlets
4. Lower the index of the negative singlets
5. Raise the index of the elements in general
6. Aspherize a surface (or surfaces)
7. Split a cemented doublet
8. Use unusual partial dispersion glasses to reduce secondary spectrum (see Chap. 6, "Telescope Objectives")

The simple, straightforward application of these techniques is no guarantee of improvement in a lens, in that they do not automatically correct the defects that they are intended to address. In general, these changes tend to reduce the aberration contributions of the modified components; in order to take full advantage of this, the aberrations of the balance of the system must be reduced as well. The operative principle is this: if large amounts of aberrations are corrected or balanced by equally large amounts of aberrations of opposite sign, then the residual aberrations also tend to be large. Conversely, if the balancing aberrations are both small, then the residuals tend to be correspondingly small.

3.2 Glass Changes: Index and V Value

The refractive characteristics of the materials used in a lens are obviously significant and important to the design. In general, for a posi-

tive element, the higher the index the better. The higher index reduces the inward Petzval curvature which plagues most lenses. It also tends to reduce most of the other aberrations as well. As an example, see Fig. 3.1, which clearly indicates the effect of higher index in reducing the spherical aberration of a single element. This sort of reduction is primarily a result of the fact that the surface curvature required to produce a given element power is inversely proportional to

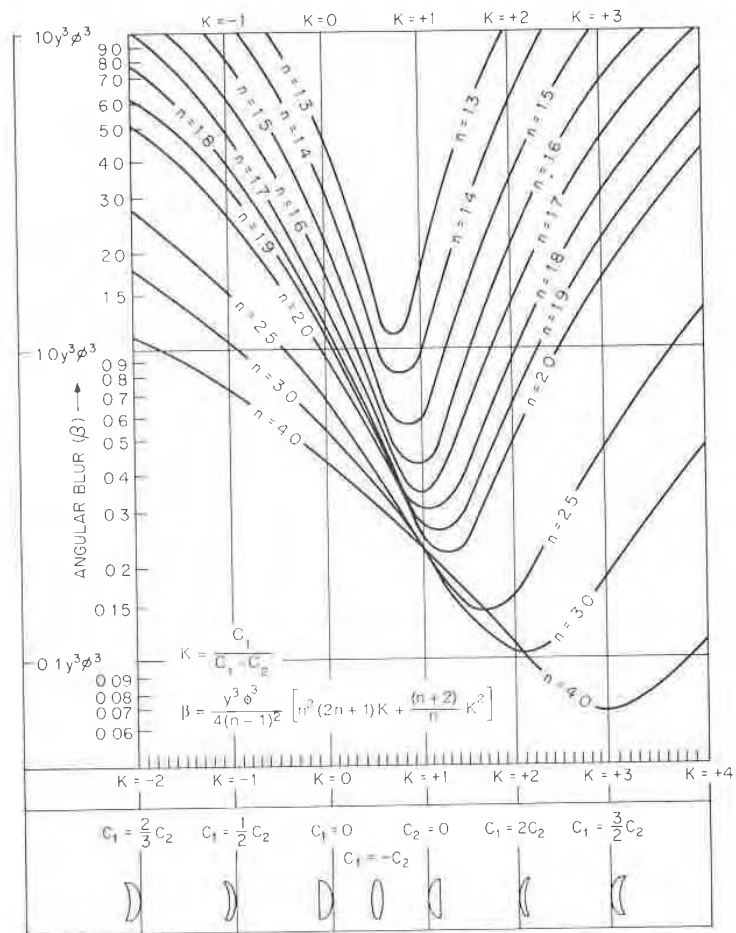


Figure 3.1 The angular spherical aberration blur of a single lens element as a function of lens shape, for various values of the index of refraction; ϕ is the element power and y is the semiaperture. The angular blur can be converted to longitudinal spherical aberration by $LA = 2B/y\phi^2$, or to transverse aberration by $TA = -2B/\phi$. (The object is at infinity.)

index the better. The higher index refractive index which plagues most lenses. It also corrects other aberrations as well. As an example, Figure 3.1 indicates the effect of higher index in the correction of a single element. This sort of reduction is due to the fact that the surface curvature required to give a certain element power is inversely proportional to

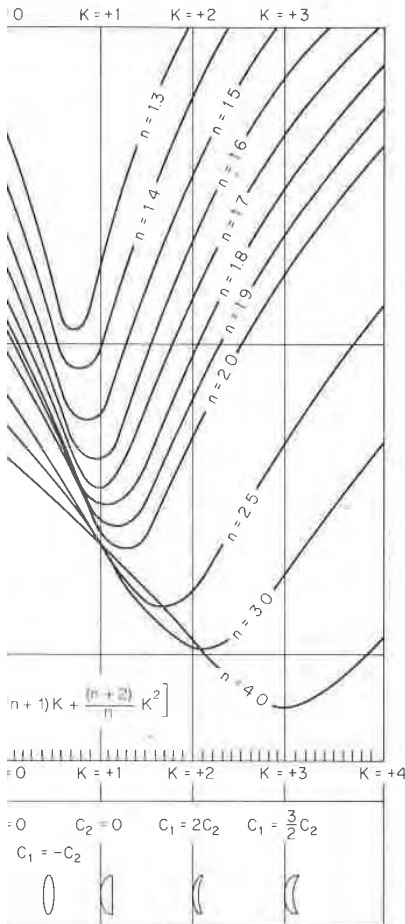


Figure 3.1. The aberration blur of a single lens element as a function of the index of refraction; ϕ is the element power. The angular blur can be converted to longitudinal blur by $A = 2B/y\phi^2$, or to transverse aberration by $(A/2)$.

$(n - 1)$. The improvement also results from the reduction of the angles of incidence at the surfaces of the element.

In a negative element, the situation is less clear. From the standpoint of the Petzval correction, a low index would increase the overcorrecting contribution of a negative element. This can help to offset the (inward) undercorrection which is a major problem in most lenses. On the other hand, a higher index would reduce the surface curvatures and have a generally desirable effect on the overall state of correction. The situation is usually resolved with the negative elements made from a glass along the glass line boundary of the glass map (Fig. 2.2).

A high V value for the positive element and a low V value for the negative element of an achromatic doublet reduce the element powers; this is ordinarily desirable. In lenses (such as the Cooke triplet) where the relative V values of separated elements control the element spacing or the system length, this desideratum may be overridden by other concerns.

Note that, as usual, when you are dealing with components of negative focal length, many of the considerations outlined above are reversed. In a negative achromatic doublet, the negative element is often made of crown glass and the positive is made of flint. Here a high-index (flint) positive element will reduce the inward Petzval curvature, as will a low-index (crown) negative element.

3.3 Splitting Elements

Splitting an element into two (or more) approximately equal parts whose total power is equal to the power of the original element can reduce the aberration contribution by a significant factor. The reason that this reduces aberrations is that it allows the angles of incidence to be reduced; the nonlinearity of Snell's law means that smaller angles introduce less aberration than do large ones. This technique is often used in high-speed lenses to reduce the zonal spherical residual and in wide-angle lenses to control astigmatism, distortion, and coma.

Figure 3.2 shows the thin lens third-order spherical aberration for spherical-surfaced positive elements which are shaped (or bent) to minimize the undercorrected spherical. The upper plot shows the spherical aberration as a function of the index of refraction for a single element with a distant object. The curve labeled $i = 2$ shows the spherical aberration for two elements whose total power is equal to that of the single element. The best split is 50-50—i.e., the split elements have equal power; this minimizes the spherical. (The same is true for a split into more than two elements, i.e., three, four, etc., as shown in the curves labeled $i = 3$ and $i = 4$.) The improvement produced by splitting an element in

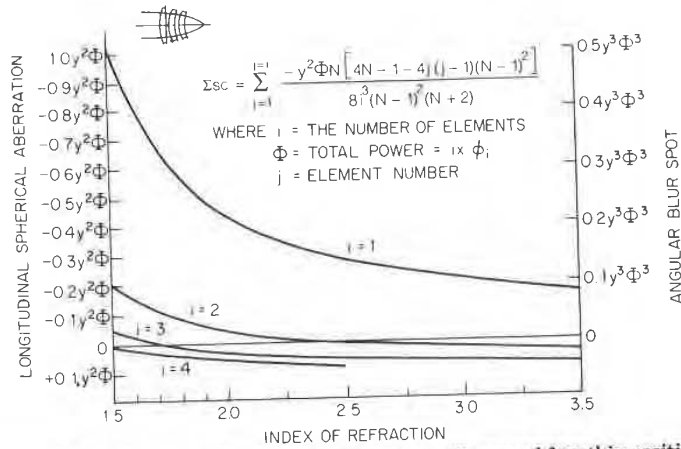
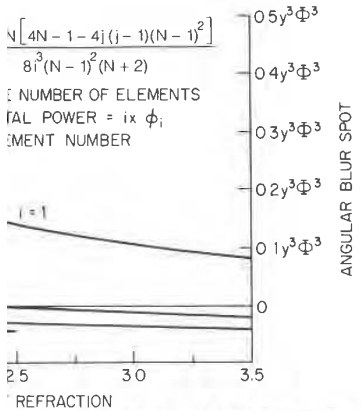


Figure 3.2 The spherical aberration of one, two, three, and four thin positive elements, each bent for minimum spherical aberration, plotted as a function of the index of refraction, and showing the reduction in the amount of aberration produced by splitting a single element into two or more elements (of the same total power). Each plot is labeled with i , the number of elements in the set. (The object is at infinity.)

two can be seen to be a factor of about 5 for lenses of index equal to 1.5. The higher the index, the greater the reduction; for an index of 1.8, the factor is about 7. At an index of 2.5 or higher, the spherical can be brought to zero or even overcorrected with just two positive elements. Most other aberrations are similarly affected by splitting, although it should be obvious that neither Petzval nor chromatic is changed by splitting.

In high-speed lenses this technique is frequently used to reduce the residual zonal spherical; the positive elements are split. This illustrates the basic idea. If the residual zonal spherical is negative (undercorrected), one splits a positive element; in the rare event that the zonal is positive (overcorrected), one would split a negative element. A similar philosophy can be applied for troublesome residuals of the other aberrations as well.

The choice of which element to split is often less apparent. The logical candidate would obviously seem to be the element which contributes most heavily to the problem aberration. (An examination of the third- and fifth-order surface contributions can often locate the source of the aberration.) However, other considerations often become significant. For example, in the Cooke triplet, the rear element is the prime candidate for the split, and such a split is quite effective in reducing



of one, two, three, and four thin positive spherical aberration, plotted as a function of refractive index. The reduction in the amount of aberration is shown for splitting one element into two or more elements (of equal power), labeled with i , the number of elements in

or of about 5 for lenses of index equal to the greater the reduction; for an index of about 2.5 or higher, the spherical aberration overcorrected with just two positive elements are similarly affected by splitting, also that neither Petzval nor chromatic is

technique is frequently used to reduce the zonal spherical aberration. This illustrates that the residual zonal spherical is negative if the original lens is overcorrected with a positive element; in the rare event that the lens is undercorrected, one would split a negative element. This technique can be applied for troublesome residuals of zonal spherical aberration.

When the lens is overcorrected, the element to split is often less apparent. The logarithmic scale seems to be the element which contributes most to the problem aberration. (An examination of the logarithmic scale contributions can often locate the source of the problem; other considerations often become significant. In a Cooke triplet, the rear element is the prime candidate for such a split is quite effective in reducing

the zonal spherical, as Figs. 14.1 and 14.2 will attest. But the better choice for the split is the front element, not because it does a better job of reducing the zonal spherical, but because the resulting lens is better corrected for the other aberrations. Figure 14.3 shows the simple split-front triplet. This is the ancestor of the Ernstar family of lenses; Figs. 14.10 through 14.15 illustrate designs which can be considered as descendants from the split-front triplet. Although they have been largely superseded by the more powerful double-Gauss form, they are nonetheless excellent design types.

Many retrofocus and wide-angle lenses which use strong outer meniscus negative elements illustrate the use of this technique for the control of coma, astigmatism, and distortion by splitting these negative elements.

The implementation of this technique with an automatic design program is often far from easy. For example, if one decides to split one of the crowns of a Cooke triplet and simply replaces one crown with two, after the computer optimization has run its course, the resultant lens may look like an ordinary triplet with a narrow cracklike airspace in the split element (a *cracked crown triplet*). The performance of the lens is the same as the original triplet; the split has not improved a thing. This is because the original lens was in a local optimum of the merit function. Aberrations other than the zonal spherical dominated the design; this caused the program to return the lens to its original design configuration. What is necessary in this situation is to force the split elements into a configuration which will accomplish the desired result.

Consider the split-front triplet. There are two ways to get to a design like Fig. 14.3. One approach is to make the lens so fast that the zonal spherical is by far the single dominant aberration in the merit function. Then the program will probably choose a form which reduces the zonal spherical; the lens shapes in Fig. 14.3 are a likely result. A difficulty with this approach may be that you aren't interested in a very fast lens, or if you are, the rays may miss the surfaces of the initial design completely, or encounter TIR. The alternative approach is to constrain the front elements to a configuration in which the zonal spherical is minimized. Simply fixing the first element to a plano-convex form (by not allowing the plano surface curvature to vary) or holding the second to an aplanatic meniscus shape is usually sufficient to obtain a stable design which is enough different from the cracked crown triplet. When this has been accomplished the constraint can be released and the automatic design routine allowed to find what is (one hopes) a new and better local optimum. The problem here is that this approach presupposes a knowledge of the configuration which will

produce a good result. Obviously a knowledge of both aberration theory and of successful design forms is a useful tool to the designer.

3.4 Separating a Cemented Doublet

Airspacing a cemented doublet can provide two additional degrees of freedom: two bendings instead of one, plus an airspace. While this technique does not have the inherent aberration reduction capability that many other modifications possess, the extra variables may indirectly make a design improvement possible. A difficulty in implementing this is that the refraction at the cemented surface is apt to become much more abrupt when it is split into two glass-air interfaces than when it was a cemented surface; in fact rays may encounter TIR if a simple split is attempted without a concomitant reduction of the angle of incidence. Manual intervention in the form of adjusting the radii to reduce the angle of incidence is often necessary.

3.5 Compounding an Element

Compounding a singlet to a doublet can be viewed in two different ways:

1. As a way of simulating a desirable but nonexistent glass type
2. As a way of introducing a cemented interface into the element in order to control the ray paths

Note that in almost all examples of Tessar-type lenses (and other types which utilize compounded elements), the doublets have positive elements with high index and high V values, while the negative element of the doublet has both a lower index and V value. See Chap. 12 for examples.

The longitudinal axial chromatic of a singlet is given by $LA_{ch} = -f/V$. Thus a fully achromatized lens (with $LA_{ch} = 0.0$) has the chromatic characteristic of a lens made from a material with a V value of infinity; a partially achromatized doublet acts like a singlet with a very high V value.

The Petzval radius of a singlet is given by $\rho = -nf$, where n is its index. An *old achromat* with a low-index crown and a higher-index flint has a shorter Petzval radius than a singlet of the crown glass. For example, an achromat of BK7 (517:649) and SF1 (717:295) has a Petzval radius $\rho = -1.37f$; in other words, in regard to Petzval field curvature, it behaves like a singlet with an index of 1.37. A *new achromat* has a high-index crown and a lower-index flint. A new

sly a knowledge of both aberration the-
rms is a useful tool to the designer.

Doublet

It can provide two additional degrees of
d of one, plus an airspace. While this
herent aberration reduction capability
s possess, the extra variables may indi-
ement possible. A difficulty in imple-
ction at the cemented surface is apt to
en it is split into two glass-air interfaces
surface; in fact rays may encounter TIR
without a concomitant reduction of the
tervention in the form of adjusting the
cidence is often necessary.

nt

doublet can be viewed in two different

desirable but nonexistent glass type

cemented interface into the element in
ths

mples of Tessar-type lenses (and other
ed elements), the doublets have positive
l high V values, while the negative ele-
a lower index and V value. See Chap. 12

chromatic of a singlet is given by
chromatized lens (with $LA_{ch} = 0.0$) has
of a lens made from a material with a V
achromatized doublet acts like a singlet

glet is given by $\rho = -nf$, where n is its
a low-index crown and a higher-index
ius than a singlet of the crown glass. For
K7 (517:649) and SF1 (717:295) has a
n other words, in regard to Petzval field
singlet with an index of 1.37. A new
crown and a lower-index flint. A new

achromat of SSKN5 (658:509) and LF5 (581:409) has a Petzval radius
 $\rho = -2.19f$ and a Petzval curvature which is characteristic of a
singlet with an index of 2.19.

Thus an achromatized (or partially achromatized) doublet with a
high-index positive element and a low-index negative element has
many of the characteristics of a lens made of a high-index, high- V -
value crown glass. (Note that for a negative focal length doublet, the
reverse is true.) Both conditions are usually to be desired, in order to
flatten the Petzval field and to achieve achromatism.

Figure 3.3 shows a singlet, an old achromat, and a new achromat,
each with the same focal length. The equivalent V value of each
achromat is, of course, equal to infinity. The Petzval radius for each is
given in the figure caption.

The cemented interface of the doublet can be used for specific control
of specific rays. In a lens such as the Tessar, where the doublet is
located well away from the aperture stop, the upper and lower rim
rays of the oblique fan have very different angles of incidence at the
cemented surface. In Fig. 3.4 it can be seen that the angle of incidence
at this surface is much larger for the upper ray than for the lower. In
this type of lens the cemented surface is typically a convergent one,
and the (trigonometric) nonlinear characteristic of Snell's law means
that the upper ray is, in this case, refracted downward more than it
would be were the refraction linear with angle. Thus the upper ray is
deviated in such a way as to reduce any positive coma of this ray. This

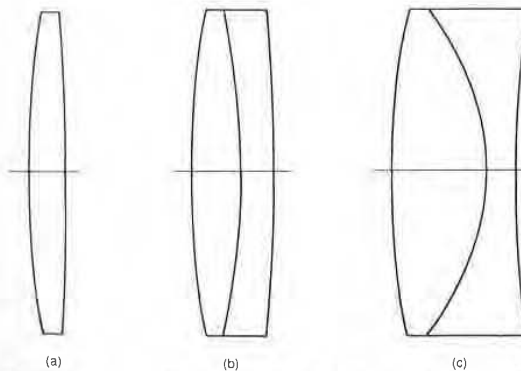


Figure 3.3 Three lenses, each with the same focal length f . (a) A singlet of BK7 (517:642) glass; Petzval radius equals $-1.52f$. (b) An old achromat of BK7 (517:642) and SF1 (717:295) glasses; Petzval radius equals $-1.37f$. (c) A new achromat of SSKN5 (658:509) and LF5 (581:409); Petzval radius is $-2.19f$.

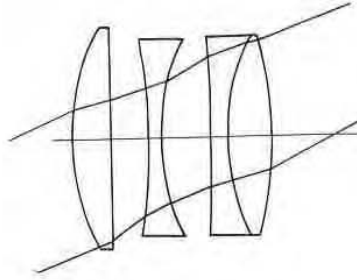


Figure 3.4 The upper and lower rim rays have significantly different angles of incidence at the cemented interface in the rear doublet of this Tessar design. Properly handled, this difference can be used to modify the correction of the coma-type aberrations.

illustrates the manner in which a cemented surface can be used for an asymmetrical effect on an oblique beam.

The Merté surface

A strongly curved, collective cemented surface with a small index break (to the order of 0.06) has an effect which can be used to reduce the undercorrected zonal spherical aberration. The central doublet of the Hektor lens shown in Fig. 3.5 illustrates this principle. The ce-

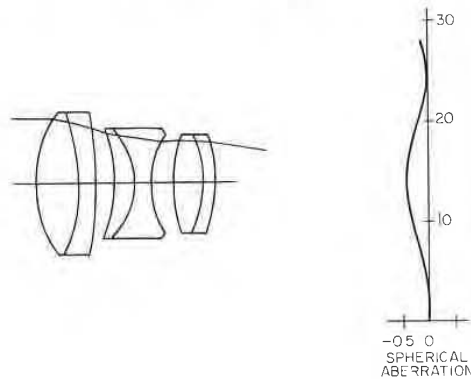
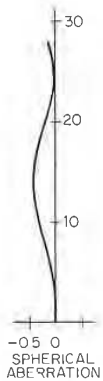


Figure 3.5 The cemented surface in the center doublet of this Hektor lens is what is called a Merté surface. The index break ($n' - n$) across the surface is small, but at the margin of the aperture the angle of incidence for the axial ray becomes quite large. This combination produces an undercorrecting seventh-order spherical aberration which, as the plot shows, dominates the spherical aberration at the margin of the aperture, causing the marginal spherical to be negative rather than the usual positive value.

Figure 3.4 The upper and lower rim rays have significantly different angles of incidence at the cemented interface in the rear doublet of this Tessar design. Properly handled, this difference can be used to modify the correction of the coma-type aberrations.

which a cemented surface can be used for an oblique beam.

tive cemented surface with a small index) has an effect which can be used to reduce spherical aberration. The central doublet of Fig. 3.5 illustrates this principle. The ce-



e in the center dou- s called a Merté sur- across the surface is perture the angle of nes quite large. This rcorrecting seventh-), as the plot shows, ion at the margin of inal spherical to be ositive value.

mented surface is a collective one (in that $[n' - n]/r$ is positive) and contributes undercorrected spherical aberration. For rays near the axis, the spherical aberration contribution of the surface is modest. However, when the ray intersection height increases and the angle of incidence becomes large, as shown in Fig. 3.5, the trigonometric nonlinearity of Snell's law causes the amount of ray deviation to be disproportionately increased. This causes the undercorrection from this surface to dominate the spherical aberration. The result is a spherical aberration characteristic like that shown in Fig. 3.5. The spherical in the central part of the aperture appears quite typical: the undercorrected third-order dominates close to the axis and the overcorrecting fifth-order causes the plot to curve back as the ray height increases. However, toward the edge of the aperture the undercorrection of the Merté surface becomes dominant and the aberration plot reverses direction again. The net result is the equivalent of a reduced zonal spherical aberration.

It is rare to see as extreme an example of the Merté surface as that illustrated in the Hektor of Fig. 3.5. Such a surface is very sensitive to fabrication errors and is thus expensive to make. It is also often best used close to the aperture stop because, if it is located away from the stop, the asymmetrical effects described two paragraphs above can become quite undesirable. However, it is well worth noting that an ordinary collective cemented surface has a tendency to behave as a mild Merté surface and to reduce the spherical zonal, at least somewhat.

3.6 Vignetting and Its Uses

Vignetting, which is simply the mechanical limitation or obstruction of an oblique beam, is usually regarded primarily as something which reduces the off-axis illumination in the image. However, vignetting often plays an essential role in determining the off-axis image quality as well as the illumination. Of course there are many applications for which vignetting cannot be tolerated; the illumination must be as uniform as possible across the entire field of view. The complexity of the lens design, therefore, must be sufficient to produce the required image quality at full aperture over the full field.

But for many applications, vignetting is, in fact, quite tolerable. In commercial applications the clear apertures may well be established so as to be just sufficient to pass the full aperture rays for the axial image. It is not at all unusual for vignetting to exceed 50 percent at the edge of the field. For a camera lens, this vignetting will, of course, completely disappear when the iris of the lens is stopped down to an aperture below the vignetting level. Since camera lenses are most of-

ten used at less than full aperture, the vignetting is not as significant as it is in a lens which is always used at full aperture, such as a microscope or projection lens.

The *benefit* of vignetting is that it cuts off the upper and/or lower rim rays of the oblique tangential fan. Since these are ordinarily the most poorly behaved rays, the image quality may well be improved by their elimination. Most lenses which cover a significant field are afflicted with oblique spherical aberration, a fifth-order aberration which looks like third-order spherical aberration, but which varies as the square of the field angle. And since its magnitude is different for sagittal than for tangential rays, it can be seen to have characteristics of both astigmatism and spherical aberration. Oblique spherical aberration usually causes the rays at the edge of the oblique bundle to show strongly overcorrected spherical aberration; vignetting is a simple way to block these aberrant rays from the image.

Another factor favoring the use of vignetting is that it results from lens elements with small diameters. In general, one can count on a smaller-diameter lens being less costly to fabricate.

For a camera lens, one must be certain that the iris diaphragm is located centrally in the oblique beam so that, when the iris is closed down, the central rays of the beam are the ones which are passed. These are usually the best-corrected rays of the oblique beam. Also this location assures that the vignetting will be eliminated at the largest possible aperture.

3.7 Eliminating a Weak Element; the Concentric Problem

Occasionally an automatic design program will produce a design with an element of very low power. Frequently this means that the element can be removed from the design without adversely affecting the quality of the design. Often a straightforward removal will not work; the design process may simply "blow up." An approach which usually works (if anything will) is to add the thickness and the surface curvatures of the element to the merit function with target values of zero, allowing them to continue as variable parameters. Sometimes targeting the difference between the two curvatures is also useful. Usually, if the element isn't necessary to the design, a few cycles of optimization, possibly with gradually increasing weights on these targets, will change the element to a very thin, nearly plane parallel plate, which can then be removed without severe trauma to the design. If your design program will not accept curvatures and thicknesses as targets, an alternative technique is to remove the curvatures and the thickness as variables and to gradually weaken the curvatures and reduce

ture, the vignetting is not as significant as for rays used at full aperture, such as a mi-

that it cuts off the upper and/or lower marginal fan. Since these are ordinarily the rays which cover a significant field, the image quality may well be improved by aspheric surfaces which cover a significant field are affected by spherical aberration, a fifth-order aberration, but which varies as the square of the field angle.

And since its magnitude is different for different rays, it can be seen to have characteristics of spherical aberration. Oblique spherical aberration is a fifth-order aberration; vignetting is a simultaneous effect of spherical aberration and vignetting.

One use of vignetting is that it results from a design which is less costly to fabricate.

It must be certain that the iris diaphragm is placed so that, when the iris is closed, the marginal rays are the ones which are passed. The corrected rays of the oblique beam. Also, the vignetting will be eliminated at the

ment; the

design program will produce a design with a spherical aberration. Frequently this means that the element is not thin without adversely affecting the quality of the design. The straightforward removal will not work; the "blow up." An approach which usually adds the thickness and the surface curvature to the merit function with target values of zero, and variable parameters. Sometimes target values for two curvatures is also useful. Usually, the design, a few cycles of optimization with increasing weights on these targets, will result in a thin, nearly plane parallel plate, which is a severe trauma to the design. If your merit function curvatures and thicknesses as targets, the design will remove the curvatures and the thicknesses, usually weaken the curvatures and reduce

the thickness (by hand) while continuing to optimize with the other variables.

An unfortunate form of the "weak" element is a fairly strongly bent meniscus, which the computer uses for a relatively important design function, such as the correction of spherical aberration or the reduction of the Petzval curvature. It is rarely possible to eliminate such an element because it is an integral part of the design. The unfortunate aspect of this situation is that, if the surfaces of the meniscus element are concentric or nearly so, the customary centering process used in optical manufacture is impossible or impractical, and the element is costly to fabricate. This situation can be ameliorated by forcing the centers of curvature of the surfaces apart by a distance sufficient to allow the use of ordinary centering techniques. Again, including the required center-to-center spacing in the merit function and reoptimizing will usually modify the offending element to a more manufacturable form without any significant damage to the system performance.

3.8 Balancing Aberrations

The optimum balance of the aberrations is not always the same in every case; the best balance varies with the application and depends on the size of the residual aberrations. In general, for well-corrected lenses, the aberrations should be balanced so as to minimize the OPD, i.e., the wavefront variance, but there are significant exceptions.

Spherical aberration

If a lens is well-corrected and the high-order residual spherical aberration is small, so that the OPD is to the order of a half-wave or less, then the best correction is almost always that with the marginal spherical corrected to zero, as illustrated in Fig. 3.6b. However, when the zonal spherical is large, there are two situations where one may want to depart from complete correction of the marginal spherical.

If the lens will always be used at full aperture (as a projection lens, for example), and if the spherical aberration residual is large (say to the order of a wave or so), the diffraction effects will be small when compared to the aberration blur; then the spherical aberration should be corrected to minimize the size of the blur spot rather than to minimize the OPD. This will produce the best contrast for an image with relatively coarse details, i.e., for a resolution well below the diffraction limit. As an example, at a speed of $f/1.6$, a 16-mm projection lens has a diffraction cutoff frequency of about 1100 line pairs per millimeter (lp/mm). But its performance is considered quite good if it resolves 100

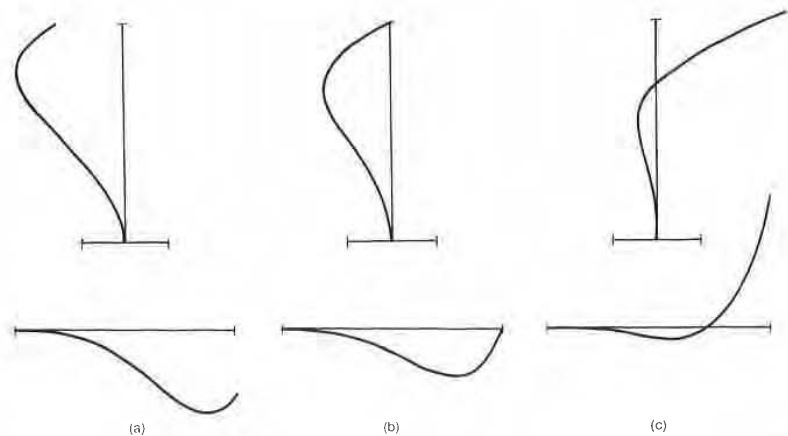
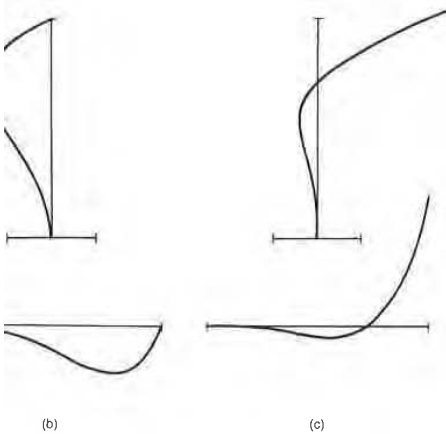


Figure 3.6 Three states of correction of spherical aberration are shown. Each has the same amount of fifth-order spherical, but different amounts of third-order. (a) Spherical aberration balanced to give the smallest possible size blur spot. This correction may be optimum when the aberration is large and the required level of resolution is low compared to the diffraction limit. (b) Spherical aberration balanced for minimum OPD. This is optimum when the system is diffraction-limited. (c) Spherical aberration balanced to minimize the focus shift as the lens aperture is stopped down. This correction is used in camera lenses when the residual spherical is large. The upper row is longitudinal spherical versus ray height; the lower row is transverse ray intercept plots.

lpm, an order of magnitude less than the diffraction limit. Such a lens can advantageously be corrected for the minimum diameter geometrical blur spot. This state of correction occurs (for third- and fifth-order spherical) when $LA_z = 1.5LA_m$, or $TA_z = 1.05TA_m$; the result is a high-contrast, but low-resolution, image. This correction is illustrated in Fig. 3.6a. See also the comments on defocusing in Secs. 2.4 and 2.7.

For a lens which is used at varying apertures, as is a typical camera lens, it is important that the best focus position not shift as the size of the aperture stop is changed. If the spherical aberration is corrected at the margin of the aperture, or corrected as described in the paragraph above, the position of the best focus will shift as the aperture is changed. The best focus will move toward the paraxial focus as the aperture is reduced. The state of correction which is often used in such a case is overcorrection of the marginal spherical, as shown on Fig. 3.6c (assuming an undercorrected zonal residual). The result is a design in which the focus is quite stable as the lens is stopped down. The *resolution* is better than it would be otherwise, but, at full aperture, the *contrast* in the image is quite low. This works out reasonably well in a high-speed camera lens because camera lenses are only infrequently used at full aperture. Typically, photographs are taken with the lens



Three different correction states of spherical aberration are shown. Each has the same amount of fifth-order spherical aberration, but different amounts of third-order. (a) Spherical aberration corrected for the smallest possible size blur spot. This correction may be used when the required level of resolution is low and the aberration is diffraction-limited. (b) Spherical aberration balanced for minimum OPD. This correction is used in most commercial lenses. (c) Spherical aberration balanced to the aperture is stopped down. This correction is used in lenses where the resolution is large. The upper row is longitudinal spherical aberration plots, and the lower row is transverse ray intercept plots.

less than the diffraction limit. Such a lens is used for the minimum diameter geometrical resolution occurs (for third- and fifth-order spherical aberration, TA_m , or $TA_z = 1.05TA_m$; the result is a diffraction-limited image. This correction is illustrated in Figs. 3.6a and 3.6b. For varying apertures, as is a typical camera lens, the best focus position not shift as the size of the aperture is changed. If the spherical aberration is corrected at the center of the aperture, the best focus will shift as the aperture is stopped down. The correction is often used in such a design where the marginal spherical aberration is large, as shown on Fig. 3.6c (the result is a design in which the resolution is low as the lens is stopped down. The resolution is low, but, at full aperture, the resolution is high. This works out reasonably well in most camera lenses are only infrequently used, photographs are taken with the lens

stopped down well below the full aperture, and, when the camera is stopped down, this state of correction yields a much better photograph.

The three correction states shown in Fig. 3.6 also indicate the manner in which the spherical aberration is changed when the third-order spherical aberration is changed. This is a typical situation often encountered in lens design: the fifth- (and higher-) order aberrations are relatively stable and difficult to change, but the third order is easily modified (by bending an element, for example). In the figure, all three illustrations have exactly the same amount of fifth-order spherical; the difference is solely in the amount of third-order. Note that, in the (upper) longitudinal plots, the change from one illustration to the next varies as y^2 , whereas in the (lower) transverse plots the differences vary as y^3 .

Chromatic aberration and spherochromatism

Here the question is how to balance the spherochromatism, which typically causes the spherical aberration at short (blue) wavelengths to be overcorrected and that at the long (red) wavelengths to be undercorrected. If the aberration is small (diffraction-limited), the best correction is probably with the chromatic aberration corrected at the 0.7 zone of the aperture. This means that the central half of the aperture area is undercorrected for color and the outer half of the aperture is overcorrected, as shown in Fig. 3.7a. But if the amount of the aberration is large, the spherical overcorrection of the blue marginal ray causes a blue flare and a low contrast in the image. In these circumstances the correction zone can advantageously be moved to (or toward) the marginal zone, as shown in Fig. 3.7b. This will probably reduce the resolution somewhat, because it increases the size of the core of the image blur, but it improves the contrast significantly and yields a more pleasing image, free of the blue flare and haze. This state of correction is accomplished by increasing the undercorrection of the chromatic aberration of the paraxial rays.

Astigmatism and Petzval field curvature

In a typical anastigmat lens the fifth-order astigmatism tends to become significantly undercorrected (i.e., negative) as the field angle is increased. In order to minimize the astigmatism over the full field, the third-order astigmatism is made enough overcorrected to balance the undercorrected fifth-order astigmatism. The result is the typical field curvature correction with the sagittal focal surface located inside the tangential focal surface in the central part of the field because of the overcorrected third-order astigmatism, and the reverse arrangement

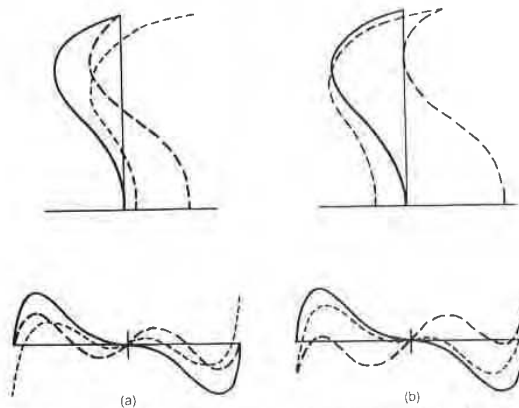
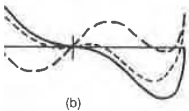
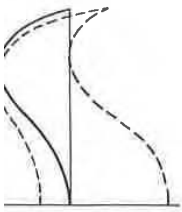


Figure 3.7 Spherochromatism. (a) Chromatic aberration balanced so that the outer half of the aperture is overcorrected and the inner half is undercorrected. This may be best if the amount of aberration is small. (b) Chromatic aberration balanced so that it is corrected at the margin. If the aberration is large, this correction eliminates the blue flare which can result from the type of correction in (a). Note that the state of correction is more easily perceived in the upper, longitudinal aberration plots, whereas the effect on the blur spot size and flare is much more apparent in the lower transverse ray intercept plots.

in the extreme outer portions. The field angle at which the s and t fields cross (i.e., where the astigmatism is zero) is called the *node*. Usually the two fields separate very rapidly outside the node, and the image quality quickly deteriorates, often suddenly. The Petzval curvature is usually made somewhat negative, so that both fields are slightly inward-curving and the effective field is as flat as possible. A typical state of correction is shown in Fig. 3.8.

Note that a field correction with the s and t focal surfaces spaced equally on either side of the focal plane (so that the compromise "smallest circle of confusion" focal surface is flat) is definitely *not* the best state of correction. In considering the correction of the field curvature, one should bear in mind that the oblique spherical aberration (a fifth-order aberration which varies as the cube of the aperture and the square of the field angle) typically goes overcorrected with increasing field angle. In addition, the oblique spherical is usually more significant for the tangential fan of rays than for the sagittal. Thus the effective field curvature for the full fan of rays is usually more backward-curving than the X_s and X_t field curves indicate. These curves indicate the imagery of a very small bundle of rays close to the principal ray, and do not take the oblique spherical of the full aperture



Chromatic aberration at the aperture is overcorrected. This may be small. (b) Chromatic aberration at the margin. If the image is overcorrected, it eliminates the blue flare effect in (a). Note that the effect perceived in the upper part of the image is the effect on the blur apparent in the lower part of the image.

The field angle at which the s and t astigmatism is zero is called the *node*. It varies very rapidly outside the node, and the astigmatism often varies, often suddenly. The Petzval curvature is somewhat negative, so that both fields are as flat as possible. The effective field is as flat as possible. As shown in Fig. 3.8.

With the s and t focal surfaces spaced so that the focal plane (so that the compromise focal surface is flat) is definitely *not* the same as the correction of the field curvature and that the oblique spherical aberration varies as the cube of the aperture and is typically goes overcorrected with increasing aperture, the oblique spherical is usually more negative than the sagittal. Thus the effective field of view is usually more negative than the sagittal. These field curves indicate. These field curves indicate. These field curves indicate.

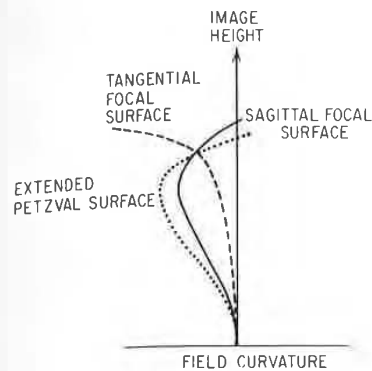


Figure 3.8 This is the typical balance of astigmatism and Petzval curvature in the presence of undercorrecting fifth-order astigmatism and overcorrecting high-order Petzval curvature. This is achieved by leaving the third-order Petzval slightly inward-curving and overcorrecting the third-order astigmatism by a small amount. This is the usual aberration balance for most anastigmats.

into account. Thus, for most designs, the astigmatism and field curvature are usually arranged somewhere between the state at which the s and t curves are superimposed (i.e., zero astigmatism) and that at which the t field is approximately flat. Often a through-focus MTF plot which includes both on-axis and off-axis plots will indicate quite clearly the effective field curvature, which is, of course, more informative than the X_s and X_t curves.

Note well that these discussions have assumed the type of higher-order residual aberrations which one ordinarily finds: overcorrected fifth-order spherical aberration, undercorrected fifth-order astigmatism, and overcorrected spherochromatism for the shorter wavelengths. Although rare, the reverse is sometimes encountered. In such circumstances the obvious move is to apply the above advice in reverse.

As an additional consideration, note that the undercorrection of either the chromatic aberration or the Petzval curvature has the usually desirable side effect of reducing the power of the elements of the lens system. Thus a secondary benefit of this undercorrection is the reduction of residual aberrations in general, because a lower-power element produces less aberration, which means that there is less higher-order residual aberration left when the aberrations are balanced out.

3.9 The Symmetrical Principle

When an optical system has mirror symmetry about the aperture stop (or a pupil), as shown in Fig. 3.9, the system is free of coma, distortion, and lateral color. This results from the fact that the components on one side of the stop have aberrations which exactly cancel the aberrations from the components on the other side of the stop. Obviously, to have mirror symmetry, the system must work at unit magnification,

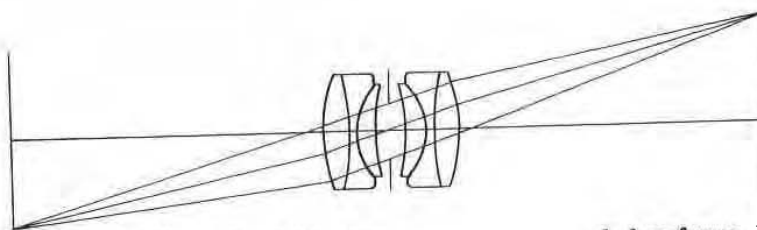


Figure 3.9 A fully (left to right) symmetrical system is completely free of coma, distortion, and lateral color, because the aberration in one half of the system exactly cancels out the aberration in the other half.

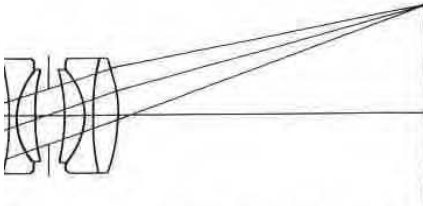
with equal object and image distances. For the symmetry to be *absolutely* complete, the object and image surfaces must be identical in shape; this then would imply separately curved sagittal and tangential surfaces at both object and image. However, the third-order coma, distortion, and lateral color are completely removed by symmetry, even with flat object and image surfaces.

Of course, most systems do not operate at unit magnification, and therefore a symmetrical construction of the lens will not completely eliminate these aberrations. However, even for a lens with an infinitely distant object, these aberrations are markedly reduced by symmetry, or even by an approximately symmetrical construction. This is why so many optical systems which cover a significant angular field display a rough symmetry of construction. Consider the Cooke triplet: it has outer crown elements which are similar, but not identical in shape, and the center flint, while not equi-concave, is bi-concave, and, except for slow-speed triplets, the airspaces are quite similar in size. The benefit of this is that the higher-order residuals of coma, distortion, and lateral color are markedly reduced by this symmetry. This is especially true for wide-angle lenses when good distortion correction is important.

3.10 Aspheric Surfaces

Many designs can be improved by the use of one or more aspheric surfaces. Except for the case of a molded or diamond-turned element, an aspheric surface is many times more expensive to fabricate than a spherical surface. A conic aspheric is easier to test than a general aspheric and is therefore somewhat less costly. For many systems, e.g., mirror objectives, aspheric surfaces are essential to the design and cannot be avoided.

One technique for introducing an aspheric into an optical system is to first vary only the conic constant. (Note that the conic constant and



A symmetrical system is completely free of coma, distortion, and spherical aberration in one half of the system exactly cancelled by the other half.

distances. For the symmetry to be absolute, the image surfaces must be identical in shape. The separately curved sagittal and tangential image surfaces. However, the third-order coma, astigmatism, and distortion are completely removed by symmetry, as are the spherical surfaces.

Systems do not operate at unit magnification, and the construction of the lens will not completely correct for distortion. However, even for a lens with an infinite number of aspheric surfaces, the aberrations are markedly reduced by symmetry. This is particularly true for systems which cover a significant angular field of view. Consider the Cooke triplet: the three lenses are similar, but not identical in shape. The first lens is biconcave, the second is biconvex, and the third is biconcave, and the airspaces are quite similar in size. The higher-order residuals of coma, distortion, and astigmatism are markedly reduced by this symmetry. This is particularly true for systems with a large number of lenses when good distortion correction

is achieved by the use of one or more aspheric surfaces. A diamond-turned or molded element, although more expensive to fabricate than a spherical lens, is easier to test than a general aspheric lens, somewhat less costly. For many systems, aspheric surfaces are essential to the design.

Incorporating an aspheric into an optical system is not a simple task. (Note that the conic constant and

the fourth-order deformation term have exactly the same effect on the third-order aberrations. Thus, allowing both to vary in an automatic design program may cause a slowing of the convergence or, in extreme cases, a failure of the process. Occasionally the difference between the effect of the conic and the fourth-order term on the fifth- and higher-order aberrations may be useful in a design, but more often than not the two are redundant.) If the effect of varying the conic constant alone is inadequate, one can then allow the sixth-order term to vary, then the eighth-order, etc. Some designs have aspherics specified to the tenth-order term when just the sixth or eighth would suffice. It is a good idea to calculate the surface deformation caused by the highest-order term used; if it is a fraction of a wave at the edge of the surface aperture, its utility may well be totally imaginary.

Occasionally one encounters a design specification or print in which the aspheric is specified by a tabulation of sagittal heights instead of an equation. The optimization program can be used to fit the constants of the standard aspheric surface equation to the tabulated data. The specification table is entered in the merit function as the sag of the intersections of (collimated) rays at the appropriate heights. The surface coefficients are allowed to vary, and the result is a least-squares fit to the sag table.

The equations of Sec. F.11 indicate the effects of a conic or a fourth-order aspheric term on the third-order aberrations. Several points are worthy of note. The conic has no effect on the Petzval curvature or on axial or lateral chromatic. Further, if the conic is located at the aperture stop or at a pupil, then the principal ray height, y_p , is zero and the conic has no effect on third-order coma, astigmatism, or distortion; it can only affect third-order spherical aberration. In the Schmidt camera the aspheric surface is located at the stop because the coma and astigmatism are already zero, because the stop is at the center of curvature of the spherical mirror; the purpose of the aspheric is to change *only* the spherical aberration. Conversely, if the purpose of an aspheric is to affect the coma, astigmatism, or distortion, then it must be located a significant distance from the aperture stop.

It is also worth noting that the primary effect of the conic, or fourth-order, deformation term is on the third-order aberrations. The primary effect of the sixth-order deformation term is on the fifth-order aberrations, etc., etc.



Evaluation: How Good Is This Design?

4.1 The Uses of a Preliminary Evaluation

At some point in the process of designing an optical system, the designer must decide whether the design is good enough for the application at hand. With modern computing power, it is not a difficult matter to calculate the MTF or the point spread function (PSF), and to accurately include the effects of diffraction in the calculations. The process does consume a finite amount of time, however (which, on a slow computer, may be a significant amount), and it is useful to be able to make a reasonable estimate of the system performance from a more limited amount of data. A good estimate can avoid wasting time and computer paper in evaluating a clearly deficient design, or it can signal an appropriate point at which to conduct a full-dress evaluation.

4.2 OPD versus Measures of Performance

The distribution of illumination in the point spread function, particularly in the diffraction pattern of a reasonably well-corrected lens, is often used as a measure of image quality. The *Strehl ratio* (or *Strehl definition*) is the ratio of the illumination at the center of an (aberrated) point image to the illumination at the center of the point image formed by an aberration-free system. Figure 4.1 illustrates the concept. Another measure of image quality uses the percentage of the total energy in the point image which is contained within the diameter of the Airy disk. This diameter remains relatively constant in size for small amounts of aberrations. The table of Fig. 4.2 gives the relationships between the wavefront deformation (or OPD), the Strehl ratio, and the energy distribution.

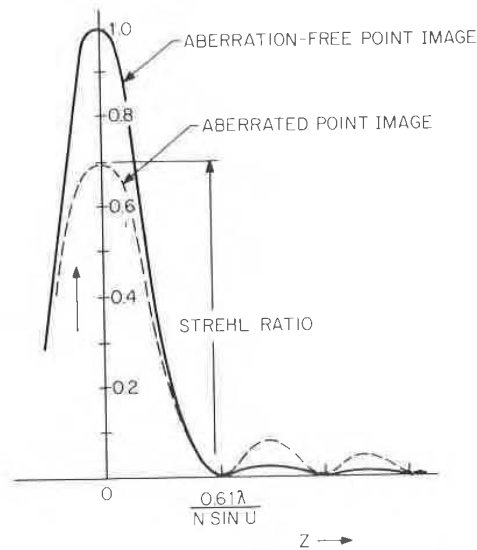


Figure 4.1 The Strehl ratio is the illumination at the center of the diffraction pattern of an aberrated image, relative to that of an aberration-free image.

Relation of Image Quality Measures to OPD				
P-V OPD	RMS OPD	Strehl Ratio	% energy in	
			Airy Disk	Rings
0.0	0.0	1.00	84	16
0.25RL = $\lambda/16$	0.018 λ	0.99	83	17
0.5RL = $\lambda/8$	0.036 λ	0.95	80	20
1.0RL = $\lambda/4$	0.07 λ	0.80	68	32
2.0RL = $\lambda/2$	0.14 λ	0.4 ^a	40	60
3.0RL = 0.75 λ	0.21 λ	0.1 ^a	20	80
4.0RL = λ	0.29 λ	0.0 ^a	10	90

^aThe smaller values of the Strehl ratio do not correlate well with image quality.

Figure 4.2 Tabulation of the Strehl ratio and the energy distribution as a function of the wavefront deformation. RL means the Rayleigh limit of one-quarter-wavelength peak-to-valley OPD.

E POINT IMAGE

NT IMAGE



Illumination at center of an aberrated image.

Image Quality Measures to OPD

Strehl Ratio	% energy in	
	Airy Disk	Rings
1.00	84	16
0.99	83	17
0.95	80	20
0.80	68	32
0.4*	40	60
0.1*	20	80
0.0*	10	90

Strehl ratio do not correlate well with image quality.

Strehl ratio and the energy distribution as a function of OPD. The Rayleigh limit of one-quarter-wavelength

Another commonly utilized measure of performance is the modulation transfer function, which describes the image modulation or contrast as a function of the spatial frequency of the object or image. The MTF of a perfect, aberration-free system is given by

$$MTF(v) = \frac{2}{\pi} (\phi - \cos \phi \sin \phi) \tag{4.1}$$

where

$$\phi = \arccos \left(\frac{\lambda v}{2NA} \right) \tag{4.2}$$

This is plotted as curve A in Figs. 4.3 and 4.4. Figure 4.3 shows the effect on the MTF of defocusing an otherwise aberration-free lens. The spatial frequency in these plots is normalized to the cutoff frequency

$$v_0 = \frac{2NA}{\lambda} = \frac{1}{\lambda(\text{f number})} \tag{4.3}$$

Figure 4.4 shows the effect of simple third-order spherical aberration on the MTF. Note that, although the curves of Figs. 4.3 and 4.4 are not identical, they are quite similar. This similarity of effect is the basis for the common rule of thumb that a given amount of OPD will de-

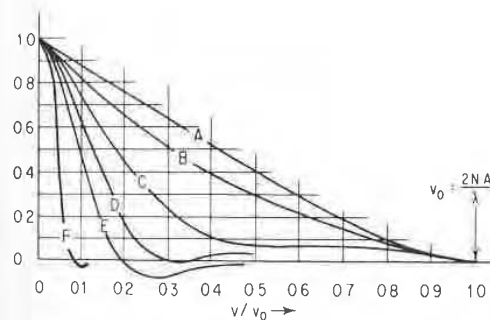


Figure 4.3 The effect of defocusing on the modulation transfer function of an aberration-free system.

- (A) In focus $\text{OPD} = \text{zero}$
 - (B) Defocus $= \lambda/2n \sin^2 U$ $\text{OPD} = \lambda/4$
 - (C) Defocus $= \lambda/n \sin^2 U$ $\text{OPD} = \lambda/2$
 - (D) Defocus $= 3\lambda/2n \sin^2 U$ $\text{OPD} = 3\lambda/4$
 - (E) Defocus $= 2\lambda/n \sin^2 U$ $\text{OPD} = \lambda$
 - (F) Defocus $= 4\lambda/n \sin^2 U$ $\text{OPD} = 2\lambda$
- (Curves are based on diffraction effects—not on a geometric calculation.)

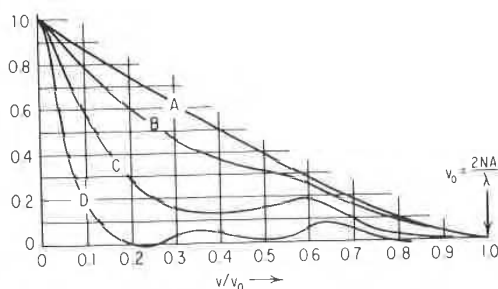


Figure 4.4 The effect of third-order spherical aberration on the modulation transfer function.

(A) $LA_M = \text{zero}$	$OPD = 0$
(B) $LA_M = 4\lambda/n \sin^2 U$	$OPD = \lambda/4$
(C) $LA_M = 8\lambda/n \sin^2 U$	$OPD = \lambda/2$
(D) $LA_M = 16\lambda/n \sin^2 U$	$OPD = \lambda$

grade the image by the same amount regardless of what type of aberration produced the OPD.

When the OPD is large (say more than one or two waves), the following geometrical approximation (derived from the geometric defocusing expression) can be used to calculate the MTF with reasonable accuracy:

$$MTF(v) = \frac{J_1[8\pi n OPD(v/v_0)]}{4\pi n OPD(v/v_0)} \quad (4.4)$$

where v_0 is the cutoff frequency (Eq. 4.3), n is the index of the image medium, OPD is the peak-to-valley wavefront deformation in waves, and

$$J_1[x] = \frac{x}{2} - \frac{(x/2)^3}{1^2 \cdot 2} + \frac{(x/2)^5}{1^2 \cdot 2^2 \cdot 3} - \dots$$

The relationships between the basic aberrations and the OPD are given in Sec. F.12, as are the relationships between rms OPD and peak-to-valley OPD and between rms OPD and the Strehl ratio.

A convenient relationship to remember is that a quarter-wave of OPD corresponds to a transverse spherical aberration (either marginal or zonal) of about

$$TA = \frac{4\lambda}{NA} \quad (4.5)$$

This is a useful way to make a quick and dirty evaluation from just the ray intercept plots.

4.3 Blur Spot Size versus Certain Aberrations

Many times, the system characteristic of interest is the size of the blur produced as the image of a point source. There are a few simple relationships which are useful in this regard:

Third-order spherical at best focus (three-fourths of the way from paraxial to marginal focus):

$$B = 0.5 LA_m \tan U_m = 0.5TA_m \tag{4.6}$$

Third- and fifth-order spherical (with the marginal spherical corrected, focused at 0.42 LA_z from the paraxial focus):

$$B = 0.84 LA_z \tan U_m = 0.59 TA_z \tag{4.7}$$

Third- and fifth-order spherical (corrected so that LA_z = 1.5 LA_m, or TA_m = 1.06 TA_z, and focused at 0.83 LA_z from the paraxial focus; this correction yields the smallest-diameter blur spot for a given amount of fifth-order spherical):

$$\begin{aligned} B &= 0.5 LA_m \tan U_m = 0.5TA_m \\ &= 0.33 LA_z \tan U_m = 0.47TA_z \end{aligned} \tag{4.8}$$

Note that the above are based on the idea of the smallest spot containing 100 percent of the energy in the image of a point. For many applications this concept is valid and useful, but for best image quality there is usually another focus or correction at which the image has a smaller, brighter core and a larger flare; this is usually judged to be better for definition and pictorial purposes.

The effect of a large amount of defocusing on a well-corrected image is to produce a uniformly illuminated blur disk with a diameter of

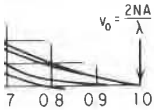
$$B = 2(\text{defocus}) \tan U_m \approx \frac{\text{defocus}}{f \text{ number}} \tag{4.9}$$

Astigmatism and field curvature can be evaluated by applying Eq. 4.9 separately in the sagittal and tangential meridians.

Although ordinary axial chromatic is also defocusing, the blur it produces is not uniformly illuminated, but has the energy centrally concentrated. At the midway focus point, the diameter of the blur containing 100 percent of the energy is

$$B = LA_{ch} \tan U_m = TA_{ch} \tag{4.10}$$

However, the central concentration leads to a situation where 75 to 90 percent of the energy is in a spot only half this size, and 40 to 60 percent is in a spot one-quarter as large. (The smaller percentages apply



spherical aberration

4
2

amount regardless of what type of aber-

7 more than one or two waves), the fol-
nation (derived from the geometric
used to calculate the MTF with reason-

$$\frac{J_1[8\pi n \text{OPD}(v/v_0)]}{4\pi n \text{OPD}(v/v_0)} \tag{4.4}$$

ty (Eq. 4.3), *n* is the index of the image
valley wavefront deformation in waves,

$$\frac{(x/2)^3}{1^2 \cdot 2} + \frac{(x/2)^5}{1^2 \cdot 2^2 \cdot 3} - \dots$$

ie basic aberrations and the OPD are
e relationships between rms OPD and
en rms OPD and the Strehl ratio.

o remember is that a quarter-wave of
erse spherical aberration (either mar-

$$TA = \frac{4\lambda}{NA} \tag{4.5}$$

a quick and dirty evaluation from just

for a uniform spectral response distribution and the larger for a triangular spectral distribution.)

For third-order coma, the blur is the typical comet shape, and has a height equal to the tangential coma and a width (in the sagittal direction) two-thirds this size. Note, however, that some 50 to 60 percent of the energy in the coma patch is in the point of the figure, whose size equals one-third the tangential coma.

4.4 MTF—The Modulation Transfer Function

The interpretation of an MTF plot is often problematical; it is not the easiest thing in the world to decide how good an image is on the basis of an examination of its MTF plot.

The limiting resolution is easily determined if the system sensor can be characterized by an aerial image modulation (AIM) curve. This is a plot of the threshold, or minimum, modulation required in the image for the sensor to produce a response. When plotted against spatial frequency, the intersection of the AIM curve and the MTF plot clearly indicates the limiting resolution, as shown in Fig. 4.5.

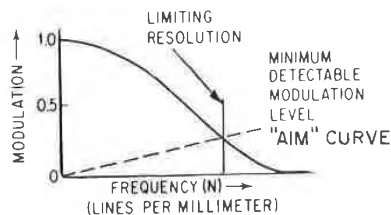


Figure 4.5 The intersection of the AIM curve and the MTF curve indicates the limiting resolution of the system.

A criterion for *excellent* performance (one which is often used as a design goal for top-of-the-line professional motion picture camera lenses) is to look for a 50 percent MTF at 50 lpm. Another criterion which has been presented for commercial 35-mm camera lenses is 20 percent MTF at 30 lpm over 90 percent of the field. Both criteria are applied at full aperture. These will give some idea of the range of the MTF values which are more or less standard for this type of work.

Lens Design Data

distribution and the larger for a trian-

is the typical comet shape, and has a coma and a width (in the sagittal direction), however, that some 50 to 60 percent of is in the point of the figure, whose size l coma.

transfer

plot is often problematical; it is not the decide how good an image is on the basis plot.

asily determined if the system sensor ial image modulation (AIM) curve. This nimum, modulation required in the im- response. When plotted against spatial he AIM curve and the MTF plot clearly n, as shown in Fig. 4.5.

E
N

RVE

AIM curve
iting reso-

formance (one which is often used as a e professional motion picture camera ent MTF at 50 lpm. Another criterion commercial 35-mm camera lenses is 20 0 percent of the field. Both criteria are will give some idea of the range of the r less standard for this type of work.

5.1 About the Sample Lenses

One of the features of this volume is a fairly large set of lens designs, their prescriptions, and their aberration plots. This set is not intended to be a complete or extensive *collection* of all or even most of the published lens designs. We happily leave that to others. The set is intended to be a *selection* of lens designs which will serve two primary purposes. These are to serve as a set of suitable starting designs and to serve as a set of designs which illustrate to the reader the principles and techniques of successful lens designs.

The designs in this book were drawn from many sources. A significant number are from the original version of OPTICS TOOLBOX.* (All of the designs in this text, plus many others which were considered but not chosen for inclusion, have been incorporated in the *Warren J. Smith Lens Library*.†) Many are derived from the patent literature, or books which include patent references. Some of the designs are from the technical literature, such as journals, proceedings, or other books about lenses. Some have never been published previously.

In most cases the published designs have been modified to some extent. For the majority of the designs, we have specified the optical glass as one of those from the Schott (Schott Glass Technologies, Inc.) catalog. We have chosen what we feel is the nearest Schott glass to that indicated in our source for the lens data. Occasionally this may constitute a significant change, but we have attempted to stay as close to the original data as possible. In a few designs, non-Schott glasses have been used.

*OPTICS TOOLBOX is a product of Genesee Optics Software, Inc.

†Warren J. Smith Lens Library is a trademark of Genesee Optics Software, Inc., and is incorporated in their optical design software products.

The aperture and field which are indicated for any given lens design are more a matter of taste than anything else. What constitutes an acceptable level of aberration depends mostly on the application to which the lens is to be put. Thus the values for field and aperture which accompany each design in this book have often been selected somewhat arbitrarily to yield a level of correction which we thought reasonable.

The choice of the clear apertures for the lens elements is equally arbitrary. Obviously, the clear aperture of an element cannot be so large that the edge thickness at that diameter becomes negative or impractically thin. We have selected what seemed to be reasonable values for the clear apertures, based on both edge thickness considerations and the choice of a vignetting factor which allows a reasonably sized oblique beam through the lens and also trims the oblique beam to eliminate the worst-behaved rays.

5.2 Lens Prescriptions, Drawings, and Aberration Plots

The lens design data and the associated graphics for this book have been produced by computer. While data input errors and other glitches are always possible, by producing the lens data table, the lens drawing, and the aberration plots all from the same lens data file, we hope to prevent most of the errors which have afflicted some other efforts of this type. The design examples have all been scaled to focal lengths which are within a few percent of 100 units in order that comparisons can be easily made. So that the details of the aberration correction will be readily apparent, the computer was programmed to select the scale of each aberration plot to make the plot fill the available space. This does, of course, have the disadvantage that each lens and its aberrations may be plotted to a different scale. In order to minimize this disadvantage we have limited the scales used to decimal factors of 2, 5, and 10.

Lens prescription

A sample is shown in Fig. 5.1. The lens construction data are tabulated in a quite straightforward way. The columns are headed *radius*, *thickness*, *mat'l*, *index*, *V-no*, and *sa* (for semiaperture); the meanings should be apparent. The radius value follows the usual sign convention that a positive radius has its center of curvature to the right of the surface. Plano surfaces (i.e., with infinite radius) are indicated by a blank entry in the radius column. The thickness and material following a surface are presented on the same line as the surface radius, and have the same number.

ch are indicated for any given lens design anything else. What constitutes an depends mostly on the application to which values for field and aperture which accom have often been selected somewhat arbitrary which we thought reasonable. rtures for the lens elements is equally aperture of an element cannot be so large that diameter becomes negative or selected what seemed to be reasonable s, based on both edge thickness consideration factor which allows a reasonably the lens and also trims the oblique beam ed rays.

Drawings, and

e associated graphics for this book have r. While data input errors and other by producing the lens data table, the lens plots all from the same lens data file, we errors which have afflicted some other ex n examples have all been scaled to focal w percent of 100 units in order that com. So that the details of the aberration content, the computer was programmed to section plot to make the plot fill the available ave the disadvantage that each lens and ed to a different scale. In order to mini ve limited the scales used to decimal fac-

5.1. The lens construction data are tabu ard way. The columns are headed *radius*, and *sa* (for semiaperture); the meanings ius value follows the usual sign conven as its center of curvature to the right of e., with infinite radius) are indicated by column. The thickness and material fold on the same line as the surface radius,

F/4.5 25.2deg TRIPLET US 1,987,878/1935 SCHNEIDER

radius	thickness	mat'l	index	V-no	sa
26.160	4.916	LAK12	1.678	55 2	11.7
1201.700	3.988	air			11.7
-83.460	1.038	SF2	1.648	33 8	10.2
25.670	4.000	air			10.2
	6.925	air			9.2
302.610	2.567	LAK22	1.651	55 9	10.3
-54.790	81.433	air			10.3

EFL = 98.56 = EFFECTIVE FOCAL LENGTH
 BFL = 81.43 = BACK FOCAL LENGTH
 NA = 0.1127 (F/4.4) = NUMERICAL APERTURE (F-NUMBER)
 GIH = 46.33 (HFOV=25.17) = IMAGE HEIGHT (HALF FIELD IN DEGREES)
 PTZ/F = 2.831 = (PETZVAL RADIUS)/EFL
 VL = 23.43 = VERTEX LENGTH
 OD = infinite conjugate = OBJECT DISTANCE

Figure 5.1 Sample lens prescription.

With few exceptions, the material names are those of Schott Glass Technologies, Inc. The index and V number values correspond to the wavelengths given with the ray intercept plot (e.g., see Fig. 5.3); for most lenses we have used the *d*, *F*, and *C* lines. The location of the aperture stop is indicated by a blank in the radius column with air on both sides of the surface. Aspheric surfaces are specified by the conic constant kappa and/or the aspheric deformation coefficients. The equation for the surface is

$$x = \frac{cy^2}{1 + [1 - (1 + \kappa)c^2y^2]^{1/2}} + ADy^4 + AEy^6 + AFy^8 + AGy^{10} \quad (5.1)$$

The data below the prescription tabulation has the following meanings:

- EFL Effective focal length
- BFL Back focal length (the distance from the last surface to the paraxial focal point)
- NA Numerical aperture (the corresponding *f* number is in parentheses)
- GIH Gaussian (paraxial) image height (half-field in degrees is in parentheses)
- PTZ/F Petzval radius as a fraction of EFL
- VL Vertex length from first to last surface
- OD Object distance

Lens drawing

A sample lens drawing is shown in Fig. 5.2. The scale of the lens drawing is indicated by the dimensioned length of the line immediately below the lens sketch. The two rays in the sketch are the marginal and principal rays corresponding to the aperture and field angle which are

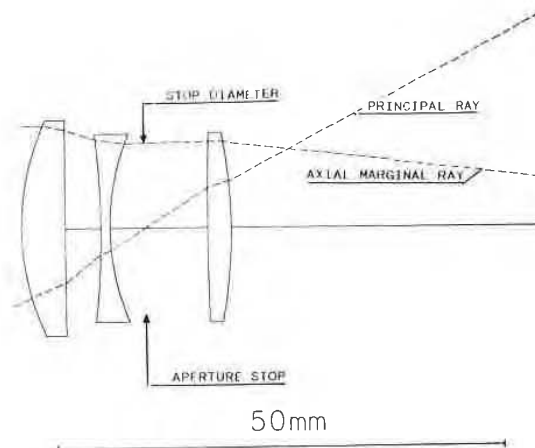


Figure 5.2 Sample lens drawing.

tabulated with the lens data. The aperture stop location is indicated by the point at which the principal ray crosses the optical axis. The lens elements are drawn to the clear apertures given in the prescription table as sa , the semiaperture.

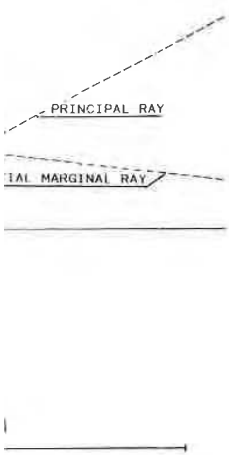
Additional rays can easily be added to the lens drawing if desired, by using a technique which is exact only for paraxial rays, but which is often accurate enough for use in estimating or drawing ray paths. A ray may be scaled by simply multiplying the heights at which it strikes the surfaces by a scaling constant. Also, rays may be added by adding their intersection heights together. In each case the result is a reasonable approximation to the path of another ray. Obviously, two rays can be scaled and then added. Thus any desired third ray can be drawn by determining its intersection heights from

$$Y_3 = AY_1 + BY_2 \quad (5.2)$$

where A and B are scaling factors and Y_1 and Y_2 are the ray heights of the rays in the lens drawing. If one defines the desired third ray by its intersection with any two surfaces (which may include the object or image surface), then a simultaneous solution for A and B may be found from the two equations which result when the appropriate values of Y_1 , Y_2 , and Y_3 are substituted into the equation above.

Aberration plots

A sample aberration plot is shown in Fig. 5.3. The aberration plots include both tangential and sagittal ray intercept plots (sometimes



a. The aperture stop location is indicated by the principal ray crossing the optical axis. The clear apertures given in the prescription are the clear apertures.

rays be added to the lens drawing if desired, but this is exact only for paraxial rays, but which can be used in estimating or drawing ray paths. A third ray may be added by simply multiplying the heights at which it intersects the surfaces together. In each case the result is a ray that follows the path of another ray. Obviously, two rays can be added. Thus any desired third ray can be added by the intersection heights from

$$Y_3 = AY_1 + BY_2 \quad (5.2)$$

where A and B are the ray height factors and Y_1 and Y_2 are the ray heights at the surfaces. If one defines the desired third ray by the intersection heights at the surfaces (which may include the object or image surfaces), a simultaneous solution for A and B may be found which result when the appropriate values are substituted into the equation above.

as shown in Fig. 5.3. The aberration plots in meridional and sagittal ray intercept plots (sometimes

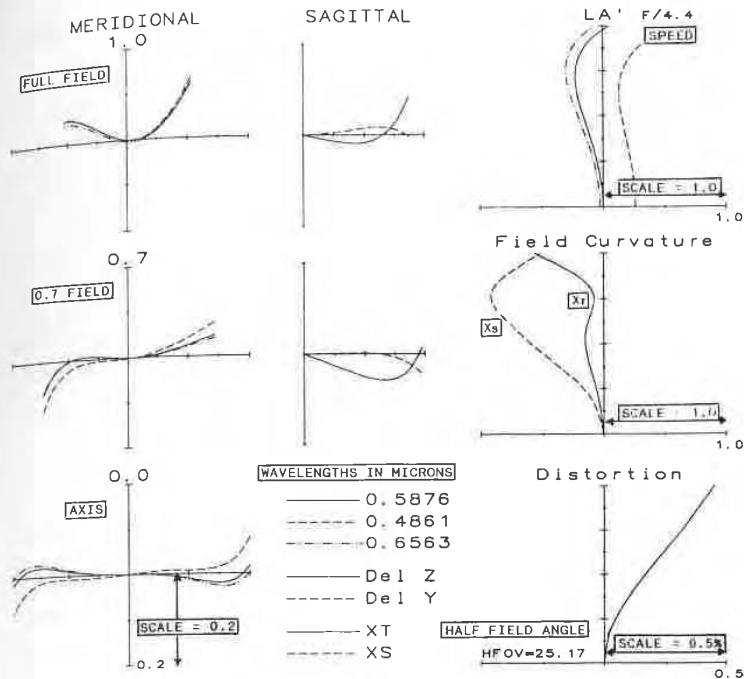


Figure 5.3 Sample aberration plot.

called H -tan U curves) for the axis, 0.7 field, and full field. The ray displacements are plotted vertically, as a function of the position of the ray in the aperture. The vertical scale is given at the lower end of the vertical bar for the axial plot; the number given is the half-length (i.e., from the origin to the end) of the vertical line in the plot. The horizontal scale is proportional to the tangent of the ray slope angle. Following the usual convention, the upper ray of the ray fan is plotted to the right. In the sagittal plots, the solid line is the transverse aberration in the z , or sagittal, direction and the dashed line is the ray displacement in the y direction (which is sagittal coma).

In addition to the ray intercept plots (which are, in general, probably the most broadly useful presentation of the aberration characteristics of a design), two aberrations are also presented as longitudinal plots. The longitudinal representations of spherical aberration and field curvature have been the classical, conventional presentation for decades, despite the fact that they give a very incomplete picture of the state of correction of the lens. However, a longitudinal plot of the spherical aberration in three wavelengths does allow a much clearer

understanding of the spherochromatism, as well as the secondary spectrum. The scale factor for this plot is the number given at the right end of the horizontal axis; the number is the half length of the horizontal line. The vertical dimension of the plot is the height of the ray at the pupil; the f number is given at the top of the plot. This is the f number of the imaging cone and is equal to $1/2\text{NA}$. The longitudinal field curvature plots yield an excellent picture of the correction of the Petzval curvature and the astigmatism. The scale for X_s and X_t is given at the right end of the horizontal axis; again the number is the half length of the horizontal line. The solid line is X_t and the dashed line is X_s . The vertical scale is the fraction of the gaussian image height (GIH); the half field angle is given at the left side of the distortion plot. The scale for distortion is in percent, and the number is the half-length of the horizontal line.

5.3 Estimating the Potential of a Design

It is relatively easy to estimate the effects of a modest redesign on the aberration plots of an existing design by applying a knowledge of third-order aberration theory. This is because the third-order aberrations of a lens are easily adjusted by changing the spaces or the shapes of the elements, whereas the amount of higher-order aberration tends to be quite stable and resistant to change.

Equations 5.3 and 5.4 are a power series expansion of the relationships between the ray intersection with the image plane (y' , z') as a function of the object height h and the ray position in the pupil (defined in polar coordinates s and θ), as shown in Fig. 5.4.

$$\begin{aligned}
 y' = & A_1 s \cos \theta + A_2 h + B_1 s^3 \cos \theta + B_2 s^2 h (2 + \cos 2\theta) \\
 & + (3B_3 + B_4) s h^2 \cos \theta + B_5 h^3 + C_1 s^5 \cos \theta + (C_2 + C_3 \cos 2\theta) s^4 h \\
 & + (C_4 + C_6 \cos^2 \theta) s^3 h^2 \cos \theta + (C_7 + C_8 \cos 2\theta) s^2 h^3 + C_{10} s h^4 \cos \theta \\
 & + C_{12} h^5 + D_1 s^7 \cos \theta + \dots
 \end{aligned} \tag{5.3}$$

$$\begin{aligned}
 z' = & A_1 s \sin \theta + B_1 s^3 \sin \theta + B_2 s^2 h \sin 2\theta \\
 & + (B_3 + B_4) s h^2 \sin \theta + C_1 s^5 \sin \theta + C_3 s^4 h \sin 2\theta \\
 & + (C_5 + C_6 \cos^2 \theta) s^3 h^2 \sin \theta + C_9 s^2 h^3 \sin 2\theta + C_{11} s h^4 \sin \theta \\
 & + D_1 s^7 \sin \theta + \dots
 \end{aligned} \tag{5.4}$$

Notice that, in the A terms, the exponents of s and h are unity. In the B terms, the exponents total 3, as in s^3 , $s^2 h$, $s h^2$, and h^3 . In the C

ochromatism, as well as the secondary for this plot is the number given at the axis; the number is the half length of the d dimension of the plot is the height of number is given at the top of the plot. This ng cone and is equal to $1/2NA$. The longi- s yield an excellent picture of the correc- re and the astigmatism. The scale for X_s end of the horizontal axis; again the num- horizontal line. The solid line is X_i and the al scale is the fraction of the gaussian im- field angle is given at the left side of the ' distortion is in percent, and the number izontal line.

al of a Design

ate the effects of a modest redesign on the ting design by applying a knowledge of y. This is because the third-order aberrat- ed by changing the spaces or the shapes amount of higher-order aberration tends ant to change.

a power series expansion of the relation- section with the image plane (y', z') as a t h and the ray position in the pupil (de- and θ), as shown in Fig. 5.4.

$$\begin{aligned} & \cos \theta + B_2 s^2 h (2 + \cos 2\theta) \\ & B_6 h^3 + C_1 s^5 \cos \theta + (C_2 + C_3 \cos 2\theta) s^4 h \\ & s \theta + (C_7 + C_8 \cos 2\theta) s^2 h^3 + C_{10} s h^4 \cos \theta \end{aligned} \tag{5.3}$$

$$\begin{aligned} & B_2 s^2 h \sin 2\theta \\ & C_1 s^5 \sin \theta + C_3 s^4 h \sin 2\theta \\ & s \theta + C_9 s^2 h^3 \sin 2\theta + C_{11} s h^4 \sin \theta \end{aligned} \tag{5.4}$$

ns, the exponents of s and h are unity. In total 3, as in s^3 , $s^2 h$, sh^2 , and h^3 . In the C

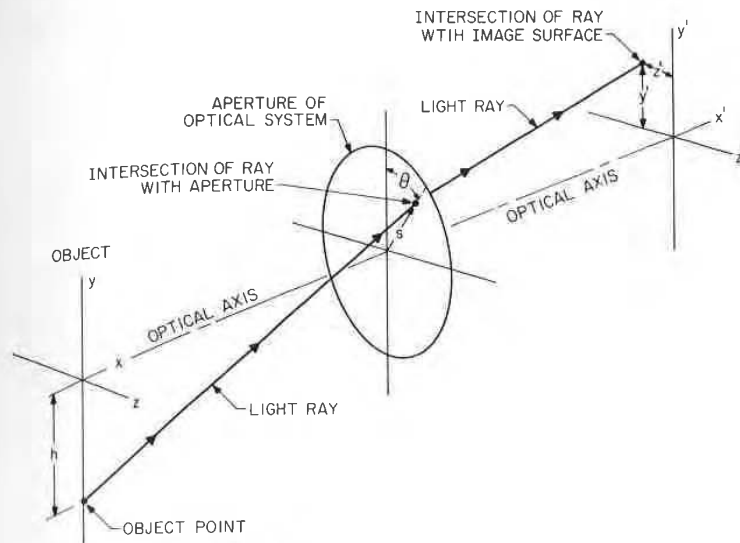


Figure 5.4 A ray from the point $y = h, z = 0.0$ in the object passes through the aperture of the optical system at a point defined by its polar coordinates (s, θ), and intersects the image surface at point y', z' .

terms, the exponents total 5, and in the D terms, 7. These are referred to as the first-order, third-order, and fifth-order terms, etc. There are 2 first-order terms, 5 third-order, 9 fifth-order, and $[(n + 3)(n + 5)/8 - 1]$ n th-order terms. In an axially symmetrical system there are no even-order terms; only odd-order terms may exist (unless we depart from symmetry as, for example, by tilting a surface or introducing a toroidal or other nonsymmetrical surface).

It is apparent that the A terms relate to the paraxial (or first-order) imagery. A_2 is simply the magnification (h'/h), and A_1 is a measure of the distance from the paraxial focus to our "image plane." All the other terms in Eqs. 5.3 and 5.4 are called *transverse aberrations*. They represent the distance by which the ray misses the ideal image point as described by the paraxial imaging equations.

The B terms are called the *third-order*, or *Seidel*, or *primary* aberrations. B_1 is spherical aberration, B_2 is coma, B_3 is astigmatism, B_4 is Petzval, and B_5 is distortion. Similarly, the C terms are called the *fifth-order* or *secondary* aberrations. C_1 is fifth-order spherical aberration; C_2 and C_3 are linear coma; $C_4, C_5,$ and C_6 are oblique spherical aberration; $C_7, C_8,$ and C_9 are elliptical coma; C_{10} and C_{11} are Petzval and astigmatism; and C_{12} is distortion.

The 14 terms in D are the seventh-order or tertiary aberrations; D_1 is the seventh-order spherical aberration. A similar expression for OPD, the wavefront deformation, is given in Sec. 5.4 (Eqs. 5.5 and 5.6).

The terms with the B coefficients are the transverse third-order aberrations. The longitudinal aberrations are equal to the transverse aberrations divided by $-u_k'$; since u_k' is a direct function of the ray height s , one can convert these into longitudinal aberrations by reducing the exponent of s by 1 (and adjusting the coefficients).

Thus one can assume that if the spherical aberration is adjusted so as to correct it at a given aperture, the change in the longitudinal aberration will be proportional to the square of the ray heights. For example, if the spherical at ray height Y_1 is to be changed by dLA_1 , then at ray height Y_2 it will change by $dLA_2 = dLA_1(Y_2/Y_1)^2$. The change of the transverse spherical will vary as a cubic function, so that the transverse change $dTA_2 = dTA_1(Y_2/Y_1)^3$. Figure 3.6 shows the effect of changing the third-order spherical (assuming a constant fifth-order spherical).

If the axial chromatic is changed, the ray intercept plots for the different colors will simply rotate with respect to each other. The secondary spectrum and spherochromatism will change very little, so that one can readily estimate the ray intercept plots which will result from a simple change in the axial chromatic. Figure 3.7 shows two different balances of axial chromatic and spherochromatism. Similarly, a lateral chromatic change will change the relative heights of the different color ray plots, and the amount of the height change will be proportioned to the image height.

The change in the longitudinal astigmatism and field curvature is proportional to the square of the image height or field angle. Thus if the field curvature is changed by dX_1 at image height H_1 , the change at H_2 is $dX_2 = dX_1(H_2/H_1)^2$. The change in the tangential field curvature X_t is three times the change in the sagittal field curvature X_s if the change is produced by changing the amount of the astigmatism. However, if the change results from a change in the Petzval curvature, both X_s and X_t are shifted by the same distance. Note that the slope of the ray intercept plot ($dH/d \tan U$) at the principal ray is equal to the tangential field curvature (X_t) (or X_s for the sagittal plot).

Changes in the third-order coma produce a parabolic-shaped change in the ray intercept plot. If the plot is raised by an amount dH at the ends of the plot, it will be raised by $(0.7)^2 dH = 0.5 dH$ at the 0.7 zones of the aperture. The amount of the coma change for other field angles will vary directly with the field angle or image height.

The change in percent distortion will vary with the square of the field angle. The change in the lateral color varies directly with the field angle.

eventh-order or tertiary aberrations; D_1 is aberration. A similar expression for OPD, given in Sec. 5.4 (Eqs. 5.5 and 5.6).

coefficients are the transverse third-order aberrations are equal to the transverse aberrance u_k' is a direct function of the ray height into longitudinal aberrations by reducing adjusting the coefficients).

if the spherical aberration is adjusted so that the change in the longitudinal aberrance to the square of the ray heights. For example, height Y_1 is to be changed by dLA_1 , then the change by $dLA_2 = dLA_1(Y_2/Y_1)^2$. The change will vary as a cubic function, so that the change is $dLA_1(Y_2/Y_1)^3$. Figure 3.6 shows the effect of spherical (assuming a constant fifth-order

aberration), the ray intercept plots for the different heights with respect to each other. The second-order spherical aberration will change very little, so that the ray intercept plots which will result from spherical aberration and spherochromatism. Figure 3.7 shows two different ray intercept plots. Similarly, a lateral change in the relative heights of the different heights of the height change will be proportional to the height change.

lateral astigmatism and field curvature is the image height or field angle. Thus if the change in the image height is dY_1 , the change in the tangential field curvature is dX_s if the change in the amount of the astigmatism is dA_s . The change in the Petzval curvature is dP if the change in the amount of the astigmatism is dA_s . Note that the change in the Petzval curvature is $dP = dH/d \tan U$ at the principal ray is dX_s (or X_s for the sagittal plot). The change in the coma produce a parabolic-shaped change in the plot is raised by an amount dH at the edge of the field by $(0.7)^2 dH = 0.5 dH$ at the 0.7 zones of the coma change for other field angles and field angle or image height.

distortion will vary with the square of the field angle and the lateral color varies directly with

Thus one can look at the aberration plots for a given design and, by applying the techniques outlined above, easily visualize what they will look like after an adjustment has been made to fit the design to the application at hand.

5.4 Scaling a Design, Its Aberrations, and Its MTF

A lens prescription can be scaled to any desired focal length simply by multiplying all of its dimensions by the same constant. All of the *linear* aberration measures will then be scaled by the same factor. Note however, that percent distortion, chromatic difference of magnification (CDM), the numerical aperture or f number, aberrations expressed as angular aberrations, and any other *angular* characteristics remain completely unchanged by scaling.

The exact *diffraction* MTF cannot be scaled with the lens data. The diffraction MTF, since it includes diffraction effects which depend on wavelength, will not scale because the wavelength is not (ordinarily) scaled with the lens. A *geometric* MTF can be scaled by dividing the spatial frequency ordinate of the MTF plot by the scaling factor. Of course, because it neglects diffraction, the geometric MTF is quite inaccurate unless the aberrations are very large (and the MTF is correspondingly poor).

A diffraction MTF can be scaled *very* approximately as follows: Determine the OPD which corresponds to the MTF value of the lens for several spatial frequencies. This can be done by comparing the MTF plot for the lens to Figs. 4.3 and 4.4, which relate the MTF to OPD. Then multiply the OPD by the scaling factor and, again using Figs. 4.3 and 4.4, determine the MTF corresponding to these scaled OPD values. Obviously the accuracy of this procedure depends on how well the simple relationships of Figs. 4.3 and 4.4 represent the usually complex mix of aberrations in a real lens.

In the event that a proposed change of aperture or field is expected to produce a change in the amount of the aberrations, one can attempt to scale the MTF as affected by aberration. This is done by determining the type of aberration which most severely limits the MTF, then scaling the OPD according to the way that this aberration scales with aperture or field, in a manner analogous to that described in Sec. 5.3. In general, OPD as a function of aperture varies as one higher exponent of the aperture than does the corresponding transverse aberration. For example, the OPD for third-order transverse spherical (which varies as Y^3) varies as the fourth power of the ray height. In a form analogous to Eqs. 5.3 and 5.4, which indicate a power series expansion of the transverse aberrations as a function of aperture and

field, Eq. 5.5 gives the relationship for OPD. As in Sec. 5.3, the terms of the equation refer to Fig. 5.4.

$$\begin{aligned} \text{OPD} = & A'_1 s^2 + A'_2 s h \cos \theta + B'_1 s^4 + B'_2 s^3 h \cos \theta \\ & + B'_3 s^2 h^2 \cos^2 \theta + B'_4 s^2 h^2 + B'_5 s h^3 \cos \theta + C'_1 s^6 + C'_2 s^5 h \cos \theta \\ & + C'_4 s^4 h^2 + C'_5 s^4 h^2 \cos^2 \theta + C'_7 s^3 h^3 \cos \theta + C'_8 s^3 h^3 \cos^3 \theta \\ & + C'_{10} s^2 h^4 + C'_{11} s^2 h^4 \cos^2 \theta + C'_{12} s h^5 \cos \theta + D'_1 s^8 + \dots \quad (5.5) \end{aligned}$$

Note that although the constants here correspond to those in Eqs. 5.3 and 5.4, they are not numerically the same. However, the expressions are related by

$$y' = \text{TA}_y = \frac{l}{N} \frac{\partial \text{OPD}}{\partial y} \quad \text{and} \quad z' = \text{TA}_z = \frac{l}{N} \frac{\partial \text{OPD}}{\partial z} \quad (5.6)$$

where l is the pupil-to-image distance and N is the image space index. Note that the exponent of the semiaperture term s is larger by 1 in the wavefront expression than in the ray-intercept equations.

5.5 Notes on the Interpretation of Ray Intercept Plots

When the image plane intersection heights of a fan of meridional rays are plotted against the slope of the rays as they emerge from the lens, the resultant curve is called a ray intercept curve, an $H' - \tan U'$ curve, or sometimes (erroneously) a rim ray curve. The shape of the intercept curve not only indicates the amount of spreading or blurring of the image directly, but also can serve to indicate which aberrations are present.

In Fig. 5.5 an oblique fan of rays from a distant object point is brought to a perfect focus at point P . If the reference plane passes through P , it is apparent that the $H' - \tan U'$ curve will be a straight horizontal line. However, if the reference plane is behind P (as shown) then the ray intercept curve becomes a tilted straight line since the height, H' , decreases as $\tan U'$ decreases. Thus it is apparent that shifting the reference plane (or focusing the system) is equivalent to a rotation of the $H' - \tan U'$ coordinates. A valuable feature of this type of aberration representation is that one can immediately assess the effects of refocusing the optical system by a simple rotation of the abscissa of the figure. Notice that the slope of the line ($\Delta H' / \Delta \tan U'$) is equal to the distance δ from the reference plane to the point of focus, so that for an oblique ray fan the tangential field curvature is equal to the slope of the ray intercept curve.

Figure 5.6 shows a number of intercept curves, each labeled with

relationship for OPD. As in Sec. 5.3, the terms are numbered 1, 2, 3, 4.

$$\begin{aligned}
 & C'_1 s^4 + B'_2 s^3 h \cos \theta \\
 & C'_3 h^2 + B'_6 s h^3 \cos \theta + C'_1 s^6 + C'_2 s^5 h \cos \theta \\
 & C'_7 s^3 h^3 \cos \theta + C'_8 s^3 h^3 \cos^3 \theta \\
 & C'_{12} s h^5 \cos \theta + D'_1 s^8 + \dots \quad (5.5)
 \end{aligned}$$

terms here correspond to those in Eqs. 5.3 and are generally the same. However, the expressions

$$\text{and } z' = \text{TA}_z = \frac{l}{N} \frac{\partial \text{OPD}}{\partial z} \quad (5.6)$$

distance and N is the image space index. The semiaperture term s is larger by 1 in the ray-intercept equations.

Construction of Ray Intercept Curve

The intersection heights of a fan of meridional rays as they emerge from the lens, the ray intercept curve, an $H' - \tan U'$ curve, or ray intercept curve. The shape of the intercept curve indicates the amount of spreading or blurring of the image. To indicate which aberrations are present, the ray intercept curve of rays from a distant object point is plotted against the slope angle U' . If the reference plane passes through the point P , the ray intercept curve will be a straight line. If the reference plane is behind P (as shown in Fig. 5.5), the intercept curve becomes a tilted straight line since the slope angle U' decreases. Thus it is apparent that the ray intercept curve for a focusing system is equivalent to a straight line in the $H' - \tan U'$ coordinates. A valuable feature of this type of curve is that one can immediately assess the effect of a change in the slope of the line ($\Delta H' / \Delta \tan U'$) is the distance from the reference plane to the point of focus, the tangential field curvature is equal to the slope of the curve.

Figure 5.5 shows several ray intercept curves, each labeled with

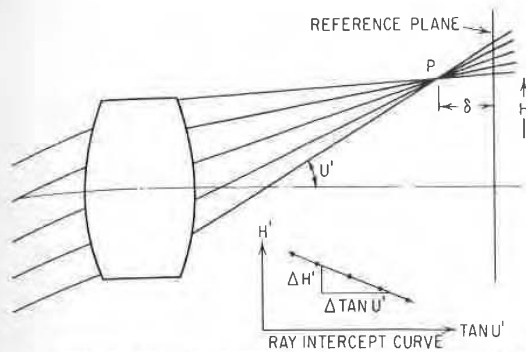


Figure 5.5 The ray intercept curve (H' versus $-\tan U'$) of an image point which does not lie in the reference plane is a tilted straight line. The slope of the line ($dH'/d \tan U'$) is mathematically identical to the distance from the reference plane to the point P . Note that this distance is equal to X_p , the tangential field curvature (if the reference plane is the paraxial focal plane).

the aberration represented. The generation of these curves can be readily understood by sketching the ray paths for each aberration and then plotting the intersection height and slope angle for each ray as a point of the curve. Distortion is not shown in Fig. 5.6; it would be represented as a vertical displacement of the curve from the paraxial image height h' . Lateral color would be represented by curves for two colors which were vertically displaced from each other. The ray intercept curves of Fig. 5.6 are generated by tracing a fan of meridional or tangential rays from an object point and plotting their intersection heights versus their slopes. The imagery in the other meridian can be examined by tracing a fan of rays in the sagittal plane (normal to the meridional plane) and plotting their z -coordinate intersection points against their slopes in the sagittal plane (i.e., the ray slope relative to the principal ray lying in the meridional plane).

It is apparent that the ray intercept curves which are "odd" functions, that is, the curves which have a rotational or point symmetry about the origin, can be represented mathematically by an equation of the form

$$y = a + bx + cx^3 + dx^5 + \dots$$

$$\text{or } H' = a + b \tan U' + c \tan^3 U' + d \tan^5 U' + \dots \quad (5.7)$$

All the ray intercept curves for axial image points are of this type. Since the curve for an axial image must have $H' = 0$ when $\tan U' = 0$,

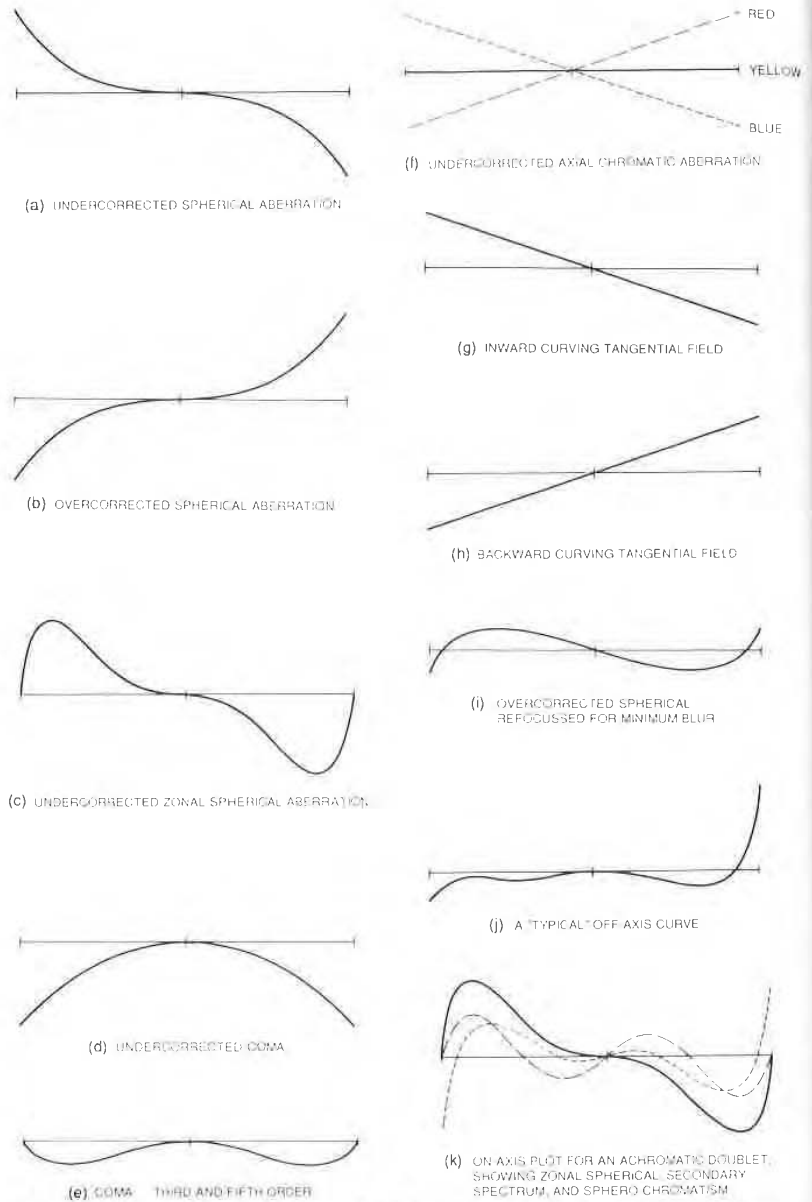
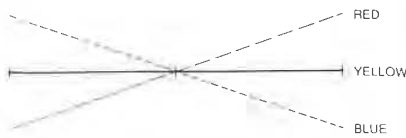
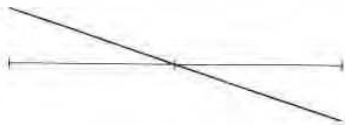


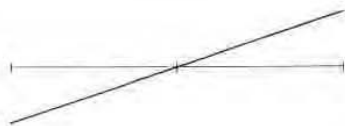
Figure 5.6 Sample ray intercept plots for various aberrations. The ordinate for each curve is the height at which the ray intersects the (paraxial) image plane; usually H is plotted relative to the principal ray height, which is set to zero. The abscissa is $\tan U$, the final slope of the ray with respect to the optical axis. Note that, regardless of the sign convention for the ray slope, it is conventional to plot the ray through the top of the lens at the right of the figure, and that the curves for image points above the axis are usually shown. Observance of these conventions makes it much easier to interpret the plots.



(f) UNDERCORRECTED AXIAL CHROMATIC ABERRATION



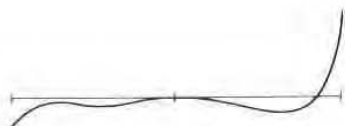
(g) INWARD CURVING TANGENTIAL FIELD



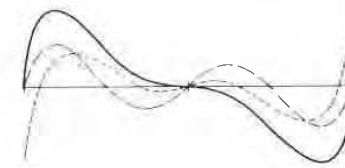
(h) BACKWARD CURVING TANGENTIAL FIELD



(i) OVERCORRECTED SPHERICAL
REFOCUSED FOR MINIMUM BLUR



(j) A "TYPICAL" OFF AXIS CURVE



(k) ON AXIS PLOT FOR AN ACHROMATIC DOUBLET
SHOWING ZONAL SPHERICAL SECONDARY
SPECTRUM AND SPHEROCHROMATISM

ts for various aberrations. The ordinate for each intersects the (paraxial) image plane; usually H is height, which is set to zero. The abscissa is $\tan U$, U to the optical axis. Note that, regardless of the conventional to plot the ray through the top of the at the curves for image points above the axis are conventions makes it much easier to interpret the

it is apparent that the constant a must be a zero. It is also apparent that the constant b for this case represents the amount the reference plane is displaced from the paraxial image plane. Thus the curve for lateral spherical aberration plotted with respect to the paraxial focus can be expressed by the equation

$$TA' = c \tan^3 U' + d \tan^5 U' + e \tan^7 U' + \dots \quad (5.8)$$

It is, of course, possible to represent the curve by a power series expansion in terms of the final angle U' , or $\sin U'$, or the ray height at the lens (Y), or even the initial slope of the ray at the object (U_0) instead of $\tan U'$. The constants will, of course, be different for each.

For simple uncorrected lenses, the first term of Eq. 5.8 is usually adequate to describe the aberration. For the great majority of corrected lenses the first two terms are dominant; in a few cases three terms (and rarely four) are necessary to satisfactorily represent the aberration. As examples, Figs. 5.6a and b can be represented by $TA' = c \tan^3 U'$, and this type of aberration is called *third-order spherical*. Figure 5.6c however, would require two terms of the expansion to represent it adequately; thus $TA' = c \tan^3 U' + d \tan^5 U'$. The amount of aberration represented by the second term is called the *fifth-order aberration*. Similarly, the aberration represented by the third term of Eq. 5.8 is called the *seventh-order aberration*. The fifth-, seventh-, ninth-, etc., order aberrations are collectively referred to as *higher-order aberrations*.

The ray intercept plot is subject to a number of interesting interpretations. It is immediately apparent that the top-to-bottom extent of the plot gives the size of the image blur. Also, a rotation of the horizontal (abscissa) lines of the graph is equivalent to a refocusing of the image and can be used to determine the effect of refocusing on the size of the blur.

Figure 5.5 shows that the ray intercept plot for a defocused images is a sloping line. If we consider the slope of the curve at any point on an H - $\tan U$ ray intercept plot, the slope is equal to the defocus of a small-diameter bundle of rays centered about the ray represented by that point. In other words, this would represent the focus of the rays passing through a pinhole aperture which was so positioned as to pass the rays at that part of the H - $\tan U$ plot. Similarly, since shifting an aperture stop along the axis is, for an oblique bundle of rays, the equivalent of selecting one part or another of the ray intercept plot, one can understand why shifting the stop can change the field curvature.

The OPD (optical path difference) or wavefront aberration can be derived from an H - $\tan U$ ray intercept plot. The area under the curve between two points is equal to the OPD between the two rays which

correspond to the two points. Ordinarily, the reference ray for OPD is either the optical axis or the principal ray (for an oblique bundle). Thus the OPD for a given ray is usually the area under the ray intercept plot between the center point and the ray.

Mathematically speaking, then, the OPD is the integral of the H - $\tan U$ plot and the defocus is the first derivative. The coma is related to the curvature or second derivative of the plot, as a glance at Fig. 5.6d will show.

It should be apparent that a ray intercept plot for a given object point can be considered as a power series expansion of the form

$$H' = h + a + bx + cx^2 + dx^3 + ex^4 + fx^5 + \dots \quad (5.9)$$

where h is the paraxial image height, a is the distortion, and x is the aperture variable (e.g., $\tan U'$). Then the art of interpreting a ray intercept plot becomes analogous to decomposing the plot into its various terms. For example, cx^2 and ex^4 represent third- and fifth-order coma, while dx^3 and fx^5 are the third- and fifth-order spherical. The bx term is due to a defocusing from the paraxial focus and could be due to curvature of field. Note that the constants a , b , c , etc., will be different for points of differing distances from the axis.

Telephoto Lenses

10.1 The Basic Telephoto

The arrangement shown in Fig. 10.1, with a positive component followed by a negative component, can produce a compact system with an effective focal length F which is longer than the overall length L of the lens. The ratio of L/F is called the *telephoto ratio*, and a lens for which this ratio is less than unity is classified as a telephoto lens. The smaller the ratio, the more difficult the lens is to design. Note that many camera lenses which are sold as telephoto lenses are simply long-focal-length lenses and are not true telephotos.

Many of the comments in Chap. 9 regarding retrofocus or reverse telephoto lenses are equally applicable to the telephoto lens. Equations 9.1 and 9.2 may also be applied to the telephoto. The usual Petzval problem is with a backward-curving field, just as with the retrofocus, and the same glass choices are appropriate for the telephoto. Since the system is unsymmetrical, each component must be individually achromatized if both axial and lateral color are to be cor-

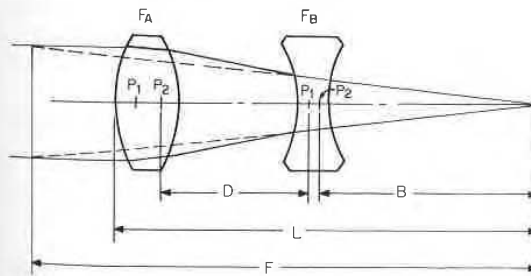


Figure 10.1 The basic power arrangement for a telephoto lens yields a compact lens with an overall length which is less than its effective focal length.

rected. The aperture stop is usually at the front member or part way toward the rear. Since a telephoto lens usually covers only a relatively small angular field, coma, distortion, and lateral color (which in many lenses are reduced by an approximate symmetry about the stop) are not as troublesome as they would be with a wider field.

10.2 Close-up or Macro lenses

The correction of a long-focal-length unsymmetrical lens is usually quite sensitive to a change in object distance, and, for most telephoto lenses, the image quality deteriorates severely when they are focused on nearby objects. Note that this effect varies inversely with the object distance expressed in focal length units; i.e., for a given design type, the image quality may remain acceptable as long as the object distance exceeds some number of focal lengths. Thus, for a given object distance, this effect is more of a problem for a long-focal-length lens than for a short. Since retrofocus lenses tend to have short focal lengths, this problem is somewhat less frequently encountered, in spite of their asymmetry.

Many newer telephoto lenses and the specialized close-focusing lenses (called *macro* lenses) utilize a floating component or separately moving elements to maintain the aberration correction when the lens is focused at a close distance. For many lenses, the spherical aberration and the astigmatism become undercorrected at close conjugates. Thus a relative motion of the elements to increase the marginal ray height on a negative (or overcorrecting) element/component can be used to stabilize the spherical. The astigmatism can be controlled by a motion which increases the height of the chief ray on a component which contributes overcorrected astigmatism, or which reduces it on an undercorrecting one.

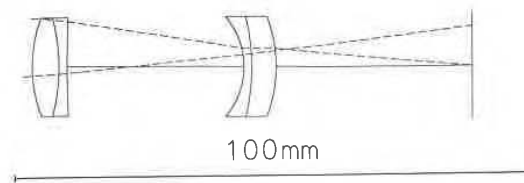
The design of such a system is carried out just like the design of a zoom lens. Two (or more) configurations are set up, one with a long (perhaps infinite) object conjugate distance and the other with a short one. The computer then uses the same lens elements with different spacings for each configuration and optimizes the merit function for both configurations simultaneously.

Figures 19.3 to 19.6, and 20.5 show nontelephoto designs with macro features.

10.3 Sample Telephoto Designs

Figures 10.2 and 10.3 show two very basic telephoto lenses; each consists of just two cemented or closely airspaced achromatic doublets, about as simple a construction as possible. Figure 10.2 covers less

ally at the front member or part way
o lens usually covers only a relatively
tion, and lateral color (which in many
imate symmetry about the stop) are
d be with a wider field.



KINGSLAKE TELEPHOTO MODIFIED BY HOPKINS

radius	thickness	mat'l	index	V-no	sa
24.607	5.080	BK7	1.517	64.2	9.2
-36.347	1.600	F2	1.620	36.4	9.2
212.138	12.300	air			9.0
	21.699				6.7
-14.123	1.520	BK7	1.517	64.2	9.4
-38.904	4.800	F2	1.620	36.4	9.4
-25.814	37.934	air			9.4

EFL = 101.6
BFL = 37.93
NA = -0.0893 (F/5.6)
GIH = 7.44
PTZ/F = -19.38
VL = 47.00
OD = infinite conjugate

length unsymmetrical lens is usually
object distance, and, for most telephoto
rates severely when they are focused
effect varies inversely with the object
th units; i.e., for a given design type,
acceptable as long as the object dis-
ocal lengths. Thus, for a given object
problem for a long-focal-length lens
cus lenses tend to have short focal
that less frequently encountered, in

s and the specialized close-focusing
ze a floating component or separately
e aberration correction when the lens
or many lenses, the spherical aberrate
undercorrected at close conjugates.
ements to increase the marginal ray
orrecting) element/component can be
he astigmatism can be controlled by a
ght of the chief ray on a component
astigmatism, or which reduces it on

s carried out just like the design of a
urations are set up, one with a long
te distance and the other with a short
te same lens elements with different
and optimizes the merit function for
sly.

0.5 show nontelephoto designs with

is

very basic telephoto lenses; each con-
osely airspaced achromatic doublets,
as possible. Figure 10.2 covers less

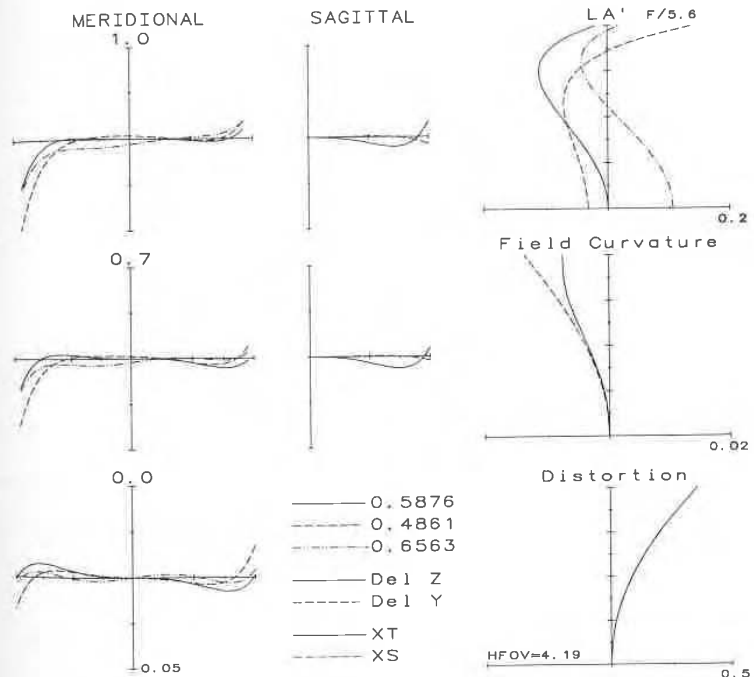
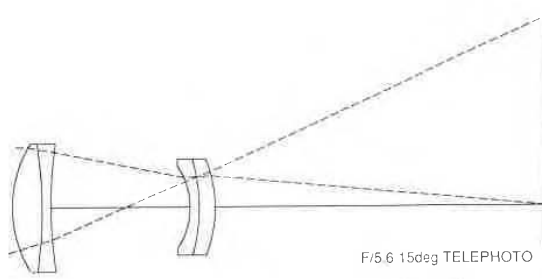


Figure 10.2



F/5.6 15deg TELEPHOTO US 2,390,387

radius	thickness	matl	index	V-no	sa
17.000	4.500	BK7	1.517	64.2	9.3
-62.570	0.006	air			9.3
-61.860	1.300	SF2	1.648	33.8	9.3
60.450	11.450	air			9.3
	9.540	air			6.1
-10.610	1.400	KF9	1.523	51.5	6.0
-24.760	0.011	air			7.0
-24.250	2.400	SF1	1.717	29.5	7.0
-18.570	50.137	air			7.0

EFL = 98.52
 BFL = 50.14
 NA = -0.0288 (F/5.6)
 GIH = 26.60 (HFOV=15.11)
 PTZ/F = 16.55
 VL = 30.61
 OD = infinite conjugate

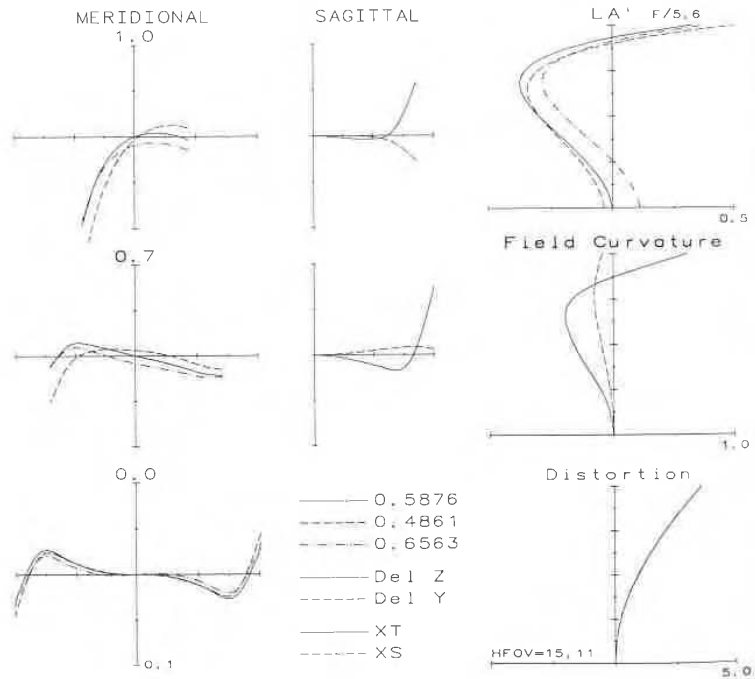
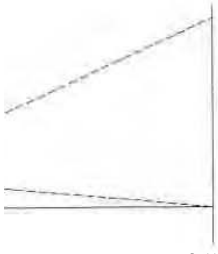


Figure 10.3

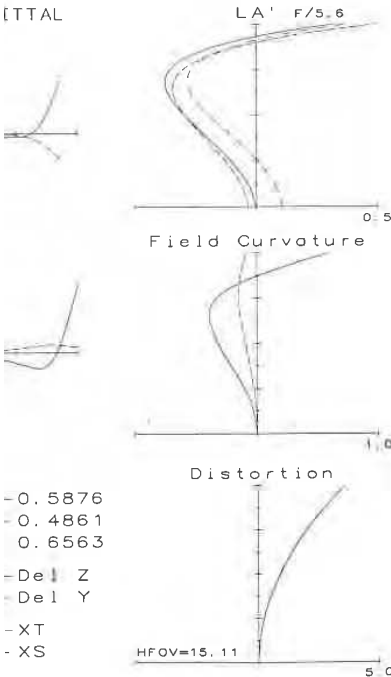


F/5.6 15deg TELEPHOTO US 2,390,387

radius	thickness	mat'l	index	V-no	sa
17 000	4 500	BK7	1 517	64 2	9.3
-62 570	0 006	air			9.3
-61 860	1 300	SF2	1 648	33 8	9.3
60 450	11 450	air			9.3
	9 540	air			6.1
-10 610	1 400	KF9	1 523	51 5	6.0
-24 760	0 011	air			7.0
-24 250	2 400	SF1	1 717	29 5	7.0
-18 570	50 137	air			7.0

EFL = 98.52
 BFL = 50.14
 NA = -0.0888 (F/5.6)
 GIH = 26.60 (HFOV=15.11)
 PTZ/F = 16.55
 VL = 30.61
 OD = infinite conjugate

TTAL



-0.5876
 -0.4861
 0.6563
 -Del Z
 -Del Y
 -XT
 -XS

than 9° at f/5.6 and has a telephoto ratio of 0.85; it uses BK7 and F2 glasses and was done as an illustrative design exercise. Figure 10.3, at the same speed, covers 3 times as large a field with a telephoto ratio of 0.81. It utilizes heavier flint glasses (higher index and lower V value) to achieve a modestly improved performance.

Figure 10.4 covers a 30° field at f/4.5 with excellent distortion correction, illustrating the benefits derived from the added degrees of freedom gained by splitting the cemented doublets into widely spaced components. The large telephoto ratio of 0.91 and the modestly high-index glasses are also helpful.

Figure 10.5 illustrates the use of unusual partial dispersion glasses (as described in Chap. 6) to reduce the secondary spectrum. The term *superachromat* implies that at least four wavelengths are brought to a common focus, whereas the term *apochromat* indicates that three wavelengths are corrected. Notice, however, that the spherochromatism and zonal spherical aberration in this lens are much larger than the axial chromatic aberration; these are the aberrations which will determine the limiting performance of this lens.

Figures 10.6, 10.7, and 10.8 each have five elements and illustrate some of the different ways that the inherent capabilities of this configuration can be utilized. In Figs. 10.6 and 10.8, the crown element of the front doublet is split into two elements to reduce the zonal spherical aberration (among others). Figure 10.6 is the result of a classroom exercise which specified a 200-mm f/5.0 lens with a telephoto ratio of 0.80 for a 35-mm camera. It uses quite ordinary glasses and achieves an excellent level of performance. Figure 10.7 uses high-index glass and a different arrangement to get to a speed of f/4.0, but falls a bit short in performance and telephoto ratio (at 0.91). Figure 10.8 uses unusual partial dispersion glasses and breaks the contact in the front doublet, to achieve what is (potentially) a high level of correction, although the telephoto ratio is only a modest 0.95.

Figure 10.9 uses seven elements to produce a well-corrected f/5.6, 6° field lens with an extremely short telephoto ratio of 0.66. Notice the overcorrected Petzval field, with $\rho/f = +2.1$; this is one reason that small telephoto ratios are troublesome.

With a telephoto ratio of 1.06, Fig. 10.10 doesn't really qualify as a true telephoto, but at a speed of f/1.8 and a field of 18°, it is an interesting lens, even if it is difficult to classify.

Figures 10.11 and 10.12 show an internal-focusing telephoto with a modest ratio of 0.92. The front component is fixed and the lens is focused for close-ups by moving the rear component toward the image plane. This could be considered as a sort of macro-style lens.

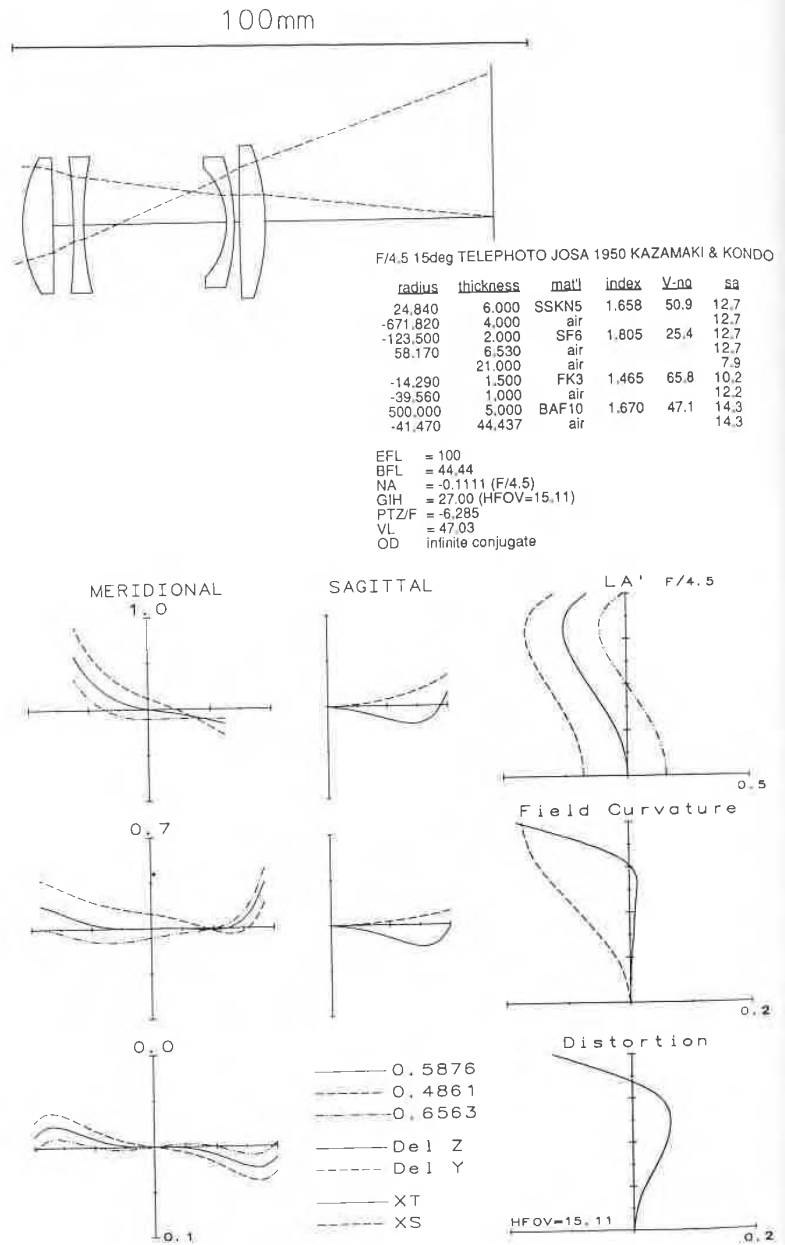
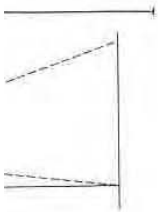


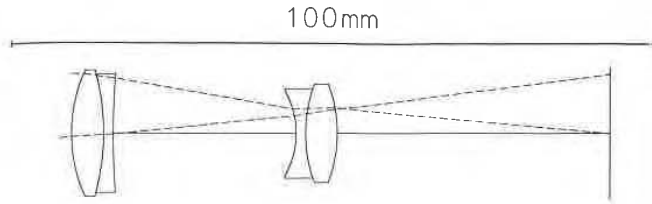
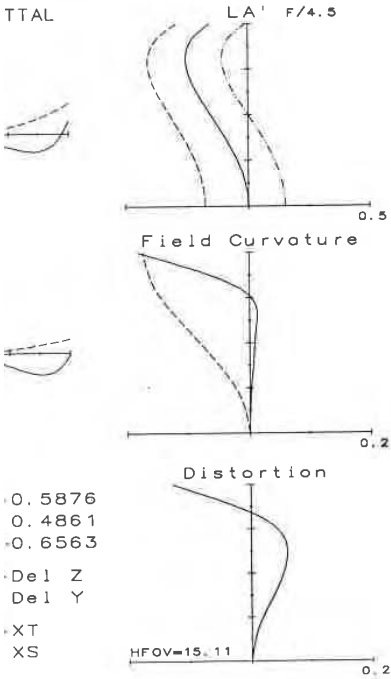
Figure 10.4



f/4.5 15deg TELEPHOTO JOSA 1950 KAZAMAKI & KONDO

radius	thickness	mat'l	index	V-no	sa
24.840	6.000	SSKN5	1.658	50.9	12.7
-671.820	4.000	air			12.7
-123.500	2.000	SF6	1.805	25.4	12.7
58.170	6.530	air			12.7
	21.000	air			7.9
-14.290	1.500	FK3	1.465	65.8	10.2
-39.560	1.000	air			12.2
500.000	5.000	BAF10	1.670	47.1	14.3
-41.470	44.437	air			14.3

iFL = 100
 BFL = 44.44
 NA = -0.1111 (F/4.5)
 GIH = 27.00 (HFOV=15.11)
 PTZ/F = -6.285
 VL = 47.03
 OD = infinite conjugate



SIGLER; SUPER ACHROMAT; TELEPHOTO EFL=254

radius	thickness	mat'l	index	V-no	sa
21.851	5.008	PK51	1.529	77.0	9.5
-34.546	1.502	KZFS9	1.599	46.9	8.9
108.705	1.127	air			8.3
	26.965	air			8.1
-12.852	1.502	KZFS1	1.613	44.3	6.3
19.813	5.008	BASF5	1.603	42.5	6.7
-20.378	42.174	air			7.4

EFL = 100
 BFL = 42.17
 NA = -0.0898 (F/5.6)
 GIH = 8.75
 PTZ/F = -40.38
 VL = 41.11
 OD = infinite conjugate

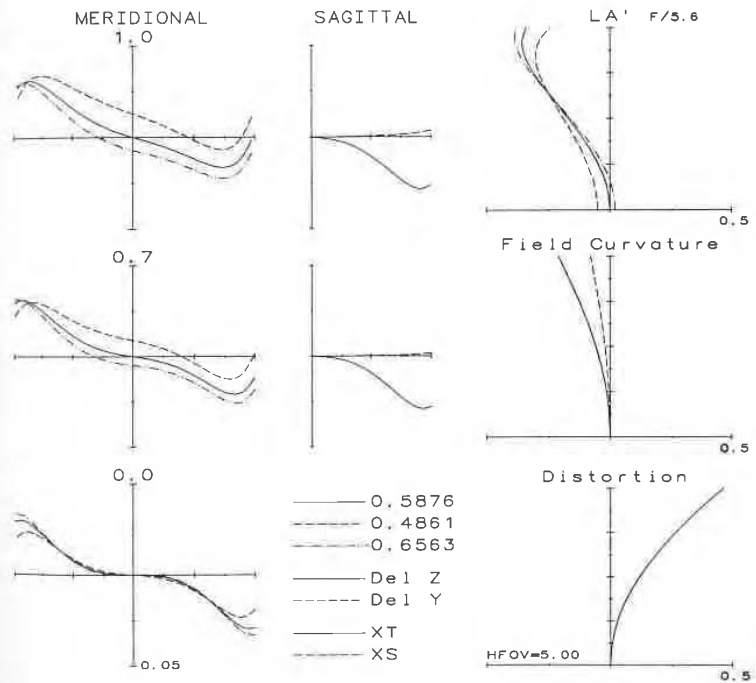
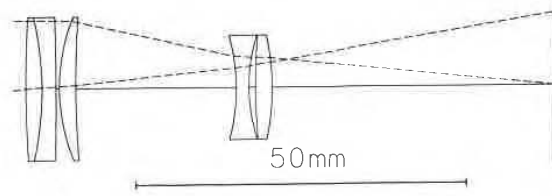


Figure 10.5



F/5.6deg TELEPHOTO

radius	thickness	matl	index	v-no	sa
149.035	2.500	SK4	1.613	58.6	10.5
-46.003	2.000	SF14	1.762	26.5	10.5
-477.921	0.500	air			10.5
26.522	2.500	SK4	1.613	58.6	10.5
132.322	24.060	air			10.5
-28.605	2.000	SK4	1.613	58.6	7.6
22.989	1.050	air			7.6
82.834	2.500	F5	1.603	38.0	7.6
-36.911	42.897	air			7.6

EFL = 100
 BFL = 42.9
 NA = 0.1000 (F/5.0)
 GlH = 10.50 (HFOV=5.99)
 PTZ/F = 7.68
 VL = 37.11
 OD = infinite conjugate

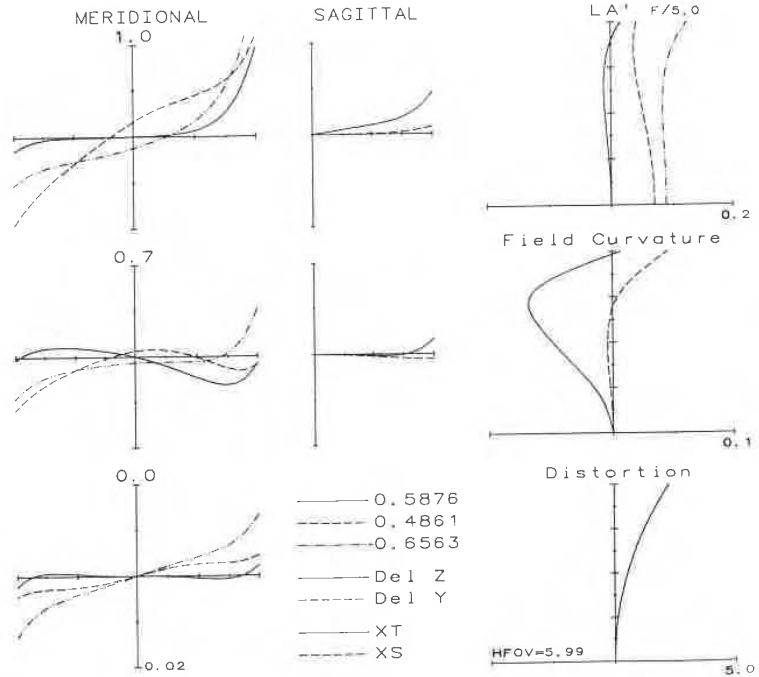
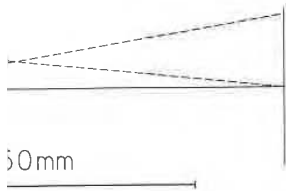
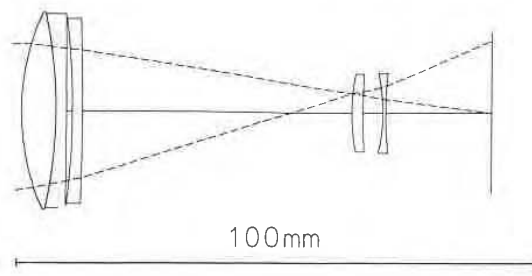
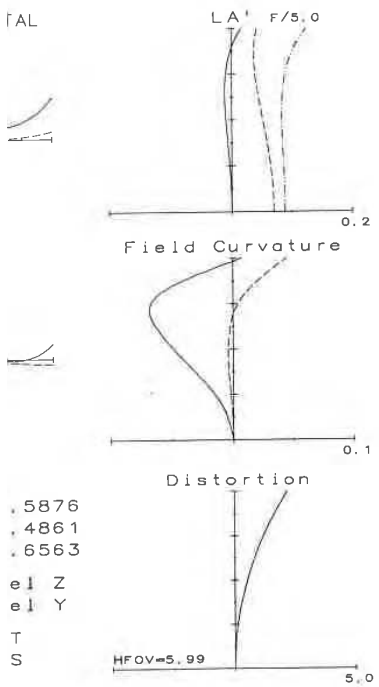


Figure 10.6



matl	index	V-no	sa
SK4	1.613	58.6	10.5
SF14	1.762	26.5	10.5
air			10.5
SK4	1.613	58.6	10.5
air			10.5
SK4	1.613	58.6	7.6
air			7.6
F5	1.603	38.0	7.6
air			7.6

(99)



J. EGGERT ET AL; USP 3388956; F/4 15 DEG. TELEPHOTO #1

radius	thickness	matl	index	V-no	sa
42.156	6.676	LAKN6	1.642	58.0	18.4
-88.214	1.945	SF10	1.728	28.4	18.2
-1800.073	1.183	air			17.4
-137.288	1.945	SF9	1.654	33.7	17.3
-530.649	40.290	air			16.8
	11.913	air			5.4
34.202	2.234	LAF11	1.757	31.7	7.3
117.496	3.859	air			7.3
-31.069	0.526	BSF10	1.650	39.1	7.3
69.782	20.320	air			7.5

EFL = 99.99
 BFL = 20.32
 NA = -0.1256 (F/4.0)
 GIH = 13.16 (HFOV=7.50)
 PTZ/F = 4.272
 VL = 70.57
 OD = infinite conjugate

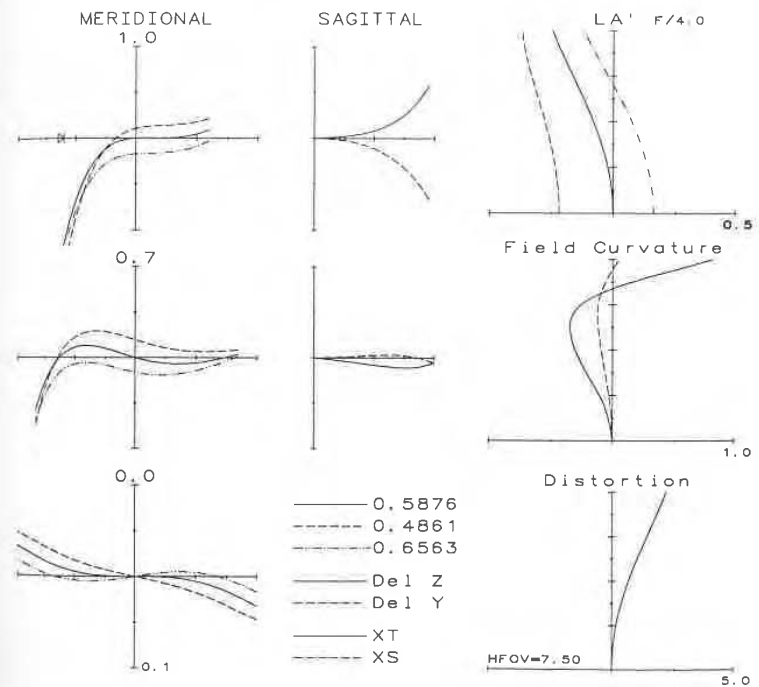
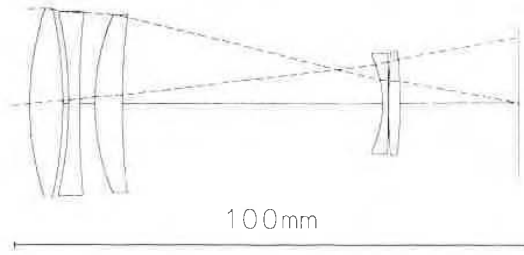


Figure 10.7



SEI MATSUI; USP 4338001; F/2.8 14 DEG. TELEPHOTO LENS #1

radius	thickness	matl	index	V-no	sa
54.585	6.667	FCD1	1.497	81.6	17.9
-77.813	1.111	air			17.7
-76.698	2.056	LAFN7	1.750	34.9	17.3
207.222	3.056	air			17.0
43.208	5.111	BED5	1.658	50.9	16.8
134.444	50.667	air			16.2
-19.462	1.111	K3	1.518	59.0	9.0
-305.556	0.056	air			9.5
121.887	2.222	TAF2	1.794	45.4	9.7
-89.277	22.862	air			9.8

EFL = 100
 BFL = 22.86
 NA = -0.1790 (F/2.8)
 GIH = 12.28 (HFOV=7.00)
 PTZ/F = -9.12
 VL = 72.06
 OD = infinite conjugate

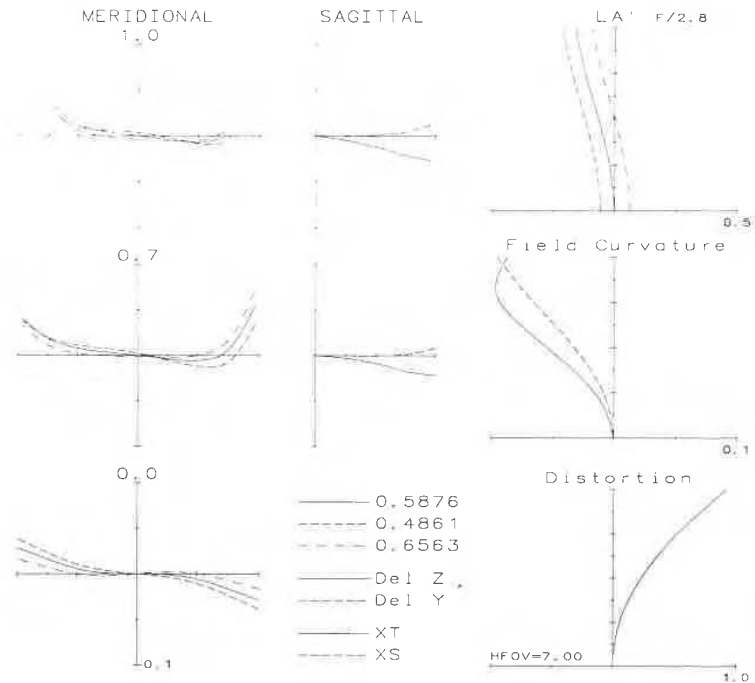
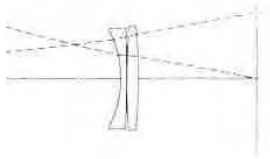


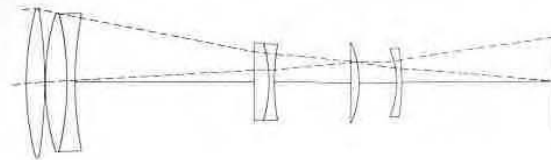
Figure 10.8



0mm

8 14 DEG. TELEPHOTO LENS #1

index	V-no	sa
1.497	81.6	17.9
		17.7
1.750	34.9	17.3
		17.0
1.658	50.9	16.8
		16.2
1.518	59.0	9.0
		9.5
1.794	45.4	9.7
		9.8



50mm

MELVYN H. KREITZER; USP 4359272; 390 MM F/5.6 6 DEG TEL #1

radius	thickness	mat'l	index	V-no	sa
33.072	2.386	C3	1.518	59.0	8.9
-53.387	0.077	air			8.9
27.825	2.857	C3	1.518	59.0	8.4
-35.934	1.025	LAF7	1.749	35.0	8.3
40.900	22.084	air			7.8
	1.794	FD110	1.785	25.7	4.7
-16.775	0.641	TAFD5	1.835	43.0	4.6
27.153	9.607	air			4.5
-120.757	1.035	CF6	1.517	52.2	4.8
-12.105	4.705	air			4.8
-9.386	0.641	TAF1	1.773	49.6	4.0
-24.331	18.960	air			4.1

EFL = 100
 BFL = 18.96
 NA = -0.0892 (F/5.6)
 GIH = 5.24
 PTZ/F = 2.097
 VL = 46.65
 OD = infinite conjugate

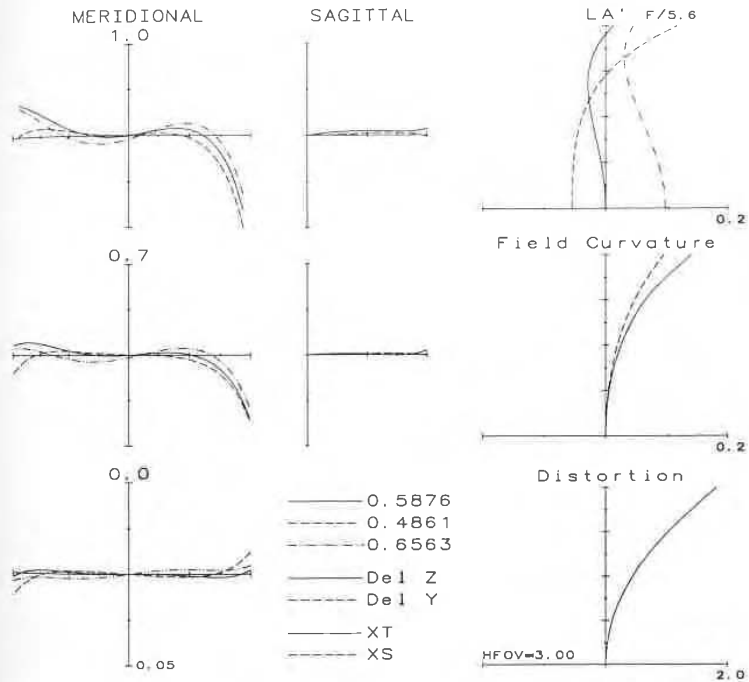
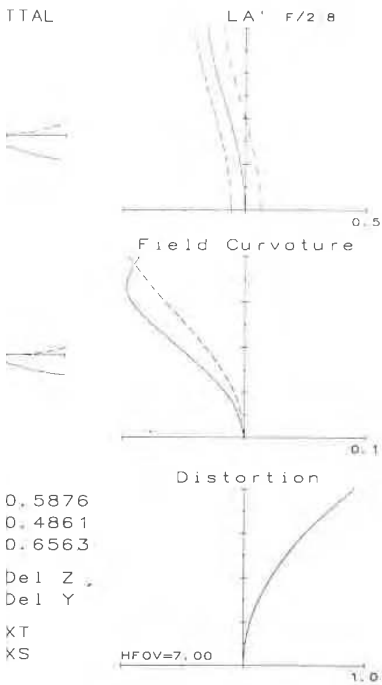


Figure 10.9

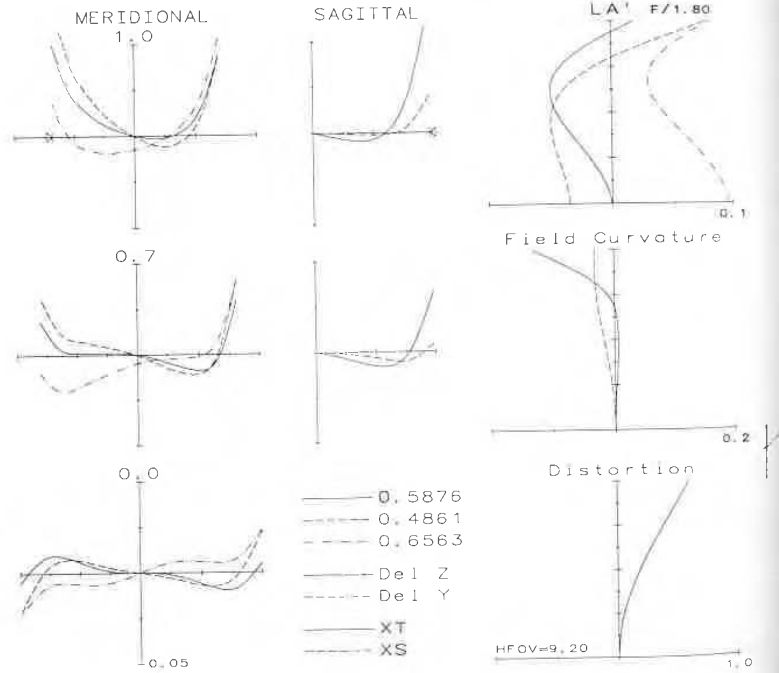
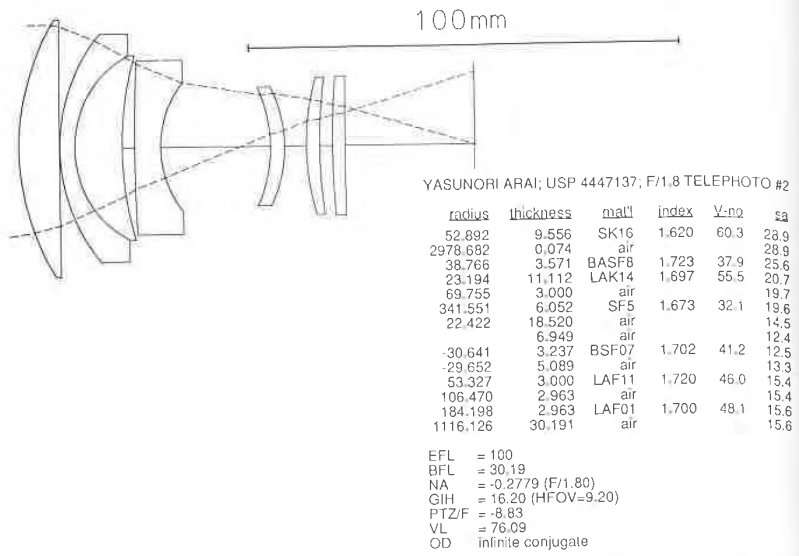
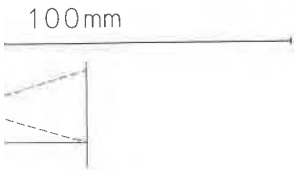


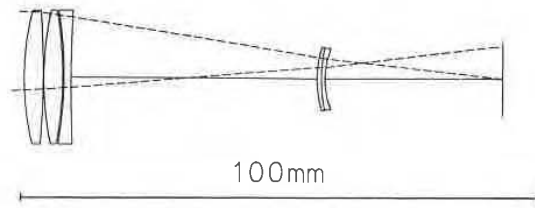
Figure 10.10



YASUNORI ARAI; USP 4447137; F/1.8 TELEPHOTO #2

radius	thickness	matl	index	V-no	sa
52.892	9.556	SK16	1.620	60.3	28.9
2978.682	0.074	air			28.9
38.766	3.571	BASF8	1.723	37.9	25.6
23.194	11.112	LAK14	1.697	55.5	20.7
69.755	3.000	air			19.7
341.551	6.052	SF5	1.673	32.1	19.6
22.422	18.520	air			14.5
	6.949	air			12.4
-30.641	3.237	BSF07	1.702	41.2	12.5
-29.652	5.089	air			13.3
53.327	3.000	LAF11	1.720	46.0	15.4
106.470	2.963	air			15.4
184.198	2.963	LAF01	1.700	48.1	15.6
1116.126	30.191	air			15.6

EFL = 100
 BFL = 30.19
 NA = -0.2779 (F/1.80)
 GIH = 16.20 (HFOV=9.20)
 PTZF = -3.83
 VL = 78.09
 OD = infinite conjugate



MOMIYAMA USP 4,037,935; F/4.5 (LONG EFL POSITION)

radius	thickness	matl	index	V-no	sa
48.796	3.645	CAF	1.434	94.9	12.6
-168.096	0.140	air			12.6
62.820	3.505	FK5	1.487	70.2	12.6
-70.733	0.303	air			12.6
-73.188	1.402	LASF3	1.806	40.9	12.6
250.187	22.431	air			12.6
	25.150	air			7.9
19.535	0.841	SF4	1.755	27.5	6.0
27.456	0.701	LSF16	1.772	49.6	5.8
14.524	34.173	air			5.7

EFL = 112.2
 BFL = 34.17
 NA = -0.1099 (F/4.5)
 GIH = 6.06
 PTZF = -4.07
 VL = 58.12
 OD = infinite conjugate

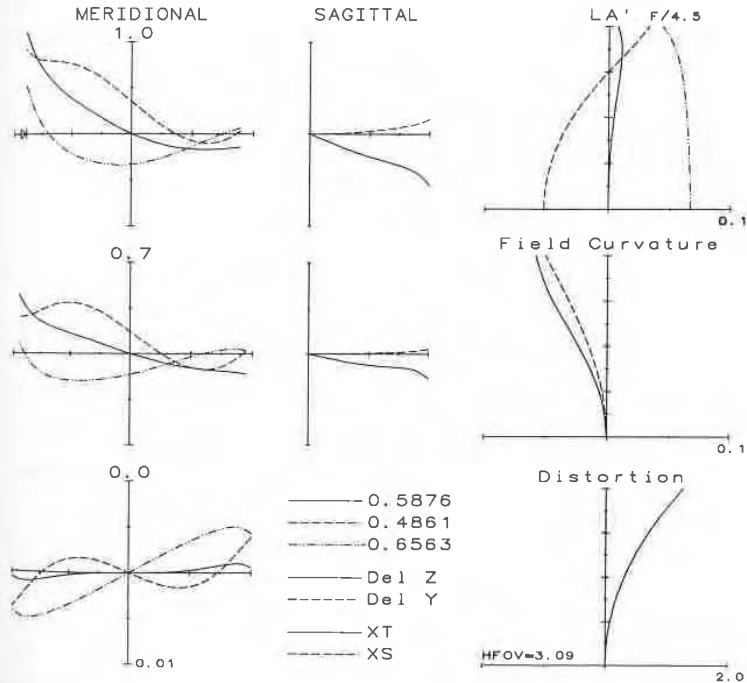
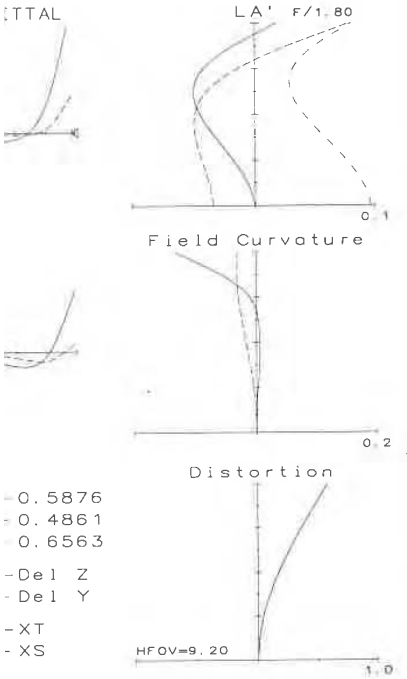
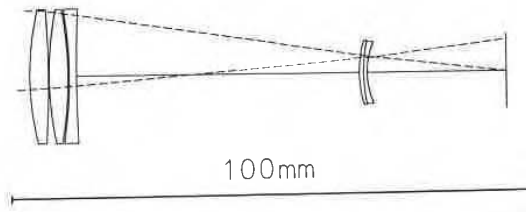


Figure 10.11



MOMIYAMA USP 4,037,935; F/4.5 (SHORT EFL POSITION)

radius	thickness	matl	index	V-no	sa
48.796	3.645	CAF	1.434	94.9	12.6
-168.096	0.140	air			12.6
62.820	3.505	FK5	1.487	70.2	12.6
-70.733	0.303	air			12.6
-73.188	1.402	LASF3	1.806	40.9	12.6
250.187	22.431	air			12.6
	32.440	air			7.9
19.535	0.841	SF4	1.755	27.5	6.0
27.456	0.701	LSF16	1.772	49.6	5.8
14.524	26.657	air			5.7

EFL = 100
 BFL = 26.66
 NA = -0.1139 (F/4.4)
 GIH = 5.93
 PTZ/F = -4.605
 VL = 65.41
 OD = 2243.07 (MAG = -0.048)

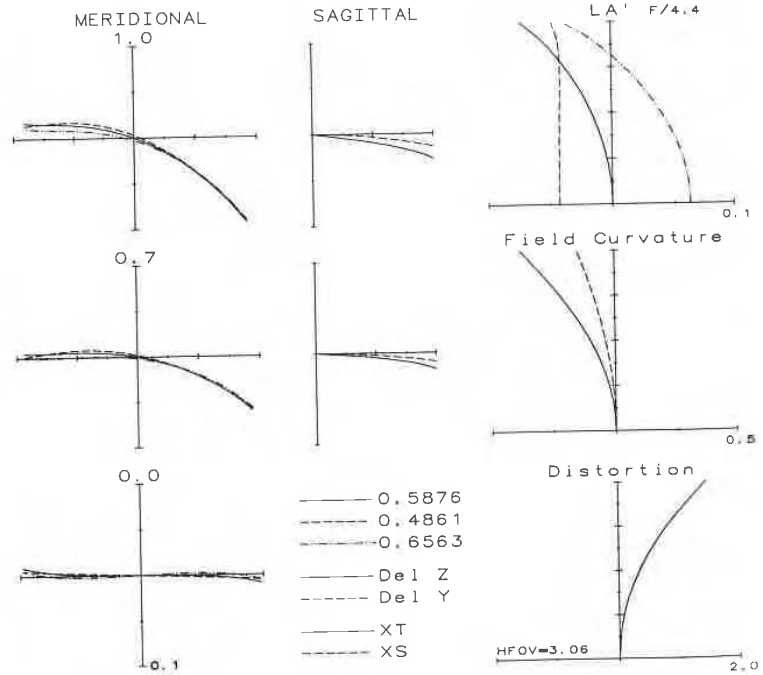


Figure 10.12

MODERN LENS DESIGN
WARREN J. SMITH ■ GENESEE OPTICS SOFTWARE

FT MEADE
GenColl

QC 385

.2

.D47 S65

1992

Copy 2

Optical Engineering



*More than 280 worked-out examples
for optical engineers*

MODERN LENS DESIGN

Finally, lens designers now have at their fingertips a practical, desktop resource of tested lens designs and methods. In addition to extensive design instruction, *Modern Lens Design* features 288 proven designs drawn from patents and the literature of everything from camera lenses to laser collimators, and each example includes:

- **The prescription:** Radii, spacings, materials, EFL, BFL, vertex length, object and image distances, magnification, Petzval radius, wavelength, clear apertures, and more.
- **A drawing of the lens and rays:** A meridional section view of the lens with the axial-marginal ray and the chief ray.
- **Lens aberrations plots:** Ray intercept plots for axis, 0.5, 0.7, and full field, field curvature, distortion, and lateral color.

The manual includes construction and performance data for each design, as well as easy-to-understand, comprehensive instruction in the lens design process, both traditional and CAD. The design examples include classical design types, improvement stages, landmark designs, recent designs/patents, and database designs from OPTICS TOOLBOX.

Beginners and experts alike will turn to this book as the definitive source of lens design examples and techniques for many years to come.

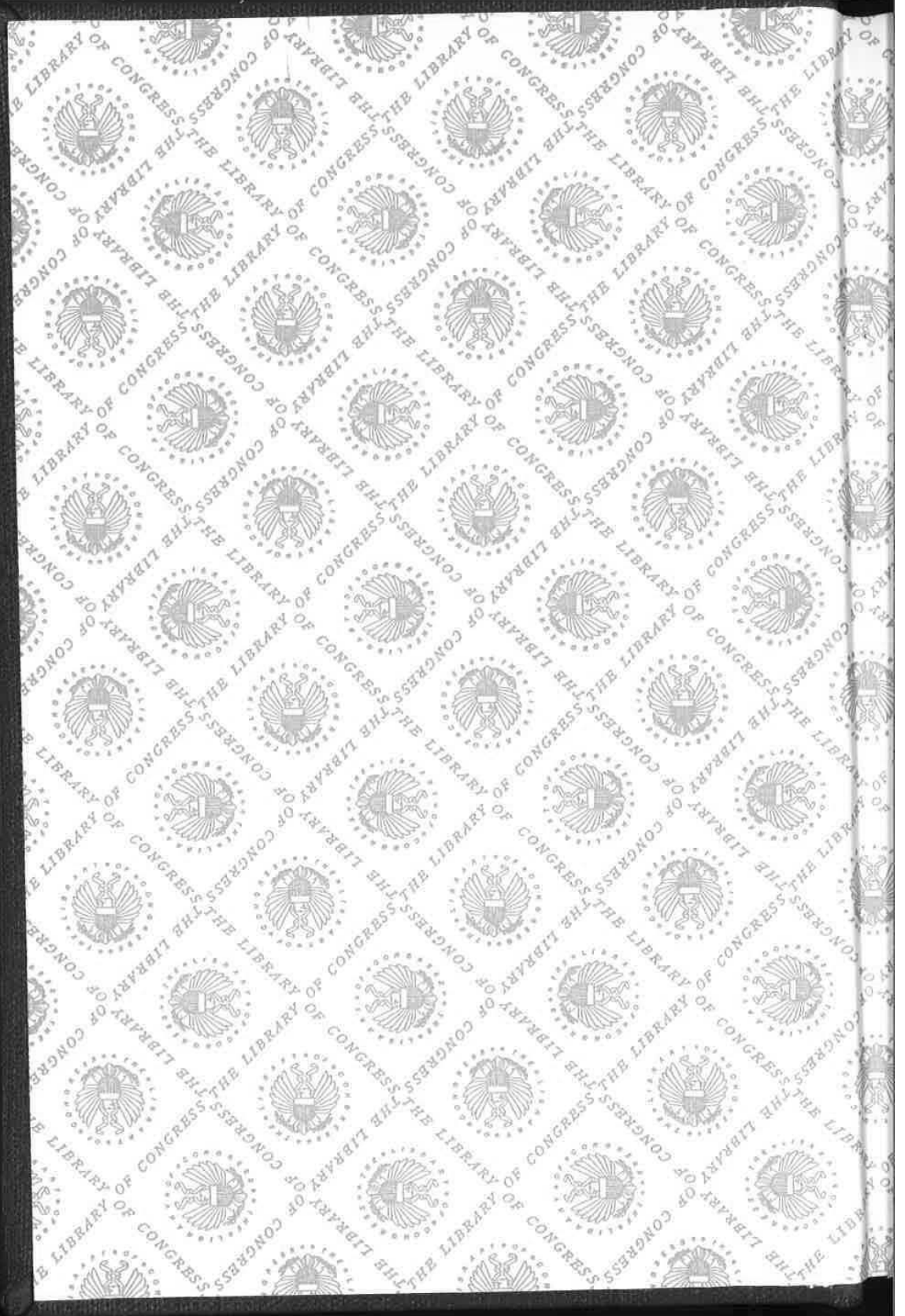
ISBN 0-07-059178-4

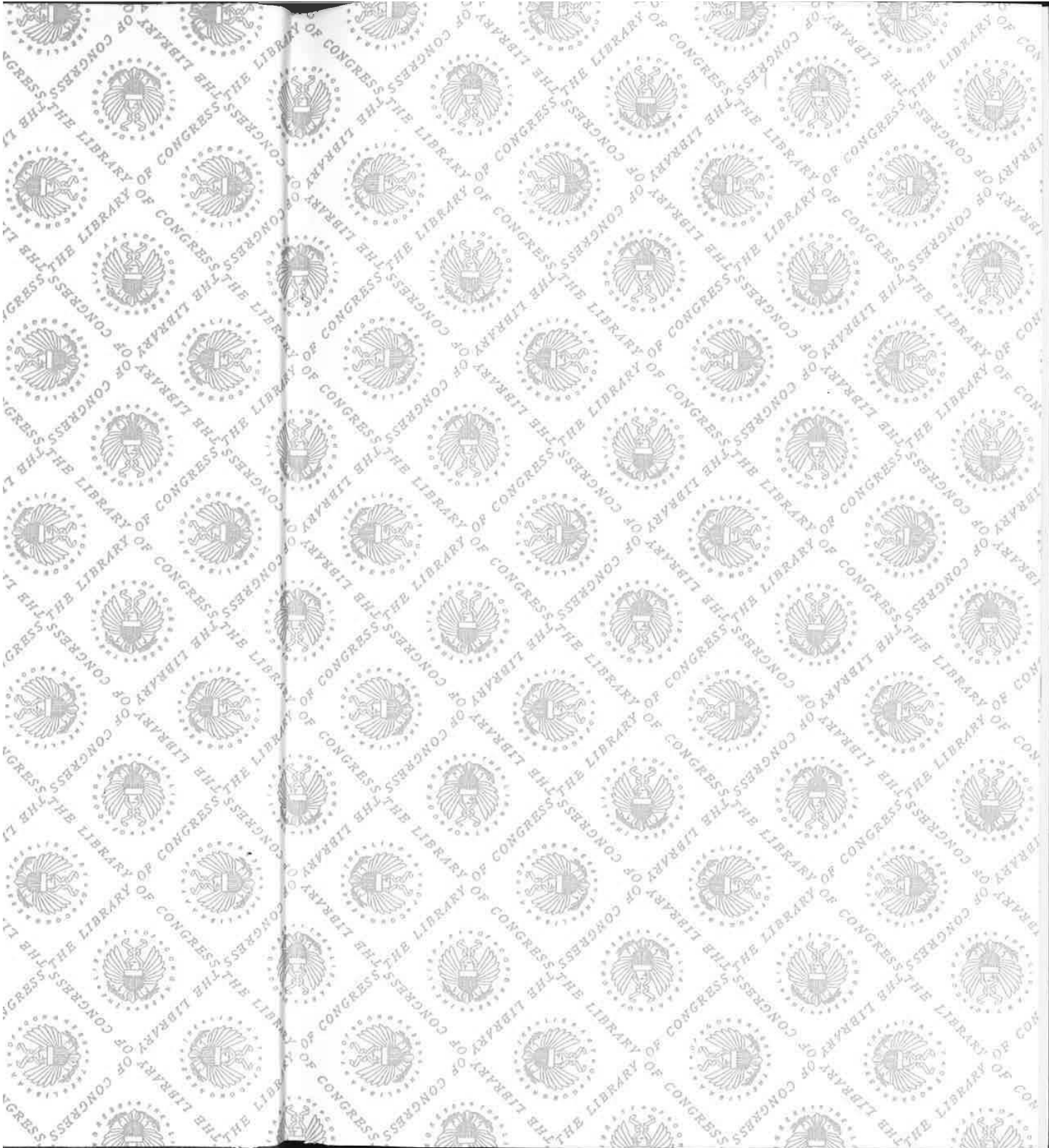


McGraw-Hill, Inc.
Serving the Need for Knowledge
1221 Avenue of the Americas
New York, NY 10020

APPENDIX D





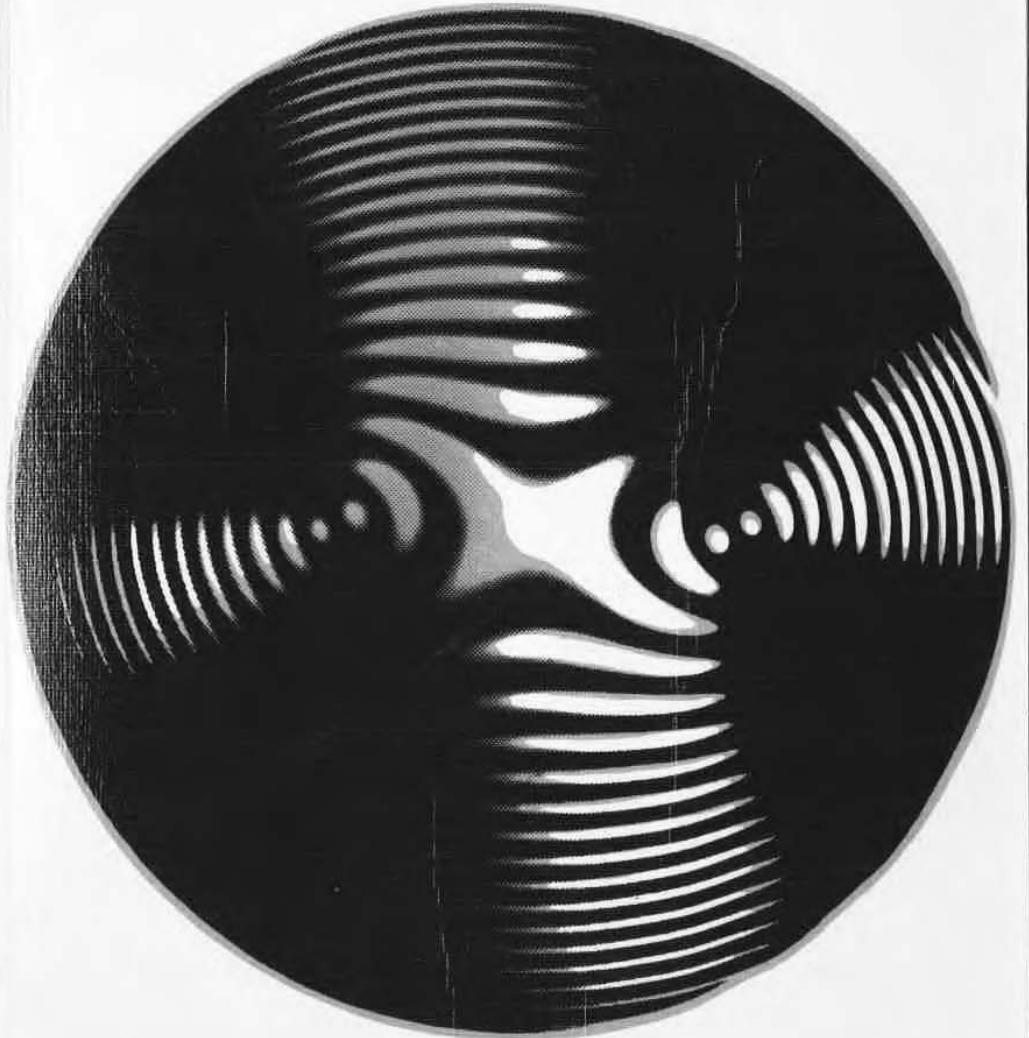


Principles of Optics

ELECTROMAGNETIC THEORY OF PROPAGATION
INTERFERENCE AND DIFFRACTION OF LIGHT

Sixth Edition

MAX BORN & EMIL WOLF



Pergamon Press

v of
NHEIMER

Principles of Optics

*Electromagnetic Theory of Propagation,
Interference and Diffraction of Light*

by

MAX BORN
M.A., Dr.Phil., F.R.S.
Nobel Laureate

*Formerly Professor at the Universities of Göttingen and Edinburgh
and*

EMIL WOLF
Ph.D., D.Sc.

Professor of Physics, University of Rochester, N.Y.

with contributions by

A. B. BHATIA, P. C. CLEMMOW, D. GABOR, A. R. STOKES,
A. M. TAYLOR, P. A. WAYMAN and W. L. WILCOCK

SIXTH EDITION



PERGAMON PRESS

OXFORD · NEW YORK · TORONTO · SYDNEY · PARIS · FRANKFURT

U.K. Pergamon Press Ltd., Headington Hill Hall,
Oxford OX3 0BW, England

U.S.A. Pergamon Press Inc., Maxwell House, Fairview Park,
Elmsford, New York 10523, U.S.A.

CANADA Pergamon of Canada, Suite 104, 150 Consumers Road,
Willowdale, Ontario M2J 1P9, Canada

AUSTRALIA Pergamon Press (Aust.) Pty. Ltd., P.O. Box 544,
Potts Point, N.S.W. 2011, Australia

FRANCE Pergamon Press SARL, 24 rue des Ecoles,
75240 Paris, Cedex 05, France

FEDERAL REPUBLIC
OF GERMANY Pergamon Press GmbH, 6242 Kronberg-Taunus,
Hammerweg 6, Federal Republic of Germany

QC 355
.2
B67
1980
copy 7

Copyright © 1980 Max Born and Emil Wolf
All Rights Reserved. No part of this publication may be reproduced, stored in a retrieval system or transmitted in any form or by any means: electronic, electrostatic, magnetic tape, mechanical, photocopying, recording or otherwise, without permission in writing from the copyright holders



First edition 1959
Second (revised) edition 1964
Third (revised) edition 1965
Fourth (revised) edition 1970
Fifth (revised) edition 1975
Reprinted 1975, 1977
Sixth edition 1980

Library of Congress Cataloging in Publication Data

Born, Max
Principles of optics. - 6th ed.
1. Optics - Collected works
I. Title II. Wolf, Emil
535 QC351 80-41470

ISBN 0-08-026482-4 hardcover
ISBN 0-08-026481-6 flexicover

Printed in Great Britain by A. Wheaton & Co. Ltd., Exeter

Readington Hill Hall,
and
Maxwell House, Fairview Park,
23, U.S.A.
Suite 104, 150 Consumers Road,
J1P9, Canada
Pty. Ltd., P.O. Box 544,
1, Australia
24 rue des Ecoles,
France
6242 Kronberg-Taunus,
Republic of Germany

Born and Emil Wolf

part of this publication may be
retrieval system or transmitted in
means: electronic, electrostatic,
magnetic, photocopying, recording or
any other means.

1964
1965
1970
1975

Logging in Publication Data

1 ed.
1975
1470
1 cover
1 cover

by A. Wheaton & Co. Ltd., Exeter

PREFACE TO THE FIRST EDITION

THE idea of writing this book was a result of frequent enquiries about the possibility of publishing in the English language a book on optics written by one of us* more than twenty-five years ago. A preliminary survey of the literature showed that numerous researches on almost every aspect of optics have been carried out in the intervening years, so that the book no longer gives a comprehensive and balanced picture of the field. In consequence it was felt that a translation was hardly appropriate; instead a substantially new book was prepared, which we are now placing before the reader. In planning this book it soon became apparent that even if only the most important developments which took place since the publication of *Optik* were incorporated, the book would become impracticably large. It was, therefore, deemed necessary to restrict its scope to a narrower field. *Optik* itself did not treat the whole of optics. The optics of moving media, optics of X-rays and γ rays, the theory of spectra and the full connection between optics and atomic physics were not discussed; nor did the old book consider the effects of light on our visual sense organ—the eye. These subjects can be treated more appropriately in connection with other fields such as relativity, quantum mechanics, atomic and nuclear physics, and physiology. In this book not only are these subjects excluded, but also the classical molecular optics which was the subject-matter of almost half of the German book. Thus our discussion is restricted to those optical phenomena which may be treated in terms of MAXWELL'S phenomenological theory. This includes all situations in which the atomistic structure of matter plays no decisive part. The connection with atomic physics, quantum mechanics, and physiology is indicated only by short references wherever necessary. The fact that, even after this limitation, the book is much larger than *Optik*, gives some indication about the extent of the researches that have been carried out in classical optics in recent times.

We have aimed at giving, within the framework just outlined, a reasonably complete picture of our present knowledge. We have attempted to present the theory in such a way that practically all the results can be traced back to the basic equations of MAXWELL'S electromagnetic theory, from which our whole consideration starts.

In Chapter I the main properties of the electromagnetic field are discussed and the effect of matter on the propagation of the electromagnetic disturbance is described formally, in terms of the usual material constants. A more physical approach to the question of influence of matter is developed in Chapter II: it is shown that in the presence of an external incident field, each volume element of a material medium may be assumed to give rise to a secondary (scattered) wavelet and that the combination of these wavelets leads to the observable, macroscopic field. This approach is of considerable physical significance and its power is illustrated in a later chapter (Chapter XII) in connection with the diffraction of light by ultrasonic waves, first treated in this way by A. B. BHATIA and W. J. NOBLE; Chapter XII was contributed by Prof. BHATIA himself.

A considerable part of Chapter III is devoted to showing how geometrical optics follows from MAXWELL'S wave theory as a limiting case of short wavelengths. In addition to discussing the main properties of rays and wave-fronts, the vectorial

* MAX BORN, *Optik* (Berlin, Springer, 1933).

aspects of the problem (propagation of the directions of the field vectors) are also considered. A detailed discussion of the foundations of geometrical optics seemed to us desirable in view of the important developments made in recent years in the related field of microwave optics (optics of short radio waves). These developments were often stimulated by the close analogy between the two fields and have provided new experimental techniques for testing the predictions of the theory. We found it convenient to separate the mathematical apparatus of geometrical optics—the calculus of variations—from the main text; an appendix on this subject (Appendix I) is based in the main part on unpublished lectures given by D. HILBERT at Göttingen University in the early years of this century. The following appendix (Appendix II), contributed by Prof. D. GABOR, shows the close formal analogy that exists between geometrical optics, classical mechanics, and electron optics, when these subjects are presented in the language of the calculus of variations.

We make no apology for basing our treatment of geometrical theory of imaging (Chapter IV) on HAMILTON's classical methods of characteristic functions. Though these methods have found little favour in connection with the design of optical instruments, they represent nevertheless an essential tool for presenting in a unified manner the many diverse aspects of the subject. It is, of course, possible to derive some of the results more simply from *ad hoc* assumptions; but, however valuable such an approach may be for the solution of individual problems, it cannot have more than illustrative value in a book concerned with a systematic development of a theory from a few simple postulates.

The defect of optical images (the influence of aberrations) may be studied either by geometrical optics (appropriate when the aberrations are large), or by diffraction theory (when they are sufficiently small). Since one usually proceeds from quite different starting points in the two methods of treatments, a comparison of results has in the past not always been easy. We have attempted to develop a more unified treatment, based on the concept of the deformation of wave-fronts. In the geometrical analysis of aberrations (Chapter V) we have found it possible and advantageous to follow, after a slight modification of his eikonal, the old method of K. SCHWARZSCHILD. The chapter on diffraction theory of aberrations (Chapter IX) gives an account of the NIJBOER-ZERNIKE theory and also includes an introductory section on the imaging of extended objects, in coherent and in incoherent illumination, based on the techniques of FOURIER transforms.

Chapter VI, contributed by Dr. P. A. WAYMAN, gives a brief description of the main image-forming optical systems. Its purpose is to provide a framework for those parts of the book which deal with the theory of image formation.

Chapter VII is concerned with the elements of the theory of interference and with interferometers. Some of the theoretical sections have their nucleus in the corresponding sections of *Optik*, but the chapter has been completely re-written by Dr. W. L. WILCOCK, who has also considerably broadened its scope.

Chapter VIII is mainly concerned with the FRESNEL-KIRCHHOFF diffraction theory and with some of its applications. In addition to the usual topics, the chapter includes a detailed discussion of the central problem of optical image formation—the analysis of the three-dimensional light distribution near the geometrical focus. An account is also given of a less familiar alternative approach to diffraction, based on the notion of the boundary diffraction wave of T. YOUNG.

The chapters so far referred to are mainly concerned with perfectly monochromatic (and therefore completely coherent) light, produced by point sources. Chapter X deals with the more realistic case of light produced by sources of finite extension and

ns of the field vectors) are also of geometrical optics seemed to ade in recent years in the related ves). These developments were e two fields and have provided ions of the theory. We found it us of geometrical optics—the idix on this subject (Appendix I) en by D. HILBERT at Göttingen llowing appendix (Appendix II), nal analogy that exists between optics, when these subjects are is.

f geometrical theory of imaging aracteristic functions. Though with the design of optical instrur presenting in a unified manner se, possible to derive some of the wever valuable such an approach not have more than illustrative oment of a theory from a few

rations) may be studied either ions are large), or by diffraction ne usually proceeds from quite tments, a comparison of results npted to develop a more unified ave-fronts. In the geometrical t possible and advantageous to d method of K. SCHWARZSCHILD. hapter IX) gives an account of n introductory section on the erent illumination, based on the

gives a brief description of the is to provide a framework for f image formation.

theory of interference and with ave their nucleus in the corre- n completely re-written by Dr. d its scope.

L-KIRCHHOFF diffraction theory usual topics, the chapter includes l image formation—the analysis ometrical focus. An account is diffraction, based on the notion

d with perfectly monochromatic by point sources. Chapter X r sources of finite extension and

covering a finite frequency range. This is the subject of partial coherence, where considerable progress has been made in recent years. In fact, a systematic theory of interference and diffraction with partially coherent light has now been developed. This chapter also includes an account of the closely related subject of partial polarization, from the standpoint of coherence theory.

Chapter XI deals with rigorous diffraction theory, a field that has witnessed a tremendous development over the period of the last twenty years,* stimulated largely by advances in the ultra-shortwave radio techniques. This chapter was contributed by Dr. P. C. CLEMMOW who also prepared Appendix III, which deals with the mathematical methods of steepest descent and stationary phase.

The last two chapters, Optics of Metals (Chapter XIII) and Optics of Crystals (Chapter XIV) are based largely on the corresponding chapters of *Optik*, but were revised and extended with the help of Prof. A. M. TAYLOR and Dr. A. R. STOKES respectively. These two subjects are perhaps discussed in less detail than might seem appropriate. However, the optics of metals can only be treated adequately with the help of quantum mechanics of electrons, which is outside the scope of this book. In crystal optics the centre of interest has gradually shifted from visible radiation to X-rays, and the progress made in recent years has been of a technical rather than theoretical nature.

Though we have aimed at producing a book which in its methods of presentation and general approach would be similar to *Optik*, it will be evident that the present book is neither a translation of *Optik*, nor entirely a compilation of known data. As regards our own share in its production, the elder co-author (M. B.) has contributed that material from *Optik* which has been used as a basis for some of the chapters in the present treatise, and has taken an active part in the general planning of the book and in numerous discussions concerning disputable points, presentation, etc. Most of the compiling, writing, and checking of the text was done by the younger co-author (E. W.).

Naturally we have tried to use systematic notation throughout the book. But in a book that covers such a wide field, the number of letters in available alphabets is far too limited. We have, therefore, not always been able to use the most elegant notation but we hope that we have succeeded, at least, in avoiding the use in any one section of the same symbol for different quantities.

In general we use vector notation as customary in Great Britain. After much reflection we rejected the use of the nabla operator alone and employed also the customary "div", "grad", and "curl". Also, we did not adopt the modern electro-technical units, as their main advantage lies in connection with purely electromagnetic measurements, and these play a negligible part in our discussions; moreover, we hope, that if ever a second volume (*Molecular and Atomic Optics*) and perhaps a third volume (*Quantum Optics*) is written, the C.G.S. system, as used in Theoretical Physics, will have returned to favour. Although, in this system of units, the magnetic permeability μ of most substances differs inappreciably from unity at optical frequencies, we have retained it in some of the equations. This has the advantage of greater symmetry and makes it possible to derive "dual" results by making use of the symmetry properties of MAXWELL's equations. For time periodic fields we have used, in complex representation, the factor $\exp(-i\omega t)$ throughout.

We have not attempted the task of referring to all the relevant publications. The

* The important review article by C. J. BOUWKAMP, *Rep. Progr. Phys.* (London, Physical Society), 17 (1954), 35, records more than 500 papers published in the period 1940-1954.

references that are given, and which, we hope, include the most important papers, are to help the reader to gain some orientation in the literature; an omission of any particular reference should not be interpreted as due to our lack of regard for its merit.

In conclusion it is a pleasure to thank many friends and colleagues for advice and help. In the first place we wish to record our gratitude to Professor D. GABOR for useful advice and assistance in the early stages of this project, as well as for providing a draft concerning his ingenious method of reconstructed wave-fronts (§ 8.10). We are also greatly indebted to Dr. F. ABELÈS, who prepared a draft, which is the backbone of § 1.6, on the propagation of electromagnetic waves through stratified media, a field to which he himself has made a substantial contribution. We have also benefited by advice on this subject from Dr. B. H. BILLINGS.

We are much indebted to Dr. H. H. HOPKINS, Dr. R. A. SILVERMAN, Dr. W. T. WELFORD and Dr. G. WYLLIE for critical comments and valuable advice, and to them and also to Dr. G. BLACK, Dr. H. J. J. BRADDICK, Dr. N. CHAKO, Dr. F. D. KAHN, Mr. A. NISBET, Dr. M. ROSS and Mr. R. M. SILLITTO for scrutinizing various sections of the manuscript. We are obliged to Polaroid Corporation for information concerning dichroic materials. Dr. F. D. KAHN helped with proof-reading and Dr. P. ROMAN and Mrs. M. PODOLANSKI with the preparation of the author index.

The main part of the writing was done at the Universities of Edinburgh and Manchester. The last stages were completed whilst one of the authors (E. W.) was a guest at the Institute of Mathematical Sciences, New York University. We are grateful to Professor M. KLINE, Head of its Division of Electromagnetic Research, for his helpful interest and for placing at our disposal some of the technical facilities of the Institute.

We gratefully acknowledge the loan of original photographs by Professor M. FRANÇON and Dr. M. CAGNET (Figs. 7.4, 7.26, 7.28, 7.60, 14.24, 14.26), Professor H. LIPSON and his co-workers at the Manchester College of Science and Technology (Figs. 8.10, 8.12, 8.15), Dr. O. W. RICHARDS (Figs. 8.34, 8.35), and Professor F. ZERNIKE and Dr. K. NIENHUIS (Figs. 9.4, 9.5, 9.8, 9.10, 9.11). Figure 7.66 is reproduced by courtesy of the Director of the Mount Wilson and Palomar Observatories. The blocks of Fig. 7.42 were kindly loaned by Messrs. Hilger and Watts, Ltd., and those of Figs. 7.64 and 7.65 by Dr. K. W. MEISSNER.

Financial assistance was provided by Messrs. Industrial Distributors Ltd., London, and we wish to acknowledge the generosity of the late Sir ERNEST OPPENHEIMER, its former head.

Finally, it is a pleasure to thank our publishers and in particular Mr. E. J. BUCKLEY, Mr. D. M. LOWE and also Dr. P. ROSBAUD, who as a former Director of Pergamon Press was closely associated with this project in its early stages, for the great care they have taken in the production of the book. It is a pleasure to pay tribute also to the printers, Pitman Press of Bath, for the excellence of their printing.

Bad Pymont and Manchester
January 1959

MAX BORN
EMIL WOLF

EDITION

le the most important papers, are
literature; an omission of any
to our lack of regard for its merit.
ads and colleagues for advice and
to Professor D. GABOR for useful
project, as well as for providing
ructed wave-fronts (§ 8.10). We
pared a draft, which is the back-
waves through stratified media,
ial contribution. We have also
BILLINGS.

Dr. R. A. SILVERMAN, Dr. W. T.
its and valuable advice, and to
k, Dr. N. CHAKO, Dr. F. D. KAHN,
for scrutinizing various sections
ration for information concerning
f-reading and Dr. P. ROMAN and
thor index.

Universities of Edinburgh and
one of the authors (E. W.) was
New York University. We are
n of Electromagnetic Research,
al some of the technical facilities

ographs by Professor M. FRANÇON
24, 14.26), Professor H. LIPSON
nce and Technology (Figs. 8.10,
and Professor F. ZERNIKE and
re 7.66 is reproduced by courtesy
Observatories. The blocks of
Watts, Ltd., and those of Figs.

ustrial Distributors Ltd., London,
late Sir ERNEST OPPENHEIMER,

in particular Mr. E. J. BUCKLEY,
a former Director of Pergamon
early stages, for the great care
is a pleasure to pay tribute also
nce of their printing.

MAX BORN
EMIL WOLF

PREFACE TO THE SECOND EDITION

ADVANTAGE has been taken in the preparation of a new edition of this work to make a number of corrections of errors and misprints, to make a few minor additions and to include some new references.

Since the appearance of the first edition almost exactly three years ago, the first optical masers (lasers) have been developed. By means of these devices very intense and highly coherent light beams may be produced. Whilst it is evident that optical masers will prove of considerable value not only for optics but also for other sciences and for technology, no account of them is given in this new edition. For the basic principles of maser action have roots outside the domain of classical electromagnetic theory on which considerations of this book are based. We have, however, included a few references to recent researches in which light generated by optical masers was utilized or which have been stimulated by the potentialities of these new optical devices.

We wish to acknowledge our gratitude to a number of readers who drew our attention to errors and misprints. We are also obliged to Dr. B. KARCEWSKI and Mr. C. L. MEHTA for assistance with the revisions.

Bad Pyrmont and Rochester
November 1962

M. B.
E. W.

PREFACE TO THE SIXTH EDITION

SOME errors found in the earlier editions of this work have been corrected, slight improvements have been made in several sections and a number of references to recent publications have been added. I am obliged to some of our readers who drew my attention to errors and misprints, especially to Drs. J. M. BENNETT, C. BOWLT, J. L. F. DE MEIJERE, MEI-SHENG DENG, A. G. LIEBERMAN, and F. RATAJCZYK.

I also wish to acknowledge my indebtedness to Dr. ARI T. FRIBERG for assistance with the revisions.

Rochester
August 1980

E. W.

CONTENTS

	PAGE
HISTORICAL INTRODUCTION	xxi
I. BASIC PROPERTIES OF THE ELECTROMAGNETIC FIELD	1
1.1. The Electromagnetic Field	1
1.1.1. Maxwell's equations	1
1.1.2. Material equations	2
1.1.3. Boundary conditions at a surface of discontinuity	4
1.1.4. The energy law of the electromagnetic field	7
1.2. The Wave Equation and the Velocity of Light	10
1.3. Scalar Waves	14
1.3.1. Plane waves	14
1.3.2. Spherical waves	15
1.3.3. Harmonic waves. The phase velocity	16
1.3.4. Wave packets. The group velocity	18
1.4. Vector Waves	23
1.4.1. The general electromagnetic plane wave	23
1.4.2. The harmonic electromagnetic plane wave	24
(a) Elliptic polarization	25
(b) Linear and circular polarization	28
(c) Characterization of the state of polarization by Stokes parameters	30
1.4.3. Harmonic vector waves of arbitrary form	32
1.5. Reflection and Refraction of a Plane Wave	36
1.5.1. The laws of reflection and refraction	36
1.5.2. Fresnel formulae	38
1.5.3. The reflectivity and transmissivity; polarization on reflection and refraction	41
1.5.4. Total reflection	47
1.6. Wave Propagation in a Stratified Medium. Theory of Dielectric Films	51
1.6.1. The basic differential equations	52
1.6.2. The characteristic matrix of a stratified medium	55
(a) A homogeneous dielectric film	57
(b) A stratified medium as a pile of thin homogeneous films	58
1.6.3. The reflection and transmission coefficients	59
1.6.4. A homogeneous dielectric film	61
1.6.5. Periodically stratified media	66
II. ELECTROMAGNETIC POTENTIALS AND POLARIZATION	71
2.1. The Electrodynamic Potentials in the Vacuum	72
2.1.1. The vector and scalar potentials	72
2.1.2. Retarded potentials	74

	PAGE
2.2. Polarization and Magnetization	76
2.2.1. The potentials in terms of polarization and magnetization	76
2.2.2. Hertz vectors	79
2.2.3. The field of a linear electric dipole	81
2.3. The Lorentz-Lorenz Formula and Elementary Dispersion Theory	84
2.3.1. The dielectric and magnetic susceptibilities	84
2.3.2. The effective field	85
2.3.3. The mean polarizability: the Lorentz-Lorenz formula	87
2.3.4. Elementary theory of dispersion	90
2.4. Propagation of Electromagnetic Waves Treated by Integral Equations	98
2.4.1. The basic integral equation	99
2.4.2. The Ewald-Oseen extinction theorem and a rigorous derivation of the Lorentz-Lorenz formula	100
2.4.3. Refraction and reflection of a plane wave, treated with the help of the Ewald-Oseen extinction theorem	104
 III. FOUNDATIONS OF GEOMETRICAL OPTICS	 109
3.1. Approximation for Very Short Wavelengths	109
3.1.1. Derivation of the eikonal equation	110
3.1.2. The light rays and the intensity law of geometrical optics	113
3.1.3. Propagation of the amplitude vectors	117
3.1.4. Generalizations and the limits of validity of geometrical optics	119
3.2. General Properties of Rays	121
3.2.1. The differential equation of light rays	121
3.2.2. The laws of refraction and reflection	124
3.2.3. Ray congruences and their focal properties	126
3.3. Other Basic Theorems of Geometrical Optics	127
3.3.1. Lagrange's integral invariant	127
3.3.2. The principle of Fermat	128
3.3.3. The theorem of Malus and Dupin and some related theorems	130
 IV. GEOMETRICAL THEORY OF OPTICAL IMAGING	 133
4.1. The Characteristic Functions of Hamilton	133
4.1.1. The point characteristic	133
4.1.2. The mixed characteristic	135
4.1.3. The angle characteristic	137
4.1.4. Approximate form of the angle characteristic of a refracting surface of revolution	138
4.1.5. Approximate form of the angle characteristic of a reflecting surface of revolution	141
4.2. Perfect Imaging	143
4.2.1. General theorems	143
4.2.2. Maxwell's "fish-eye"	147
4.2.3. Stigmatic imaging of surfaces	149

	PAGE
	76
on and magnetization	76
	79
	81
tary Dispersion Theory	84
ibilities	84
	85
tz-Lorenz formula	87
	90
ated by Integral Equations	98
	99
n and a rigorous derivation	100
wave, treated with the help	104
orem	104
TICS	109
as	109
	110
of geometrical optics	113
rs	117
lidity of geometrical optics	119
	121
ys	121
t	124
roperties	126
ics	127
	127
	128
ad some related theorems	130
IMAGING	133
	133
	133
	135
	137
aracteristic of a refracting	138
aracteristic of a reflecting	141
	143
	143
	147
	149

4.3. Projective Transformation (Collineation) with Axial Symmetry	150
4.3.1. General formulae	151
4.3.2. The telescopic case	154
4.3.3. Classification of projective transformations	154
4.3.4. Combination of projective transformations	155
4.4. Gaussian Optics	157
4.4.1. Refracting surface of revolution	157
4.4.2. Reflecting surface of revolution	160
4.4.3. The thick lens	161
4.4.4. The thin lens	163
4.4.5. The general centred system	164
4.5. Stigmatic Imaging with Wide-angle Pencils	166
4.5.1. The sine condition	167
4.5.2. The Herschel condition	169
4.6. Astigmatic Pencils of Rays	169
4.6.1. Focal properties of a thin pencil	169
4.6.2. Refraction of a thin pencil	171
4.7. Chromatic Aberration. Dispersion by a Prism	174
4.7.1. Chromatic aberration	174
4.7.2. Dispersion by a prism	177
4.8. Photometry and Apertures	181
4.8.1. Basic concepts of photometry	181
4.8.2. Stops and pupils	186
4.8.3. Brightness and illumination of images	188
4.9. Ray Tracing	190
4.9.1. Oblique meridional rays	191
4.9.2. Paraxial rays	193
4.9.3. Skew rays	194
4.10. Design of Aspheric Surfaces	197
4.10.1. Attainment of axial stigmatism	197
4.10.2. Attainment of aplanatism	200
V. GEOMETRICAL THEORY OF ABERRATIONS	203
5.1. Wave and Ray Aberrations; the Aberration Function	203
5.2. The Perturbation Eikonal of Schwarzschild	207
5.3. The Primary (Seidel) Aberrations	211
5.4. Addition Theorem for the Primary Aberrations	218
5.5. The Primary Aberration Coefficients of a General Centred Lens System	220
5.5.1. The Seidel formulae in terms of two paraxial rays	220
5.5.2. The Seidel formulae in terms of one paraxial ray	224
5.5.3. Petzval's theorem	225
5.6. Example: The Primary Aberrations of a Thin Lens	226
5.7. The Chromatic Aberration of a General Centred Lens System	230

	PAGE
VI. IMAGE-FORMING INSTRUMENTS	233
6.1. The Eye	233
6.2. The Camera	235
6.3. The Refracting Telescope	239
6.4. The Reflecting Telescope	245
6.5. Instruments of Illumination	250
6.6. The Microscope	251
VII. ELEMENTS OF THE THEORY OF INTERFERENCE AND INTERFEROMETERS	256
7.1. Introduction	257
7.2. Interference of Two Monochromatic Waves	257
7.3. Two-beam Interference: Division of Wave-front	260
7.3.1. Young's experiment	260
7.3.2. Fresnel's mirrors and similar arrangements	261
7.3.3. Fringes with quasi-monochromatic and white light	264
7.3.4. Use of slit sources; visibility of fringes	265
7.3.5. Application to the measurement of optical path difference: the Rayleigh interferometer	268
7.3.6. Application to the measurement of angular dimensions of sources: the Michelson stellar interferometer	271
7.4. Standing Waves	277
7.5. Two-beam Interference: Division of Amplitude	281
7.5.1. Fringes with a plane parallel plate	281
7.5.2. Fringes with thin films; the Fizeau interferometer	286
7.5.3. Localization of fringes	291
7.5.4. The Michelson interferometer	300
7.5.5. The Twyman-Green and related interferometers	302
7.5.6. Fringes with two identical plates: the Jamin interferometer and interference microscopes	306
7.5.7. The Mach-Zehnder interferometer; the Bates wave-front shearing interferometer	312
7.5.8. The coherence length; the application of two-beam interference to the study of the fine structure of spectral lines	316
7.6. Multiple-beam Interference	323
7.6.1. Multiple-beam fringes with a plane parallel plate	323
7.6.2. The Fabry-Perot interferometer	329
7.6.3. The application of the Fabry-Perot interferometer to the study of the fine structure of spectral lines	333
7.6.4. The application of the Fabry-Perot interferometer to the comparison of wavelengths	338
7.6.5. The Lummer-Gehrcke interferometer	341
7.6.6. Interference filters	347
7.6.7. Multiple-beam fringes with thin films	351

	PAGE
	233
	233
	235
	239
	245
	250
	251
INTERFERENCE AND	
	256
	257
	257
front	260
	260
ments	261
nd white light	264
es	265
optical path difference: the	268
	268
ular dimensions of sources:	
r	271
	277
tude	281
	281
interferometer	286
	291
	300
erferometers	302
the Jamin interferometer	306
; the Bates wave-front	312
n of two-beam interference	
f spectral lines	316
	323
parallel plate	323
	329
nterferometer to the study	
es	333
interferometer to the com-	
	338
r	341
	347
s	351

CONTENTS		xv
		PAGE
7.6.8. Multiple-beam fringes with two plane parallel plates		360
(a) Fringes with monochromatic and quasi-monochromatic light		360
(b) Fringes of superposition		364
7.7. The Comparison of Wavelengths with the Standard Metre		367
VIII. ELEMENTS OF THE THEORY OF DIFFRACTION		370
8.1. Introduction		370
8.2. The Huygens-Fresnel Principle		370
8.3. Kirchhoff's Diffraction Theory		375
8.3.1. The integral theorem of Kirchhoff		375
8.3.2. Kirchhoff's diffraction theory		378
8.3.3. Fraunhofer and Fresnel diffraction		382
8.4. Transition to a Scalar Theory		387
8.4.1. The image field due to a monochromatic oscillator		387
8.4.2. The total image field		390
8.5. Fraunhofer Diffraction at Apertures of Various Forms		392
8.5.1. The rectangular aperture and the slit		393
8.5.2. The circular aperture		395
8.5.3. Other forms of aperture		398
8.6. Fraunhofer Diffraction in Optical Instruments		401
8.6.1. Diffraction gratings		401
(a) The principle of the diffraction grating		401
(b) Types of grating		407
(c) Grating spectrographs		412
8.6.2. Resolving power of image-forming systems		414
8.6.3. Image formation in the microscope		418
(a) Incoherent illumination		418
(b) Coherent illumination—Abbe's theory		419
(c) Coherent illumination—Zernike's phase contrast method of observation		424
8.7. Fresnel Diffraction at a Straight Edge		428
8.7.1. The diffraction integral		428
8.7.2. Fresnel's integrals		430
8.7.3. Fresnel diffraction at a straight edge		433
8.8. The Three-dimensional Light Distribution near Focus		435
8.8.1. Evaluation of the diffraction integral in terms of Lommel functions		435
8.8.2. The distribution of intensity		439
(a) Intensity in the geometrical focal plane		441
(b) Intensity along the axis		441
(c) Intensity along the boundary of the geometrical shadow		441
8.8.3. The integrated intensity		442
8.8.4. The phase behaviour		445
8.9. The Boundary Diffraction Wave		449

	PAGE
8.10. Gabor's Method of Imaging by Reconstructed Wave-fronts (Holography)	453
8.10.1. Producing the positive hologram	453
8.10.2. The reconstruction	455
 IX. THE DIFFRACTION THEORY OF ABERRATIONS	 459
9.1. The Diffraction Integral in the Presence of Aberrations	460
9.1.1. The diffraction integral	462
9.1.2. The displacement theorem. Change of reference sphere	462
9.1.3. A relation between the intensity and the average deformation of wave-fronts	463
9.2. Expansion of the Aberration Function	464
9.2.1. The circle polynomials of Zernike	464
9.2.2. Expansion of the aberration function	466
9.3. Tolerance Conditions for Primary Aberrations	468
9.4. The Diffraction Pattern Associated with a Single Aberration	473
9.4.1. Primary spherical aberration	475
9.4.2. Primary coma	477
9.4.3. Primary astigmatism	479
9.5. Imaging of Extended Objects	480
9.5.1. Coherent illumination	481
9.5.2. Incoherent illumination	484
 X. INTERFERENCE AND DIFFRACTION WITH PARTIALLY COHERENT LIGHT	 491
10.1. Introduction	491
10.2. A Complex Representation of Real Polychromatic Fields	494
10.3. The Correlation Functions of Light Beams	499
10.3.1. Interference of two partially coherent beams. The mutual coherence function and the complex degree of coherence	499
10.3.2. Spectral representation of mutual coherence	503
10.4. Interference and Diffraction with Quasi-monochromatic Light	505
10.4.1. Interference with quasi-monochromatic light. The mutual intensity	505
10.4.2. Calculation of mutual intensity and degree of coherence for light from an extended incoherent quasi-monochromatic source	508
(a) The Van Cittert-Zernike theorem	508
(b) Hopkins' formula	512
10.4.3. An example	513
10.4.4. Propagation of mutual intensity	516

	PAGE	CONTENTS	PAGE
ruacted Wave-fronts	453	10.5. Some Applications	518
	453	10.5.1. The degree of coherence in the image of an extended incoherent quasi-monochromatic source	518
	455	10.5.2. The influence of the condenser on resolution in a microscope	522
RRATIONS	459	(a) Critical illumination	522
Aberrations	460	(b) Köhler's illumination	524
	462	10.5.3. Imaging with partially coherent quasi-monochromatic illumination	526
of reference sphere	462	(a) Transmission of mutual intensity through an optical system	526
d the average deformation	463	(b) Images of transilluminated objects	528
	464	10.6. Some Theorems Relating to Mutual Coherence	532
	464	10.6.1. Calculation of mutual coherence for light from an incoherent source	532
	466	10.6.2. Propagation of mutual coherence	534
	468	10.7. Rigorous Theory of Partial Coherence	535
Single Aberration	473	10.7.1. Wave equations for mutual coherence	535
	475	10.7.2. Rigorous formulation of the propagation law for mutual coherence	537
	477	10.7.3. The coherence time and the effective spectral width	540
	479	10.8. Polarization Properties of Quasi-monochromatic Light	544
	480	10.8.1. The coherency matrix of a quasi-monochromatic plane wave	544
	481	(a) Completely unpolarized light (Natural light)	548
	484	(b) Completely polarized light	549
		10.8.2. Some equivalent representations. The degree of polarization of a light wave	550
		10.8.3. The Stokes parameters of a quasi-monochromatic plane wave	554
WITH PARTIALLY	491	XI. RIGOROUS DIFFRACTION THEORY	556
	491	11.1. Introduction	556
romatic Fields	494	11.2. Boundary Conditions and Surface Currents	557
	499	11.3. Diffraction by a Plane Screen: Electromagnetic Form of Babinet's Principle	559
erent beams. The mutual	499	11.4. Two-dimensional Diffraction by a Plane Screen	560
lex degree of coherence	503	11.4.1. The scalar nature of two-dimensional electromagnetic fields	560
herence	503	11.4.2. An angular spectrum of plane waves	561
nonochromatic Light	505	11.4.3. Formulation in terms of dual integral equations	564
matic light. The mutual	505	11.5. Two-dimensional Diffraction of a Plane Wave by a Half-plane	565
id degree of coherence for	508	11.5.1. Solution of the dual integral equations for <i>E</i> -polarization	565
erent quasi-monochromatic	508	11.5.2. Expression of the solution in terms of Fresnel integrals	567
	512	11.5.3. The nature of the solution	570
	513	11.5.4. The solution for <i>H</i> -polarization	574
	516	11.5.5. Some numerical calculations	575
		11.5.6. Comparison with approximate theory and with experimental results	577

	PAGE
11.6. Three-dimensional Diffraction of a Plane Wave by a Half-plane	578
11.7. Diffraction of a Localized Source by a Half-plane	580
11.7.1. A line-current parallel to the diffracting edge	580
11.7.2. A dipole	584
11.8. Other Problems	587
11.8.1. Two parallel half-planes	587
11.8.2. An infinite stack of parallel, staggered half-planes	589
11.8.3. A strip	589
11.8.4. Further problems	591
11.9. Uniqueness of Solution	591
XII. DIFFRACTION OF LIGHT BY ULTRASONIC WAVES	593
12.1. Qualitative Description of the Phenomenon and Summary of Theories Based on Maxwell's Differential Equations	593
12.1.1. Qualitative description of the phenomenon	593
12.1.2. Summary of theories based on Maxwell's equations	596
12.2. Diffraction of Light by Ultrasonic Waves as Treated by the Integral Equation Method	599
12.2.1. Integral equation for <i>E</i> -polarization	600
12.2.2. The trial solution of the integral equation	601
12.2.3. Expressions for the amplitudes of the light waves in the diffracted and reflected spectra	603
12.2.4. Solution of the equations by a method of successive approximations	604
12.2.5. Expressions for the intensities of the first and second order lines for some special cases	607
12.2.6. Some qualitative results	608
12.2.7. The Raman-Nath approximation	609
XIII. OPTICS OF METALS	611
13.1. Wave Propagation in a Conductor	611
13.2. Refraction and Reflection at a Metal Surface	615
13.3. Elementary Electron Theory of the Optical Constants of Metals	624
13.4. Wave Propagation in a Stratified Conducting Medium. Theory of Metallic Films	627
13.4.1. An absorbing film on a transparent substrate	628
13.4.2. A transparent film on an absorbing substrate	632
13.5. Diffraction by a Conducting Sphere; Theory of Mie	633
13.5.1. Mathematical solution of the problem	635
(a) Representation of the field in terms of Debye's potentials	635
(b) Series expansions for the field components	640
(c) Summary of formulae relating to the associated Legendre functions and to the cylindrical functions	646

	PAGE
Wave by a Half-plane	578
E-plane	580
ring edge	580
	584
	587
	587
and half-planes	589
	589
	591
	591
ONIC WAVES	593
mon and Summary of	
l Equations	593
monon	593
rell's equations	596
s Treated by the Integral	
	599
	600
ation	601
the light waves in the	
	603
od of successive approxi-	
	604
ie first and second order	
	607
	608
	609
	611
	611
ice	615
l Constants of Metals	624
ting Medium. Theory of	
	627
substrate	628
substrate	632
ry of Mie	633
n	635
of Debye's potentials	635
onents	640
the associated Legendre	
unctions	646

CONTENTS		xix
13.5.2. Some consequences of Mie's formulae		PAGE
(a) The partial waves		647
(b) Limiting cases		649
(c) Intensity and polarization of the scattered light		652
13.5.3. Total scattering and extinction		657
(a) Some general considerations		657
(b) Computational results		661
XIV. OPTICS OF CRYSTALS		665
14.1. The Dielectric Tensor of an Anisotropic Medium		665
14.2. The Structure of a Monochromatic Plane Wave in an Anisotropic Medium		667
14.2.1. The phase velocity and the ray velocity		667
14.2.2. Fresnel's formulae for the propagation of light in crystals		670
14.2.3. Geometrical constructions for determining the velocities of propagation and the directions of vibration		673
(a) The ellipsoid of wave normals		673
(b) The ray ellipsoid		676
(c) The normal surface and the ray surface		676
14.3. Optical Properties of Uniaxial and Biaxial Crystals		678
14.3.1. The optical classification of crystals		678
14.3.2. Light propagation in uniaxial crystals		679
14.3.3. Light propagation in biaxial crystals		681
14.3.4. Refraction in crystals		684
(a) Double refraction		684
(b) Conical refraction		686
14.4. Measurements in Crystal Optics		690
14.4.1. The Nicol prism		690
14.4.2. Compensators		691
(a) The quarter-wave plate		691
(b) Babinet's compensator		692
(c) Soleil's compensator		694
(d) Berek's compensator		694
14.4.3. Interference with crystal plates		694
14.4.4. Interference figures from uniaxial crystal plates		698
14.4.5. Interference figures from biaxial crystal plates		701
14.4.6. Location of optic axes and determination of the principal refractive indices of a crystalline medium		702
14.5. Stress Birefringence and Form Birefringence		703
14.5.1. Stress birefringence		703
14.5.2. Form birefringence		705
14.6. Absorbing Crystals		708
14.6.1. Light propagation in an absorbing anisotropic medium		708
14.6.2. Interference figures from absorbing crystal plates		713
(a) Uniaxial crystals		714
(b) Biaxial crystals		715
14.6.3. Dichroic polarizers		716

	PAGE
APPENDICES	719
I. <i>The Calculus of Variations</i>	719
1. Euler's equations as necessary conditions for an extremum	719
2. Hilbert's independence integral and the Hamilton-Jacobi equation	720
3. The field of extremals	722
4. Determination of all extremals from the solution of the Hamilton-Jacobi equation	724
5. Hamilton's canonical equations	725
6. The special case when the independent variable does not appear explicitly in the integrand	726
7. Discontinuities	727
8. Weierstrass' and Legendre's conditions (sufficiency conditions for an extremum)	729
9. Minimum of the variational integral when one end point is constrained to a surface	731
10. Jacobi's criterion for a minimum	732
11. Example I: Optics	732
12. Example II: Mechanics of material points	734
II. <i>Light Optics, Electron Optics and Wave Mechanics</i>	738
1. The Hamiltonian analogy in elementary form	738
2. The Hamiltonian analogy in variational form	740
3. Wave mechanics of free electrons	743
4. The application of optical principles to electron optics	745
III. <i>Asymptotic Approximations to Integrals</i>	747
1. The method of steepest descent	747
2. The method of stationary phase	752
3. Double integrals	753
IV. <i>The Dirac Delta Function</i>	755
V. <i>A Mathematical Lemma used in the Rigorous Derivation of the Lorentz-Lorenz Law</i> (§ 2.4.2)	760
VI. <i>Propagation of Discontinuities in an Electromagnetic Field</i> (§ 3.1.1)	763
1. Relations connecting discontinuous changes in field vectors	763
2. The field on a moving discontinuity surface	765
VII. <i>The Circle Polynomials of Zernike</i> (§ 9.2.1)	767
1. Some general considerations	767
2. Explicit expressions for the radial polynomials $R_n^{\pm m}(\rho)$	769
VIII. <i>Proof of an Inequality</i> (§ 10.7.3)	773
IX. <i>Evaluation of Two Integrals</i> (§ 12.2.2)	775
AUTHOR INDEX	779
SUBJECT INDEX	790

Let c be the distance between the focal points F'_0 and F_1 . Since the image space of the first transformation coincides with the object space of the second,

$$Z_1 = Z'_0 - c, \quad Y_1 = Y'_0. \quad (23)$$

Elimination of the coordinates of the intermediate space from (22) by means of (23) gives

$$\left. \begin{aligned} Y'_1 &= \frac{Z'_1 Y_1}{f'_1} = \frac{Z'_1 Y'_0}{f'_1} = \frac{Z'_1 f_0 Y_0}{f'_1 Z_0} = \frac{f_0 f_1 Y_0}{f_0 f'_0 - c Z_0}, \\ Z'_1 &= \frac{f_1 f'_1}{Z_1} = \frac{f_1 f'_1}{Z'_0 - c} = \frac{f_1 f'_1}{\frac{f_0 f'_0}{Z_0} - c} = \frac{f_1 f'_1 Z_0}{f_0 f'_0 - c Z_0} \end{aligned} \right\} \quad (24)$$

Let

$$\left. \begin{aligned} Y &= Y_0, & Z &= Z_0 - \frac{f_0 f'_0}{c}, \\ Y' &= Y'_1, & Z' &= Z'_1 + \frac{f_1 f'_1}{c}. \end{aligned} \right\} \quad (25)$$

Equations (25) express a change of coordinates, the origins of the two systems being shifted by distances $f'_0 f_0/c$ and $-f_1 f'_1/c$ respectively in the Z -direction. In terms of these variables, the equations of the combined transformation become

$$\frac{Y'}{Y} = \frac{f}{Z} = \frac{Z'}{f'}, \quad (26)$$

where

$$f = -\frac{f_0 f_1}{c}, \quad f' = \frac{f'_0 f'_1}{c}. \quad (27)$$

The distance between the origins of the new and the old systems of coordinates, i.e. the distances $\delta = F_0 F'$ and $\delta' = F'_1 F'$ of the foci of the equivalent transformation from the foci of the individual transformations are seen from (25) to be

$$\delta = \frac{f_0 f'_0}{c}, \quad \delta' = -\frac{f_1 f'_1}{c}. \quad (28)$$

If $c = 0$, then $f = f' = \infty$ so that the equivalent collineation is telescopic. The equations (24) then reduce to

$$\left. \begin{aligned} Y'_1 &= \frac{f_1}{f'_0} Y_0, \\ Z'_1 &= \frac{f_1 f'_1}{f_0 f'_0} Z_0; \end{aligned} \right\} \quad (29)$$

the constants α and β in (18) of the equivalent transformation, are therefore

$$\alpha = \frac{f_1}{f'_0}, \quad \beta = \frac{f_1 f'_1}{f_0 f'_0}. \quad (30)$$

The angular magnification is now

$$\frac{\tan \gamma'}{\tan \gamma} = \frac{\alpha}{\beta} = \frac{f_0}{f'_1}. \quad (31)$$

If one or both of the transformations are telescopic, the above considerations must be somewhat modified.

F'_0 and F_1 . Since the image space of the first system is the object space of the second,

$$Y_1 = Y'_0. \quad (23)$$

Eliminate Y_1 from (22) by means of (23)

$$\left. \begin{aligned} \frac{Y_0}{c} &= \frac{f_0 f_1 Y_0}{f_0 f'_0 - c Z_0}, \\ \frac{f'_1}{-c} &= \frac{f_1 f'_1 Z_0}{f_0 f'_0 - c Z_0} \end{aligned} \right\} \quad (24)$$

$$\left. \begin{aligned} Z_0 - \frac{f_0 f'_0}{c} \\ Z'_1 + \frac{f_1 f'_1}{c} \end{aligned} \right\} \quad (25)$$

the origins of the two systems being respectively in the Z -direction. In terms of the transformation become

$$\frac{Z'}{f'} \quad (26)$$

$$= \frac{f_0 f'_1}{c} \quad (27)$$

and the old systems of coordinates, i.e. the foci of the equivalent transformation are seen from (25) to be

$$= -\frac{f_1 f'_1}{c} \quad (28)$$

the equivalent collineation is telescopic. The

$$\left. \begin{aligned} & \\ & \end{aligned} \right\} \quad (29)$$

the transformation, are therefore

$$= \frac{f_1 f'_1}{f_0 f'_0} \quad (30)$$

$$= \frac{f_0}{f'_1} \quad (31)$$

For a telescopic collineation, the above considerations must

4.4 GAUSSIAN OPTICS

We shall now study the elementary properties of lenses, mirrors, and their combinations. In this elementary theory only those points and rays will be considered which lie in the immediate neighbourhood of the axis; terms involving squares and higher powers of off-axis distances, or of the angles which the rays make with the axis, will be neglected. The resulting theory is known as Gaussian optics.*

4.4.1 Refracting surface of revolution

Consider a pencil of rays incident on a refracting surface of revolution which separates two homogeneous media of refractive indices n_0 and n_1 . To begin with, points and rays in both media will be referred to the same Cartesian reference system, whose origin will be taken at the pole O of the surface, with the z -direction along the axis of symmetry.

Let $P_0(x_0, y_0, z_0)$ and $P_1(x_1, y_1, z_1)$ be points on the incident and on the refracted ray respectively. Neglecting terms of degree higher than first, it follows from § 4.1 (29), § 4.1 (40), and § 4.1 (44) that the coordinates of these points and the components of the two rays are connected by the relations

$$\left. \begin{aligned} x_0 - \frac{p_0}{n_0} z_0 &= \frac{\partial T^{(2)}}{\partial p_0} = 2\mathcal{A}p_0 + \mathcal{C}p_1, \\ x_1 - \frac{p_1}{n_1} z_1 &= -\frac{\partial T^{(2)}}{\partial p_1} = -2\mathcal{B}p_1 - \mathcal{C}p_0, \end{aligned} \right\} \quad (1a)$$

$$\left. \begin{aligned} y_0 - \frac{q_0}{n_0} z_0 &= \frac{\partial T^{(2)}}{\partial q_0} = 2\mathcal{A}q_0 + \mathcal{C}q_1, \\ y_1 - \frac{q_1}{n_1} z_1 &= -\frac{\partial T^{(2)}}{\partial q_1} = -2\mathcal{B}q_1 - \mathcal{C}q_0, \end{aligned} \right\} \quad (1b)$$

where, according to § 4.1 (45),

$$\mathcal{A} = \mathcal{B} = \frac{1}{2} \frac{r}{n_1 - n_0}, \quad \mathcal{C} = -\frac{r}{n_1 - n_0} \quad (2)$$

r being the paraxial radius of curvature of the surface.

Let us examine under what conditions all the rays from P_0 (which may be assumed to lie in the plane $x = 0$) will, after refraction, pass through P_1 . The coordinates of P_1 will then depend only on the coordinates of P_0 and not on the components of the rays, so that when q_1 is eliminated from (1b), q_0 must also disappear.

Now from the first equation (1b)

$$q_1 = \frac{1}{\mathcal{C}} \left\{ y_0 - q_0 \left(2\mathcal{A} + \frac{1}{n_0} z_0 \right) \right\}, \quad (3)$$

and substituting this into the second equation, we obtain

$$y_1 = - \left(2\mathcal{B} - \frac{1}{n_1} z_1 \right) \frac{1}{\mathcal{C}} y_0 + \left[\frac{1}{\mathcal{C}} \left(2\mathcal{B} - \frac{1}{n_1} z_1 \right) \left(2\mathcal{A} + \frac{1}{n_0} z_0 \right) - \mathcal{C} \right] q_0. \quad (4)$$

* As before, the usual sign convention of analytical geometry (Cartesian sign convention) is used. The various sign conventions employed in practice are very fully discussed in a Report on the Teaching of Geometrical Optics published by the Physical Society (London) in 1934.

Hence P_1 will be a stigmatic image of P_0 if

$$\left(2\mathcal{A} + \frac{1}{n_0}z_0\right)\left(2\mathcal{B} - \frac{1}{n_1}z_1\right) = \mathcal{C}^2, \quad (5)$$

or, on substituting from (2), if

$$\left[\frac{r}{n_1 - n_0} + \frac{z_0}{n_0}\right]\left[\frac{r}{n_1 - n_0} - \frac{z_1}{n_1}\right] = \frac{r^2}{(n_1 - n_0)^2}. \quad (6)$$

(6) may be written in the form

$$n_0\left[\frac{1}{r} - \frac{1}{z_0}\right] = n_1\left[\frac{1}{r} - \frac{1}{z_1}\right]. \quad (7)$$

It is seen that, within the present degree of approximation, every point gives rise to a stigmatic image; and the distances of the conjugate planes from the pole O of the surface are related by (7). Moreover, equation (4), subject to (5), implies that the imaging is a *projective transformation*.

The expressions on either side of (7) are known as *Abbe's (refraction) invariant* and play an important part in the theory of optical imaging. (7) may also be written in the form

$$\frac{n_1}{z_1} - \frac{n_0}{z_0} = \frac{n_1 - n_0}{r}. \quad (8)$$

The quantity $(n_1 - n_0)/r$ is known as the *power* of the refracting surface and will be denoted by \mathcal{P} ,

$$\mathcal{P} = \frac{n_1 - n_0}{r}. \quad (9)$$

According to (4) and (5) the lateral magnification y_1/y_0 is equal to unity when $z_1/n_1 = 2\mathcal{B} + \mathcal{C}$. But by (2), $2\mathcal{B} + \mathcal{C} = 0$. Hence the unit points U_0 and U_1 are given by $z_0 = z_1 = 0$, i.e. *the unit points coincide with the pole of the surface*. Further, from (8),

$$z_0 \rightarrow -\frac{n_0 r}{n_1 - n_0} \quad \text{as } z_1 \rightarrow \infty$$

and

$$z_1 \rightarrow \frac{n_1 r}{n_1 - n_0} \quad \text{as } z_0 \rightarrow -\infty,$$

so that the abscissae of the foci F_0 and F_1 are $-n_0 r/(n_1 - n_0)$ and $n_1 r/(n_1 - n_0)$ respectively. The focal lengths $f_0 = F_0 U_0$, $f_1 = F_1 U_1$ are therefore given by

$$\left. \begin{aligned} f_0 &= \frac{n_0 r}{n_1 - n_0}, \\ f_1 &= -\frac{n_1 r}{n_1 - n_0}; \end{aligned} \right\} \quad (10)$$

and

$$\frac{1}{n_1} z_1) = \mathcal{C}^2, \tag{5}$$

$$\frac{z_1}{n_1} = \frac{r^2}{(n_1 - n_0)^2}. \tag{6}$$

$$\frac{1}{r} - \frac{1}{z_1}. \tag{7}$$

roximation, every point gives rise to a conjugate planes from the pole O of the surface (4), subject to (5), implies that the

n as Abbe's (refraction) invariant and imaging. (7) may also be written in

$$\frac{-n_0}{r}. \tag{8}$$

of the refracting surface and will be

$$0. \tag{9}$$

ication y_1/y_0 is equal to unity when hence the unit points U_0 and U_1 are with the pole of the surface. Further,

$$z_1 \rightarrow \infty$$

$$z_0 \rightarrow -\infty,$$

re $-n_0 r / (n_1 - n_0)$ and $n_1 r / (n_1 - n_0)$ $F_1 U_1$ are therefore given by

$$\left. \begin{aligned} & \\ & \\ & \end{aligned} \right\} \tag{10}$$

or, in terms of the power \mathcal{P} of the surface,*

$$\frac{n_0}{f_0} = -\frac{n_1}{f_1} = \mathcal{P}. \tag{11}$$

Since f_0 and f_1 have different signs, the imaging is *concurrent* (cf. § 4.3.3). If the surface is convex towards the incident light ($r > 0$) and if $n_0 < n_1$ then $f_0 > 0$, $f_1 < 0$, and the imaging is convergent. If $r > 0$ and $n_0 > n_1$ it is *divergent* (Fig. 4.12). When the surface is concave towards the incident light the situation is reversed.

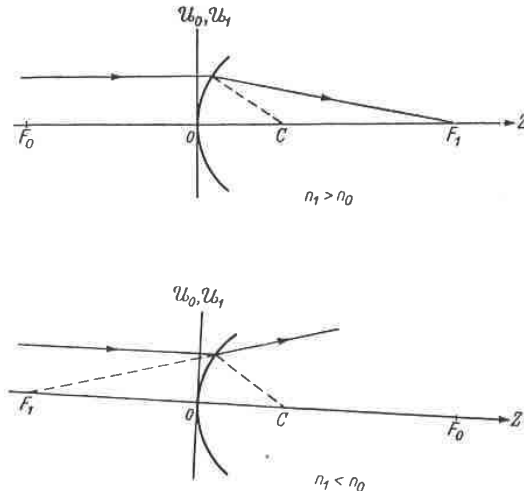


Fig. 4.12. Position of the cardinal points for refraction at a surface of revolution.

Using the expressions (10) for the focal lengths, (8) becomes

$$\frac{f_0}{z_0} + \frac{f_1}{z_1} = -1; \tag{12}$$

and the coefficients (2) may be written in the form

$$\mathcal{A} = \frac{f_0}{2n_0}, \quad \mathcal{B} = -\frac{f_1}{2n_1}, \quad \mathcal{C} = -\frac{f_0}{n_0} = \frac{f_1}{n_1}. \tag{13}$$

Let us introduce separate coordinate systems in the two spaces, with the origins at the foci, and with the axes parallel to those at O :

$$\begin{aligned} X_0 &= x_0, & X_1 &= x_1, \\ Y_0 &= y_0, & Y_1 &= y_1, \\ Z_0 &= z_0 + f_0, & Z_1 &= z_1 + f_1. \end{aligned}$$

* It will be seen later that the relation $n_0/f_0 = -n_1/f_1$ is not restricted to a single refracting surface, but holds in general for any centred system, the quantities with suffix zero referring to the object space, those with the suffix 1 to the image space. (11) may therefore be regarded as defining the power of a general centred system. The practical unit of power is a *diopetre*; it is the reciprocal of the focal length, when the focal length is expressed in meters. The power is positive when the system is convergent ($f_0 > 0$) and negative when it is divergent ($f_0 < 0$).

Equations (12) and (4), subject to (5), then reduce to the standard form § 4.3 (10):

$$\frac{Y_1}{Y_0} = \frac{f_0}{Z_0} = \frac{Z_1}{f_1}. \quad (14)$$

4.4.2 Reflecting surface of revolution

It is seen that with a notation strictly analogous to that used in the previous section, equations of the form (1a) and (1b) also hold when reflection takes place on a surface of revolution, the coefficients \mathcal{A} , \mathcal{B} and \mathcal{C} now being replaced by the corresponding coefficients \mathcal{A}' , \mathcal{B}' and \mathcal{C}' of § 4.1.5. It has been shown in § 4.1.5 that \mathcal{A}' , \mathcal{B}' and \mathcal{C}' can be obtained from \mathcal{A} , \mathcal{B} and \mathcal{C} on setting $n_0 = -n_1 = n$, n denoting the refractive index of the medium in which the rays are situated. Hence the appropriate

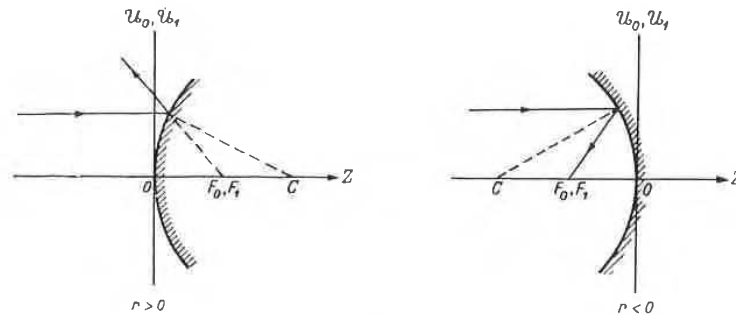


Fig. 4.13. Position of the cardinal points for reflection on a mirror of revolution.

formulae for reflection may be immediately written down by making this substitution in the preceding formulae. In particular, (7) gives

$$\frac{1}{z_0} - \frac{1}{r} = -\frac{1}{z_1} + \frac{1}{r}, \quad (15)$$

the expression on either side of (15) being *Abbe's (reflection) invariant*. (15) may also be written as

$$\frac{1}{z_0} + \frac{1}{z_1} = \frac{2}{r}. \quad (16)$$

The focal lengths f_0 and f_1 are now given by

$$f_0 = f_1 = -\frac{r}{2}, \quad (17)$$

and the power \mathcal{P} is

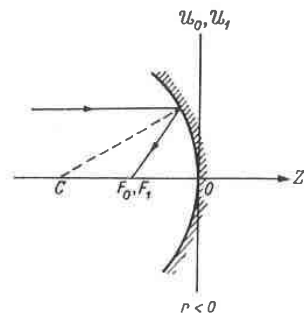
$$\mathcal{P} = -\frac{2n}{r}. \quad (18)$$

Since $f_0 f_1 > 0$, the imaging is *contracurrent* (katoptric). When the surface is convex towards the incident light ($r > 0$) $f_0 < 0$, and the imaging is then divergent; when it is concave towards the incident light, ($r < 0$), $f_0 > 0$ and the imaging is convergent (Fig. 4.13).

luc to the standard form § 4.3 (10):

$$\frac{Z_1}{f_1} \tag{14}$$

s to that used in the previous section, en reflection takes place on a surface being replaced by the corresponding n shown in § 4.1.5 that \mathcal{A}' , \mathcal{B}' and \mathcal{C}' , $= -n_1 = n$, n denoting the refrac- are situated. Hence the appropriate



eflection on a mirror of revolution.

ten down by making this substitution ves

$$+ \frac{1}{r} \tag{15}$$

's (reflection) invariant. (15) may also

$$\tag{16}$$

$$\frac{r}{2'} \tag{17}$$

$$\tag{18}$$

optric). When the surface is convex ie imaging is then divergent; when it $r_0 > 0$ and the imaging is convergent

4.4.3 The thick lens

Next we derive the Gaussian formulae relating to imaging by two surfaces which are rotationally symmetrical about the same axis.

Let n_0 , n_1 and n_2 be the refractive indices of the three regions, taken in the order in which light passes through them, and let r_1 and r_2 be the radii of curvature of the surfaces at their axial points, measured positive when the surface is convex towards the incident light.

By (10), the focal lengths of the first surface are given by

$$f_0 = \frac{n_0 r_1}{n_1 - n_0}, \quad f'_0 = -\frac{n_1 r_1}{n_1 - n_0} \tag{19}$$

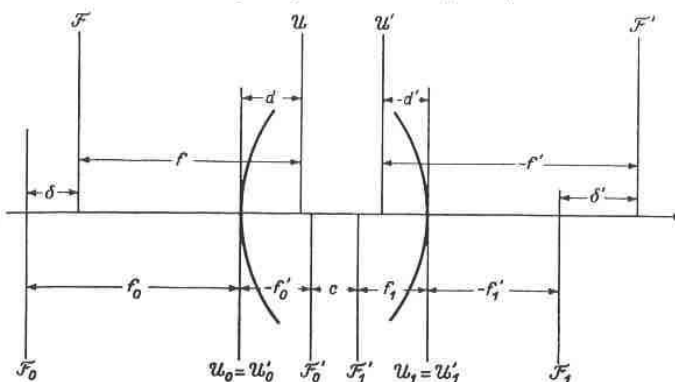


Fig. 4.14. The cardinal points of a combined system (thick lens).

and of the second surface by

$$f_1 = \frac{n_1 r_2}{n_2 - n_1}, \quad f'_1 = -\frac{n_2 r_2}{n_2 - n_1} \tag{20}$$

According to § 4.3 (27) the focal lengths of the combination are

$$f = -\frac{f_0 f_1}{c}, \quad f' = \frac{f'_0 f'_1}{c} \tag{21}$$

where c is the distance between the foci F'_0 and F_1 . Let t be the axial thickness of the lens, i.e. the distance between the poles of the two surfaces; then (see Fig. 4.14)

$$c = t + f'_0 - f_1 \tag{22}$$

On substituting into (22) for f'_0 and for f_1 we obtain

$$c = \frac{D}{(n_1 - n_0)(n_2 - n_1)}, \tag{23}$$

where

$$D = (n_1 - n_0)(n_2 - n_1)t - n_1[(n_2 - n_1)r_1 + (n_1 - n_0)r_2]. \tag{24}$$

The required expressions for the focal lengths of the combination are now obtained on substituting for f_0 , f_1 , f'_0 , f'_1 and c into (21). This gives

$$f = -n_0 n_1 \frac{r_1 r_2}{D}; \quad f' = n_1 n_2 \frac{r_1 r_2}{D} \tag{25}$$

Since ff' is negative, the imaging is concurrent. The power \mathcal{P} of the lens is

$$\begin{aligned}\mathcal{P} &= \frac{n_0}{f} = -\frac{n_2}{f'} = -\frac{1}{n_1} \frac{D}{r_1 r_2} \\ &= \mathcal{P}_1 + \mathcal{P}_2 - \frac{t}{n_1} \mathcal{P}_1 \mathcal{P}_2,\end{aligned}\quad (26)$$

where \mathcal{P}_1 and \mathcal{P}_2 are the powers of the two surfaces.

By § 4.3 (28), the distances $\delta = F_0 F'$ and $\delta' = F'_1 F'$ are seen to be

$$\delta = -n_0 n_1 \frac{n_2 - n_1}{n_1 - n_0} \frac{r_1^2}{D}, \quad \delta' = n_1 n_2 \frac{n_1 - n_0}{n_2 - n_1} \frac{r_2^2}{D}.\quad (27)$$

The distances d and d' of the principal planes \mathcal{U} and \mathcal{U}' from the poles of the surfaces are (see Fig. 4.14)

$$\left. \begin{aligned}d &= \delta + f - f_0 = -n_0(n_2 - n_1) \frac{r_1^2 t}{D}, \\ d' &= \delta' + f' - f'_1 = n_2(n_1 - n_0) \frac{r_2^2 t}{D}.\end{aligned}\right\} \quad (28)$$

Of particular importance is the case where the media on both sides of the lens are of the same refractive index, i.e. when $n_2 = n_0$. If we set $n_1/n_0 = n_1/n_2 = n$, the formulae then reduce to

$$\left. \begin{aligned}f &= -f' = -\frac{n r_1 r_2}{\Delta}, \\ \delta &= n \frac{r_1^2}{\Delta}, \quad \delta' = -n \frac{r_2^2}{\Delta}, \\ d &= (n-1) \frac{r_1^2 t}{\Delta}, \quad d' = (n-1) \frac{r_2^2 t}{\Delta},\end{aligned}\right\} \quad (29)$$

where

$$\Delta = (n-1)[n(r_1 - r_2) - (n-1)t].\quad (30)$$

Referred to axes at the foci F and F' , the abscissae of the unit points are $Z = f$ and $Z' = f'$, and the nodal points are given by $Z = -f'$, $Z = -f$. Since $f = -f'$ the unit points and the nodal points now coincide. The formula § 4.3 (16) which relates the distances ζ and ζ' of conjugate planes from the unit planes becomes

$$\frac{1}{\zeta} - \frac{1}{\zeta'} = -\frac{1}{f}.\quad (31)$$

The lens is *convergent* ($f > 0$) or *divergent* ($f < 0$) according as

$$f = -n \frac{r_1 r_2}{\Delta} \geq 0,\quad (32)$$

i.e. according as

$$\frac{1}{r_2} - \frac{1}{r_1} \leq \frac{n-1}{n} \frac{t}{r_1 r_2}.\quad (33)$$

When $f = \infty$, we have the intermediate case of *telescopic* imaging. Then $\Delta = 0$, i.e.

$$r_1 - r_2 = \frac{n-1}{n} t.\quad (34)$$

The power \mathcal{P} of the lens is

$$-\frac{1}{n_1 r_1 r_2} \mathcal{P}_1 \mathcal{P}_2, \tag{26}$$

faces.

$F_1'F'$ are seen to be

$$= n_1 n_2 \frac{n_1 - n_0 r_2^2}{n_2 - n_1 D}, \tag{27}$$

and \mathcal{U}' from the poles of the surfaces

$$\left. \begin{aligned} n_2 - n_1 \frac{r_1 t}{D}, \\ - n_0 \frac{r_2 t}{D} \end{aligned} \right\} \tag{28}$$

media on both sides of the lens are n_0 . If we set $n_1/n_0 = n_1/n_2 = n$, the

$$\left. \begin{aligned} \frac{2}{\Delta}, \\ (n-1) \frac{r_2 t}{\Delta} \end{aligned} \right\} \tag{29}$$

$$-(n-1)t]. \tag{30}$$

issue of the unit points are $Z = f$ and $-f'$, $Z = -f$. Since $f = -f'$ the The formula § 4.3 (16) which relates the unit planes becomes

$$\frac{1}{f} \tag{31}$$

< 0) according as

$$0, \tag{32}$$

$$\frac{t}{r_1 r_2} \tag{33}$$

telescopic imaging. Then $\Delta = 0$, i.e.

$$\frac{1}{-t}. \tag{34}$$

The three cases may be illustrated by considering a double convex lens, $r_1 > 0$, $r_2 < 0$ (cf. Fig. 4.15). If, for simplicity, we assume that both radii are numerically equal, i.e. $r_1 = -r_2 = r$, the imaging will be convergent or divergent according as $t \lesseqgtr 2nr/(n-1)$ and telescopic when $t = 2nr/(n-1)$.

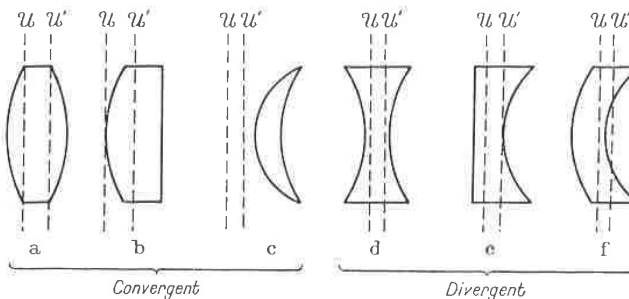


Fig. 4.15. Common types of lenses:

- (a) Double-convex; (b) Plano-convex; (c) Convergent meniscus;
- (d) Double-concave; (e) Plano-concave; (f) Divergent meniscus.

\mathcal{U} and \mathcal{U}' are the unit planes, light being assumed to be incident from the left.

4.4.4 The thin lens

The preceding formulae take a particularly simple form when the lens is so thin that the axial thickness t may be neglected. Then, according to (28), $d = d' = 0$, so that the unit planes pass through the axial point of the (infinitely thin) lens. Consequently, the rays which go through the centre of the lens will not suffer any deviation; this implies that *imaging by a thin lens is a central projection from the centre of the lens.*

From (26) it follows, on setting $t = 0$, that

$$\mathcal{P} = \mathcal{P}_1 + \mathcal{P}_2 = \frac{n_1 - n_0}{r_1} + \frac{n_2 - n_1}{r_2}, \tag{35}$$

i.e. the power of a thin lens is equal to the sum of the powers of the surfaces forming it.

If the media on the two sides of the lens are of equal refractive indices ($n_0 = n_2$), we have from (25)

$$\frac{1}{f} = -\frac{1}{f'} = (n-1) \left(\frac{1}{r_1} - \frac{1}{r_2} \right), \tag{36}$$

where as before, $n = n_1/n_0 = n_1/n_2$. Assuming that $n > 1$, as is usually the case, f is seen to be positive or negative according as the curvature $1/r_1$ of the first surface is greater or smaller than the curvature $1/r_2$ of the second surface (an appropriate sign being associated with the curvature). This implies that thin lenses whose thickness decreases from centre to the edge are convergent, and those whose thickness increases to the edge are divergent.

For later purposes we shall write down an expression for the focal lengths f and f' of a system consisting of two centred thin lenses, situated in air. According to § 4.3 (27) we have, since $f_0 = -f_0', f_1 = -f_1'$,

$$\frac{1}{f} = -\frac{1}{f'} = -\frac{c}{f_0 f_1}, \tag{37}$$

c being the distance between the foci F'_0 and F_1 (see Fig. 4.16). If l is the distance between the two lenses, then

$$l = f_0 + c + f_1. \tag{38}$$

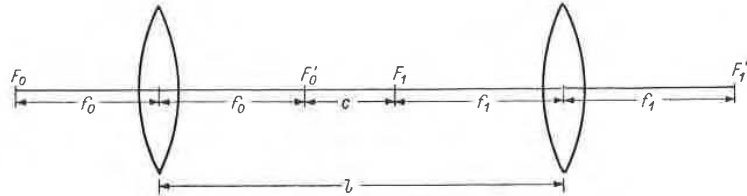


Fig. 4.16. System formed by two centred thin lenses.

Hence

$$\frac{1}{f} = -\frac{1}{f'} = \frac{1}{f_0} + \frac{1}{f_1} - \frac{l}{f_0 f_1}. \tag{39}$$

When the lenses are in contact ($l = 0$), (39) may also be written in the form, $\mathcal{P} = \mathcal{P}_1 + \mathcal{P}_2$, so that the power of the combination is then simply equal to sum of the powers of the two lenses.

4.4.5 The general centred system

Within the approximations of Gaussian theory, a refraction or a reflection at a surface of revolution was seen to give rise to a projective relationship between the object and the image spaces.* Since according to § 4.3 successive applications of projective transformations are equivalent to a single projective transformation, it follows that imaging by a centred system is, to the present degree of approximation, also a transformation of this type. The cardinal points of the equivalent transformation may be found by the application of the formulae of § 4.4.1, § 4.4.2 and § 4.3.4. We shall mainly confine our discussion to the derivation of an important invariant relation valid (within the present degree of accuracy) for any centred system.

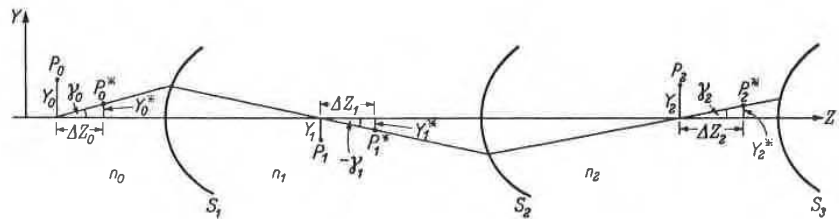


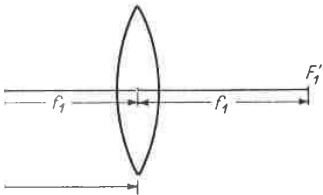
Fig. 4.17. Illustrating the SMITH-HELMHOLTZ formula.

Let S_1, S_2, \dots, S_m be the successive surfaces of the system, f_0, f_1, \dots, f_{m-1} the corresponding focal lengths, and n_0, n_1, \dots, n_m the refractive indices of the successive spaces (Fig. 4.17). Further, let P_0, P_0^* be two points in the object space, situated in a

* As in the case of a single surface, the object and the image spaces are regarded as superposed on to each other and extending indefinitely in all directions. The part of the object space which lies in front of the first surface (counted in the order in which the light traverses the system) is said to form the real portion of the object space and the portion of the image space which follows the last surface is called the real portion of the image space. The remaining portions of the two spaces are said to be *virtual*. In a similar manner we may define the real and virtual parts of any of the intermediate spaces of the system.

n_1 (see Fig. 4.16). If l is the distance

$$f_1. \tag{38}$$

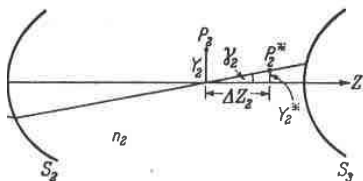


o centred thin lenses.

$$\frac{l}{f_1} - \frac{l}{f_0 f_1}. \tag{39}$$

may also be written in the form, nation is then simply equal to sum of

a refraction or a reflection at a surface e relationship between the object and successive applications of projective ective transformation, it follows that nt degree of approximation, also a nts of the equivalent transformation lae of § 4.4.1, § 4.4.2 and § 4.3.4. We ion of an important invariant relation r any centred system.



-HELMHOLTZ formula.

s of the system, f_0, f_1, \dots, f_{m-1} the he refractive indices of the successive ints in the object space, situated in a

ie image spaces are regarded as superposed tions. The part of the object space which n which the light traverses the system) is e portion of the image space which follows space. The remaining portions of the two ay define the real and virtual parts of any

meridional plane, and let $P_1, P_1', P_2, P_2', \dots$, be their images in the successive surfaces. Referred to axes at the foci of the first surface, the coordinates of P_0, P_0' and P_1, P_1' are related by eq. (14), viz.

$$\frac{Y_1}{Y_0} = \frac{f_0}{Z_0} = \frac{Z_1}{f_1}, \tag{40}$$

$$\frac{Y_1'}{Y_0'} = \frac{f_0}{Z_0'} = \frac{Z_1'}{f_1}. \tag{41}$$

Hence

$$\frac{Z_1' - Z_1}{f_1} = \frac{Y_1'}{Y_0'} - \frac{Y_1}{Y_0} = \frac{Y_0 Y_1' - Y_1 Y_0'}{Y_0 Y_0'}, \tag{42}$$

and

$$\frac{Z_0' - Z_0}{f_0} = \frac{Y_0'}{Y_1'} - \frac{Y_0}{Y_1} = \frac{Y_1 Y_0' - Y_0 Y_1'}{Y_1 Y_1'}. \tag{43}$$

Let

$$\left. \begin{aligned} Z_0' - Z_0 &= \Delta Z_0, \\ Z_1' - Z_1 &= \Delta Z_1. \end{aligned} \right\} \tag{44}$$

Then from (42) and (43),

$$\frac{f_0 Y_0 Y_0'}{\Delta Z_0} = - \frac{f_1 Y_1 Y_1'}{\Delta Z_1}. \tag{45}$$

Now by (10), $f_0/f_1 = -n_0/n_1$, so that this equation may be written as

$$\frac{n_0 Y_0 Y_0'}{\Delta Z_0} = \frac{n_1 Y_1 Y_1'}{\Delta Z_1}. \tag{46}$$

Similarly, for refraction at the second surface,

$$\frac{n_1 Y_1 Y_1'}{\Delta Z_1} = \frac{n_2 Y_2 Y_2'}{\Delta Z_2}, \tag{47}$$

and generally

$$\frac{n_{i-1} Y_{i-1} Y_{i-1}'}{\Delta Z_{i-1}} = \frac{n_i Y_i Y_i'}{\Delta Z_i} \quad (1 \leq i \leq m). \tag{48}$$

Hence $n_i Y_i Y_i' / \Delta Z_i$ is an invariant in the successive transformations. This result plays an important part in the geometrical theory of image formation. If we set $Y_i' / \Delta Z_i = \tan \gamma_i$ (see Fig. 4.17), (48) becomes

$$n_{i-1} Y_{i-1} \tan \gamma_{i-1} = n_i Y_i \tan \gamma_i.$$

Since to the present degree of accuracy, $\tan \gamma$ and $\tan \gamma'$ may be replaced by γ and γ' respectively, we obtain the *Smith-Helmholtz formula**

$$n_{i-1} Y_{i-1} \gamma_{i-1} = n_i Y_i \gamma_i. \tag{49}$$

The quantity $n_i Y_i \gamma_i$ is known as the *Smith-Helmholtz invariant*.

From (48) and (49) a number of important conclusions may be drawn. As one is usually interested only in relations between quantities pertaining to the first and the last medium (object and image space), we shall drop the suffixes and denote quantities which refer to these two spaces by unprimed and primed symbols respectively.

* This formula is also associated with the names of LAGRANGE and CLAUDIUS. It was actually known in more restricted forms to earlier writers, e.g. HUYGENS and COTES. (Cf. Lord RAYLEIGH, *Phil. Mag.*, (5) 21 (1886), 466).

PO 6th Ed. - 0

Let (Y, Z) and $(Y + \delta Y, Z + \delta Z)$ be two neighbouring points in the object space and (Y', Z') and $(Y' + \delta Y', Z' + \delta Z')$ the conjugate points. The SMITH-HELMHOLTZ formula gives, by successive application, the following relation:

$$\frac{nY(Y + \delta Y)}{\delta Z} = \frac{n'Y'(Y' + \delta Y')}{\delta Z'}. \quad (50)$$

In the limit as $\delta Y \rightarrow 0$ and $\delta Z \rightarrow 0$, this reduces to

$$\frac{dZ'}{dZ} = \frac{n' Y'^2}{n Y^2}. \quad (51)$$

According to § 4.3 (11), we may write $Y'/Y = (dY'/dY)_{Z=\text{const.}}$, and (51) becomes

$$\frac{dZ'}{dZ} = \frac{n'}{n} \left(\frac{dY'}{dY} \right)_{Z=\text{const.}}^2, \quad (52)$$

known as *Maxwell's elongation formula*. It implies that the *longitudinal magnification is equal to the square of the lateral magnification multiplied by the ratio n'/n of the refractive indices*. Now in § 4.3 we derived an analogous formula [(13)] connecting the magnifications and the ratio of the focal lengths. On comparing these two formulae it is seen that

$$\frac{f'}{f} = -\frac{n'}{n}, \quad (53)$$

i.e. the ratio of the focal lengths of the instrument is equal to the ratio n'/n of the refractive indices, taken with a negative sign.

From the SMITH-HELMHOLTZ formula it also follows, that

$$\frac{dY' \gamma'}{dY \gamma} = \frac{n}{n'}, \quad (54)$$

showing that the product of the lateral and the angular magnification is independent of the choice of the conjugate planes.

It has been assumed so far that the system consists of refracting surfaces only. If one of the surfaces (say the i th one) is a mirror, we obtain in place of (48),

$$\frac{Y_{i-1} Y_{i-1}^*}{\Delta Z_{i-1}} = -\frac{Y_i Y_i^*}{\Delta Z_i},$$

the negative sign arising from the fact that for reflection $f_{i-1}/f_i = 1$, whereas for refraction $f_{i-1}/f_i = -n_{i-1}/n_i$. In consequence n' must be replaced by $-n'$ in the final formulae. More generally n' must be replaced by $-n'$ when the system contains an odd number of mirrors; when it contains an even number of mirrors, the final formulae remain unchanged.

4.5 STIGMATIC IMAGING WITH WIDE-ANGLE PENCILS

The laws of Gaussian Optics were derived under the assumption that the size of the object and the angles which the rays make with the axis are sufficiently small. Often one also has to consider systems where the object is of small linear dimensions, but where the inclination of the rays is appreciable. There are two simple criteria, known

ighbouring points in the object space imitate points. The SMITH-HELMHOLTZ following relation:

$$\frac{\delta Y' + \delta Y'}{\delta Z'} \quad (50)$$

as to

$$\frac{\delta^2}{\delta^2} \quad (51)$$

$(dY'/dY)_{Z=\text{const.}}$, and (51) becomes

$$\frac{\delta^2}{\delta^2} \quad (52)$$

ies that the longitudinal magnification m multiplied by the ratio n'/n of the analogous formula [(13)] connecting the s. On comparing these two formulae

$$(53)$$

equal to the ratio n'/n of the refractive

follows, that

$$\frac{\delta^2}{\delta^2} \quad (54)$$

ngular magnification is independent of

onsists of refracting surfaces only. If we obtain in place of (48),

$$\frac{Y_i Y_i^*}{\Delta Z_i}$$

for reflection $f_{i-1}/f_i = 1$, whereas for n' must be replaced by $-n'$ in the ced by $-n'$ when the system contains an even number of mirrors, the final

WIDE-ANGLE PENCILS

er the assumption that the size of the the axis are sufficiently small. Often ject is of small linear dimensions, but There are two simple criteria, known

as the *sine condition** and the *Herschel condition*† relating to the stigmatic imaging in such instruments.

Let O_0 be an axial object point and P_0 any point in its neighbourhood, not necessarily on the axis. Assume that the system images these two points stigmatically, and let O_1 and P_1 be the stigmatic images.

Let (x_0, y_0, z_0) and (x_1, y_1, z_1) be the coordinates of P_0 and P_1 respectively, P_0 being referred to rectangular axes at O_0 and P_1 to parallel axes at O_1 , the z -directions being taken along the axis of the system (Fig. 4.18). By the principle of equal optical path, the path lengths of all the rays joining P_0 and P_1 are the same. Hence, if V denotes the point characteristic of the medium,

$$V(x_0, y_0, z_0; x_1, y_1, z_1) - V(0, 0, 0; 0, 0, 0) = F(x_0, y_0, z_0; x_1, y_1, z_1), \quad (1)$$

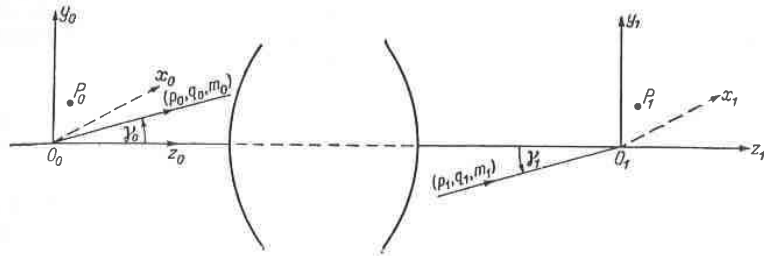


Fig. 4.18. Illustrating the sine condition and the HERSCHEL condition.

F being some function which is independent of the ray components. Using the basic relations § 4.1 (7) which express the ray component in terms of the point characteristic, we have from (1), if terms above the first power in distances are neglected,

$$(p_1^{(0)}x_1 + q_1^{(0)}y_1 + m_1^{(0)}z_1) - (p_0^{(0)}x_0 + q_0^{(0)}y_0 + m_0^{(0)}z_0) = F(x_0, y_0, z_0; x_1, y_1, z_1), \quad (2)$$

$(p_0^{(0)}, q_0^{(0)}, m_0^{(0)})$ and $(p_1^{(0)}, q_1^{(0)}, m_1^{(0)})$ being the ray components of any pair of corresponding rays through O_0 and O_1 . It is to be noted that, although the points P_0 and P_1 are assumed to be in the neighbourhood of O_0 and O_1 , no restriction as to the magnitude of the ray components is imposed.

Two cases are of particular interest, namely when (i) P_0 and P_1 lie in the planes $z_0 = 0$ and $z_1 = 0$ respectively, and (ii) when P_0 and P_1 are on the axis of symmetry. The two cases will be considered separately.

4.5.1 The sine condition

Without loss of generality we may again consider only points in a meridional plane ($x_0 = x_1 = 0$). If P_0 lies in the plane $z_0 = 0$ and P_1 in the plane $z_1 = 0$, (2) becomes

$$q_1^{(0)}y_1 - q_0^{(0)}y_0 = F(0, y_0, 0; 0, y_1, 0). \quad (3)$$

* The sine condition was first derived by R. CLAUSIUS (*Pogg. Ann.*, **121** (1864), 1) and by H. HELMHOLTZ (*Pogg. Ann. Jubelband* (1874), 557) from thermodynamical considerations. Its importance was, however, not recognized until it was rediscovered by E. ABBE (*Jenaisch. Ges. Med. Naturw.* 1879), 129, also *Carl. Repert. Phys.*, **16** (1880), 303).

† The derivations given here are essentially due to C. HOCKIN, *J. Roy. Micro. Soc.* (2) **4** (1884), 337.

† J. F. W. HERSCHEL, *Phil. Trans. Roy. Soc.*, **111** (1821), 226.

This relation holds for each pair of conjugate rays. In particular it must, therefore, hold for the axial pair $p_0^{(0)} = q_0^{(0)} = 0$, $p_1^{(0)} = q_1^{(0)} = 0$. Hence

$$F(0, y_0, 0; 0, y_1, 0) = 0. \quad (4)$$

Relation (3) becomes

$$q_1^{(0)} y_1 = q_0^{(0)} y_0, \quad (5)$$

or, more explicitly,

$$n_1 y_1 \sin \gamma_1 = n_0 y_0 \sin \gamma_0, \quad (6)$$

γ_0 and γ_1 being the angles which the corresponding rays through O_0 and O_1 make with the z -axis, and n_0 and n_1 being the refractive indices of the object and image spaces. (6) is known as the *sine condition*, and is the required condition under which a small region of the object plane in the neighbourhood of the axis is imaged sharply by a pencil of any angular divergence. If the angular divergence is sufficiently small, $\sin \gamma_0$ and $\sin \gamma_1$ may be replaced by γ_0 and γ_1 respectively, and the sine condition reduces to the SMITH-HELMHOLTZ formula, § 4.4 (49).

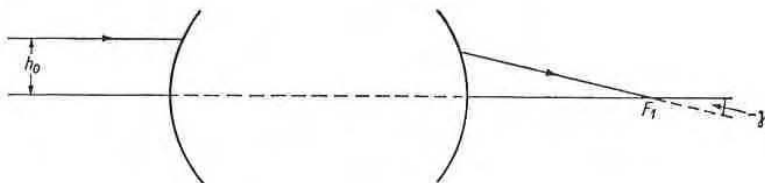


Fig. 4.19. The sine condition, when the object is at infinity.

If the object lies at infinity, the sine condition takes a different form. Assume first that the axial object point is at a great distance from the first surface. If Z_0 is the abscissa of this point referred now to axes at the first focus, and h_0 is the height above the axis at which a ray from the axial point meets the first surface, then $\sin \gamma_0 \sim -h_0/Z_0$; more precisely $Z_0 \sin \gamma_0/h_0 \rightarrow -1$ as $Z_0 \rightarrow -\infty$ whilst h_0 is kept fixed. Hence, if Z_0 is large enough, (6) may be written as

$$\frac{n_0}{n_1} h_0 = -\frac{y_1}{y_0} Z_0 \sin \gamma_1. \quad (7)$$

But by § 4.3 (10), $y_1 Z_0/y_0 = f_0$, and by § 4.4 (53) $n_0/n_1 = -f_0/f_1$, so that in the limit (6) reduces to (see Fig. 4.19)

$$\frac{h_0}{\sin \gamma_1} = f_1. \quad (8)$$

This implies that each ray which is incident in the direction parallel to the axis intersects its conjugate ray on a sphere of radius f_1 , which is centred at the focus F_1 .

Axial points which are stigmatic images of each other, and which, in addition, have the property that conjugate rays which pass through them satisfy the sine condition, are said to form an *aplanatic* pair. We have already encountered such point pairs when studying the refraction at a spherical surface (§ 4.2.3).

In the terminology of the theory of aberrations (cf. Chapter V), axial stigmatism implies the absence of all those terms in the expansion of the characteristic function which do not depend on the off-axis distance of the object, i.e. it implies the absence of spherical aberration of all orders. If, in addition, the sine condition is satisfied, then all terms in the characteristic function which depend on the first power of the

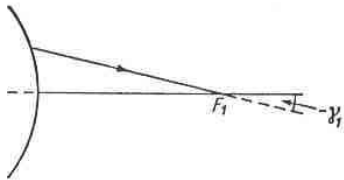
rays. In particular it must, therefore, $q_1^{(0)} = 0$. Hence

$$0) = 0. \tag{4}$$

$$y_0, \tag{5}$$

$$0 \sin \gamma_0, \tag{6}$$

ing rays through O_0 and O_1 make with indices of the object and image spaces. required condition under which a small d of the axis is imaged sharply by a gular divergence is sufficiently small, 1 respectively, and the sine condition .4 (49).



the object is at infinity.

ition takes a different form. Assume distance from the first surface. If Z_0 axes at the first focus, and h_0 is the axial point meets the first surface, then $\rightarrow -1$ as $Z_0 \rightarrow -\infty$ whilst h_0 is kept written as

$$0 \sin \gamma_1. \tag{7}$$

3) $n_0/n_1 = -f_0/f_1$, so that in the limit

$$i. \tag{8}$$

the direction parallel to the axis inter- which is centred at the focus F_1 . ch other, and which, in addition, have rough them satisfy the sine condition, already encountered such point pairs rface (§ 4.2.3). ions (cf. Chapter V), axial stigmatism xpansion of the characteristic function of the object, i.e. it implies the absence dition, the sine condition is satisfied, hich depend on the first power of the

off-axis distance must also vanish; these terms represent aberrations known as *circular coma*.

Since the sine condition gives information about the quality of the off-axis image in terms of the properties of axial pencils it is of great importance for optical design.

4.5.2 The Herschel condition

Next consider the case when P_0 and P_1 lie on the axis of the system ($x_0 = y_0 = 0, x_1 = y_1 = 0$). The condition (2) for sharp imaging reduces to

$$m_1^{(0)}z_1 - m_0^{(0)}z_0 = F(0, 0, z_0; 0, 0, z_1), \tag{9}$$

or, in terms of γ_0 and γ_1 ,

$$n_1z_1 \cos \gamma_1 - n_0z_0 \cos \gamma_0 = F(0, 0, z_0; 0, 0, z_1). \tag{10}$$

In particular for the axial ray this gives

$$F(0, 0, z_0; 0, 0, z_1) = n_1z_1 - n_0z_0. \tag{11}$$

Hence (10) may be written as

$$n_1z_1 \sin^2(\gamma_1/2) = n_0z_0 \sin^2(\gamma_0/2). \tag{12}$$

This is one form of the *Herschel condition*. Since the distances from the origin are assumed to be small, we have, by § 4.4 (52),

$$\frac{z_1}{z_0} = \frac{n_1}{n_0} \left(\frac{y_1}{y_0} \right)^2, \tag{13}$$

so that the HERSCHEL condition may also be written in the form

$$n_1y_1 \sin(\gamma_1/2) = n_0y_0 \sin(\gamma_0/2). \tag{14}$$

When the HERSCHEL condition is satisfied, an element of the axis in the immediate neighbourhood of O_0 will be imaged sharply by a pencil of rays, irrespective of the angular divergence of the pencil.

It is to be noted that the sine condition and the HERSCHEL condition cannot hold simultaneously unless $\gamma_1 = \gamma_0$. Then $y_1/y_0 = z_1/z_0 = n_0/n_1$, i.e. the longitudinal and lateral magnifications must then be equal to the ratio of the refractive indices of the object and image space.

4.6 ASTIGMATIC PENCILS OF RAYS

Rectilinear rays which have a point in common are said to form a *homocentric pencil*. The associated wave-fronts are then spherical, centred on their common point of intersection. It was with such pencils that we were concerned in the preceding sections.

In general, the homocentricity of a pencil is destroyed on refraction or reflection. It will therefore be useful to study the properties of more general pencils of rectilinear rays.

4.6.1 Focal properties of a thin pencil

Let S denote one of the orthogonal trajectories (wave-fronts) of a pencil of rectilinear rays, and let P be any point on it (Fig. 4.20). We take a plane through the ray at P and denote by C the curve in which this plane intersects S . Since the rays of the

pencil are all normal to S , the centre of the circle of curvature at P will be on the ray through P .

If now the plane is gradually rotated around the ray, the curve C and consequently the radius of curvature will change continuously. When the plane has undergone a rotation of 180° , the radius of curvature will have passed through its maximum and minimum values. It can be shown by elementary geometry* that the two planes which contain the shortest and the longest radius of curvature are perpendicular to each other. These two planes are known as the *principal planes*† at P and the corresponding radii are called *principal radii of curvature*. The curves on S which have the property that at each point they are tangential to the principal planes form two mutually orthogonal families of curves, called the *lines of curvature*.

In general two normals at adjacent points of a surface do not intersect, to first order. But if they are drawn from adjacent points on a line of curvature they will intersect to this order, and their point of intersection is a focus of the congruence formed by

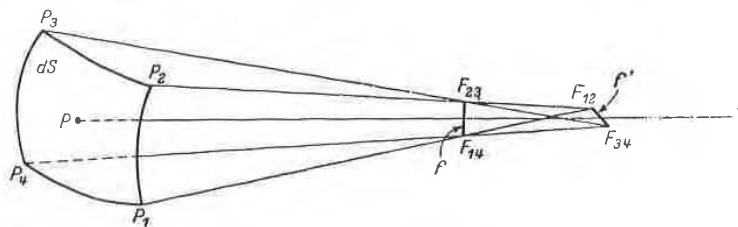


Fig. 4.20. A thin pencil of rays.

the normals (rays). Hence, in agreement with the general conclusions of § 3.2.3 there are two foci on each normal, these being the two principal centres of curvature. The caustic surface of a pencil of rectilinear rays has therefore, in general, two branches and is the *evolute* of the wave-fronts; conversely the wave-fronts are the *involutives* of the caustic surface. If the wave-fronts are surfaces of revolution, one branch of the caustic surface degenerates into a segment of the axis of revolution; the other is a surface of revolution whose meridional section is the evolute of the meridional section of the wave-front.

Let us consider a thin pencil consisting of all rays which intersect an element dS of the wave-front. It will be convenient to take as boundary of dS two pairs of lines of curvature, which may be assumed to be arcs of circles. Two of them (P_1P_2 and P_4P_3) may be taken to be vertical, and the other two (P_1P_4 and P_2P_3) to be horizontal (Fig. 4.20).

To the first order in small quantities, all the rays which pass through the arc P_1P_2 will intersect in a focus F_{12} , and those through P_3P_4 will intersect at F_{34} . The line f' joining F_{12} and F_{34} is known as a *focal line* of the pencil and is seen to be horizontal. Similarly the rays through P_1P_4 and P_2P_3 will give rise to a vertical focal line f .

If the lines of curvature are drawn through any point on dS , the corresponding two foci will lie on the two focal lines, and conversely. Hence an *approximate model of a thin pencil of rays is obtained by joining all pairs of points on two mutually orthogonal elements of lines*.

* See, for example, C. E. WEATHERBURN, *Differential Geometry of Three Dimensions* (Cambridge University Press, 1927), p. 185.

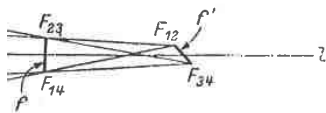
† The terms principal planes and focal planes have now a different meaning than in connection with projective transformations discussed in § 4.3.

The pencil, astigmatism f' and It is n that t centra wave-f about surface point) the cur contain at the dicular coincic that p at the is not

It was two fo surface refract namely

princip meets Take and O_y Furt pencils $z = \zeta_0$ dicular corres focus; the sec

le of curvature at P will be on the ray the ray, the curve C and consequently ly. When the plane has undergone a ave passed through its maximum and itary geometry* that the two planes lius of curvature are perpendicular to the *principal planes*† at P and the of curvature. The curves on S which angular to the principal planes form led the *lines of curvature*. surface do not intersect, to first order, a line of curvature they will intersect a focus of the congruence formed by



encil of rays.

the general conclusions of § 3.2.3 there o principal centres of curvature. The as therefore, in general, two branches ly the wave-fronts are the *involut*es of faces of revolution, one branch of the the axis of revolution; the other is a s the evolute of the meridional section

rays which intersect an element dS of s boundary of dS two pairs of lines of circles. Two of them (P_1P_2 and P_4P_3) wo (P_1P_4 and P_2P_3) to be horizontal

rays which pass through the arc P_1P_2 P_3P_4 will intersect at F_{34} . The line f' he pencil and is seen to be horizontal. l give rise to a vertical focal line f . ny point on dS , the corresponding two ely. Hence an approximate model of a rs of points on two mutually orthogonal

l Geometry of Three Dimensions (Cambridge now a different meaning than in connection

The ray l through the centre point P is called the *central (or principal) ray* of the pencil, and the distance between the focal lines, measured along this ray, is called the *astigmatic focal distance* of the pencil. The two planes specified by f and l , and by f' and l , are known as the *focal planes* of the pencil, and are mutually perpendicular. It is not, however, necessarily true (as is often incorrectly asserted in the literature) that the focal lines are perpendicular to the central ray. Consider for example a family of wave-fronts which have cylindrical symmetry about a common axis (Fig. 4.21). Let dS be a surface element (assumed not to contain an axial point) of one of the wave-fronts, and let ds be the curve of intersection of dS with a plane which contains the axis. Then, clearly, the focal line f at the centre of curvature K of ds is perpendicular to this plane. The other focal line, f' , coincides with a portion of the axis, namely with that portion which is bounded by the normals at the end points of ds . In general this focal line is not perpendicular to l .

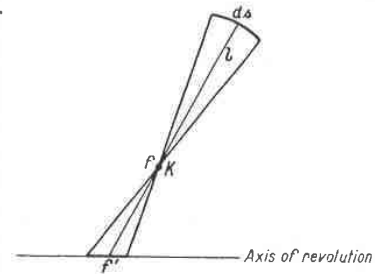


Fig. 4.21. Focal lines of a wave-front with cylindrical symmetry.

4.6.2 Refraction of a thin pencil

It was seen that a thin pencil of rays is completely specified by its central ray and its two focal lines. Suppose that a pencil specified in this way is incident on a refracting surface. It is of importance to determine the central ray and the focal lines of the refracted pencil. We shall consider the case of particular importance in practice, namely, when one of the principal planes of the incident pencil coincides with a

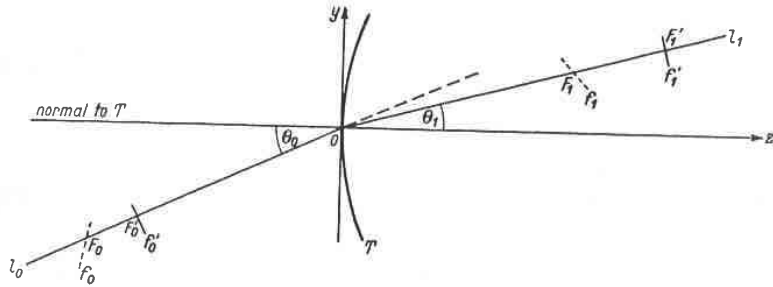


Fig. 4.22. Refraction of a thin astigmatic pencil.

principal plane of curvature of the surface at the point O at which the central ray meets it (Fig. 4.22).

Take Cartesian axes at O , with Oz along the normal to the surface T and with Ox and Oy in the direction of the principal lines of curvature of T .

Further, let θ_0 and θ_1 be the angles which the central rays l_0 and l_1 of the two pencils make with Oz . Let F_0 and F'_0 be the foci of the incident pencil, situated at $z = \zeta_0$ and $z = \zeta'_0$ respectively. The focal line at F_0 will be assumed to be perpendicular to the plane of incidence; F_0 is then said to be a *primary focus*, and the corresponding focal line f_0 the *primary focal line*. The focus F'_0 is called the *secondary focus*; the corresponding focal line f'_0 (which lies in the plane of incidence) is known as the *secondary focal line*. In the case of a centred system, the primary and secondary

focus of a pencil whose central ray lies in the meridional plane are known as the *tangential* and the *sagittal focus* respectively.

To find the focal lines of the refracted pencil it is necessary to write down first an expression for the angle characteristic of the refracting surface. If the radii of curvature of the surface in the principal directions Ox and Oy are r_x and r_y respectively, the equation of the surface is

$$z = \frac{x^2}{2r_x} + \frac{y^2}{2r_y} + \dots \quad (1)$$

Now according to § 4.1 (34), the angle characteristic referred to a set of axes at O is (taking $a_0 = a_1 = 0$)

$$T = (p_0 - p_1)x + (q_0 - q_1)y + (m_0 - m_1)z. \quad (2)$$

From the law of refraction it follows, in a way similar to that described in § 4.1 (which corresponds to the case $r_x = r_y$), when terms of the lowest degree only are retained, that

$$\left. \begin{aligned} x &= -r_x \frac{p_0 - p_1}{m_0 - m_1}, \\ y &= -r_y \frac{q_0 - q_1}{m_0 - m_1} \end{aligned} \right\} \quad (3)$$

Substitution into (1) gives

$$z = \frac{1}{2\mu^2} [r_x(p_0 - p_1)^2 + r_y(q_0 - q_1)^2], \quad (4)$$

with

$$\mu = m_1 - m_0 = n_1 \cos \theta_1 - n_0 \cos \theta_0. \quad (5)$$

Substitution from (3) and (4) then leads to the required expression for the angle characteristic:

$$T(p_0, q_0; p_1, q_1) = \frac{1}{2\mu} [r_x(p_0 - p_1)^2 + r_y(q_0 - q_1)^2] + \dots \quad (6)$$

On using this expression in § 4.1 (29), the equations of the incident and refracted ray are obtained:

$$x_0 - \frac{p_0}{m_0} z_0 = \frac{1}{\mu} r_x (p_0 - p_1), \quad (7)$$

$$x_1 - \frac{p_1}{m_1} z_1 = \frac{1}{\mu} r_x (p_0 - p_1), \quad (8)$$

the corresponding equations involving the y coordinates being strictly analogous.

Consider now the changes in the various quantities as we pass from the central ray to a neighbouring ray. From (7) and (8)

$$\delta x_0 - \frac{p_0}{m_0} \delta z_0 = z_0 \delta \left(\frac{p_0}{m_0} \right) + r_x \left\{ \delta \left(\frac{p_0}{\mu} \right) - \delta \left(\frac{p_1}{\mu} \right) \right\}, \quad (9)$$

$$\delta x_1 - \frac{p_1}{m_1} \delta z_1 = z_1 \delta \left(\frac{p_1}{m_1} \right) + r_x \left\{ \delta \left(\frac{p_0}{\mu} \right) - \delta \left(\frac{p_1}{\mu} \right) \right\} \quad (10)$$

meridional plane are known as the

it is necessary to write down first an
acting surface. If the radii of curva-
and Oy are r_x and r_y respectively, the

... (1)

istic referred to a set of axes at O is

$$y + (m_0 - m_1)z. \quad (2)$$

milar to that described in § 4.1 (which
f the lowest degree only are retained,

$$\left. \begin{array}{l} \frac{p_1}{m_1} \\ \frac{q_1}{m_1} \end{array} \right\} \quad (3)$$

$$r_y(q_0 - q_1)^2, \quad (4)$$

$$\lambda_1 - n_0 \cos \theta_0. \quad (5)$$

he required expression for the angle

$$+ r_y(q_0 - q_1)^2 + \dots \quad (6)$$

tions of the incident and refracted ray

$$p_0 - p_1, \quad (7)$$

$$p_0 - p_1, \quad (8)$$

ordinates being strictly analogous.
ities as we pass from the central ray

$$\left\{ \delta \left(\frac{p_0}{\mu} \right) - \delta \left(\frac{p_1}{\mu} \right) \right\}, \quad (9)$$

$$\left\{ \delta \left(\frac{p_0}{\mu} \right) - \delta \left(\frac{p_1}{\mu} \right) \right\} \quad (10)$$

Now the components of the central ray of the incident pencil are

$$p_0 = 0, \quad q_0 = n_0 \sin \theta_0, \quad m_0 = n_0 \cos \theta_0, \quad (11)$$

so that

$$\begin{aligned} \delta \left(\frac{p_0}{m_0} \right) &= \frac{1}{m_0^2} (m_0 \delta p_0 - p_0 \delta m_0) \\ &= \frac{1}{n_0} \sec \theta_0 \delta p_0, \end{aligned} \quad (12)$$

and

$$\begin{aligned} \delta \left(\frac{q_0}{m_0} \right) &= \frac{1}{m_0^2} (m_0 \delta q_0 - q_0 \delta m_0) \\ &= \frac{1}{n_0} \sec^3 \theta_0 \delta q_0. \end{aligned} \quad (13)$$

Here use was made of the identity $m_0 \delta m_0 + p_0 \delta p_0 + q_0 \delta q_0 = 0$.

Equations (9) and (10) become

$$\delta x_0 = \frac{z_0}{n_0} \sec \theta_0 \delta p_0 - \frac{1}{\mu} r_x (\delta p_1 - \delta p_0), \quad (14)$$

$$\delta x_1 = \frac{z_1}{n_1} \sec \theta_1 \delta p_1 - \frac{1}{\mu} r_x (\delta p_1 - \delta p_0). \quad (15)$$

In deriving (15) use was also made of the fact that $p_1 = 0$; this result follows from the law of refraction and the assumption that $p_0 = 0$. In a similar way we find

$$\delta y_0 - (\tan \theta_0) \delta z_0 = \frac{z_0}{n_0} (\sec^3 \theta_0) \delta q_0 - r_y \left\{ \delta \left(\frac{q_1}{\mu} \right) - \delta \left(\frac{q_0}{\mu} \right) \right\}, \quad (16)$$

$$\delta y_1 - (\tan \theta_1) \delta z_1 = \frac{z_1}{n_1} (\sec^3 \theta_1) \delta q_1 - r_y \left\{ \delta \left(\frac{q_1}{\mu} \right) - \delta \left(\frac{q_0}{\mu} \right) \right\}. \quad (17)$$

Consider now those rays of the pencil which pass through the focus F_0 . Then $z_0 = \zeta_0$, $\delta x_0 = \delta y_0 = \delta z_0 = 0$. Since all these rays also intersect the focal line f'_0 , $\delta p_0 = 0$. With this substitution (14) and (16) give

$$\delta p_1 = 0, \quad (14a)$$

and

$$\frac{\zeta_0}{n_0} \sec^3 \theta_0 \delta q_0 - \frac{1}{\mu} r_y (\delta q_1 - \delta q_0) = 0. \quad (16a)$$

(14a) shows that the corresponding refracted rays lie in the yz -plane. Now since all the rays from F_0 pass through the focus F_1 ($z_1 = \zeta_1$), (17) must hold with $z_1 = \zeta_1$, $\delta x_1 = \delta y_1 = \delta z_1 = 0$, whatever the value of δq_0 , so that

$$\frac{\zeta_1}{n_1} \sec^3 \theta_1 \delta q_1 - \frac{1}{\mu} r_y (\delta q_1 - \delta q_0) = 0. \quad (17a)$$

Equations (16a) and (17a) can be satisfied simultaneously for an arbitrary value of δq_0 only if

$$\frac{n_0 \cos^3 \theta_0}{\zeta_0} - \frac{n_1 \cos^3 \theta_1}{\zeta_1} = \frac{n_0 \cos \theta_0 - n_1 \cos \theta_1}{r_y}. \quad (18)$$

This relation gives the position of the focus F_1 of the refracted rays. From (14a) it is seen that the focal line through F_1 is perpendicular to the yz -plane so that F_1 is a *primary focus*.

To find the position of the other focus, consider the rays which proceed from F'_0 . Then $z_0 = \zeta'_0$, $\delta x_0 = \delta y_0 = \delta z_0 = 0$. Since all these rays intersect the focal line f_0 , $\delta q_0 = \delta m_0 = 0$. Equations (14) and (16) now give

$$\frac{\zeta'_0}{n_0} \sec \theta_0 \delta p_0 - \frac{1}{\mu} r_x (\delta p_1 - \delta p_0) = 0, \quad (14b)$$

and

$$\delta q_1 = 0. \quad (16b)$$

(16b) shows that the refracted rays now lie in the xz -plane. All these rays will pass through the other focus $F'_1(z_1 = \zeta'_1)$, so that (15) must be satisfied with $z_1 = \zeta'_1$, $\delta x_1 = \delta y_1 = \delta z_1 = 0$, whatever the value of δp_0 . Hence,

$$\frac{\zeta'_1}{n_1} \sec \theta_1 \delta p_1 - \frac{1}{\mu} r_x (\delta p_1 - \delta p_0) = 0. \quad (15b)$$

Since (15b) and (14b) hold simultaneously for any arbitrary value of δp_0 , it follows that

$$\frac{n_0 \cos \theta_0}{\zeta'_0} = \frac{n_1 \cos \theta_1}{\zeta'_1} = \frac{n_0 \cos \theta_0 - n_1 \cos \theta_1}{r_x}. \quad (19)$$

This relation gives the position of the *secondary focus* F'_1 .

It is often convenient to specify the position of the foci by means of their distances from O rather than by means of their z coordinates. If $OF_0 = d_0^{(t)}$, $OF'_0 = d_0^{(s)}$, $OF_1 = d_1^{(t)}$, $OF'_1 = d_1^{(s)}$ (in Fig. 4.22 $d_0^{(t)} < 0$, $d_0^{(s)} < 0$, $d_1^{(t)} > 0$, $d_1^{(s)} > 0$), then

$$\left. \begin{aligned} \zeta_0 &= d_0^{(t)} \cos \theta_0, & \zeta_1 &= d_1^{(t)} \cos \theta_1, \\ \zeta'_0 &= d_0^{(s)} \cos \theta_0, & \zeta'_1 &= d_1^{(s)} \cos \theta_1, \end{aligned} \right\} \quad (20)$$

and the two relations (18) and (19) become

$$\frac{n_0 \cos^2 \theta_0}{d_0^{(t)}} = \frac{n_1 \cos^2 \theta_1}{d_1^{(t)}} = \frac{n_0 \cos \theta_0 - n_1 \cos \theta_1}{r_y}, \quad (21)$$

and

$$\frac{n_0}{d_0^{(s)}} = \frac{n_1}{d_1^{(s)}} = \frac{n_0 \cos \theta_0 - n_1 \cos \theta_1}{r_x}. \quad (22)$$

The corresponding relations for reflection may be obtained by setting $n_1 = -n_0$.

4.7 CHROMATIC ABERRATION. DISPERSION BY A PRISM

In Chapter II it was shown that the refractive index is not a material constant but depends on colour, i.e. on the wavelength of light. We shall now discuss some elementary consequences of this result in relation to the performance of lenses and prisms.

4.7.1 Chromatic aberration

If a ray of polychromatic light is incident upon a refracting surface, it is split into a set of rays, each of which is associated with a different wavelength. In traversing an optical system, light of different wavelengths will therefore, after the first refraction, follow slightly different paths. In consequence, the image will not be sharp and the system is said to suffer from *chromatic aberration*.

of the refracted rays. From (14a) it is clear that the rays are perpendicular to the yz -plane so that F_1 is a

consider the rays which proceed from F'_0 . These rays intersect the focal line f_0 and give

$$-\delta p_0 = 0, \tag{14b}$$

$$\tag{16b}$$

in the xz -plane. All these rays will pass through F_1 . Hence, (15) must be satisfied with $z_1 = \zeta'_1$.

$$-\delta p_0 = 0. \tag{15b}$$

For any arbitrary value of δp_0 , it follows that

$$\frac{\cos \theta_0 - n_1 \cos \theta_1}{r_x} \tag{19}$$

is the y focus F'_1 . The coordinates of the foci by means of their distances from the origin. If $OF_0 = d_0^{(t)}$, $OF'_0 = d_0^{(s)}$, $d_0^{(s)} < 0$, $d_1^{(t)} > 0$, $d_1^{(s)} > 0$, then

$$\left. \begin{aligned} &= d_1^{(t)} \cos \theta_1, \\ &= d_1^{(s)} \cos \theta_1, \end{aligned} \right\} \tag{20}$$

$$\frac{\cos \theta_0 - n_1 \cos \theta_1}{r_y} \tag{21}$$

$$\frac{d_0 - n_1 \cos \theta_1}{r_x} \tag{22}$$

can be obtained by setting $n_1 = -n_0$.

DISPERSION BY A PRISM

The refractive index is not a material constant but varies with wavelength. We shall now discuss some elements of the performance of lenses and prisms.

When a ray passes through a refracting surface, it is split into a spectrum of different wavelengths. In traversing an optical system, it will therefore, after the first refraction, be dispersed. If, the image will not be sharp and the spectrum will be on.

We shall again confine our attention to points and rays in the immediate neighbourhood of the axis, i.e. it will be assumed that the imaging in each wavelength obeys the laws of Gaussian optics. The chromatic aberration is then said to be of the first order, or primary. If Q_α and Q_β are the images of a point P in two different wavelengths (Fig. 4.23), the projections of $Q_\alpha Q_\beta$ in the directions parallel and perpendicular to the axis are known as longitudinal and lateral chromatic aberration respectively.

Consider the change δf in the focal length of a thin lens, due to a change δn in the refractive index. According to § 4.4 (36) the quantity $(n - 1)f$ will, for a given lens, be independent of the wavelength. Hence

$$\frac{\delta f}{f} + \frac{\delta n}{n - 1} = 0. \tag{1}$$

The quantity

$$\Delta = \frac{n_F - n_C}{n_D - 1} \tag{2}$$

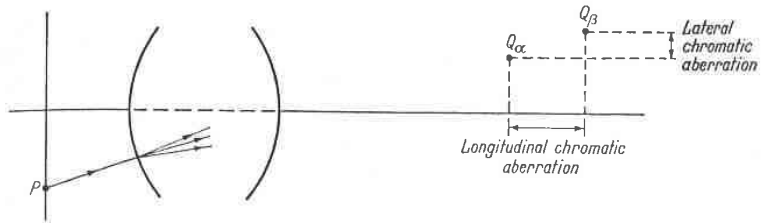


Fig. 4.23. The longitudinal and lateral chromatic aberration.

where n_F , n_D and n_C are the refractive indices for the Fraunhofer F , D and C lines ($\lambda = 4861 \text{ \AA}$, 5893 \AA , 6563 \AA respectively) is a rough measure of the dispersive properties of the glass, and is called the *dispersive power*. From (1) it is seen that it is approximately equal to the distance between the red and blue image divided by the focal length of the lens, when the object is at infinity. The variation with wavelength, of the refractive index of the usual types of glass employed in optical systems is shown in Fig. 4.24. The corresponding values of Δ lie between about 1/60 and 1/30.

To obtain an image of good quality, the monochromatic as well as the chromatic aberrations must be small. Usually a compromise has to be made, since in general it is impossible to eliminate all the aberrations simultaneously. Often it is sufficient to eliminate the chromatic aberration for two selected wavelengths only. The choice of these wavelengths will naturally depend on the purpose for which the system is designed; for example, since the ordinary photographic plate is more sensitive to the blue region than is the human eye, photographic objectives are usually "achromatized" for colours nearer to the blue end of the spectrum than is the case in visual instruments. Achromatization with respect to two wavelengths does, of course, not secure a complete removal of the colour error. The remaining chromatic aberration is known as the *secondary spectrum*.

Let us now examine under what conditions two thin lenses will form an achromatic combination with respect to their focal lengths. According to § 4.4 (39) the reciprocal of the focal length of a combination of two thin lenses separated by a distance l is given by

$$\frac{1}{f} = \frac{1}{f_1} + \frac{1}{f_2} - \frac{l}{f_1 f_2} \tag{3}$$

It is seen that $\delta f = 0$ when

$$\frac{\delta f_1}{f_1^2} + \frac{\delta f_2}{f_2^2} - \frac{l}{f_1 f_2} \left[\frac{\delta f_1}{f_1} + \frac{\delta f_2}{f_2} \right] = 0. \tag{4}$$

If the achromatization is made for the C and F lines, we have, using (1) and (2),

$$l = \frac{\Delta_1 f_2 + \Delta_2 f_1}{\Delta_1 + \Delta_2}, \tag{5}$$

where Δ_1 and Δ_2 are the dispersive powers of the two lenses.

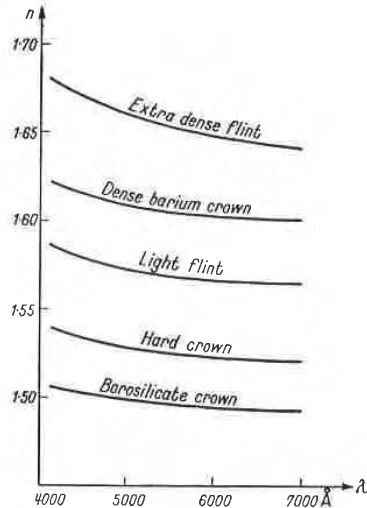


Fig. 4.24. Typical dispersion curves of various types of glass.

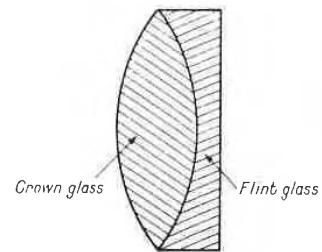


Fig. 4.25. An achromatic doublet.

One method of reducing the chromatic aberration is to employ two thin lenses in contact (Fig. 4.25), one made of crown glass, and the other of flint glass. In this case, since $l = 0$, we have, according to (5),

$$\frac{\Delta_1}{f_1} + \frac{\Delta_2}{f_2} = 0, \tag{6}$$

or, using (3),

$$\frac{1}{f_1} = \frac{1}{f} \frac{\Delta_2}{\Delta_2 - \Delta_1}, \quad \frac{1}{f_2} = -\frac{1}{f} \frac{\Delta_1}{\Delta_2 - \Delta_1}. \tag{7}$$

Now for given glass, and with a fixed value of the focal length f , (7) specifies f_1 and f_2 uniquely. But f_1 and f_2 depend on three radii of curvature; hence one of the radii may be chosen arbitrarily. This degree of freedom is sometimes used to make the spherical aberration as small as possible.

Another method of obtaining an achromatic system is to employ two thin lenses made of the same glass ($\Delta_1 = \Delta_2$) and separated by a distance equal to half of the sum of their focal lengths

$$l = \frac{1}{2}(f_1 + f_2). \tag{8}$$

That such a combination is achromatic follows immediately from (5).

$$+ \frac{\delta f_2}{f_2} = 0. \quad (4)$$

From (1) and (2),

$$\frac{\Delta_2 f_1}{\Delta_2} = \frac{\delta f_1}{f_1} \quad (5)$$

the two lenses.

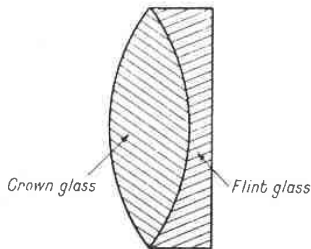


Fig. 4.25. An achromatic doublet.

ration is to employ two thin lenses in d the other of flint glass. In this case,

$$0, \quad (6)$$

$$= -\frac{1}{f} \frac{\Delta_1}{\Delta_2 - \Delta_1}. \quad (7)$$

he focal length f , (7) specifies f_1 and f_2 curvature; hence one of the radii may sometimes used to make the spherical

system is to employ two thin lenses ed by a distance equal to half of the

$$f_2). \quad (8)$$

immediately from (5).

An instrument consisting of several components cannot, in general, be made achromatic with respect to both position and magnification, unless each component is itself achromatic in this sense. We shall prove this for the case of two centred thin lenses separated by a distance l . Since according to § 4.4.4 the imaging by a thin lens is a central projection from the centre of the lens, we have (see Fig. 4.26)

$$\frac{Y'_1}{Y_1} = -\frac{\zeta'_1}{\zeta_1}, \quad \frac{Y'_2}{Y_2} = -\frac{\zeta'_2}{\zeta_2}. \quad (9)$$

Since $Y_2 = Y'_1$, the magnification is

$$\frac{Y'_2}{Y_1} = \frac{\zeta'_1}{\zeta_1} \cdot \frac{\zeta'_2}{\zeta_2}. \quad (10)$$

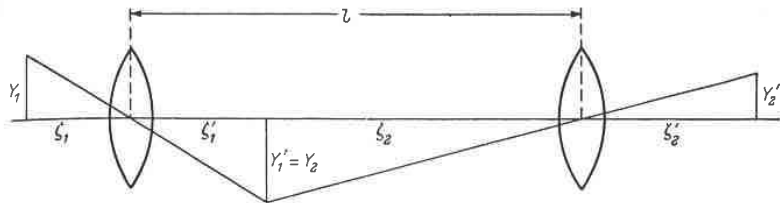


Fig. 4.26. Achromatization of two thin lenses.

If now the wavelength is altered, ζ_1 will remain unchanged, and if the position of the image is assumed to be achromatized, ζ'_2 will also remain unchanged. Hence the condition for achromatization of the magnification may be expressed by the formula

$$\delta \left(\frac{\zeta'_1}{\zeta_2} \right) = \frac{1}{\zeta_2} (\zeta_2 \delta \zeta'_1 - \zeta'_1 \delta \zeta_2) = 0. \quad (11)$$

Since $\zeta'_1 + \zeta_2 = l$, $\delta \zeta'_1 = -\delta \zeta_2$, and it is seen that (11) can only be satisfied if $\delta \zeta'_1 = \delta \zeta_2 = 0$, i.e. if each of the lenses is achromatized.

So far we have only considered the primary chromatic aberration of a thin lens and of a combination of two such lenses. Expressions for the primary chromatic aberration of a general centred system will be derived in Chapter V.

4.7.2 Dispersion by a prism

We shall now briefly discuss the passage of light through a prism.

Let α be the angle between the two faces of the prism. It is assumed that the edge A in which the two faces meet is perpendicular to the plane which contains the incident, transmitted, and emergent rays (Fig. 4.27). To begin with the light will be assumed to be strictly monochromatic.

Let B_1 and B_2 be the points of intersection of the incident and the emergent ray with the two faces, ϕ_1 and ψ_1 the angles of incidence and refraction at B_1 , and ψ_2 and ϕ_2 the inner and outer angles at B_2 (i.e. the angles which the ray $B_1 B_2$ and the emergent ray make with the normal at B_2). Further let C be the point of intersection of the normals to the prism at B_1 and B_2 , and D the point of intersection of the incident and the emergent rays, when these are prolonged sufficiently far.

If ε is the angle of deviation, i.e. the angle which the emergent ray makes with the incident ray, then

$$\phi_1 + \phi_2 = \varepsilon + \alpha, \tag{12}$$

$$\psi_1 + \psi_2 = \alpha. \tag{13}$$

Further, by the law of refraction,

$$\left. \begin{aligned} \sin \phi_1 &= n \sin \psi_1, \\ \sin \phi_2 &= n \sin \psi_2, \end{aligned} \right\} \tag{14}$$

where n is the refractive index of the glass with respect to the surrounding air. The deviation ε will have an extremum when

$$\frac{d\varepsilon}{d\phi_1} = 0. \tag{15}$$

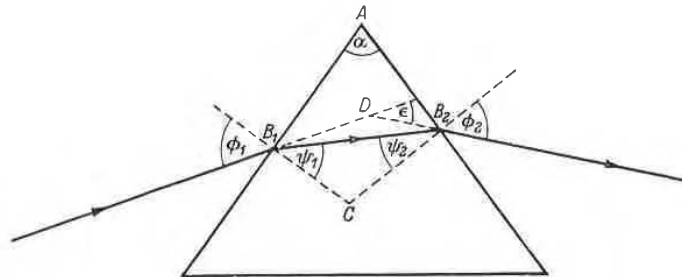


Fig. 4.27. Passage of a ray through a prism.

Using (12) this implies that

$$\left(\frac{d\phi_2}{d\phi_1} \right)_{\text{extr.}} = -1. \tag{16}$$

Now we have from (13) and (14),

$$\left. \begin{aligned} \frac{d\psi_1}{d\phi_1} &= -\frac{d\psi_2}{d\phi_1}, \\ \cos \phi_1 &= n \cos \psi_1 \frac{d\psi_1}{d\phi_1}, \\ \cos \phi_2 \frac{d\phi_2}{d\phi_1} &= n \cos \psi_2 \frac{d\psi_2}{d\phi_1} \end{aligned} \right\} \tag{17}$$

and hence, on elimination

$$\frac{d\phi_2}{d\phi_1} = -\frac{\cos \phi_1 \cos \psi_2}{\cos \psi_1 \cos \phi_2}. \tag{18}$$

From (16) and (18) it follows, that for an extremum,

$$\frac{\cos \phi_1 \cos \psi_2}{\cos \psi_1 \cos \phi_2} = 1, \tag{19}$$

whence, on squaring and using (14)

$$\frac{1 - \sin^2 \phi_1}{n^2 - \sin^2 \phi_1} = \frac{1 - \sin^2 \phi_2}{n^2 - \sin^2 \phi_2}. \tag{20}$$

4.7]
This equ
then
To de
and (18)

When
Since
that the
the ray
In ter
first fa
so that
This f
measu
Inst
throug
lens D
B' be
pass t

which the emergent ray makes with the

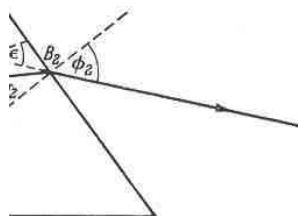
$$+ \alpha, \tag{12}$$

$$\tag{13}$$

$$\left. \begin{matrix} \psi_1, \\ \psi_2, \end{matrix} \right\} \tag{14}$$

with respect to the surrounding air. The

$$\tag{15}$$



through a prism.

$$- 1. \tag{16}$$

$$\left. \begin{matrix} \frac{d\psi_1}{d\phi_1}, \\ \frac{d\psi_2}{d\phi_1}, \end{matrix} \right\} \tag{17}$$

$$\frac{\cos \psi_2}{\cos \phi_2} \tag{18}$$

$$= 1, \tag{19}$$

$$\frac{-\sin^2 \phi_2}{-\sin^2 \phi_2} \tag{20}$$

4.7]

This equation is satisfied by

$$\left. \begin{matrix} \phi_1 = \phi_2; \\ \psi_1 = \psi_2. \end{matrix} \right\} \tag{21}$$

To determine the nature of the extremum we must evaluate $d^2\epsilon/d\phi_1^2$. From (12) and (18),

$$\begin{aligned} \frac{d^2\epsilon}{d\phi_1^2} &= \frac{d^2\phi_2}{d\phi_1^2} = \frac{d\phi_2}{d\phi_1} \frac{d}{d\phi_1} \left[\log \left(-\frac{d\phi_2}{d\phi_1} \right) \right] \\ &= \frac{d\phi_2}{d\phi_1} \left[-\tan \phi_1 - \tan \psi_2 \frac{d\psi_2}{d\phi_1} + \tan \psi_1 \frac{d\psi_1}{d\phi_1} + \tan \phi_2 \frac{d\phi_2}{d\phi_1} \right]. \end{aligned} \tag{22}$$

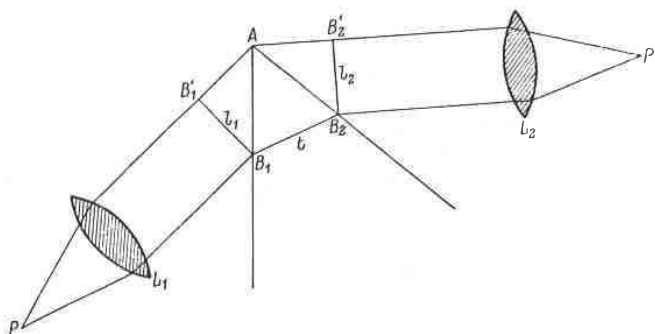


Fig. 4.28. Dispersion by a prism.

When $\phi_1 = \phi_2, \psi_1 = \psi_2$, this becomes with the help of (16), (17) and (14),

$$\left(\frac{d^2\epsilon}{d\phi_1^2} \right)_{\text{extr.}} = 2 \tan \phi_1 - 2 \tan \psi_1 \frac{\cos \phi_1}{n \cos \psi_1} = 2 \tan \phi_1 \left(1 - \frac{\tan^2 \psi_1}{\tan^2 \phi_1} \right). \tag{23}$$

Since $n > 1, \phi_1 > \psi_1$; also since $0 < \phi_1 < \pi/2, \tan \phi_1 > 0$. Hence $(d^2\epsilon/d\phi_1^2) > 0$, so that the deviation is a minimum. According to (21) it takes place when the passage of the rays through the prism is symmetrical. The minimal value of the deviation then is

$$\epsilon_{\text{min}} = 2\phi_1 - \alpha. \tag{24}$$

In terms of ϵ_{min} and α , the angle of incidence and the angle of refraction at the first face of the prism are

$$\phi_1 = \frac{1}{2}(\epsilon_{\text{min}} + \alpha), \quad \psi_1 = \frac{1}{2}\alpha, \tag{25}$$

so that

$$n = \frac{\sin \phi_1}{\sin \psi_1} = \frac{\sin [\frac{1}{2}(\epsilon_{\text{min}} + \alpha)]}{\sin (\frac{1}{2}\alpha)}. \tag{26}$$

This formula is often used in determinations of the refractive index of glass. One measures ϵ_{min} and α with the help of a spectrometer and evaluates n from (26).

Instead of a single ray, let us now consider the passage of a pencil of parallel rays through the prism, for example from a point source P placed in the focal plane of a lens L_1 (Fig. 4.28), the light still being assumed to be monochromatic. Let B_1' and B_2' be the feet of the perpendiculars dropped from B_1 and B_2 on to the rays which pass through the edge A . Then B_1B_1' and B_2B_2' are the lines of intersection of two

wave-fronts with the plane of incidence (plane of the figure). These two lines are inclined to each other at the angle of deviation ε . We set

$$B_1B'_1 = l_1, \quad B_2B'_2 = l'_2, \quad B_1B_2 = t. \quad (27)$$

Consider now a parallel beam of polychromatic instead of monochromatic light. If the lens L_1 is corrected for chromatic aberration, $B_1B'_1$ will still be in the wave front of the incident pencil. On the other hand the line $B_2B'_2$ will no longer be unique, but will depend on the wavelength λ . For the refractive index of the prism is a function of the wavelength,

$$n = n(\lambda), \quad (28)$$

and consequently the deviation ε also depends on λ :

$$\varepsilon = \varepsilon(\lambda). \quad (29)$$

The quantity

$$\frac{d\varepsilon}{d\lambda} = \frac{d\varepsilon}{dn} \frac{dn}{d\lambda} \quad (30)$$

formed for a constant value of the angle of incidence ϕ_1 is often called the *angular dispersion of the prism*. In (30) the first factor on the right depends entirely on the geometry of the arrangement, whilst the second factor characterizes the dispersive power of the glass of which the prism is made. Since $\phi_1 = \text{constant}$, we have from (12) and (13)

$$\frac{d\varepsilon}{dn} = \frac{d\phi_2}{dn}, \quad \frac{d\psi_1}{dn} = -\frac{d\psi_2}{dn}, \quad (31)$$

and from (14)

$$\begin{aligned} \sin \psi_1 + n \cos \psi_1 \frac{d\psi_1}{dn} &= 0, \\ \cos \phi_2 \frac{d\phi_2}{dn} &= \sin \psi_2 + n \cos \psi_2 \frac{d\psi_2}{dn}, \end{aligned} \quad (32)$$

whence on elimination

$$\frac{d\varepsilon}{dn} = \frac{\sin(\psi_1 + \psi_2)}{\cos \phi_2 \cos \psi_1} = \frac{\sin \alpha}{\cos \phi_2 \cos \psi_1}. \quad (33)$$

From the triangle AB_1B_2 , we have, by the sine theorem,

$$AB_2 = \frac{\cos \psi_1}{\sin \alpha} t, \quad (34)$$

and from the triangle $AB_2B'_2$,

$$AB_2 = l_2 \sec \phi_2. \quad (35)$$

Using (34) and (35), (33) gives

$$\frac{d\varepsilon}{d\lambda} = \frac{t}{l_2} \frac{dn}{d\lambda}. \quad (36)$$

In the position of minimum deviation, we have by symmetry $l_1 = l_2$. If, moreover, the lenses are so large that the pencil completely fills the prism, then t will be equal to the length b of the base of the prism. Equation (36) then gives for the *angular dispersion* $\delta\varepsilon$, i.e. for the angle by which the emergent wave-front is rotated when the wavelength is changed from λ to $\lambda + \delta\lambda$, the following expression:

$$\delta\varepsilon = \frac{b}{l_1} \frac{dn}{d\lambda} \delta\lambda. \quad (37)$$

of the figure). These two lines are ϵ . We set

$$B_1 B_2 = t. \quad (27)$$

atic instead of monochromatic light, ration, $B_1 B_1'$ will still be in the wave the line $B_2 B_2'$ will no longer be unique, refractive index of the prism is a func-

$$(28)$$

on λ :

$$(29)$$

$$\frac{n}{\lambda} \quad (30)$$

idence ϕ_1 is often called the *angular* ' on the right depends entirely on the and factor characterizes the dispersive ' . Since $\phi_1 = \text{constant}$, we have from

$$= - \frac{d\psi_2}{dn} \quad (31)$$

$$\frac{d\psi_1}{dn} = 0, \quad (32)$$

$$n \cos \psi_2 \frac{d\psi_2}{dn},$$

$$\frac{\sin \alpha}{\cos \phi_2 \cos \psi_1} \quad (33)$$

e theorem,

$$\frac{\psi_1}{\alpha} t, \quad (34)$$

$$c \phi_2. \quad (35)$$

$$\frac{n}{\lambda} \quad (36)$$

by symmetry $l_1 = l_2$. If, moreover, the lls the prism, then t will be equal to the 6) then gives for the *angular dispersion* wave-front is rotated when the wave-ving expression:

$$\delta \lambda. \quad (37)$$

4.8 PHOTOMETRY AND APERTURES

The branch of optics concerned with the measurement of light is called *photometry*. Strictly, photometry is not part of geometrical optics, but it seems appropriate to include a short account of it in the present chapter, since in many practical applications the approximate geometrical picture of an optical field forms an adequate basis for photometric investigations. We shall, therefore, take over the geometrical model according to which light is regarded as the flow of luminous energy along the geometrical rays, subject to the geometrical law of conservation of energy. This states (cf. § 3.1, eq. (31)), that the energy which is transmitted in unit time through any cross-section of a tube of rays is constant.

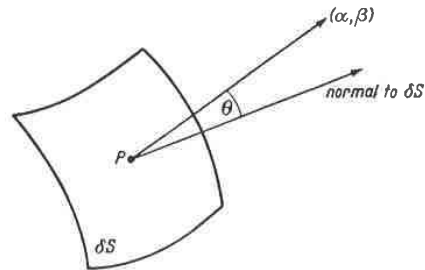


Fig. 4.29. Energy transmission from a surface element.

4.8.1 Basic concepts of photometry*

In photometry we are concerned essentially with the light energy emerging from a portion of a surface S . This surface may be fictitious, or it may coincide with the actual radiating surface of a source, or with an illuminated surface of a solid. If the latter is opaque, it is the reflected light which is considered; if it is transparent or semi-transparent (in which case the light is partly absorbed or scattered), it is the transmitted light which is usually measured.

Let $P(\xi, \eta)$ be a typical point on S referred to any convenient set of curvilinear coordinates on the surface. The (time averaged) amount of energy which emerges per unit time from the element δS of the surface at P and which falls within an element $\delta\Omega$ of the solid angle around a direction specified by the polar angles (α, β) , may be expressed in the form

$$\delta F = B \cos \theta \delta S \delta\Omega. \quad (1)$$

Here θ is the angle which the direction (α, β) makes with the normal to the surface element (see Fig. 4.29), and B is a factor which in general depends on (ξ, η) and (α, β) ,

$$B = B(\xi, \eta; \alpha, \beta). \quad (2)$$

The factor $\cos \theta$ is introduced in (1) since it is the projection of δS on to a plane normal to the direction (α, β) , rather than δS itself, which is the physically significant quantity. B is called the *photometric brightness* at the point (ξ, η) in the direction (α, β) . It must be distinguished from the visual sensation of brightness, from which

* Only the fundamental notions of photometry will be discussed. For further information and for the description of instruments used for measuring light see, for example, J. W. T. WALSH, *Photometry* (London, Constable, 2nd ed., 1953) or *Measurement of Radiant Energy* (McGraw-Hill, New York and London, 1937), edited by W. E. FORSYTHE.

it will in general differ, because the eye is not equally sensitive to all colours;* this point will be discussed more fully later.

δF is usually decomposed in two different ways, to show the explicit dependence on $\delta\Omega$ and δS :

$$\delta F = \delta I \delta\Omega = \delta E \delta S. \quad (3)$$

Comparison of (1) and (3) gives

$$\delta I = \frac{\delta F}{\delta\Omega} = B \cos \theta \delta S, \quad (4)$$

$$\delta E = \frac{\delta F}{\delta S} = B \cos \theta \delta\Omega. \quad (5)$$

The integral

$$I(\alpha, \beta) = \int B \cos \theta dS \quad (6)$$

taken over a piece of surface is called the *photometric intensity*† in the direction (α, β) , and the integral

$$E(\xi, \eta) = \int B \cos \theta d\Omega \quad (7)$$

taken throughout a solid angle is called the *photometric illumination at the point* (ξ, η) .

The variation of B with direction will depend on the nature of the surface, especially on whether it is rough or smooth, whether it is self-luminous, or whether it transmits or reflects other light. Often it is permissible to assume that, to a good approximation, B is independent of the direction. The radiation is then said to be *isotropic*. If the radiation is isotropic and if the radiating surface is plane, (6) reduces to

$$I(\alpha, \beta) = I_0 \cos \theta, \quad (8)$$

where

$$I_0 = \int B dS.$$

The photometric intensity in any direction then varies as the cosine of the angle between that direction and the normal to the surface. (8) is known as *Lambert's (cosine) law*, and when satisfied one speaks of *diffuse emission* or *diffuse reflection*, according as to whether the surface is emitting or reflecting.

The measurement of the quantities F , B , I and E involves the determination of a time interval, an area, a direction, a solid angle and an energy. The averages involved are often small and consequently sensitive instruments have to be used. They are essentially of two kinds. First, those which react to the heat developed in an absorbing medium (e.g. bolometer, thermo-couple, etc.) and are mainly used in studying heat

* We use the adjective "photometric" when we wish to stress that a particular quantity is evaluated with regard to its true physical, rather than its visual, effect.

† In Chapter I the light intensity was defined as the time average of the amount of energy which crosses per second a unit area perpendicular to the direction of the flow. This quantity must not be confused with the photometric intensity as defined by (6). It is unfortunate that the same word is used to denote two different quantities. Except in the present section we shall always understand by "intensity" the quantity introduced in Chapter I. If the surface element δS at P is orthogonal to the Poynting vector, the intensity (in the sense of Chapter I) is equal to the photometric illumination δE at P .

radiation
effect, in
incidence
of emitted
incident
in photo

In the
construction
energy
eye as a
is based

Let δ
with the
 δS per

direction
geometrical

Hence,

(10) is the
law of
proportion
of simple
and Q_2
sources
photometric

With the
son with

* The
tion with
zero, which
remains
In calculation
when its

qually sensitive to all colours;* this

s, to show the explicit dependence on

$$E\delta S. \quad (3)$$

$$E\theta\delta S, \quad (4)$$

$$E\theta\delta\Omega. \quad (5)$$

$$E\theta\delta S \quad (6)$$

metric intensity† in the direction (α, β) ,

$$E\theta\delta\Omega \quad (7)$$

metric illumination at the point (ξ, η) .

n the nature of the surface, especially self-luminous, or whether it transmits assume that, to a good approximation, n is then said to be *isotropic*. If the is plane, (6) reduces to

$$E\theta, \quad (8)$$

n varies as the cosine of the angle surface. (8) is known as *Lambert's diffuse emission* or *diffuse reflection*, or reflecting.

d E involves the determination of a and an energy. The averages involved uments have to be used. They are to the heat developed in an absorbing d are mainly used in studying heat

h to stress that a particular quantity is its visual, effect.

the time average of the amount of energy the direction of the flow. This quantity defined by (6). It is unfortunate that the

Except in the present section we shall used in Chapter I. If the surface element sity (in the sense of Chapter I) is equal to

radiation (infra-red); secondly, those which are based on the (surface) photo-electric effect, i.e. on the phenomenon of emission of electrons from a metal, caused by the incidence of light on the surface of the metal (in monochromatic light the number of emitted electrons, i.e. the current produced, is proportional to the energy of the incident light). Instruments of this kind are used, for instance, as exposure meters in photography.

In technical photometry, however, indirect methods are used. One defines and constructs a standard source of light, and expresses its photometric data in absolute energy units. Measurements are then made relative to this source, often using the eye as a null indicator, namely as an indicator of equal brightness. The comparison is based on a simple law which holds for the illumination due to a very small source* Q :

Let δS be a surface element at P and let $QP = r$. If θ is the angle which QP makes with the normal to δS (see Fig. 4.30), then the energy which the source sends through δS per unit time is $I\delta\Omega$, where I is the photometric intensity of the source in the

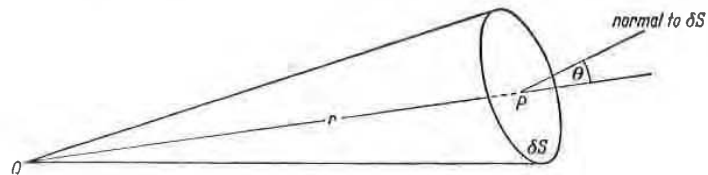


Fig. 4.30. Illumination from a point source.

direction QP , and $\delta\Omega$ is the solid angle which δS subtends at Q . Now by elementary geometry,

$$\cos \theta \delta S = r^2 \delta\Omega. \quad (9)$$

Hence, using (3), we have

$$E = \frac{I \cos \theta}{r^2}. \quad (10)$$

(10) is the basic equation of practical photometry. It expresses the so-called *cosine law of illumination* (E proportional to $\cos \theta$) and the *inverse square law* (E inversely proportional to r^2), and enables a comparison of the intensities of sources with the help of simple geometry. If a surface element δS is illuminated by two point sources Q_1 and Q_2 of photometric intensities I_1 and I_2 , and if the lines connecting δS with the sources make angles θ_1 and θ_2 with the normal to δS (Fig. 4.31) then, when the photometric illuminations are equal, we have

$$I_1 : I_2 = \frac{r_1^2}{\cos \theta_1} : \frac{r_2^2}{\cos \theta_2}. \quad (11)$$

With the help of (11), the strength of a given source may be determined by a comparison with a standard source.

* The photometric intensity I of a point source is defined by a procedure often used in connection with limiting concepts. Let us suppose that the area of the surface decreases towards zero, while at the same time B increases towards infinity, in such a way that the integral (6) remains finite. Then I is a function of α and β and of the position of the point source.

In calculating the photometric illumination, the finite extension of the source is usually neglected when its linear dimensions are less than about $1/20$ of its distance from the illuminated surface.

The equality of the illumination produced by two sources can be detected either by physical means, or directly, by the eye. The comparison by the eye is relatively easy when the light from the two sources is monochromatic and of the same frequency, but in general one has to compare sources which emit light of different spectral compositions.

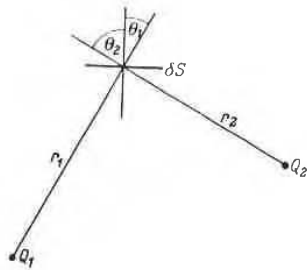


Fig. 4.31. Comparison of the intensities of two point sources.

This simple procedure can then no longer be used, since the eye is not equally sensitive to light of all wavelengths. Filters, each of which transmits light in a narrow range around a known wavelength of the spectrum, must be used instead; the determination of equality of illumination for different colours is then reduced to the determination of the relative energy values, taking into account the *relative visibility curve* of the eye. This is the curve obtained by plotting the reciprocal \$K_\lambda\$ of that amount of flux which produces the same sensation of brightness, against the wavelength. The curve depends to some extent on the strength of the illumination. For bright light it has a maximum near 550 m\$\mu\$.

(See Fig. 4.32 and Table XIII.) With decreasing strength of illumination the curve retains its shape but the maximum shifts towards the blue end of the spectrum, being at about 507 m\$\mu\$ for very faint light. This phenomenon is known as the *Purkinje effect*.

If the flux of energy is evaluated with respect to the visual sensation which it

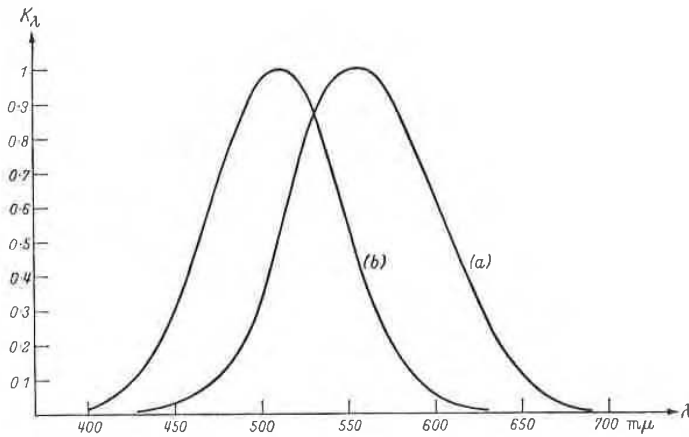


Fig. 4.32. The relative visibility curve \$K_\lambda\$ of the average human eye: (a) for bright light and (b) for feeble light.

produces, rather than with regard to its true physical magnitude, one speaks of the *luminous energy* \$F'\$:

$$F' = \frac{\int K_\lambda F_\lambda d\lambda}{\int K_\lambda d\lambda} \tag{12}$$

two sources can be detected either by comparison by the eye is relatively easy. Two sources of the same frequency, but of different spectral composition, can then no longer be detected if the eye is not equally sensitive to light of different wavelengths.

Filters, each of which transmits a narrow range around a known wavelength, must be used instead; the determination of illumination for different wavelengths is reduced to the determination of the relative sensitivity of the eye. This is the curve shown in Fig. 4.8, which gives the reciprocal K_λ of that amount of illumination which produces the same sensation of brightness as a given wavelength. The curve depends on the strength of the illumination; it has a maximum near 550 $m\mu$; with increasing strength of illumination the curve shifts towards the blue end of the spectrum. This phenomenon is known as the Purkinje effect. It is due to the fact that the eye is more sensitive to light of shorter wavelengths than it is to light of longer wavelengths.

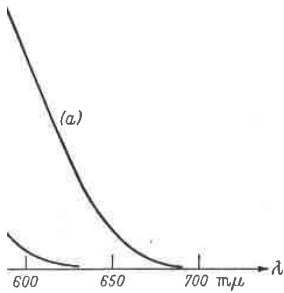


Fig. 4.8. Relative visibility factor K_λ of the average human eye; K_λ is the reciprocal of the relative sensitivity of the eye to light of wavelength λ .

physical magnitude, one speaks of

$$\lambda \quad (12)$$

$F_\lambda d\lambda$ being the amount of energy in the range $(\lambda, \lambda + d\lambda)$, K_λ the relative visibility and the integration being taken throughout the spectral range. The quantities B', I' and E' , which bear the same relations to B, I and E as F' bears to F , are usually called the *luminance*, the *luminous intensity* (or *candle power*) and the *illumination* respectively. These concepts are extensively used in visual photometry.

There are practical units for each of the four quantities F', B', I' and E' . Since it is easier to maintain a standard of luminous intensity rather than of luminous flux, the unit of luminous intensity is usually considered to be the basic photometric unit, and those for F', B' and E' are expressed in terms of it. The adopted standard of luminous intensity was at one time the *international candle*, a standard preserved by

TABLE XIII

The Relative Visibility Factor K_λ of an average human eye (bright light)

λ (in $m\mu$)	K_λ	λ (in $m\mu$)	K_λ
400	0.0004	600	0.631
410	0.0012	610	0.503
420	0.0040	620	0.381
430	0.0116	630	0.265
440	0.023	640	0.175
450	0.038	650	0.107
460	0.060	660	0.061
470	0.091	670	0.032
480	0.139	680	0.017
490	0.208	690	0.0082
500	0.323	700	0.0041
510	0.503	710	0.0021
520	0.710	720	0.00105
530	0.862	730	0.00052
540	0.954	740	0.00025
550	0.995	750	0.00012
560	0.995	760	0.00006
570	0.952		
580	0.870		
590	0.757		

a number of carbon lamps kept at various national laboratories. In more recent times it has been replaced by a new standard called the *candela* (cd); this is defined as one-sixtieth of the luminous intensity per square centimetre of a black body radiator at the temperature of solidification of platinum (2042°K approx.). The value of the luminous intensity of light of a different spectral composition must be evaluated by the procedure already explained, taking into account the relative visibility curve.

The unit of luminous flux is called the *lumen*. It is the luminous flux emitted within a unit solid angle by a uniform point source of luminous intensity 1 candela.

The unit of illumination depends on the unit of length employed. The metric unit of illumination is the *lux* (lx), sometimes also called the *metre-candle*; it is the illumination of a surface area of one square metre receiving a luminous flux of one lumen. The British unit is the lumen per square foot, formerly called the *foot-candle* (f.c.).

The unit of luminance is the candela per square centimetre, termed the *stilb* (sb),

and the candela per square metre termed the *nit*. In the British system, the units used are the candela per square inch or candela per square foot.

Other units are also used, but for their definitions and their relation to the units here discussed we must refer to books on photometry.

4.8.2 Stops and pupils*

The amount of light which reaches the image space of an optical system depends not only on the brightness of the object but also on the dimensions of the optical elements (lenses, mirrors) and of the stops. A stop (or diaphragm) is an opening, usually circular, in an opaque screen. The opaque parts of the screen prevent some of the severely aberrated rays from reaching the image. For the purposes of the present

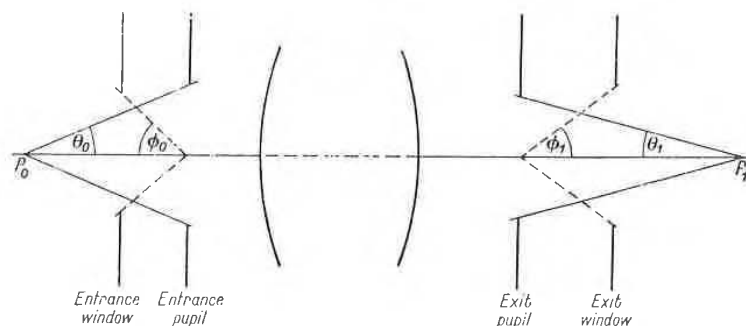


Fig. 4.33. Stops and pupils.

discussion it will be convenient to include the edges of the lenses and mirrors as well as diaphragms in the term "stop".

Consider all the rays from the axial object point P_0 . The stop which determines the cross-section of the image-forming pencil is called the *aperture stop*. To determine its position, the Gaussian image of each stop must be found in the part of the system which precedes it; the image which subtends the smallest angle at P_0 is called the *entrance pupil*. The physical stop which gives rise to the entrance pupil is the aperture stop. (If it lies in front of the first surface it is identical with the entrance pupil.) The angle $2\theta_0$ which the diameter of the entrance pupil subtends at P_0 is called the *angular aperture on the object side*, or simply *angular aperture* (Fig. 4.33).

The image of the aperture stop formed by the part of the system which follows it (also the image of the entry pupil by the whole system) is known as the *exit pupil*; the angle $2\theta_1$ which its diameter subtends at the image P_1 may be called the *angular aperture on the image side* (sometimes also the *projection angle*).

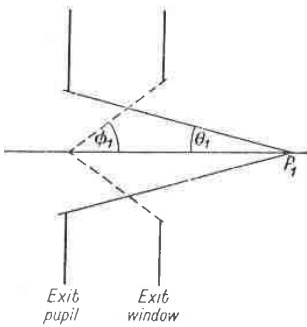
In the pencil of rays which proceeds from each object point, there will be a ray which passes through the centre of the entrance pupil. This special ray is known as the *principal ray* (also the *chief* or the *reference ray*) of the pencil, and is of particular importance in the theory of aberrations. In the absence of aberrations, the principal ray will also pass through the centre of the aperture stop and through the centre of the exit pupil.

If the aperture stop is situated in the back focal plane of that part of the system which precedes it, then the entrance pupil will be at infinity and all the principal rays

* The theory of stops was formulated by E. ABBE, *Jena Z. Naturwiss.*, 6 (1871), 263, and was extended by M. VON ROHR, *Zentr. Ztg. Opt. Mech.*, 41 (1920), 145, 159, 171.

4. In the British system, the units per square foot. Dimensions and their relation to the units of metric.

space of an optical system depends on the dimensions of the optical stop (or diaphragm) is an opening, the parts of the screen prevent some light. For the purposes of the present



pupils.

s of the lenses and mirrors as well as

point P_0 . The stop which determines the smallest angle at P_0 is called the *aperture stop*. To determine which part of the system subtends the smallest angle at P_0 is the entrance pupil. The part of the system which follows it is known as the *exit pupil*; image P_1 may be called the *angular field angle*.

At an object point, there will be a ray which subtends the smallest angle at the centre of the entrance pupil. This special ray is known as the *chief ray*. In the absence of aberrations, the principal ray passes through the centre of the aperture stop and through the centre of the exit pupil.

At infinity and all the principal rays

Z. Naturwiss., 6 (1871), 263, and was 1920), 145, 159, 171.

in the object space will be parallel to the axis. Such a system is said to be *telecentric on the object side*. If the aperture stop is in the front focal plane of the part of the system which follows it, then the exit pupil will be at infinity and the principal rays in the image space will be parallel to the axis; the system is then said to be *telecentric on the image side*. Telecentric arrangements are useful in measurements of the size of the object.

If other parameters are kept fixed, the angular aperture is a measure of the amount of light which traverses the system. There are other quantities which are frequently used to specify the "light-gathering power" of an optical system, for example the *numerical aperture* (N.A.) of a microscope objective. This is defined as the sine of the angular semi-aperture in the object space multiplied by the refractive index of the object space,

$$N.A. = n \sin \theta_0. \quad (13)$$

When a system is designed to work with objects at a great distance, as in the case of telescopes or certain photographic lenses, a convenient measure of its light-gathering

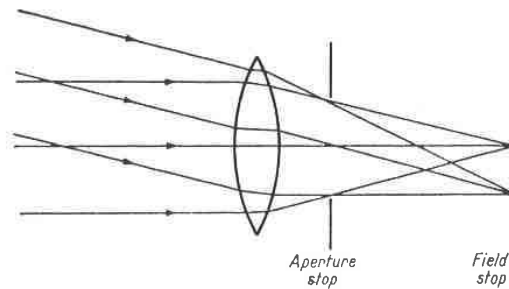


Fig. 4.34. Illustrating the distinction between the aperture stop and a field stop.

power is the so-called "*F number*" or "*nominal focal ratio*". It is the ratio of the focal length f of the system to the diameter d of the entrance pupil:

$$F = f/d. \quad (14)$$

Thus for a lens of 10 cm focal length which works with an aperture of 2 cm, $F = 5$. It is called an $f/5$ lens and is said to work at a "speed" of $f/5$.

Quantities such as the angular aperture, the numerical aperture, and the F number, which may be taken as the measure of the light-gathering power of the instrument, are often called *relative apertures*.

In addition to aperture stops, optical systems also possess *field stops*; they determine what proportion of the surface of an extended object is imaged by the instrument. The distinction between the two types of stops is illustrated in Fig. 4.34.

To determine the field stop, we again find first the image of each stop in the part of the system which precedes it. That image which subtends the smallest angle ($2\phi_0$ in Fig. 4.33) at the centre of the entrance pupil is called the *entrance window*, and the angle $2\phi_0$ is called the *field angle* or the *angular field of view*. The physical stop which corresponds to the entrance window is then the required field stop.

The image of the entrance window by the instrument (that is also the image of the field stop by the part of the system which follows it), is called the *exit window*. The angle ($2\phi_1$ in Fig. 4.33) which the diameter of the exit window subtends at the centre of the exit pupil is sometimes called the *image field angle*.

It may happen that, although the aperture stop is smaller than the lenses, some of the rays miss part of a lens entirely and parts of a lens may receive no light at all from certain regions of the object. This effect is known as *vignetting*, and is illustrated in Fig. 4.35. It is seldom encountered in systems like telescopes which have a relatively

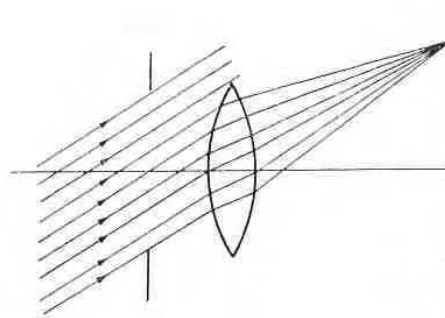


Fig. 4.35. Vignetting.

small field of view, but is of importance in other instruments, such as photographic objectives. Designers sometimes rely on vignetting to obliterate undesirable off-axis aberrations.

4.8.3 Brightness and illumination of images

We shall now briefly consider the relations between the basic photometric quantities which characterize the radiation in the image and object space.

Assume that the object is a small plane element of area δS_0 , perpendicular to the axis and radiating in accordance with LAMBERT'S law. The photometric brightness B_0 is then independent of direction. The amount of energy δF_0 which falls per unit time on to an annular element of the entry pupil centred on the axis is

$$\delta F_0 = B_0 \cos \gamma_0 \delta S_0 \delta \Omega_0, \quad (15)$$

where

$$\delta \Omega_0 = 2\pi \sin \gamma_0 \delta \gamma_0, \quad (16)$$

γ_0 being the angle which a typical ray passing through the annulus makes with the axis. Hence if θ_0 denotes, as before, the angular semi-aperture on the object side, the total flux of energy which falls on to the entrance pupil per unit time is

$$\begin{aligned} F_0 &= 2\pi B_0 \delta S_0 \int_0^{\theta_0} \sin \gamma_0 \cos \gamma_0 d\gamma_0 \\ &= \pi B_0 \delta S_0 \sin^2 \theta_0. \end{aligned} \quad (17)$$

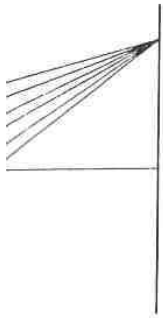
The energy flux F_1 emerging from the exit pupil may be expressed in a similar form:

$$F_1 = \pi B_1 \delta S_1 \sin^2 \theta_1. \quad (18)$$

F_1 cannot exceed F_0 and can only be equal to it if there are no losses due to reflection, absorption or scattering within the system; hence

$$B_1 \sin^2 \theta_1 \delta S_1 \leq B_0 \sin^2 \theta_0 \delta S_0. \quad (19)$$

p is smaller than the lenses, some of the lenses may receive no light at all from the object as *vignetting*, and is illustrated in Fig. 4.35.



ing.

instruments, such as photographic cameras, are designed to obliterate undesirable off-axis light.

Let us define the basic photometric quantities in the object space.

Let δS_0 be an area perpendicular to the optical axis. The photometric brightness B_0 is the energy δF_0 which falls per unit area δS_0 centred on the axis is

$$\delta F_0 = B_0 \delta S_0 \sin^2 \theta_0 \quad (15)$$

$$\delta F_0 = B_0 \delta S_0 \sin^2 \theta_0 \quad (16)$$

through the annulus makes with the optical axis. The semi-aperture on the object side, the angle θ_0 subtended by the exit pupil per unit time is

$$\cos \gamma_0 d\gamma_0 = \sin^2 \theta_0 \quad (17)$$

may be expressed in a similar form:

$$\quad (18)$$

there are no losses due to reflection,

$$B_1 = B_0 \delta S_0 \quad (19)$$

4.8]

Now the ratio $\delta S_1/\delta S_0$ is equal to the square of the lateral magnification M :

$$\frac{\delta S_1}{\delta S_0} = M^2. \quad (20)$$

If further it is assumed that the system obeys the sine condition (§ 4.5, eq. (6)),

$$\frac{n_0 \sin \theta_0}{n_1 \sin \theta_1} = M. \quad (21)$$

On substituting from (20) and (21) into (19) it follows that

$$B_1 < \left(\frac{n_1}{n_0}\right)^2 B_0. \quad (22)$$

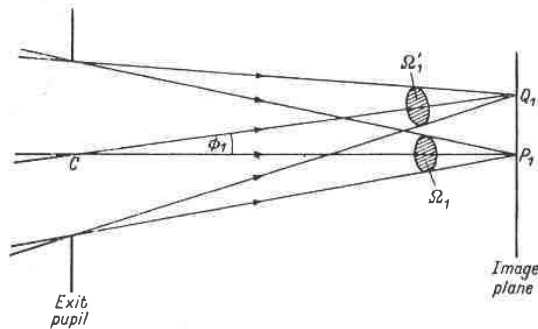


Fig. 4.36. Illumination at an off-axis image point.

In particular, if the refractive indices of the object and image spaces are equal, then according to (22), the photometric brightness of the image cannot exceed that of the object, and can only be equal to it if the losses of light within the system are negligible.

From (18) and (22) it follows, assuming the losses to be negligible, that

$$F_1 = \pi \left(\frac{n_1}{n_0}\right)^2 B_0 \delta S_1 \sin^2 \theta_1, \quad (23)$$

so that the photometric illumination $E_1 = F_1/\delta S_1$ at the axial point P_1 of the image is

$$E_1 = \pi \left(\frac{n_1}{n_0}\right)^2 B_0 \sin^2 \theta_1. \quad (24)$$

If θ_1 is small, the solid angle Ω_1 , which the exit pupil subtends at P_1 , is approximately equal to $\pi \sin^2 \theta_1$, so that (24) may then be written as

$$E_1 = \left(\frac{n_1}{n_0}\right)^2 B_0 \Omega_1. \quad (25)$$

This relation applies to the axial image, but the off-axis image may be treated in a similar way. If ϕ_1 is the angle which the principal ray CQ_1 makes with the axis (see Fig. 4.36), then we have in place of (25),

$$E_1 = \left(\frac{n_1}{n_0}\right)^2 B_0 \Omega_1' \cos \phi_1, \quad (26)$$

Ω_1' being the solid angle which the exit pupil subtends at Q_1 . With the help of (9) it follows that

$$\frac{\Omega_1'}{\Omega_1} = \cos \phi_1 \left(\frac{CP_1}{CQ_1} \right)^2 = \cos^3 \phi_1, \quad (27)$$

so that

$$E_1 = \left(\frac{n_1}{n_0} \right)^2 B_0 \Omega_1 \cos^4 \phi_1. \quad (28)$$

This formula shows that *the illumination in the image decreases as the fourth power of the cosine of the angle which the principal ray through the image point makes with the axis*, it being assumed that the object radiates according to LAMBERT'S law, that there are no losses of light within the system, and that the angular semi-aperture θ_1 is small.

In applying the preceding formulae, it should be remembered that they have been derived with the help of the laws of geometrical optics. For a very small source they may no longer give a good approximation. For example, the image of a point source is not a point but a bright disc surrounded by rings (the AIRY pattern, see § 8.5.2.); the light is then distributed over the whole diffraction pattern, and consequently the illumination at the geometrical focus is smaller than that given by (24).

4.9 RAY TRACING*

In designing optical instruments it is necessary to determine the path of the light with a greater accuracy than that given by Gaussian optics. This may be done by algebraic analysis, taking into account the higher-order terms in the expansion of the characteristic function, a procedure discussed in the next chapter. Alternatively one may determine the path of the light rays accurately with the help of elementary geometry, by successive application of the law of refraction (or reflection); this method, which will now be briefly described, is known as *ray tracing* and is extensively employed in practice.

4.9.1 Oblique meridional rays†

We consider first the tracing of an oblique meridional ray, i.e. a meridional ray from an extra-axial object point. Let A be the pole of the first surface of the system. The surface will be assumed to be a spherical refracting surface of radius r centred at a point C , and separating media of refractive indices n and n' . An incident ray OP (see Fig. 4.37) in the meridional plane is specified by the angle U which it makes with the axis, and by the distance $L = AB$ between the pole of A and the point B at which it meets the axis. Let I be the angle between the incident ray and the normal

* For a fuller discussion of ray tracing, see for example A. E. CONRADY, *Applied Optics and Optical Design*, Part I (Oxford University Press, 1929; reprinted by Dover Publications, Inc., New York, 1957); M. VON ROHR, *The Geometrical Investigation of Formation of Images in Optical Systems*, translated from German by R. KANTHACK (London, H.M. Stationery Office, 1920), and M. HERZBERGER, *Modern Geometrical Optics* (New York, Interscience Publishers, 1958). A method for the tracing of rays with the help of electronic computing machines was described by G. BLACK, *Proc. Phys. Soc. B*, **68** (1954), 569. A method for the tracing of rays through non-spherical surfaces was proposed by T. SMITH, *Proc. Phys. Soc.*, **57** (1945), 286; see also W. WEINSTEIN, *Proc. Phys. Soc. B*, **65** (1952), 731.

† In § 4.9.1, § 4.9.2, and § 4.10 the notation and the sign convention usually employed in a meridional ray trace is used. The sign convention for angles differs from the Cartesian sign convention used throughout the rest of the book; to revert to the Cartesian sign convention set $U = -\gamma$, $U' = -\gamma'$.

intersects at Q_1 . With the help of (9) it

$$= \cos^3 \phi_1, \tag{27}$$

$$\cos^4 \phi_1. \tag{28}$$

image decreases as the fourth power of the distance from the image point makes with the axis, according to LAMBERT'S law, that there are no aberrations if the angular semi-aperture θ_1 is small.

It should be remembered that they have been obtained for the case of simple optics. For a very small source the image is blurred (the AIRY pattern, see § 8.5.2.); the diffraction pattern, and consequently the resolution, is better than that given by (24).

RAY TRACING*

To determine the path of the light with accuracy, this may be done by algebraic methods in the expansion of the characteristic function in powers of the height. Alternatively one may use the method of elementary geometry, which is simpler (or reflection); this method, which is simpler and is extensively employed in

meridional ray, i.e. a meridional ray from the pole of the first surface of the system. The radius of curvature of the refracting surface of radius r centred at a point A on the axis. An incident ray OP is incident at the point P by the angle U which it makes with the normal PA at the pole of A and the point B at the intersection of the incident ray and the normal

* See for example A. E. CONRADY, *Applied Optics and Geometrical Optics*; reprinted by Dover Publications, Inc., *Investigation of Formation of Images in Optical Systems* (London, H.M. Stationery Office, 1920), and W. W. COLEMAN, *Optics* (New York, Interscience Publishers, 1958). The method of ray tracing on electronic computing machines was described by G. W. COLEMAN, *Proc. Phys. Soc.*, **57** (1945), 286; see also

The sign convention usually employed in a meridional ray trace differs from the Cartesian sign convention. In the Cartesian sign convention set $U = -\gamma$,

PC . The corresponding quantities relating to the refracted ray are denoted by primed symbols.

The following sign convention is used: The quantities r , L and L' are taken to be positive when C , B and B' are to the right of A , the light being assumed to be incident from the left. The angles U and U' are considered to be positive if the axis can be brought into coincidence with the rays PB and PB' by a clockwise rotation of less than 90° about B or B' respectively. The angles I and I' are taken to be positive if the incident and the refracted rays may be made to coincide with the normal PC by a clockwise rotation of less than 90° about the point P of incidence.

The quantities L and U which specify the incident ray may be assumed to be known.

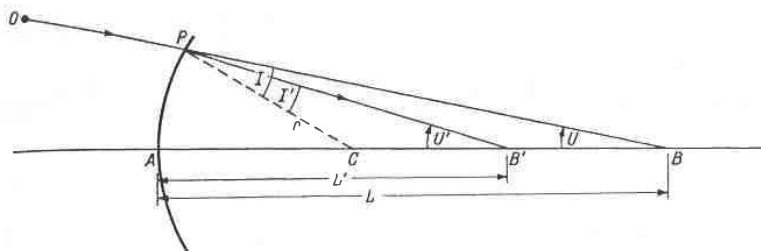


Fig. 4.37. Notation used in an oblique meridional ray trace.

It is then necessary to calculate L' and U' . Assuming also for the moment that both L and r are finite, we have, from the triangle PCB :

$$\sin I = \frac{L - r}{r} \sin U. \tag{1}$$

By the law of refraction

$$\sin I' = \frac{n}{n'} \sin I. \tag{2}$$

Also from the figure

$$U' = U + I - I'. \tag{3}$$

Finally, from the triangle PCB' ,

$$L' = \frac{\sin I'}{\sin U'} r + r. \tag{4}$$

By successive application of the refraction equations (1)–(4), the quantities L' and U' , which specify the refracted ray PB' , are obtained.

The refracted ray PB' now becomes the incident ray for the second surface. Writing L'_1 in place of L' and U'_1 in place of U' , and denoting by L_2 , U_2 the corresponding values, with L_2 referred to the pole of the second surface, we have the transfer equations

$$L_2 = L'_1 - d, \tag{5}$$

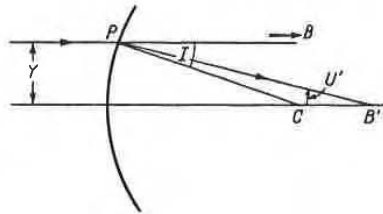
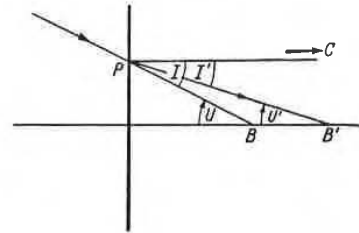
$$U_2 = U'_1, \tag{6}$$

where $d > 0$ is the distance between the poles of the two surfaces.

Next the "incident values" given by (5) and (6) are substituted into the refraction equations (1)–(4). Solving for the primed quantities, the ray is then traced through the

second surface. In this way, by the repeated application of the refraction and the transfer equations, the values L' and U' , relating to the ray in the image space, are obtained. The point of intersection of this ray with the image plane may then be determined. In practice, one would naturally trace not a single ray, but a number of suitably selected rays through the system; their intersection points with the image plane then give a rough estimate of the performance of the system.

If one of the surfaces (say the k th) is a mirror, the appropriate formulae to be used may be formally deduced from the preceding ones by setting $n'_k = -n_k$. Then d_k must be considered to be negative. Moreover all the remaining refractive indices and

Fig. 4.38 (a). The special case $L = \infty$.Fig. 4.38 (b). The special case $r = \infty$.

the subsequent d values must also be considered to be negative, unless a second reflection takes place, when they revert to positive signs.

Next consider the two special cases which were so far excluded. If the incident ray is parallel to the axis ($L = \infty$) the equation

$$\sin I = \frac{Y}{r}, \quad (7)$$

is used in place of (1), where Y is the distance of the ray from the axis (see Fig. 4.38(a)).

If the surface is plane ($r = \infty$) we have, in place of (1)–(4), the following set of equations (cf. Fig. 4.38(b)):

$$I = -U, \quad (8)$$

$$\sin U' = \frac{n}{n'} \sin U, \quad (9)$$

$$I' = -U', \quad (10)$$

$$L' = \frac{\tan U}{\tan U'} L. \quad (11)$$

On account of (9), equation (11) may also be written in the form

$$L' = \frac{n' \cos U'}{n \cos U} L, \quad (11a)$$

which is more convenient for computation than (11) if the angles are small.

application of the refraction and the sign to the ray in the image space, are the same with the image plane may then be taken as not a single ray, but a number of rays intersecting points with the image plane of the system.

the appropriate formulae to be used are obtained by setting $n'_k = -n_k$. Then d_k and the remaining refractive indices and

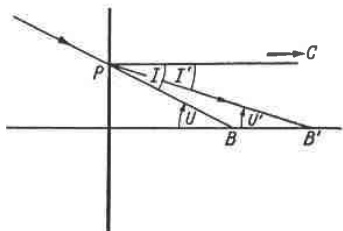


Fig. 4.38 (b). The special case $r = \infty$.

is to be negative, unless a second sign is used.

is so far excluded. If the incident ray

$$(7)$$

distance of the ray from the axis (see

place of (1)-(4), the following set of

$$(8)$$

U ,

$$(9)$$

,

$$(10)$$

L .

$$(11)$$

written in the form

$$L, \tag{11a}$$

(11) if the angles are small.

4.9]

It is useful to determine also the coordinates (Y_k, Z_k) of the point P_k of incidence at the k th surface, and the distance $D_k = P_k P_{k+1}$ between two successive points of incidence (see Fig. 4.39).

From the figure,

$$Y_k = r_k \sin (U_k + I_k), \tag{12}$$

$$Z_k = r_k - r_k \cos (U_k + I_k) = \frac{Y_k^2}{[1 + \cos (U_k + I_k)] r_k}, \tag{13}$$

$$D_k = \{d_k + Z_{k+1} - Z_k\} \sec U'_k. \tag{14}$$

In terms of Y_k, Z_k and U'_k ,

$$L'_k = Z_k + \frac{Y_k}{\tan U'_k}. \tag{15}$$

This relation may be used as a check on the value computed from (11a) or (11).

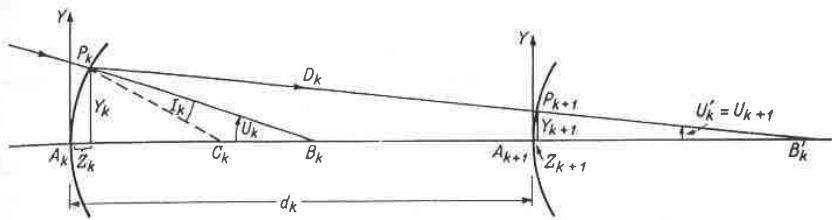


Fig. 4.39. Oblique meridional ray trace through two successive refracting surfaces.

In the special case when L_k is infinite, $U_k = 0$, and (12)-(15) still holds. If r_k is infinite, Y_k may be computed from the relation

$$Y_k = L_k \tan U_k, \tag{16}$$

Z_k then being zero.

4.9.2 Paraxial rays

If the inclination of a ray to the axis is sufficiently small, the sines of the various angles may be replaced, in the preceding formulae, by the angles themselves. The formulae then reduce to the Gaussian approximation for the path of the light. Such "paraxial ray-tracing formulae" are used in practice for computing the Gaussian magnification and the focal length of the system. A brief summary of these formulae will therefore be given here.

It is customary to denote quantities which refer to the paraxial region by small letters. The refraction equations (1)-(4) become

$$i = \frac{l - r}{r} u, \tag{17}$$

$$i' = \frac{n}{n'} i, \tag{18}$$

$$u' = u + i - i', \tag{19}$$

$$l' = \frac{i'}{u'} r + r. \tag{20}$$

The transfer equations (5) and (6) take the form

$$l_2 = l'_1 - d, \quad (21)$$

$$u_2 = u'_1. \quad (22)$$

In a similar way the paraxial equations for the cases $L = \infty$ and $r = \infty$ are obtained from (7)–(11a).

The paraxial equation for the incidence height, needed later, follows from (12):

$$y_k = r_k(u_k + i_k). \quad (23)$$

Although the relations (17)–(20) involve the angles which the incident ray and the refracted ray make with the axis, l' is independent of these quantities. This result, established in a different manner in § 4.4.1 follows when i , i' and u' are eliminated from the above relations. It is then found that u also disappears, and we obtain

$$n' \left(\frac{1}{r} - \frac{1}{l'} \right) = n \left(\frac{1}{r} - \frac{1}{l} \right). \quad (24)$$

This will be recognized as **ABBE'S** relation § 4.4 (7).

To determine the lateral Gaussian magnification M , it is only necessary to trace a paraxial ray from the axial object point. Then according to § 4.4 (54),

$$M = \frac{n_l u_l}{n_1 u_1}, \quad (25)$$

where the subscripts 1 and l refer to the first and last medium.

The focal length f' of the system may be obtained by tracing a paraxial ray at any desired height y_1 from an infinitely distant object. The equation of the conjugate ray in the image space, referred to axes at the second focal point, is then $y_l/z_l = -u'_l$, and it follows from § 4.3 (10) that

$$f' = -\frac{y_1}{u'_l}. \quad (26)$$

4.9.3 Skew rays

So far only rays which lie in a meridional plane were considered. We shall now briefly discuss the tracing of *skew* rays, i.e. rays which are not coplanar with the axis. The tracing of such rays is much more laborious and is usually carried out only in the design of systems with very high apertures.

A ray will now be specified by its direction cosines and by the coordinates of the point at which it meets a particular surface of the system. We take Cartesian rectangular axes at the pole A_1 of the first surface, with the Z -axis along the axis of the system. Let L_1 , M_1 , N_1 , ($L_1^2 + M_1^2 + N_1^2 = 1$) be the direction cosines of a ray incident at the point $P_1(X_1, Y_1, Z_1)$ (see Fig. 4.40).

The first step is to calculate the cosine of the angle I_1 of incidence. If r_1 is the radius of the first surface, the direction cosines of the normal at P_1 are

$$\bar{L}_1 = -\frac{X_1}{r_1}, \quad \bar{M}_1 = -\frac{Y_1}{r_1}, \quad \bar{N}_1 = \frac{r_1 - Z_1}{r_1},$$

so that

$$\begin{aligned} \cos I_1 &= L_1 \bar{L}_1 + M_1 \bar{M}_1 + N_1 \bar{N}_1 \\ &= N_1 - \frac{1}{r_1} (L_1 X_1 + M_1 Y_1 + N_1 Z_1). \end{aligned} \quad (27)$$

The next step is to determine the direction cosines L'_1, M'_1, N'_1 of the refracted ray. This is done in two stages: One calculates first the cosine of the angle of refraction, using the law of refraction in the form

$$n' \cos I'_1 = \sqrt{n'^2 - n^2 + n^2 \cos^2 I_1} \tag{28}$$

One then uses the fact that the refracted ray lies in the plane specified by the incident ray and the surface normal. Denoting by s_1, s'_1 and \bar{s}_1 the unit vectors along the incident ray, the refracted ray, and the normal, i.e. the vectors with components $(L_1, M_1, N_1), (L'_1, M'_1, N'_1)$ and $(\bar{L}_1, \bar{M}_1, \bar{N}_1)$, the coplanarity condition gives

$$s'_1 = \lambda s_1 + \mu \bar{s}_1, \tag{29}$$

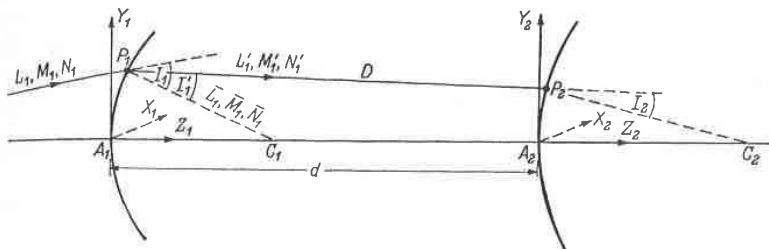


Fig. 4.40. Tracing of a skew ray.

where λ and μ are certain scalar functions. To determine λ and μ we first multiply (29) scalarly by s_1 , and use the fact that (see Fig. 4.40) $s_1 \cdot s'_1 = \cos(I_1 - I'_1)$, $s_1 \cdot \bar{s}_1 = \cos I_1$. This gives

$$\cos(I_1 - I'_1) = \lambda + \mu \cos I_1.$$

Next we multiply (29) scalarly by \bar{s}_1 , and use the relations $\bar{s}_1 \cdot s'_1 = \cos I'_1$, $\bar{s}_1 \cdot s_1 = \cos I_1$. We then obtain

$$\cos I'_1 = \lambda \cos I_1 + \mu.$$

From the last two relations it follows that

$$\lambda = \frac{\sin I'_1}{\sin I_1} = \frac{n}{n'}, \quad \mu = \frac{1}{n'} (n' \cos I'_1 - n \cos I_1),$$

and (29) then gives the following three equations for the direction cosines of the refracted ray:

$$\left. \begin{aligned} n' L'_1 &= n L_1 - \sigma X_1, \\ n' M'_1 &= n M_1 - \sigma Y_1, \\ n' N'_1 &= n N_1 - \sigma (Z_1 - r_1), \end{aligned} \right\} \tag{30}$$

where

$$\sigma = \frac{1}{r_1} (n' \cos I'_1 - n \cos I_1). \tag{31}$$

This completes the ray trace through the first surface, by means of the refraction equations (27), (28), (30) and (31).

The refracted ray now becomes the incident ray for the second surface. Taking parallel axes at the pole A_2 of the second surface, we have the transfer equations for the direction cosines

$$L_2 = L'_1, \quad M_2 = M'_1, \quad N_2 = N'_1. \tag{32}$$

$$(21)$$

$$(22)$$

ses $L = \infty$ and $r = \infty$ are obtained

, needed later, follows from (12):

$$(23)$$

angles which the incident ray and the ... of these quantities. This result, ... ws when i, i' and u' are eliminated ... u also disappears, and we obtain

$$-\frac{1}{l} \tag{24}$$

7).

n M , it is only necessary to trace a ... ccording to § 4.4 (54),

$$(25)$$

l last medium.

ied by tracing a paraxial ray at any

The equation of the conjugate ray ... d focal point, is then $y_i/z_i = -u'_i$,

$$(26)$$

ie were considered. We shall now ... hich are not coplanar with the axis. ... nd is usually carried out only in the

sines and by the coordinates of the ... ie system. We take Cartesian recti- ... ith the Z -axis along the axis of the ...) be the direction cosines of a ray

ngle I_1 of incidence. If r_1 is the radius ... ormal at P_1 are

$$\bar{N}_1 = \frac{r_1 - Z_1}{r_1},$$

$$N_1 \bar{N}_1$$

$$M_1 Y_1 + N_1 Z_1. \tag{27}$$

Let d be the distance A_1A_2 between the poles of the two surfaces. Denoting by X_1^+ , Y_1^+ , Z_1^+ the coordinates of the point P_1 referred to the axes at A_2 , we have the transfer equations for the coordinates

$$X_1^+ = X_1, \quad Y_1^+ = Y_1, \quad Z_1^+ = Z_1 - d. \quad (33)$$

Next the coordinates (X_2, Y_2, Z_2) of the point P_2 in which the refracted ray meets the second surface must be determined. If D denotes the distance from P_1 and P_2 , then

$$\left. \begin{aligned} X_2 &= X_1^+ + L_2 D, \\ Y_2 &= Y_1^+ + M_2 D, \\ Z_2 &= Z_1^+ + N_2 D. \end{aligned} \right\} \quad (34)$$

To determine D we use the fact that P_2 lies on the second surface. If r_2 is the radius of this surface, then

$$X_2^2 + Y_2^2 + Z_2^2 - 2Z_2 r_2 = 0. \quad (35)$$

On substituting into this equation from (34) the following equation for D is obtained:

$$D^2 - 2Fr_2 D + Gr_2 = 0, \quad (36)$$

where

$$\left. \begin{aligned} F &= N_2 - \frac{1}{r_2} (L_2 X_1^+ + M_2 Y_1^+ + N_2 Z_1^+), \\ G &= \frac{1}{r_2} [(X_1^+)^2 + (Y_1^+)^2 + (Z_1^+)^2] - 2Z_1^+. \end{aligned} \right\} \quad (37)$$

Equation (36) gives the following expression for D , if we also make use of the fact that $D = d$ for the axial ray:

$$D = r_2 \left(F - \sqrt{F^2 - \frac{1}{r_2} G} \right). \quad (38)$$

The coordinates of P_2 are determined on substituting for D into (34).

Finally, to complete the cycle, the cosine of the angle I_2 of incidence at the second surface must be calculated. It is given by a relation strictly analogous to (27):

$$\cos I_2 = N_2 - \frac{1}{r_2} (L_2 X_2 + M_2 Y_2 + N_2 Z_2), \quad (39)$$

or, using (34) and (38)

$$\begin{aligned} \cos I_2 &= F - \frac{1}{r_2} D \\ &= \sqrt{F^2 - \frac{1}{r_2} G}. \end{aligned} \quad (40)$$

Hence the last stage consists of the evaluation of the formulae (40), (38) and (34).

Because of the labour involved in the tracing of a general skew ray, the calculations are sometimes restricted to skew rays which lie in the immediate neighbourhood of a selected principal ray. Such skew rays may be traced through the system with the help of simplified schemes,* which are similar to those used for paraxial ray trace and are adequate for determining the position of the sagittal focal surface.

* Cf. H. H. HOPKINS, *Proc. Phys. Soc.*, **58** (1946), 663; also his *Wave Theory of Aberrations* (Oxford, Clarendon Press, 1950), pp. 59, 65.

In the p
of whic
such sin
tion of s
in optic
the ulti
reason,
called
K. SCH
aspheric

In 19
a new t
lens pla
more fu
it is pos
times la
camera
which u
type tel
low-disp
microsc

By m
to ensu
system
the desi

4.10.1

Conside
rays fro
points.
will be
pensate
pencil;
new sur
any pre
On ac
space w
the ang
intersec

* K. S
Königl. O
Two t
Universi
† Seo,
‡ The
(1947), 7
R. K. Lu
at Brown
Berkeley

PO 6th Es.

of the two surfaces. Denoting by d the distance from the axes at A_2 , we have the

$$Z_1^\dagger = Z_1 - d. \quad (33)$$

P_2 in which the refracted ray meets the second surface. Z_2 denotes the distance from P_1 and P_2 ,

$$\left. \begin{aligned} D, \\ \frac{1}{2}D, \\ D. \end{aligned} \right\} \quad (34)$$

of the second surface. If r_2 is the radius

$$Z_2 r_2 = 0. \quad (35)$$

The following equation for D is obtained:

$$Z_2 = 0, \quad (36)$$

$$\left. \begin{aligned} Y_1^\dagger + N_2 Z_1^\dagger, \\ [Z_1^\dagger]^2 - 2Z_1^\dagger. \end{aligned} \right\} \quad (37)$$

of D , if we also make use of the fact

$$-\frac{1}{r_2} G. \quad (38)$$

Substituting for D into (34).

The angle I_2 of incidence at the second surface is strictly analogous to (27):

$$M_2 Y_2 + N_2 Z_2, \quad (39)$$

$$\frac{1}{2} G. \quad (40)$$

of the formulae (40), (38) and (34). For a general skew ray, the calculations in the immediate neighbourhood of a ray are traced through the system with the same methods as those used for paraxial ray trace and sagittal focal surface.

63; also his *Wave Theory of Aberrations*

4.10 DESIGN OF ASPHERIC SURFACES

In the great majority of optical systems lenses and mirrors are employed, the surfaces of which have plane, spherical or paraboloidal form. The restriction to surfaces of such simple form is mainly due to the practical difficulties encountered in the production of surfaces of more complicated shapes with the high degree of precision required in optics. The restriction to surfaces of simple form naturally imposes limitations on the ultimate performance which systems of conventional design can attain. For this reason, in spite of the difficulties of manufacture, surfaces of more complicated form, called *aspheric* surfaces, are employed in certain systems. As early as 1905, K. SCHWARZSCHILD* considered a class of telescope objectives consisting of two aspheric mirrors, and showed that such systems can be made aplanatic.

In 1930, BERNHARD SCHMIDT, an optician of Hamburg, constructed a telescope of a new type, which consisted of a spherical mirror and a suitably designed aspheric lens placed at its centre of curvature. The performance of this system (considered more fully in § 6.4) was found to be quite outstanding. By means of such a telescope it is possible to photograph on one plate a very large region of the sky, many hundred times larger than can be obtained with telescopes of conventional design. The *Schmidt camera* has since become an important tool in astronomical research. Aspheric systems which use the principle of the SCHMIDT camera are also employed in certain projection-type television receivers,† in X-ray fluorescent screen photography, and certain fast low-dispersion spectrographs. Aspheric surfaces find also useful application in microscopy (cf. § 6.6).

By making one surface of any centred system aspherical, it is possible, in general, to ensure exact axial stigmatism; by means of two aspheric surfaces any centred system may in general be made aplanatic. In this section formulae will be derived for the design of such aspheric surfaces.

4.10.1 Attainment of axial stigmatism‡

Consider the rays from an axial object point P . In the image space of the system the rays from different zones of the exit pupil will in general intersect the axis at different points. Let $S^{(0)}$ be the last surface of the system and O its axial point (Fig. 4.41). It will be shown that it is possible to modify the profile of $S^{(0)}$ in such a way as to compensate exactly for the departure from the homocentricity of the image-forming pencil; more precisely we shall show that it is possible in general to replace $S^{(0)}$ by a new surface S which will ensure that all the rays in the image space meet the axis at any prescribed point Q .

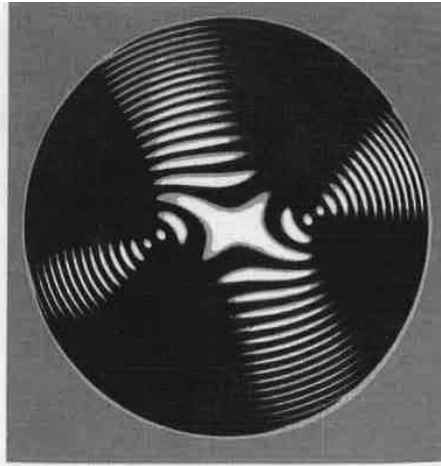
On account of symmetry only meridional rays need be considered. Each ray in the space which precedes the last surface will be specified by the following parameters: the angle U which it makes with the axis and the distance $H = OM$ at which it intersects the Y -axis (see Fig. 4.41). It will be convenient to label the rays: Let t be

* K. SCHWARZSCHILD, *Astr. Mitt. Königl. Sternwarte Göttingen* (1905). Reprinted from *Abh. Königl. Ges. Wiss. Göttingen, Math. Phys. Klasse*, 4 (1905-1906), No. 2.

Two telescopes of this type were later constructed, one with aperture of 24 in. at the University of Indiana and another, with a 12-in. aperture, at Brown University.

† See, for example, I. G. MALLOFF and D. W. EPSTEIN, *Electronics*, 17 (1944), 98.

‡ The methods here described are due to E. WOLF and W. S. PREDDY, *Proc. Phys. Soc.*, 59 (1947), 704; also E. WOLF, *Proc. Phys. Soc.*, 61 (1948), 494. Similar formulae were also given by R. K. LUNEBURG in his *Mathematical Theory of Optics* (mimeographed notes of lectures delivered at Brown University, R.I. (1944); printed version published by University of California Press, Berkeley and Los Angeles (1964), § 24.



Principles of Optics

**ELECTROMAGNETIC THEORY OF PROPAGATION
INTERFERENCE AND DIFFRACTION OF LIGHT**

MAX BORN & EMIL WOLF

Sixth Edition

The latest edition of the authors' classic work in the field of Physical Optics incorporating revisions to the text and illustrations as well as references to recent contributions to the literature.

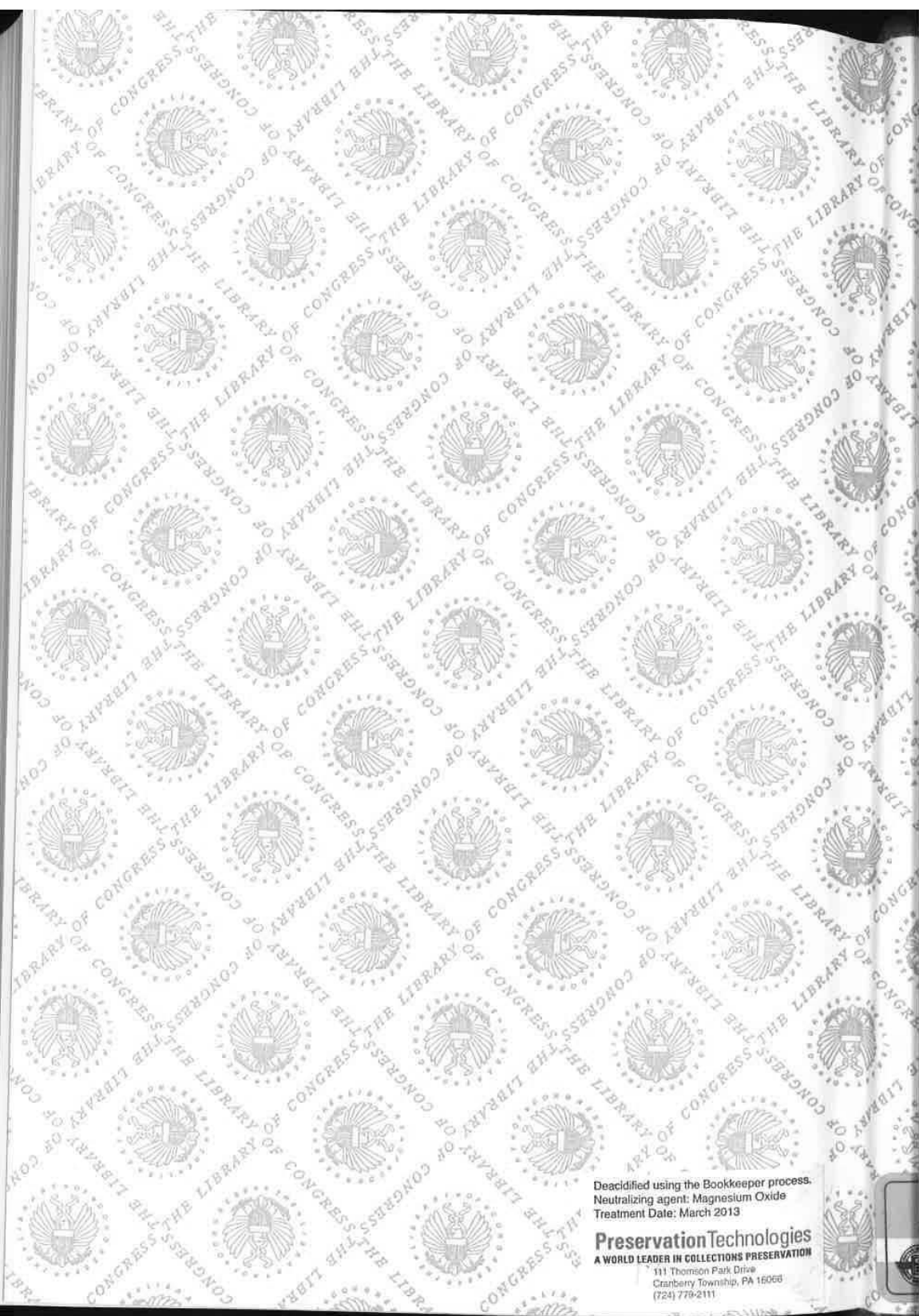
Contents: Historical Introduction. Basic Properties of the Electromagnetic Field. Electromagnetic Potentials and Polarization. Foundations of Geometrical Optics. Geometrical Theory of Optical Imaging. Geometrical Theory of Aberrations. Image Forming Instruments. Elements of the Theory of Aberrations. Interference and Diffraction with Partially Coherent Light. Rigorous Diffraction Theory. Diffraction of Light by Ultrasonic Waves. Optics of Metals. Optics of Crystals.

"Principles of Optics still stands out as the central source of information for any serious student or research worker of optical science." **Applied Optics**

"It can be recommended without reserve as the one that every serious worker in optics should have on his bookshelf." **Optics and Laser**

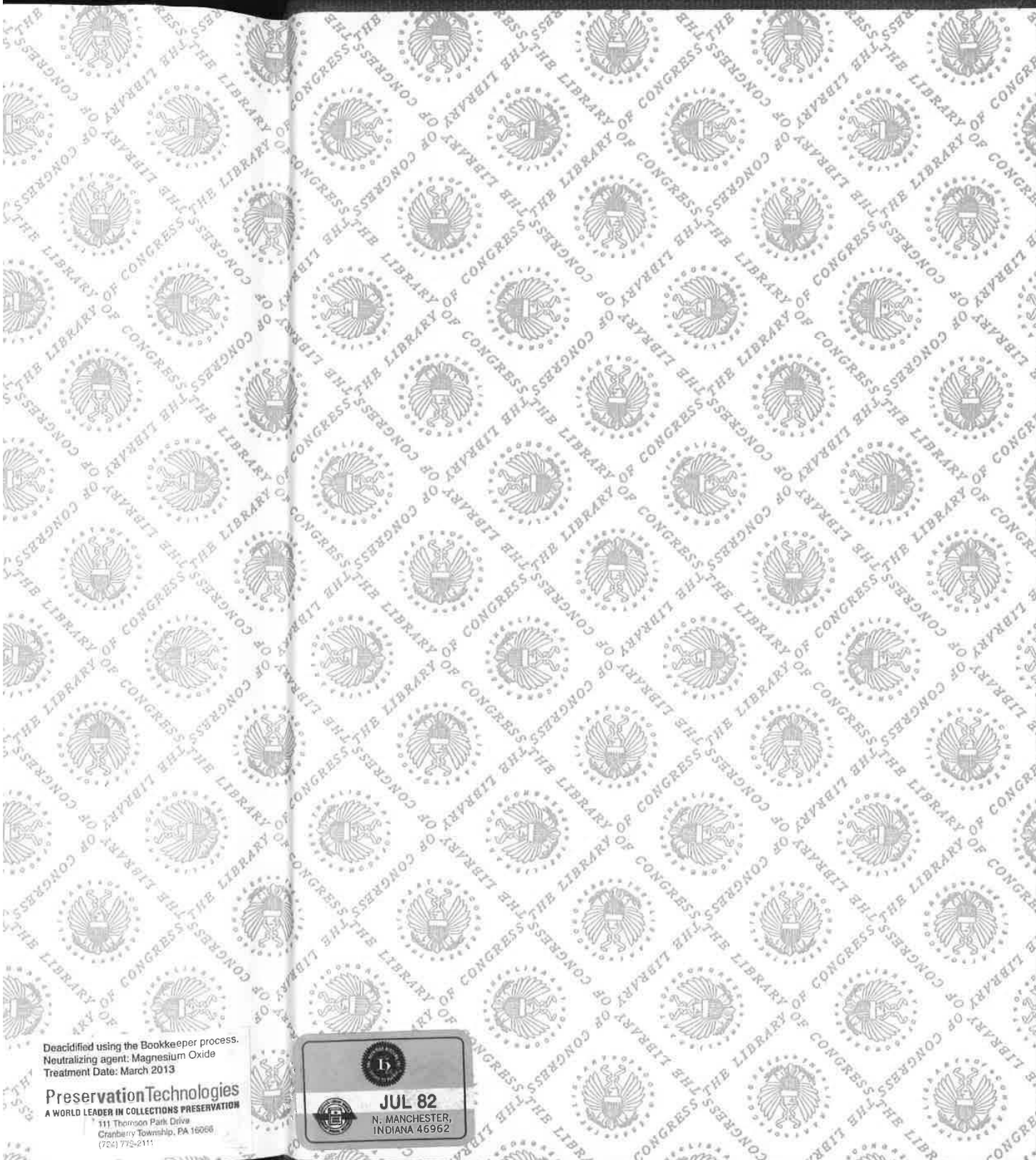
"As a result of the rigor, completeness, and elegance in the presentation of classical optics by Born and Wolf, the Principles of Optics will very likely remain for many more years the unsurpassed reference book for the mature, experienced, and serious optical scientist and engineer." **Circuits and Systems**

0 08 026431 6



Deacidified using the Bookkeeper process.
Neutralizing agent: Magnesium Oxide
Treatment Date: March 2013

Preservation Technologies
A WORLD LEADER IN COLLECTIONS PRESERVATION
111 Thomson Park Drive
Cranberry Township, PA 16066
(724) 779-2111



Decidified using the Bookkeeper process.
Neutralizing agent: Magnesium Oxide
Treatment Date: March 2013

Preservation Technologies
A WORLD LEADER IN COLLECTIONS PRESERVATION
111 Thomson Park Drive
Cranberry Township, PA 16066
(724) 772-2111



JUL 82
N. MANCHESTER,
INDIANA 46962





BORN

PRINCIPLES
OF OPTICS

FT MEADE
GenColl

QC 355
.2
.B67

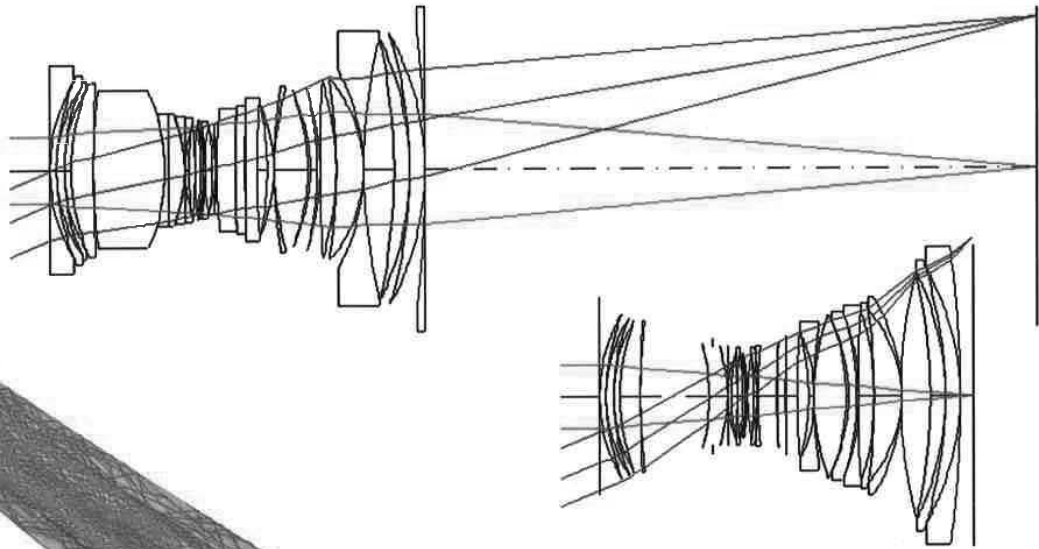
1980

Copy 2

APPENDIX E

S 510
I55
006
t. 1
copy 2

International Optical Design Conference 2006



4-8 June 2006
Vancouver, British Columbia
Canada

G. Groot Gregory
Joseph M. Howard
R. John Koshel
Chairs/Editors

SPIE Volume 6342
Part One of Two Parts

International Optical Design Conference 2006

**G. Groot Gregory
Joseph M. Howard
R. John Koshel**
Chairs/Editors

**4-8 June 2006
Vancouver, British Columbia, Canada**

Sponsored and Published by
OSA—Optical Society of America
SPIE—The International Society for Optical Engineering

Technical Cosponsor
American Society for Precision Engineering

**SPIE Volume 6342
Part One of Two Parts**

The papers included in this volume were part of the technical conference cited on the cover and title page. Papers were selected and subject to review by the editors and conference program committee. Some conference presentations may not be available for publication. The papers published in these proceedings reflect the work and thoughts of the authors and are published herein as submitted. The publisher is not responsible for the validity of the information or for any outcomes resulting from reliance thereon.

e-First Publication for Proceedings: As of July 2005, papers in the Proceedings of SPIE are first published electronically in the SPIE Digital Library (www.spiedl.org), and subsequently in print and CD-ROM.

Pagination system: The new citation format uses six-digit article identifier numbers (CIDs). Utilization of article CIDs allows proceedings articles to be fully citable as soon as they are published online, using the same identifier for both online and print versions.

The structure of the six-digit article CID number for Proceedings of SPIE is:

- The first four digits indicate the SPIE volume number.
- The last two digits indicate publication order within the volume using a Base 36 numbering system employing both numerals and letters. The CID number appears on each page, followed by the page number within the actual article.

Please use the following format to cite material from this book:

Author(s), "Title of Paper," in *International Optical Design Conference 2006*, edited by G. Groot Gregory, Joseph M. Howard, R. John Koshel, Proceedings of SPIE-OSA, SPIE Vol. 6342, Article CID Number (2006).

ISSN 0277-786X
ISBN 0-8194-6427-9

Copublished by
OSA—Optical Society of America
2010 Massachusetts Ave., N.W., D.C., 20036 USA
Telephone 1 202/223-8130 (Eastern Time) • Fax 1 202/223-1096
<http://www.osa.org>
and
SPIE—The International Society for Optical Engineering
P.O. Box 10, Bellingham, Washington 98227-0010 USA
Telephone 1 360/676-3290 (Pacific Time) • Fax 1 360/647-1445
<http://www.spie.org>

Copyright © 2006, Optical Society of America and The Society of Photo-Optical Instrumentation Engineers

Copying of material in this book for internal or personal use, or for the internal or personal use of specific clients, beyond the fair use provisions granted by the U.S. Copyright Law is authorized by OSA and SPIE subject to payment of copying fees. The Transactional Reporting Service base fee for this volume is \$15.00 per article (or portion thereof), which should be paid directly to the Copyright Clearance Center (CCC), 222 Rosewood Drive, Danvers, MA 01923. Payment may also be made electronically through CCC Online at <http://www.copyright.com>. Other copying for republication, resale, advertising or promotion, or any form of systematic or multiple reproduction of any material in this book is prohibited except with permission in writing from the publisher. The CCC fee code is 0277-786X/06/\$15.00.

Printed in the United States of America.

Contents

Part One

xiii	<i>Conference Committees</i>
xvii	<i>Introduction</i>
xxi	<i>Tribute to W. Lewis Hyde</i>
xxiii	<i>Tribute to Hilda and Rudolf Kingslake</i>
xxvii	<i>Tribute to Walter Mandler</i>
xxix	<i>Tribute to James Gilbert Baker</i>
xxxiii	<i>Tribute to Frank Cooke</i>

IODC OVERVIEW

634201	The first optical convention (in English): the 1905 Optical Convention in London, England [6342-05] K. P. Thompson, Optical Research Associates (USA)
634202	Double Gauss lens design: a review of some classics [6342-06] R. P. Jonas, M. D. Thorpe, ELCAN Optical Technologies (Canada)
634203	Twenty-first century optical tolerancing: a look at the past and improvements for the future (Invited Paper) [6342-07] R. N. Youngworth, Ball Aerospace & Technologies Corp. (USA)
634204	Alignment of optical systems (Invited Paper) [6342-08] R. E. Parks, Optical Perspectives Group, LLC (USA)
634205	Use of an application programming interface (API) to allow non-optical designers to perform specific optical evaluations [6342-09] M. C. Sanson, Corning Tropel Corp. (USA)
634206	The current state of the international standard for exchange of optical data in electronic form [6342-10] P. M. J. H. Wormell, Imperial College London (United Kingdom)

ABERRATION THEORY

634207	Wavefront correction using micromirror arrays: comparing the efficacy of tip-tilt-piston and piston-only micromirror arrays [6342-11] W. C. Sweatt, O. B. Spahn, W. D. Cowan, D. V. Wick, Sandia National Labs. (USA)
634208	Interpretation of pupil aberrations in imaging systems [6342-12] J. Sasian, College of Optical Sciences, Univ. of Arizona (USA)
634209	General sine condition for plane-symmetric imaging systems and some example aplanatic designs [6342-13] C. Zhao, College of Optical Sciences, Univ. of Arizona (USA)

TX 6-517-012



iii

- 63420A **Third-order aberrations of an AGRIN thin lens as a function of the shape and conjugate variables** [6342-14]
J. A. Díaz, Univ. de Granada (Spain); C. Pizarro, J. Arasa, Univ. Politècnica de Catalunya (Spain)
- 63420B **Description of spherical aberration and coma of a microlens using vector diffraction theory** [6342-15]
G. D. Gillen, Air Force Research Lab. (USA) and Anteon Corp. (USA); S. Guha, Air Force Research Lab. (USA)
- 63420C **Subwavelength grating induced wavefront aberrations: a case study** [6342-16]
K. Crabtree, R. A. Chipman, College of Optical Sciences, Univ. of Arizona (USA)

MEDICAL OPTICS

- 63420D **Human eye modeling using a single equation of gradient index crystalline lens for relaxed and accommodated states** [6342-17]
Y. Huang, Univ. of Rochester (USA); D. T. Moore, The Institute of Optics, Univ. of Rochester (USA)
- 63420E **Ultra-high-performance microscope objectives: the state of the art in design, manufacturing, and testing (Invited Paper)** [6342-18]
T. Sure, Leica Microsystems CMS GmbH (Germany); L. Danner, Vistec Semiconductor Systems GmbH (Germany); P. Euteneuer, Leica Microsystems CMS GmbH (Germany); G. Hoppen, Vistec Semiconductor Systems GmbH (Germany); A. Pausch, Leica Microsystems CMS GmbH (Germany); W. Vollrath, Vistec Semiconductor Systems GmbH (Germany)
- 63420F **2mm catheter design for endoscopic optical coherence tomography** [6342-19]
K.-S. Lee, C. Koehler, E. G. Johnson, CREOL, College of Optics and Photonics, Univ. of Central Florida (USA); E. V. Teuma, O. Ilegbusi, Univ. of Central Florida (USA); M. Costa, Univ. of Florida Health Science Ctr., Shands Hospital (USA); H. Xie, Univ. of Florida (USA); J. P. Rolland, CREOL, College of Optics and Photonics, Univ. of Central Florida (USA)
- 63420G **Apochromatic immersion objective for in vivo imaging for low-coherence confocal microscopy** [6342-20]
J. L. Bentley, Corning Tropel Corp. (USA) and The Institute of Optics, Univ. of Rochester (USA); C. Glazowski, J. M. Zavislan, The Institute of Optics, Univ. of Rochester (USA)
- 63420H **Dynamic-focusing microscope objective for optical coherence tomography** [6342-21]
S. Murali, J. Rolland, CREOL, College of Optics and Photonics, Univ. of Central Florida (USA)
- 63420I **A miniaturized fluorescence imaging system for detecting disease genes on a micro PCR biochip** [6342-22]
Y. Tan, H. Gong, N. Ramalingam, Q. Wang, L. Deng, Nanyang Technological Univ. (Singapore)

RAY TRACING AND OPTIMIZATION

- 63420J **Ray-tracing CAD objects** [6342-59]
M. Nicholson, K. Moore, ZEMAX Development Corp. (USA); I. Hörsch, Sick AG (Germany)

- 63420K **Forward tracing technique for diffraction analysis of apertures in optical systems** [6342-60]
A. Cifuentes, J. Arasa, C. Pizarro, Technical Univ. of Catalonia (Spain)
- 63420L **Designing lithographic objectives by constructing saddle points** [6342-61]
O. Marinescu, F. Bociort, Delft Univ. of Technology (Netherlands)
- 63420M **Using global synthesis to find tolerance-insensitive design forms** [6342-62]
J. R. Rogers, Optical Research Associates (USA)
- 63420N **Lens design: global optimization of both performance and tolerance sensitivity** [6342-63]
M. Isshiki, Isshiki Optics (Japan); D. C. Sinclair, Sinclair Optics (USA); S. Kaneko, Chart Inc. (Japan)
- 63420O **Designing easily manufactured lenses using a global method** [6342-64]
J. P. McGuire, Jr., Optical Research Associates (USA)

LIGHTPIPES

- 63420P **Optimization of parameterized lightpipes** [6342-65]
R. J. Koshel, Lambda Research Corp. (USA) and College of Optical Sciences, Univ. of Arizona (USA)
- 63420Q **Non-rotationally symmetric mixing rods** [6342-66]
W. J. Cassarly, T. L. R. Davenport, Optical Research Associates (USA)
- 63420R **Etendue preserving mixing and projection optics for high brightness LEDs applied to automotive headlamps** [6342-67]
A. Cvetković, CEDINT, Technical Univ. of Madrid (Spain); O. Dross, LPI Europe (Spain); J. Chaves, Light Prescriptions Innovators LLC (USA); P. Benítez, J. C. Miñano, CEDINT, Technical Univ. of Madrid (Spain); R. Mohedano, LPI Europe (Spain)
- 63420S **Equiangular-spiral non-loss bent lightpipe and its applications** [6342-68]
S.-C. Chu, J.-L. Chern, National Chiao Tung Univ. (Taiwan)
- 63420T **Optimizing density patterns to achieve desired light extraction for displays** [6342-69]
T. L. R. Davenport, W. J. Cassarly, Optical Research Associates (USA)
- 63420U **Off the beaten path with total internal reflection (Invited Paper)** [6342-70]
L. A. Whitehead, M. A. Mossman, Univ. of British Columbia (Canada)

DISPLAYS

- 63420V **Stereoscopic vision and the design of stereoscopic displays** [6342-71]
J. M. Cobb, Corning Tropel Corp. (USA)
- 63420W **Dual-element off-axis eyeglass-based display** [6342-72]
O. Cakmakci, CREOL, College of Optics and Photonics, Univ. of Central Florida (USA); A. Oranchak, Human Artifact R&D (USA); J. Rolland, CREOL, College of Optics and Photonics, Univ. of Central Florida (USA)

- 63420X **Dual-purpose lens for an eye-tracked projection head-mounted display** [6342-73]
C. Curatu, CREOL, College of Optics and Photonics, Univ. of Central Florida (USA); H. Hua, College of Optical Sciences, Univ. of Arizona (USA); J. Rolland, CREOL, College of Optics and Photonics, Univ. of Central Florida (USA)
- 63420Y **Catadioptric projection optical system for flat panel exposure tool** [6342-74]
M. Kohno, K. Fukami, H. Yoshioka, S. Watanabe, A. Suzuki, Canon Inc. (Japan)
- 63420Z **High definition DLP zoom projector lens design with TIR prism for high-definition television (HDTV)** [6342-75]
Y. C. Fang, W. T. Lin, H. L. Tsai, National Kaohsiung First Univ. of Science and Technology (Taiwan)
- 634210 **Wide angle hybrid magnifier for micro-display source** [6342-76]
D. Lingwood, M. Jeffs, Qioptiq (United Kingdom)

ILLUMINATION DESIGN AND SOURCE MODELING

- 634211 **Freeform optical systems with prescribed irradiance properties in near-field (Invited Paper)** [6342-77]
V. Oliker, Emory Univ. (USA)
- 634212 **Parametric design of non-imaging collimators** [6342-78]
S. Kudaev, P. Schreiber, Fraunhofer Institute for Applied Optics and Precision Engineering (Germany)
- 634213 **High-concentration mirror-based Kohler integrating system for tandem solar cells** [6342-79]
R. Winston, P. Benitez, A. Cvetkovic, Univ. of California, Merced (USA)
- 634214 **Geodesic lens: new designs for illumination engineering** [6342-80]
J. C. Miñano, P. Benítez, Univ. Politécnica de Madrid (Spain) and Light Prescriptions Innovators LLC (USA); B. Parkyn, Light Prescriptions Innovators LLC (USA); D. Grabovickic, F. García, A. Santamaría, J. Blen, Univ. Politécnica de Madrid (Spain); J. Chaves, W. Falicoff, Light Prescriptions Innovators LLC (USA)
- 634215 **A near-field goniospectroradiometer for LED measurements (Invited Paper)** [6342-81]
I. Ashdown, M. Salisbury, TIR Systems Ltd. (Canada)
- 634216 **Spatial distribution of LED radiation** [6342-82]
I. Moreno, Univ. Autonoma de Zacatecas (Mexico)
- 634217 **Optical modeling for LED in mid-field region** [6342-83]
C.-C. Sun, T.-X. Lee, S.-H. Ma, Y.-L. Lee, S.-M. Huang, National Central Univ. (Taiwan)

DIFFRACTIVE OPTICS

- 634218 **Novel lens design for free-space optical interconnects** [6342-84]
J. L. Ramsey, Univ. of Ottawa (Canada); W. Pijitrojana, Thammasat Univ. (Thailand); T. J. Hall, Univ. of Ottawa (Canada)

- 634219 **Diffractive nano-focusing and nano-imaging** [6342-85]
Q. Cao, FernUniv. Hagen (Germany)
- 63421A **Optical spatial filter for two-dimensional speed measurement, position monitoring, and particle sizing** [6342-86]
S. Bergeler, H. Krambeer, H. Ewald, Univ. of Rostock (Germany)
- 63421B **En-squared power-based optical design for page-based holographic storage systems** [6342-87]
Y. Takashima, L. Hesselink, Stanford Univ. (USA)
- 63421C **GASIR 1: a promising material for dual waveband systems** [6342-88]
M. C. de la Fuente, Indra Sistemas SA (Spain)

Part Two

OPTICS FOR DIGITAL SYSTEMS

- 63421D **Panamorph lenses: a new type of panoramic lens** [6342-89]
S. Thibault, ImmerVision (Canada)
- 63421E **Digital correction of lens aberrations in light field photography (Invited Paper)** [6342-90]
R. Ng, P. Hanrahan, Stanford Univ. (USA)
- 63421F **The optics of miniature digital camera modules** [6342-91]
J. Bateau, P. P. Clark, Flextronics Optical Technology Ctr. (USA)
- 63421G **Joint design of lens systems and digital image processing** [6342-92]
M. D. Robinson, D. G. Stork, Ricoh Innovations (USA)
- 63421H **Impact of the 2D structured noise in the post-processing of hybrid optical-digital imaging systems** [6342-93]
S. Bosch, R. Tudela, Univ. de Barcelona (Spain); M. C. de la Fuente, Indra Sistemas SA (Spain); J. Ferré-Borrull, Univ. Rovira i Virgili (Spain)
- 63421I **Two times optical digital zoom lens with short total length and extremely small front aperture for two-million pixel CMOS on mobile phones** [6342-94]
Y.-C. Fang, H.-L. Tsai, National Kaohsiung First Univ. of Science and Technology (Taiwan); Y.-H. Chien, W.-Y. Wu, C.-C. Hu, H.-W. Su, OES/Industrial Technology Research Institute (Taiwan)

TELESCOPES AND SPACE OPTICS

- 63421J **Four-mirror compact afocal telescope with dual exit pupil** [6342-95]
J. M. Rodgers, Optical Research Associates (USA)
- 63421L **Diffraction-limited constant-resolution zoom lens across multi-wavelengths for the Advanced Technology Solar Telescope** [6342-97]
H. K. An, S. K. Pitalo, Univ. of Alabama in Huntsville (USA)

- 63421M **Design of an infrared integral field spectrograph specialized for direct imaging of exoplanets** [6342-98]
J.-F. Lavigne, Univ. de Montréal (Canada), Institut National d'Optique (Canada), and Herzberg Institute of Astrophysics (Canada); R. Doyon, Univ. de Montréal (Canada); S. Thibault, Univ. Laval (Canada) and Immervision (Canada); M. Wang, Institut National d'Optique (Canada)
- 63421N **Corrected calculation of star trails caused by differential atmospheric refraction** [6342-99]
E. H. Richardson, Univ. of Victoria (Canada)
- 63421O **The SCUBA-2 polarimeter** [6342-100]
M. R. Leclerc, INO (Canada); P. Bastien, Univ. de Montréal (Canada); S. Bernier, INO (Canada); E. Bissonnette, Univ. de Montréal (Canada); P. A. R. Ade, G. Pisano, G. Savini, Cardiff Univ. (United Kingdom)

INFRARED AND LITHOGRAPHIC DESIGN SYSTEMS

- 63421P **Optical design of a panoramic, wide spectral band, infrared fisheye lens** [6342-101]
H. M. Spencer, DRS Sensors and Targeting Systems (USA); J. M. Rodgers, J. M. Hoffman, Optical Research Associates (USA)
- 63421Q **All-reflective zoom systems for infrared optics (Invited Paper)** [6342-102]
J. Chang, Y. Wang, T. Zhang, M. M. Talha, Beijing Institute of Technology (China); Z. Weng, H. Yang, Changchun Institute of Optics, Fine Mechanics and Physics (China)
- 63421R **Extreme ring fields in microlithography** [6342-103]
A. Epple, Carl Zeiss SMT AG (Germany)
- 63421S **Use of diffractive lenses in lithographic projection lenses** [6342-104]
H.-J. Rostalski, A. Epple, H. Feldmann, Carl Zeiss SMT AG (Germany)
- 63421T **The optical design for microlithographic lenses** [6342-105]
Y. Ohmura, Nikon Corp. (Japan)

IODC PROBLEM SESSION

- 63421U **2006 IODC lens design problem: the lens shuffler** [6342-107]
R. C. Juergens, Raytheon Missile Systems (USA); P. K. Manhart, Advanced Refractive (USA)
- 63421V **2006 IODC illumination design problem** [6342-110]
P. Benitez, Univ. of California, Merced (USA)

INTERFEROMETRY AND TESTING

- 63421W **Determination of measurement uncertainty in the developed instantaneous phase shifting interferometer** [6342-46]
N. R. Sivakumar, Concordia Univ. (Canada); B. Tan, K. Venkatakrishnan, Ryerson Univ. (Canada)

- 63421X **Maximum likelihood estimation as a general method of combining subaperture data for interferometric testing** [6342-47]
P. Su, J. Burge, R. A. Sprowl, J. Sasian, College of Optical Sciences, Univ. of Arizona (USA)
- 63421Y **CGH null test design and fabrication for off-axis aspherical mirror tests** [6342-48]
M. Wang, D. Asselin, P. Topart, J. Gauvin, INO (Canada); P. Berlioz, EADS Astrium SAS (France); B. Harnisch, European Space Agency (Netherlands)
- 63421Z **High-precision measurements of reflectance** [6342-49]
P. Voarino, S. Petitrenaud, H. Piombini, F. Sabary, D. Marteau, CEA Le Ripault (France)
- 634220 **Overview of the line-imaging VISAR diagnostic at the National Ignition Facility (NIF)** [6342-50]
R. M. Malone, G. A. Capelle, Bechtel Nevada (USA); J. R. Celeste, P. M. Celliers, Lawrence Livermore National Lab. (USA); B. C. Frogget, R. L. Guyton, M. I. Kaufman, Bechtel Nevada (USA); T. L. Lee, B. J. MacGowan, E. W. Ng, Lawrence Livermore National Lab. (USA); I. P. Reinbachs, Bechtel Nevada (USA); R. B. Robinson, L. G. Seppala, Lawrence Livermore National Lab. (USA); T. W. Tunnell, P. W. Watts, Bechtel Nevada (USA)

DESIGN FOR FABRICATION

- 634223 **Localized slope errors and their impact on image performance requirements** [6342-53]
M. C. Sanson, C. T. Tienvieri, S. VanKerkhove, Corning Tropel Corp. (USA)
- 634224 **Numerical Integration of an aspheric surface profile** [6342-54]
J. L. Rayces, Consultant (USA); X. Cheng, Tsinghua Univ. (China)
- 634225 **Sensitivity control to surface irregularity** [6342-55]
A. Yabe, Consultant (Germany)
- 634226 **Approximation of shranked aspheres** [6342-56]
R. Schoene, D. Hintermann, T. Hanning, Univ. of Passau (Germany)
- 634227 **Improvements in lenticular lens arrays design and fabrication** [6342-57]
R. B. Johnson, Consultant (USA)
- 634228 **Systematic design processes to improve the manufacturability of zoom lenses** [6342-58]
C.-W. Chang, C.-L. Wang, C.-C. Chang, Y.-L. Wu, C.-C. Cheng, W.-C. Chao, Industrial Technology Research Institute (Taiwan)

POSTER SESSION

- 634229 **Fast and low noise adaptive optics system for the correction of micro-aberrations of laser beam** [6342-23]
S. Avino, E. Calloni, R. De Rosa, Univ. Federico II di Napoli (Italy) and INFN (Italy); L. Di Fiore, INFN (Italy); L. Milano, Univ. Federico II di Napoli (Italy) and INFN (Italy); S. R. Restaino, Naval Research Lab. (USA); A. Tierno, Univ. Federico II di Napoli (Italy) and INFN (Italy)
- 63422B **Mathematical and computer model for designing a telescope with a segmented mirror** [6342-39]
D. Cheng, Y. Wang, J. Chang, M. M. Talha, Beijing Institute of Technology (China)

- 63422C **Performance comparison of an anamorphic spatial heterodyne spectrometer with conventional spectrometer** [6342-40]
I. Powell, P. Cheben, National Research Council Canada (Canada)
- 63422D **Aberration functions for microlithographic lens** [6342-41]
T. Matsuyama, T. Ujike, Nikon Corp. (Japan)
- 63422E **Merit function segmentation dependence on the isoplanatic patch criterion** [6342-42]
C. Pizarro, Technical Univ. of Catalonia (Spain); J. A. Díaz, Univ. de Granada (Spain)
- 63422F **Design of aspheric lens to collimate and uniform irradiance of a light source with Lambertian angular distribution** [6342-43]
C.-J. Cheng, J.-L. Chern, National Chiao Tung Univ. (Taiwan)
- 63422G **Application of global optimization to design of an aspheric pickup head for multiple wavelengths** [6342-44]
C.-H. Tsao, J.-L. Chern, National Chiao Tung Univ. (Taiwan)
- 63422H **Optical design with aspheric surfaces and exact ray tracing: an analytical method** [6342-45]
O. García-Lievanos, S. Vazquez-Montiel, J. A. Hernandez-Cruz, J. Castro-Ramos, Instituto Nacional de Astrofísica, Óptica y Electrónica (Mexico)
- 63422I **A polarization fidelity tracking mount optical geometry and comparison with Az El mount: polarization and throughput modeling using ZEMAX** [6342-24]
R. F. Horton, ad hoc Optics (USA)
- 63422J **Analytical and exact method for design diffractive lenses free of spherical aberration** [6342-25]
J. A. Hernández-Cruz, S. Vázquez-Montiel, O. García-Liévanos, J. Castro-Ramos, Instituto Nacional de Astrofísica, Óptica y Electrónica (Mexico)
- 63422K **Jones calculus for step polarization states of lightwave** [6342-26]
C. Li, Beihang Univ. (China)
- 63422N **Optical design of a compact and anastigmatic telescope with three mirrors** [6342-29]
J. Herrera Vázquez, S. Vázquez y Montiel, Instituto Nacional de Astrofísica, Óptica y Electrónica (Mexico)
- 63422O **Design and implementation of organic LED-based displays for signage application** [6342-30]
P. Sharma, H. Kwok, Univ. of Victoria (Canada)
- 63422Q **Designing pillow optics for signal lighting** [6342-106]
R. S. Mulder, Optical Research Associates (USA)
- 63422S **Optical design compensation from engineering to production manufacturing** [6342-35]
C. T. Tienvieri, T. Rich, Corning Tropol Corp. (USA)
- 63422U **Infrared Fabry-Perot spectrometer optical design: optimization and simulation** [6342-37]
C. B. Chen, S. C. Fry, Raytheon Co. (USA)

x

- 63422V **A proposal for a photoelastic stress multiplier** [6342-38]
C. Li, Beihang Univ. (China)
- 63422W **Design of a foveated imaging system using a two-axis MEMS mirror** [6342-108]
S. Liu, C. Pansing, H. Hua, College of Optical Sciences, Univ. of Arizona (USA)
- 63422X **Tapered gradient index microlenses for compound lens arrays** [6342-109]
G. R. Schmidt, D. T. Moore, The Institute of Optics, Univ. of Rochester (USA)

PLENARY PAPER

- 63422Y **The past, present, and future of optical design** [6342-111]
W. J. Smith, Rockwell Collins Optronics (USA); E. Betensky, Light Capture, Inc. (Canada);
D. Williamson, Nikon Research Corp. of America (USA); J. C. Miñano, Univ. Politécnica de
Madrid (Spain); R. J. Koshel, Lambda Research Corp. (USA) and College of Optical
Sciences, Univ. of Arizona (USA)

Author Index

Conference Committees

Conference Chairs

G. Groot Gregory, Lambda Research Corporation (USA)
Joseph M. Howard, NASA Goddard Space Flight Center (USA)
R. John Koshel, Lambda Research Corporation (USA) and College of Optical Sciences, University of Arizona (USA)

Program Committee

Geoff Adams, Optical Software, Inc. (United Kingdom)
Miguel Alonso, The Institute of Optics, University of Rochester (USA)
Pablo Benítez, Universidad Politécnica de Madrid (Spain)
Julie L. Bentley, Corning Tropol Corporation (USA)
Florian Bociort, Delft University of Technology (Netherlands)
William J. Cassarly, Optical Research Associates (USA)
Jyh-Long Chern, National Chiao Tung University (Taiwan)
Peter Clark, Flextronics (USA)
Jasmin Cote, Side by Side Optical Engineering (Canada)
Edward English, 3M (USA)
Alexander Epple, Carl Zeiss (Germany)
Stephen Fatone, Optikos (USA)
Leo R. Gardner, Lambda Research Corporation (USA)
John E. Greivenkamp, University of Arizona (USA)
Anurag Gupta, Optical Research Associates (USA)
John Hall, OPTICS 1, Inc. (USA)
Jürgen Jahns, FernUniversität Gesamthochschule in Hagen (Germany)
R. Barry Johnson, Consultant (USA)
Richard C. Juergens, Raytheon Missile Systems (USA)
Tina E. Kidger, Kidger Optics Associates (United Kingdom)
Douglas Kreysar, Radiant Imaging (USA)
Osuk Kwon, Space Imaging (USA)
Jong-Ung Lee, Chongju University (South Korea)
Scott A. Lerner, Hewlett-Packard Company (USA)
Virendra N. Mahajan, The Aerospace Corporation (USA)
Daniel Malacara, Centro de Investigaciones en Óptica, AC (Mexico)
Paul K. Manhart, Consultant (USA)
Jon Maxwell, Cooke Optics Ltd. (United Kingdom)
Juan C. Miñano, Universidad Politécnica de Madrid (Spain)
Kenneth Moore, ZEMAX Development Corporation (USA)
Pantazis Mouroulis, Jet Propulsion Laboratory (USA)
Hiroshi Ooki, Nikon Corporation (Japan)
Richard Pfisterer, Photon Engineering (USA)
Andrew Rakich, EOS (Australia)
Harald Ries, OEC (Germany)

John R. Rogers, Optical Research Associates (USA)
Jannick P. Rolland, CREOL, College of Optics and Photonics, University of Central Florida (USA)
Jose M. Sasian, University of Arizona (USA)
Vesselin Shaoulov, CREOL, University of Central Florida (USA)
Narkis Shatz, Sciences Applications International Corporation (USA)
Colin Sheppard, National University of Singapore (Singapore)
Bryan D. Stone, Optical Research Associates (USA)
Akiyoshi Suzuki, Canon Inc. (Japan)
Kimio Tatsuno, Hitachi (Japan)
Thomas Thoeniss, Linos Photonics GmbH (Germany)
Kevin P. Thompson, Optical Research Associates (USA)
Mary Turner, Breault Research Organization (USA)
Wilhelm Ulrich, Carl Zeiss (Germany)
John Van Derlofske, Rensselaer Polytechnic Institute (USA)
Wolfgang Vollrath, Vistec Semiconductor Systems GmbH (Germany)
Yongtian Wang, Beijing Institute of Technology (China)
David M. Williamson, Nikon Research Corporation (USA)
Roland Winston, University of California at Merced (USA)
Andrew Wood, Thales Optics Ltd. (United Kingdom)
Kimiaki Yamamoto, Olympus Advanced Technical Research Center (Japan)
Richard N. Youngworth, Ball Aerospace & Technologies Corporation (USA)

Lens Design Problem Committee

Julie L. Bentley, Corning Tropel Corporation (USA)
R. Barry Johnson, Consultant (USA)
Richard C. Juergens, Raytheon Missile Systems (USA)
Scott A. Lerner, Hewlett-Packard Company (USA)
Paul K. Manhart, Consultant (USA)
Andrew Rakich, EOS (Australia)
Wilhelm Ulrich, Carl Zeiss (Germany)
Wolfgang Vollrath, Vistec Semiconductor Systems GmbH (Germany)
Yongtian Wang, Beijing Institute of Technology (China)
David M. Williamson, Nikon Research Corporation (USA)
Richard N. Youngworth, Ball Aerospace & Technologies Corporation (USA)

Illumination Problem Committee

Miguel Alonso, The Institute of Optics, University of Rochester (USA)
Pablo Benítez, Universidad Politécnica de Madrid (Spain)
Jyh-Long Chern, National Chiao Tung University (Taiwan)
Anurag Gupta, Optical Research Associates (USA)
Vesselin Shaoulov, CREOL, University of Central Florida (USA)
Narkis Shatz, Sciences Applications International Corporation (USA)
John Van Derlofske, Rensselaer Polytechnic Institute (USA)

Session Chairs

IODC Overview

G. Groot Gregory, Lambda Research Corporation (USA)

Aberration Theory

Virendra N. Mahajan, The Aerospace Corporation (USA)

Medical Optics

Alexander Epple, Carl Zeiss (Germany)

Ray Tracing and Optimization

Scott A. Lerner, Hewlett-Packard Company (USA)

Lightpipes

Jasmin Cote, Side by Side Optical Engineering (Canada)

Displays

William J. Cassarly, Optical Research Associates (USA)

Illumination Design and Source Modeling

R. John Koshel, Lambda Research Corporation (USA) and College of Optical Sciences, University of Arizona (USA)

Diffraction Optics

R. Barry Johnson, Consultant (USA)

Optics for Digital Systems

Kevin P. Thompson, Optical Research Associates (USA)

Telescopes and Space Optics

Paul K. Manhart, Consultant (USA)

Infrared and Lithographic Design Systems

Jose M. Sasian, University of Arizona (USA)

IODC Problem Session

G. Groot Gregory, Lambda Research Corporation (USA)

Interferometry and Testing

Alexander Sohn, North Carolina State University (USA)

Design for Fabrication

Richard N. Youngworth, Ball Aerospace & Technologies Corporation (USA)

Introduction

Many changes have occurred in the four years since the previous IODC: new technologies, new fields of application, and new faces in the design community. Unfortunately, we have also lost some of the people that have made the field exciting and rich with history, and who have set a standard with which we can only hope to maintain. These individuals are:

- W. Lewis Hyde,
- Hilda and Rudolf Kingslake,
- Walter Mandler,
- James Gilbert Baker, and
- Frank Cooke.

These proceedings are dedicated to them.

IODC 2006 took place at the Sheraton Wall Centre in Vancouver, British Columbia, Canada during the week of 4–8 June. By all indications it was a rousing success. The IODC has a rich history, starting in 1905 in London, England (see Kevin Thompson's paper about the roots of the IODC conference), and has met for the past few decades every four years. Past meeting locations have been:

- 1986: Cherry Hill, New Jersey, USA
- 1990: Monterey, California, USA
- 1994: Rochester, New York, USA
- 1998: Kona, Hawaii, USA
- 2002: Tucson, Arizona, USA
- 2006: Vancouver, British Columbia, Canada.

This history shows that the meeting has been held in Western North America for the last three events, thus it is expected that the meeting will follow a route to the East for the 2010 conference. Also, note that only this year's conference has ventured outside the United States, albeit just across the border for the first time in many years.

IODC 2006 was managed by the Optical Society of America (OSA), and was sponsored by both OSA and SPIE—The International Society for Optical Engineering. New this year was the addition of the American Society of Precision Engineers (ASPE) as a technical cosponsor. Two U.S. government sponsors supplied funding support for travel: the Defense Advanced Research Projects Agency (DARPA) and the Air Force Office of Scientific Research (AFOSR). Three companies sponsored conferences events during the week: Coastal Optics (Monday morning coffee break and Session ThB: Design for Fabrication), Optical Research Associates (registration bags, Tuesday morning coffee break, Session

TuA: Ray Tracing and Optimization, and Session TuD: Illumination Design and Source Modeling), and Lambda Research Corporation (Illumination and Lens Design Awards Event). Finally, 10 companies exhibited at the conference: Kreischer Optics, Ltd., Lambda Research Corporation, Optical Perspectives Group, LLC, Optical Research Associates, Optimax Systems Inc., OPTIS North America, Photon Engineering LLC, Photonics Spectra, Schott North America – Optics for Devices, and ZEMAX Development Corporation.

Attendance and participation at IODC is growing. We had 267 registered attendees and 20 guests, which is a 25% improvement over the 2002 IODC. Notably, this increase in attendance is quite encouraging since in 2002 IODC was co-located with the Diffractive Optics and Micro Optics and Optics Fabrication and Testing meetings. The conference accepted 70 oral, 26 poster, and 2 post-deadline poster presentations, and there were 13 invited speakers. Like the attendance, the number of contributed papers presented was also up over 25% compared to 2002.

Every day was filled with oral presentations, and each evening included a special event on the three full days of the conference. The plenary session kicked off the conference, and was entitled, "The past, present, and future of optical design." It featured four imminent speakers ranging across the many subfields of optical design:

- Warren Smith: Discussion of lens designs from the past,
- Ellis Betensky: The design of zoom lenses,
- David Williamson: The state of lithographic systems, and
- Juan Miñano: Nonimaging and illumination optics designs.

The plenary session was transcribed and is included in these proceedings along with graphics from the four presentations; please see the last paper of the volume. The sessions following the plenary on the Monday of the conference were an overview and history of optical design, aberration theory, and medical optics. Monday evening was dedicated to the poster session. Tuesday was geared to the ever-growing illumination design subfield. The sessions for the day were ray tracing and optimization, lightpipes, displays, and illumination design and source modeling. The day ended with a relaxing reception held in the hotel's outdoor patio area. Wednesday had sessions devoted to diffractive optics, optics for digital systems, telescopes and space optics, and infrared and lithographic design and systems. The Wednesday evening event was a presentation of the Illumination and Lens Design Awards, which is described in more detail below. Thursday was the last day of the conference, and it included a half day of oral sessions dedicated to interferometry and testing and design for fabrication. While each of the days were very busy, the coffee breaks, special evening events, and lunch breaks provided enough time to unwind or even continue the discussions of the previous sessions.

As in previous IODCs, the design problem presentation proved to be the focal point of the meeting. This year the event was expanded by offering the first Illumination Design Problem in conjunction with the traditional Lens Design Problem. The awards event started with David M. Williamson presenting the 2006 Michael Kidger Memorial Scholarship to Blair L. Unger, a graduate student at The Institute of Optics, University of Rochester under the supervision of Prof. Duncan Moore. Additionally, Blair is conducting a portion of his work at NASA under the supervision of Joseph Howard. His submission entitled, "Optical design of astronomical spectrographic systems," won him the award, which recognizes "a person with outstanding talents in optical design during the very early phases of their career." Next, Pablo Benítez provided the results for the first illumination design problem, called "Illuminating the Red Cross." In its first year, William Cassarly (Optical Research Associates) won the prize. Following this presentation, Rick Juergens presented the lens design problem, called "The lens shuffler," which was won for the first time by Akira Yabe (consultant in Germany). Both of the lens design problems are presented in papers included in these proceedings. Additionally, the cover of this Proceedings volume shows the winning solutions from the two design contests.

We the chairs want to express our thanks to the many people, groups, and companies that made IODC 2006 a success. First, we thank the authors and attendees that made the conference such a success. The engaging papers and questions made for a great week of technical presentations. Second, we thank the sponsors and companies who committed to IODC, which includes the OSA, SPIE, ASPE, DARPA, AFOSR, Michael Kidger Memorial Scholarship Committee, and the companies that exhibited or sponsored events. Finally, IODC 2006 would not have run smoothly without the assistance of the conference staff and the Sheraton Wall Centre personnel. We especially want to thank:

- Kristin Mirabal (OSA) – Meeting Manager,
- Heather Schoch (OSA) – Meeting Coordinator,
- Brian Hanrahan (OSA) – Technical Editor,
- Cathryn Wanders (OSA) – Exhibit Coordinator,
- Lori Paulette (OSA) – Sponsorship Coordinator, and
- the SPIE staff.

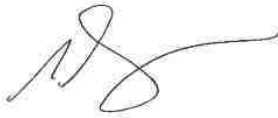
Without their help our jobs would have been a lot harder.

Finally, what is planned for IODC 2010? We anticipate the conference to head East, and the location expected to be selected by the end of 2006. We anticipate the conference to take a more International flavor in future years since a large portion of the attendees do come from non-U.S. locations, but that has to be weighed against the majority coming from the U.S. The continued growth of illumination design content at IODC will continue, and we anticipate additional content from potential partnering societies to enrich the future of IODC. If you have suggestions, would like to assist with the development of IODC 2010, or

have other questions, do not hesitate to use the IODC archival website at www.iodc.info.

It was a pleasure working on IODC 2006, and we look forward to seeing you in 2010!

Sincerely,



G. Groot Gregory



Joseph M. Howard



R. John Koshel

xx

Author Index

Ade, P.A. R., 1O
An, Hyun Kyoung, 1L
Arasa, Josep, 0A, 0K
Ashdown, Ian, 15
Asselin, Daniel, 1Y
Avino, S., 29
Bareau, Jane, 1F
Bastien, Pierre, 1O
Benítez, Pablo, 0R, 13, 14, 1V
Bentley, Julie L., 0G
Bergeler, S., 1A
Berlioz, Philippe, 1Y
Bernier, Sophie, 1O
Betensky, Ellis, 2Y
Bissonnette, Eric, 1O
Blen, José, 14
Bociort, Florian, 0L
Bosch, Salvador, 1H
Burge, Jim, 1X
Cakmakci, Ozan, 0W
Calloni, E., 29
Cao, Qing, 19
Capelle, Gene A., 20
Cassarly, William J., 0Q, 0T
Castro-Ramos, J., 2H, 2J
Celeste, John R., 20
Celliers, Peter M., 20
Chang, Chir-Weei, 28
Chang, Chuan-Chung, 28
Chang, Jun, 1Q, 2B
Chao, Wei-Chung, 28
Chaves, Julio, 0R, 14
Cheben, Pavel, 2C
Chen, Chungte Bill, 2U
Cheng, Chen-Chin, 28
Cheng, Chieh-Jen, 2F
Cheng, Dewen, 2B
Cheng, Xuemin, 24
Chern, Jyh-Long, 0S, 2F, 2G
Chien, Yu-Han, 1I
Chipman, Russell A., 0C
Chu, Shu-Chun, 0S
Cifuentes, A., 0K
Clark, Peter P., 1F
Cobb, Joshua M., 0V
Costa, Marco, 0F
Cowan, William D., 07
Crabtree, Karlton, 0C
Curatu, Costin, 0X
Cvetković, Aleksandra, 0R, 13
Danner, Lambert, 0E
Davenport, Thomas L. R., 0Q, 0T
de la Fuente, Marta C., 1C, 1H
Deng, Liqun, 0I
De Rosa, R., 29
Díaz, José A., 0A, 2E
Di Fiore, L., 29
Doyon, René, 1M
Dross, Oliver, 0R
Epple, Alexander, 1R, 1S
Euteneuer, Peter, 0E
Ewald, H., 1A
Falicoff, Waqidi, 14
Fang, Yi Chin, 0Z, 1I
Feldmann, H., 1S
Ferré-Borrull, Josep, 1H
Frogget, Brent C., 20
Fry, Stephen C., 2U
Fukami, Kiyoshi, 0Y
García, Fernando, 14
García-Liévanos, O., 2H, 2J
Gauvin, Jonny, 1Y
Gillen, Glen D., 0B
Glazowski, Chris, 0G
Gong, Haiqing, 0I
Grabovickic, Dejan, 14
Guha, Shekhar, 0B
Guyton, Robert L., 20
Hall, T. J., 18
Hanning, T., 26
Hanrahan, Pat, 1E
Harnisch, Bernd, 1Y
Hernández-Cruz, J. A., 2H, 2J
Herrera Vázquez, Joel, 2N
Hesselink, Lambertus, 1B
Hintermann, D., 26
Hoffman, Jeffrey M., 1P
Hoppen, Gerhard, 0E
Hörsch, Ingolf, 0J
Horton, Richard F., 2I
Hu, Chao-Chang, 1I
Hua, Hong, 0X, 2W
Huang, Shih-Ming, 17
Huang, Yanqiao, 0D
Ilegbusi, Olusegun, 0F
Isshiki, Masaki, 0N
Jeffs, Mark, 10
Johnson, Eric G., 0F
Johnson, R. Barry, 27
Jonas, Reginald P., 02
Juergens, Richard C., 1U
Kaneko, Seichi, 0N
Kaufman, Morris I., 20
Koehler, Chuck, 0F
Kohnno, Michio, 0Y
Koshel, R. John, 0P, 2Y

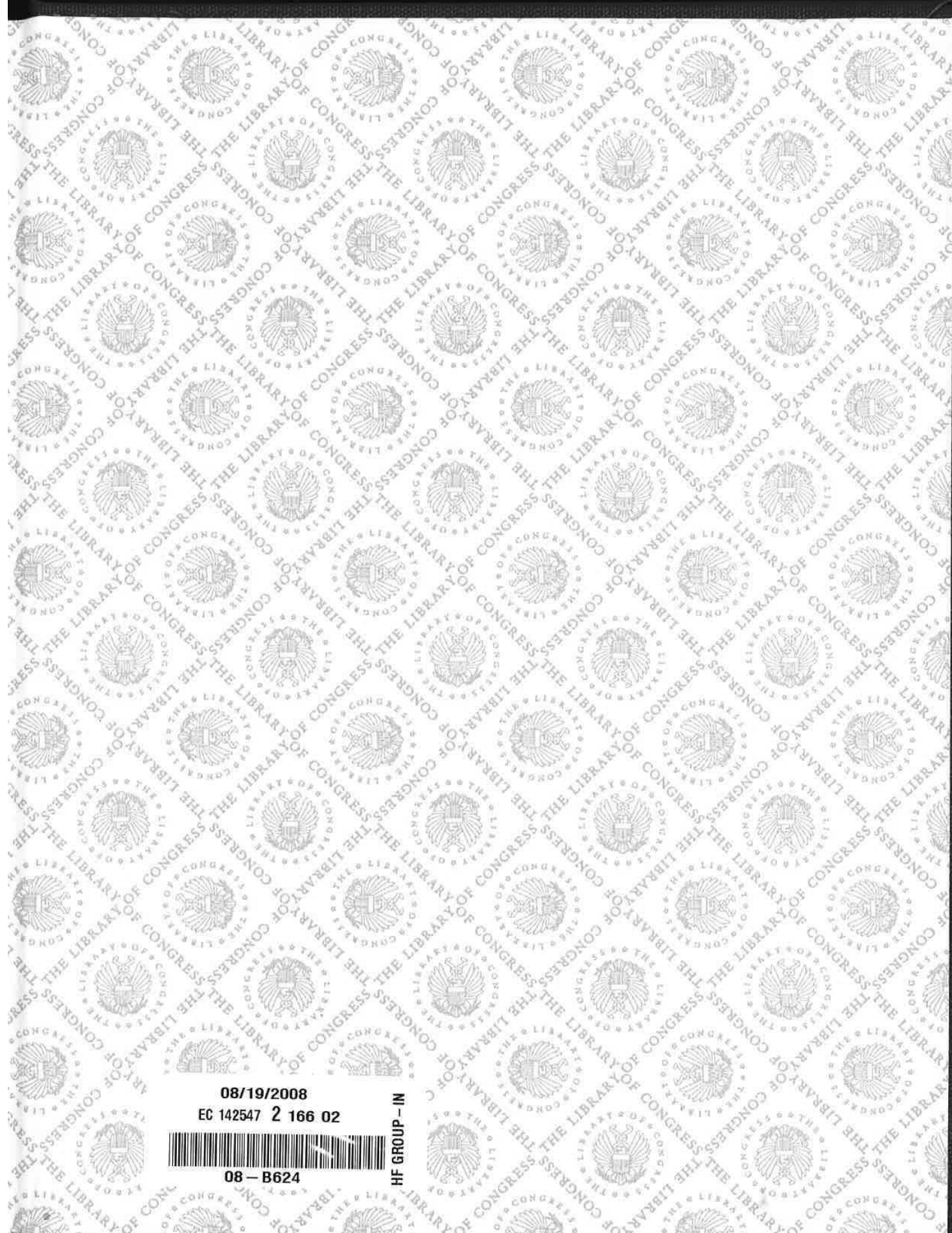
Krambeer, H., 1A
Kudaev, Sergey, 12
Kwok, Harry, 2O
Lavigne, Jean-François, 1M
Leclerc, Mélanie R., 1O
Lee, Kye-Sung, 0F
Lee, Tony L., 2O
Lee, Tsung-Xian, 17
Lee, Ya-Luan, 17
Li, Changsheng, 2K, 2V
Lin, Wei Teng, 0Z
Lingwood, David, 1O
Liu, Sheng, 2W
Ma, Shih-Hsin, 17
MacGowan, Brian J., 3O
Malone, Robert M., 2O
Manhart, Paul K., 1U
Marinescu, Oana, 0L
Marteau, Daniel, 1Z
Matsuyama, Tomoyuki, 2D
McGuire, James P., Jr., 0O
Milano, L., 29
Miñano, Juan C., 0R, 14, 2Y
Mohedano, Rubén, 0R
Moore, Duncan T., 0D, 2X
Moore, Kenneth, 0J
Moreno, Ivan, 16
Mossman, Michele A., 0U
Mulder, R. S., 2Q
Murali, Supraja, 0H
Ng, Edmund W., 2O
Ng, Ren, 1E
Nicholson, Mark, 0J
Ohmura, Yasuhiro, 1T
Oliker, Vladimir, 1I
Oranchak, Adam, 0W
Pansing, Craig, 2W
Parks, Robert E., 04
Parkyn, Bill, 14
Pausch, Armin, 0E
Petitrenaud, Sébastien, 1Z
Pijitrojana, W., 18
Piombini, Hervé, 1Z
Pisano, Giampaolo, 1O
Pitalo, Stephen K., 1L
Pizarro, Carles, 0A, 0K, 2E
Powell, Ian, 2C
Ramalingam, Naveen, 0I
Ramsey, J. L., 18
Rayces, Juan L., 24
Reinbachs, Imants P., 2O
Restaino, S. R., 29
Rich, Tim, 2S
Richardson, Eric Harvey, 1N
Robinson, M. Dirk, 1G
Robinson, Ronald B., 2O
Rodgers, J. Michael, 1J, 1P
Rogers, John R., 0M
Rolland, Jannick P., 0F, 0H, 0W, 0X
Rostalski, H.-J., 1S

Sabary, Frédéric, 1Z
Salsbury, Marc, 15
Sanson, Mark C., 05, 23
Santamaría, Asunción, 14
Sasian, Jose M., 08, 1X
Savini, Giorgio, 1O
Schmidt, Greg R., 2X
Schoene, R., 26
Schreiber, Peter, 12
Seppala, Lynn G., 2O
Sharma, Pratibha, 2O
Sinclair, Douglas C., 0N
Sivakumar, N. R., 1W
Smith, Warren J., 2Y
Spahn, Olga B., 07
Spencer, Harvey M., 1P
Sprowl, Robert A., 1X
Stork, David G., 1G
Su, Han-Wei, 1I
Su, Peng, 1X
Sun, Ching-Cherng, 17
Sure, Thomas, 0E
Suzuki, Akiyoshi, 0Y
Sweatt, William C., 07
Takashima, Yuzuru, 1B
Talha, M. M., 1Q, 2B
Tan, B., 1W
Tan, Yin, 0I
Teuma, Eric Valaski, 0F
Thibault, Simon, 1D, 1M
Thompson, Kevin P., 0I
Thorpe, Michael D., 02
Tienvieri, C. Theodore, 23, 2S
Tierno, A., 29
Topart, Patrice, 1Y
Tsai, Hsien Lin, 0Z, 1I
Tsao, Chao-Hsi, 2G
Tudela, Raul, 1H
Tunnell, Thomas W., 2O
Ujike, Tomoko, 2D
VanKerkhove, Steven, 23
Vázquez y Montiel, Sergio, 2H, 2J, 2N
Venkatakishnan, K., 1W
Voarino, Philippe, 1Z
Vollrath, Wolfgang, 0E
Wang, Chy-Lin, 28
Wang, Min, 1M, 1Y
Wang, Qinghui, 0I
Wang, Yongtian, 1Q, 2B
Watanabe, Shu, 0Y
Watts, Phillip W., 2O
Weng, Zhicheng, 1Q
Whitehead, Lorne A., 0U
Wick, David V., 07
Williamson, David M., 2Y
Winston, Roland, 13
Wormell, Prudence M. J. H., 06
Wu, Wen-Yi, 1I
Wu, Yi-Ling, 28
Xie, Huikai, 0F

Yabe, Akira, 25
Yang, Haoming, 1Q
Yoshioka, Hitoshi, 0Y
Youngworth, Richard N., 03
Zavislan, James M., 0G
Zhang, Tingcheng, 1Q
Zhao, Chunyu, 09

LC COPYRIGHT
0 022 804 561 5

ISBN 0-8194-6427-9
ISSN 0277-786X



08/19/2008

EC 142547 2 166 02



08 - B624

HF GROUP - IN

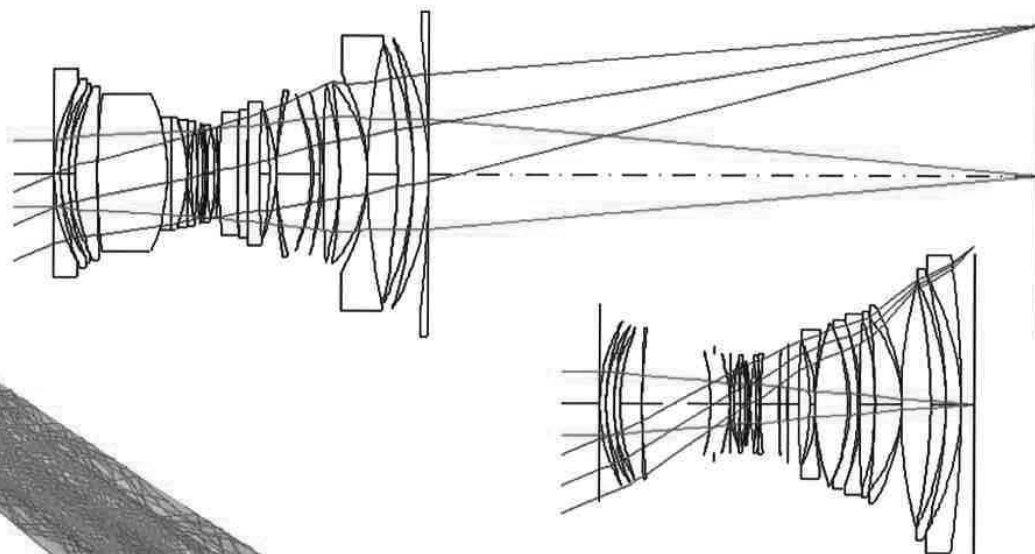
INTERNATIONAL OPTICAL DESIGN CONFERENCE

TS 510
.I55
2006
Pt 1
Copy 2



TS 510
.155
2006
pt. 2
Copy 2

International Optical Design Conference 2006



4-8 June 2006
Vancouver, British Columbia
Canada

G. Groot Gregory
Joseph M. Howard
R. John Koshel
Chairs/Editors

SPIE Volume 6342
Part Two of Two Parts

International Optical Design Conference 2006

**G. Groot Gregory
Joseph M. Howard
R. John Koshel**
Chairs/Editors

**4-8 June 2006
Vancouver, British Columbia, Canada**

Sponsored and Published by
OSA—Optical Society of America
SPE—The International Society for Optical Engineering

Technical Cosponsor
American Society for Precision Engineering

**SPIE Volume 6342
Part Two of Two Parts**



The papers included in this volume were part of the technical conference cited on the cover and title page. Papers were selected and subject to review by the editors and conference program committee. Some conference presentations may not be available for publication. The papers published in these proceedings reflect the work and thoughts of the authors and are published herein as submitted. The publisher is not responsible for the validity of the information or for any outcomes resulting from reliance thereon.

e-First Publication for Proceedings: As of July 2005, papers in the Proceedings of SPIE are first published electronically in the SPIE Digital Library (www.spiedl.org), and subsequently in print and CD-ROM.

Pagination system: The new citation format uses six-digit article identifier numbers (CIDs). Utilization of article CIDs allows proceedings articles to be fully citable as soon as they are published online, using the same identifier for both online and print versions.

The structure of the six-digit article CID number for Proceedings of SPIE is:

- The first four digits indicate the SPIE volume number.
- The last two digits indicate publication order within the volume using a Base 36 numbering system employing both numerals and letters. The CID number appears on each page, followed by the page number within the actual article.

Please use the following format to cite material from this book:

Author(s), "Title of Paper," in *International Optical Design Conference 2006*, edited by G. Groot Gregory, Joseph M. Howard, R. John Koshel, Proceedings of SPIE-OSA, SPIE Vol. 6342, Article CID Number (2006).

ISSN 0277-786X
ISBN 0-8194-6427-9

Copublished by
OSA—Optical Society of America
2010 Massachusetts Ave., N.W., D.C., 20036 USA
Telephone 1 202/223-8130 (Eastern Time) • Fax 1 202/223-1096
<http://www.osa.org>

and
SPIE—The International Society for Optical Engineering
P.O. Box 10, Bellingham, Washington 98227-0010 USA
Telephone 1 360/676-3290 (Pacific Time) • Fax 1 360/647-1445
<http://www.spie.org>

Copyright © 2006, Optical Society of America and The Society of Photo-Optical Instrumentation Engineers

Copying of material in this book for internal or personal use, or for the internal or personal use of specific clients, beyond the fair use provisions granted by the U.S. Copyright Law is authorized by OSA and SPIE subject to payment of copying fees. The Transactional Reporting Service base fee for this volume is \$15.00 per article (or portion thereof), which should be paid directly to the Copyright Clearance Center (CCC), 222 Rosewood Drive, Danvers, MA 01923. Payment may also be made electronically through CCC Online at <http://www.copyright.com>. Other copying for republication, resale, advertising or promotion, or any form of systematic or multiple reproduction of any material in this book is prohibited except with permission in writing from the publisher. The CCC fee code is 0277-786X/06/\$15.00.

Printed in the United States of America.

Contents

Part One

xiii	<i>Conference Committees</i>
xvii	<i>Introduction</i>
xxi	<i>Tribute to W. Lewis Hyde</i>
xxiii	<i>Tribute to Hilda and Rudolf Kingslake</i>
xxvii	<i>Tribute to Walter Mandler</i>
xxix	<i>Tribute to James Gilbert Baker</i>
xxxiii	<i>Tribute to Frank Cooke</i>

IODC OVERVIEW

634201	The first optical convention (in English): the 1905 Optical Convention in London, England [6342-05] K. P. Thompson, Optical Research Associates (USA)
634202	Double Gauss lens design: a review of some classics [6342-06] R. P. Jonas, M. D. Thorpe, ELCAN Optical Technologies (Canada)
634203	Twenty-first century optical tolerancing: a look at the past and improvements for the future (Invited Paper) [6342-07] R. N. Youngworth, Ball Aerospace & Technologies Corp. (USA)
634204	Alignment of optical systems (Invited Paper) [6342-08] R. E. Parks, Optical Perspectives Group, LLC (USA)
634205	Use of an application programming interface (API) to allow non-optical designers to perform specific optical evaluations [6342-09] M. C. Sanson, Corning Tropel Corp. (USA)
634206	The current state of the international standard for exchange of optical data in electronic form [6342-10] P. M. J. H. Wormell, Imperial College London (United Kingdom)

ABERRATION THEORY

634207	Wavefront correction using micromirror arrays: comparing the efficacy of tip-tilt-piston and piston-only micromirror arrays [6342-11] W. C. Sweatt, O. B. Spahn, W. D. Cowan, D. V. Wick, Sandia National Labs. (USA)
634208	Interpretation of pupil aberrations in imaging systems [6342-12] J. Sasian, College of Optical Sciences, Univ. of Arizona (USA)
634209	General sine condition for plane-symmetric imaging systems and some example aplanatic designs [6342-13] C. Zhao, College of Optical Sciences, Univ. of Arizona (USA)

The Optics of Miniature Digital Camera Modules

Jane Bateau and Peter P. Clark

Flextronics Optical Technology Center, 1 Upland Road, Norwood, MA, USA 02062

ABSTRACT

Designing lenses for cell phone cameras is different from designing for traditional imaging systems; the format poses unique challenges. Most of the difficulty stems from the scale of the system, which is based on the size of the sensor.

Keywords: Optical design, lens design, digital cameras

1. INTRODUCTION

The scale of cell phone camera systems creates particular challenges for the lens designer that are unique to this format. Both the size and the low-cost requirements have many implications for the design, fabrication and assembly processes.



Fig.1: This 3.6 μ m pixel VGA camera module is 6.05 x 6.05 x 4.5 mm.
The most critical dimension is the 4.5 mm axial length.

For those of us who have been involved in the design and manufacturing of consumer and commercial imaging systems using lens elements with diameters in the 12–40mm range, the switch to much smaller elements with diameters in the 3–5mm range takes some adjustment. When designing a camera module lens, it is not always helpful to begin with a traditional larger-scale imaging lens. Scaling down such a lens will result in a system that is unmanufacturable. If the design includes molded plastic optics, a scaled down system will result in element edge thicknesses shrinking to the point where the flow of plastic is affected. For glass elements, the edge thicknesses will become too thin to be fabricated without chipping. To achieve a successful design we have to modify our lens forms and adjust the proportions of the elements.

Layout drawings can be very misleading. Many times we find ourselves surprised when the mechanical layout of a lens barrel that looked reasonable on paper turns out to be very difficult or impossible to fabricate. Tabs on a barrel that appear substantial in a drawing, are found to be too flimsy to function on the actual part, “sharp” edges on molded stops don’t fill completely because the features are too small. The size of the lenses and mechanical details on the flanges and barrels affect all aspects of the manufacturing process. Diamond tools have to be redesigned to be able to generate large changes in angle over small areas. Handling the lenses becomes difficult even with tweezers, all inspection and screening has to be done with a microscope. Measuring basic dimensions and the surfaces of the lenses becomes very challenging. Center thickness and surface decenter measurements in particular are difficult at the high levels of accuracy required for current designs. The ability to fabricate accurate and robust fixtures for measurement of individual elements has become absolutely critical.

International Optical Design Conference 2006, edited by G. Groot Gregory,
Joseph M. Howard, R. John Koshel, SPIE Vol. 6342, 63421F,
© 2006 SPIE-OSA · 0277-786X/06/\$15 · doi: 10.1117/12.692291

SPIE-OSA/ Vol. 6342 63421F-1

Another process that has been affected is assembly. Assembly must be done in clean conditions, with visual aids to ensure proper lens orientation and seating. Once an assembly is complete it needs to be tested. Testing assemblies with barrel outer dimensions of 6mm pose similar fixturing challenges as those in the fixturing of individual elements, with the additional requirement that they must be aligned with a test target for MTF or resolution testing. This target or series of targets must provide adequate sampling over an area representing the sensor, to characterize the lens, which could be anywhere from 1/10" diagonal to 1/3" diagonal. Fixturing for both MTF testing and resolution testing must minimize tilt of the lens barrel with respect to the target.

2. CMOS Focal Planes

Development of sensors has been moving steadily towards smaller pixels and higher density formats. The initial cell phone cameras were based around VGA and QVGA modules with 5.6um pixels. Generally formats were between 1/7" and 1/4" in size. Next, the sensor manufacturers began offering VGA and SXGA sensors with 3.2-3.8um pixels in 1/6-1/4" formats. Then the sensors moved to 2.8um pixels offered in VGA, 1.3MP and 2MP, 1/8", 1/4" and 1/3" formats respectively, a full 50% reduction in pixel size from the original sensors. Today we are designing for 2-3MP sensors in 2.2um pixels, 1/4" and 1/3" formats, and there are plans for 5MP sensors with 1.75um(!) pixels coming soon.

Over the past couple of years, pixel areas have been reduced by 75%, then 85%, soon to be 90%, compared with 5.6 micron pixels. Lower pixel count formats (VGA and 1.3mp) have gotten correspondingly smaller, and higher resolution sensors (2mp and 3mp) have been introduced. The higher resolution formats have made the job of the lens designer extremely challenging because, while the basic imaging problem has remained the same, each reduction in pixel size has required an increase in lens performance, and the overall length of the system is often required to be shorter. VGA systems pose different, but no less daunting problems. VGA sensors have scaled with the pixel size from 1/4" with the original 5.6um pixels to the current 1/11" format based on a 2.2um pixel. As the pixels have shrunk, the lenses for VGA systems have become so small that contamination is now a major issue and the scratch/dig requirements for each lens surface are very tight making the lenses very difficult to manufacture.

3. The Problem of Scale



Fig.2: 3-element lens, disassembled. Barrel, three plastic aspheric lenses, thin sheet aperture stop and baffle.

It is interesting to consider the differences between these miniature camera module lenses and lenses for conventional photography, such as the 35 mm format. The goal is the same: Produce pleasing images of snapshot quality. However, the scale of the optical system is reduced by roughly a factor of ten!

	<u>35 mm point and shoot</u>	<u>35 mm single use</u>	<u>¼" CMOS</u>
Film format diagonals:	43 mm	43 mm	4.4 mm
Lens EFL:	37.5 mm	37.5 mm	3.8 mm
f/number:	2.8, variable	11, fixed	2.8, fixed
Entrance pupil diam:	13.4 mm	3.4 mm	1.36 mm
Spatial frequencies:	10 – 40 /mm	10 – 20 /mm	50 – 100 /mm
Cost:	\$10 (est.)	\$0.50 (est.)	\$1 (est.)

If we were able to simply scale the 35 mm lens design by 1/10x, we would encounter a few issues:

- 1) Smaller entrance pupil: Depth of field will be much greater, but diffraction will limit performance sooner than with larger formats.
- 2) Surface figure tolerances: Figure tolerances (fringes of irregularity, for example) will be somewhat tighter, because spatial frequencies of interest are higher, but because the surfaces are smaller, they will be easier to achieve in practice.
- 3) Geometric tolerances: Scaling the system's size requires linear tolerances to scale as well. So center thickness tolerances and surface and element decenter tolerances will be tighter by a factor of ten. This proves to be the greatest challenge of producing these lenses.
- 4) Angular tolerances: Lens tilt tolerances do not scale down, but small defects on flanges or mounting surfaces will have a larger effect on tilt.
- 5) Stray light considerations: An aperture or baffle feature that has an acceptably small dimension at the large scale should be scaled down by 1/10. However, some parts cannot be made thin enough, or they may become translucent, so they will cause a larger fraction of the light to scatter from their edges, resulting in flare or veiling glare.
- 6) Scratch/Dig and Contamination: The smaller system is much more sensitive to defects and contamination causing shadowing on the image. Acceptable defect dimensions scale with the format size, and the situation is often worse in practice, because the back focal distance is very short and defects close to the image are more visible.

4. Specifications

The following are typical lens specifications for a ¼" sensor format:

FOV	60 degrees
Image Circle	4.6 mm diam.
TTL	5.0mm
f/no	f/2.8
Distortion	<2%
Chief Ray Angle	<22 degrees
Relative Illumination	>50%

FOV - The field of view for these systems is typically 60 to 66 degrees across the sensor diagonal, but the design must include a slightly larger angle to allow for correction over the image circle.

Image Circle - This is the diameter of the image over which the lens has to be well corrected to allow for lateral displacement of the sensor relative to the optical axis. Lens to sensor centration errors are caused mostly by uncertainty in the placement of the sensor on its circuit board. To allow for those errors, the lens image circle is increased by at least 0.2 mm. As sensors get smaller sensor placement accuracy must improve.

TTL- The total track length is the distance from the front of the barrel to the image plane, this has to be longer than the optical track length by at least 0.050mm in order to protect the front of the lens. This is extremely important to the cell phone designers because of the market pressure to produce thinner phones.

f/number – Although most camera module customers specify $f/2.8$, it is not uncommon to see lenses at $f/3.0$ and $f/3.3$ when the increased f no has a significant effect on performance or manufacturability. However, smaller pixel sensors have less light gathering capability and will suffer at slower f /numbers.

Distortion – The usual distortion requirement is $<2\%$ optical distortion or $<1\%$ TV distortion. Although this sounds like a much more stringent requirement than the 4% typically allowed in traditional 35mm camera lenses, the distortion curve can vary significantly from assembly to assembly due to build tolerances. In fact the approximate effect of tolerances is to add positive or negative slope to the nominal distortion curve.

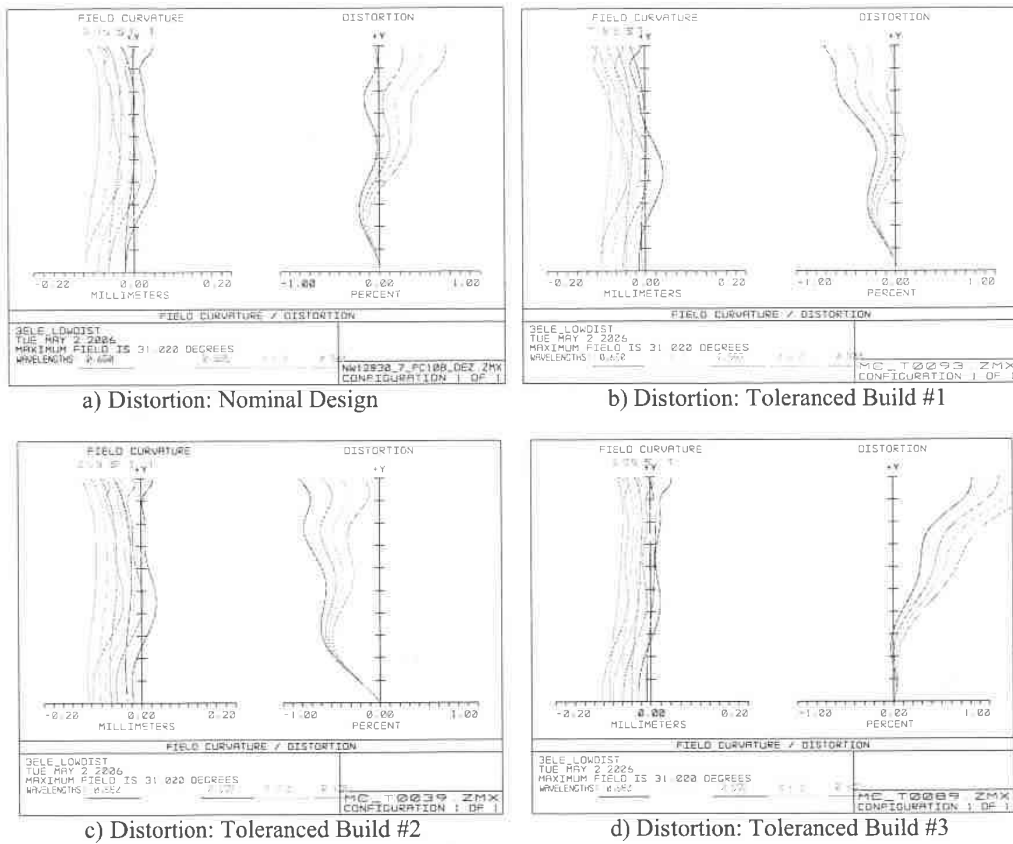
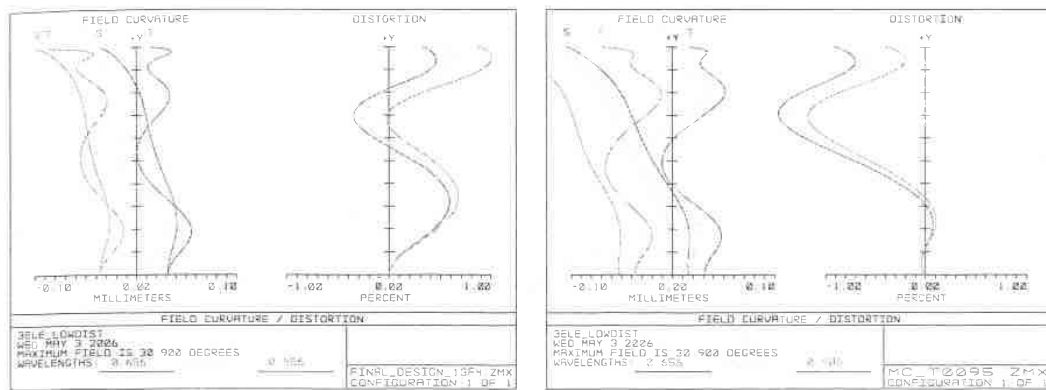


Fig.3: a) Nominal design distortion curve, b) Distortion curve for a simulated toleranced build, displaying moderate tilt, c) Another sample of a simulated build with induced tilt in the distortion curve, d) Distortion curve representing the simulated build with the maximum amount of tilt generated for this design.

As demonstrated in fig.3, a nominal design with distortion $<0.3\%$ can easily generate distortion $>1\%$ when fabricated. An even more critical factor in ensuring good performance is to limit the slope and rate of change of slope of the distortion curve. The added tilt due to tolerances applied to a fast changing distortion curve can result in extremely steep slopes that are objectionable in an image.



a) Distortion: Nominal Design

b) Distortion: Toleranced Build

Fig.4: a) Nominal design distortion is low in magnitude but fast changing over the field, b) Distortion curve for simulated build displaying unacceptable tilt and variation in slope as a result of build tolerances.

Even though absolute distortion values may be low, large changes in slope over a small area will be noticeable in an image. For this reason it is important to control both the shape and the magnitude of the distortion curve.

Chief Ray Angle (CRA)– The CRA is the incidence angle of the chief ray at the image plane for any field point. The CRA is usually specified as a maximum value that cannot be exceeded anywhere in the field. Most camera module lens CRA curves increase monotonically with field to a maximum value and then drop off at the edge of the image, because of pupil aberrations. See fig.5.

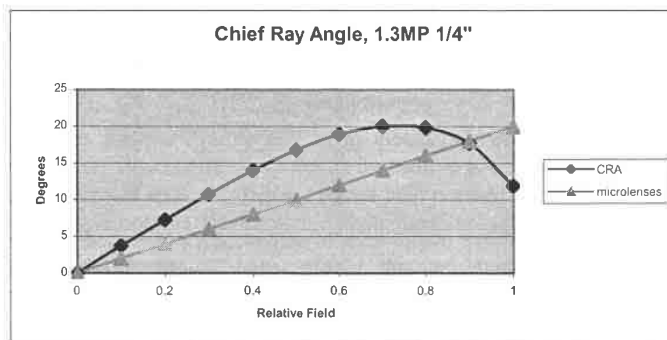


Fig.5: Chief Ray Angle and Microlens Optimum Acceptance Angle as a Function of Relative Field

To better illustrate the source of this requirement, let's first take a closer look at the structure of the focal plane. The CMOS sensor array is an array of sensors with color filters integrated, to produce the standard Bayer pattern of red, green and blue detectors:

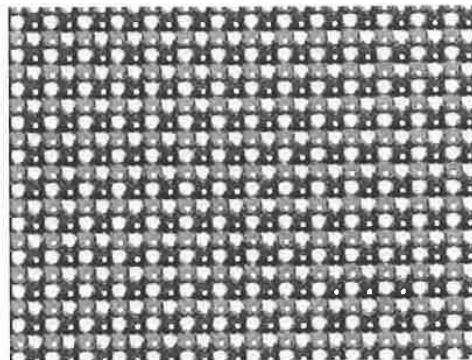


Fig.6: Photomicrograph of a portion of a Bayer pattern sensor. 2.8um pixels.
Note the specular highlights from microlens surfaces.

The surface of the detectors is not uniformly sensitive, though. Circuitry integrated with the sensor reduces the active area significantly. To improve sensitivity, an array of microlenses is applied to the top of the sensor:

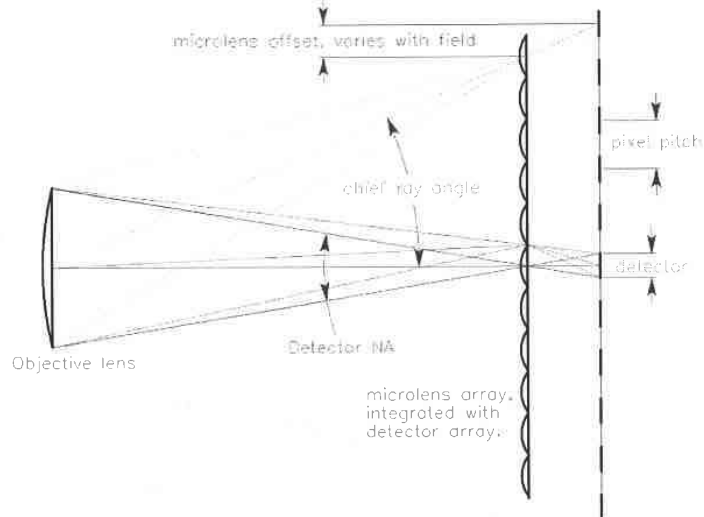


Fig.7: Microlenses located above active area of sensor, are positioned relative to pixel location based on expected incident angle and enhance the sensor's light collecting ability by magnifying the effective area of each pixel. [Highly schematic drawing, not to scale.]

These lenses act as condensers, relaying the sensor image to the exit pupil of the lens. This increases the apparent size of the detectors, improving sensitivity, because the diameter of the microlens becomes the apparent size of the detectors. The plane of microlenses is effectively the image plane of the system. The microlensed detectors now have limited angular response; if the exit pupil of the taking lens is increased beyond the size of the detector image, system sensitivity does NOT increase. In practice, the microlenses are not perfectly formed, so their imaging is crude, but they do improve performance.

The CRA curve illustrated in fig.5 represents a lens designed for a maximum CRA value of 20 degrees. The purpose of the CRA constraint is to maximize the light collection efficiency of the microlenses. Instead of centering each microlens on its pixel, the sensor manufacturers have offset the center of each microlens in order to compensate for the incidence angle of chief rays. Ideally the microlens distribution would exactly match the CRA variation of the lens it was to be used with, but this is not generally seen in practice. Typically the microlens offsets vary linearly with radial position from the center of the sensor, and are designed to minimize CRA/microlens mismatch based on expected lens CRA

curves. The effect of mismatch is a drop in light collection efficiency or decreased relative illumination at the image, or cross-talk between microlenses and adjacent pixels, resulting in false coloration.

Today, maximum CRA specifications for different sensor formats are readily available in the <12 degree to <26 degree range, with the larger CRA allowances corresponding to smaller VGA formats (2.2um, 3.6um). The demand for shorter TTL's is putting pressure on sensor manufacturers to increase their maximum allowable CRA values. Added constraints and fewer elements are lessening the lens designer's ability to deliver good image quality performance and low CRA's.

Relative Illumination – The relative illumination is the level of light energy incident at the image plane for a given field point relative to that at the center of the image.

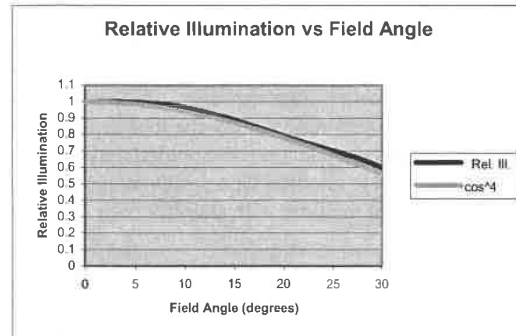


Fig.8: Relative Illumination and Cos⁴ as a Function of Field Angle

The blue curve in fig.8 is a typical relative illumination plot. Lens specifications usually require a value greater than 50% at the edge of the field. This corresponds roughly to cos⁴, so there is rarely enough corner illumination to allow vignetting for aberration control. If relative illumination meets the requirements, the final image is corrected electronically. Also, it's important that the drop in the relative illumination curve is not precipitous towards full field, or a slight decenter of the sensor relative to the optical axis will cause one corner of an image to appear noticeably dark.

5. Designing

When first beginning a lens design, it is not obvious how many elements to use or which materials. The biggest challenge in designing these systems is to create a lens that is insensitive to tolerances and will perform well when built. Each additional element adds tolerances that will degrade the as-built performance. But each element also adds variables that can be used to increase nominal performance while meeting system and manufacturing constraints.

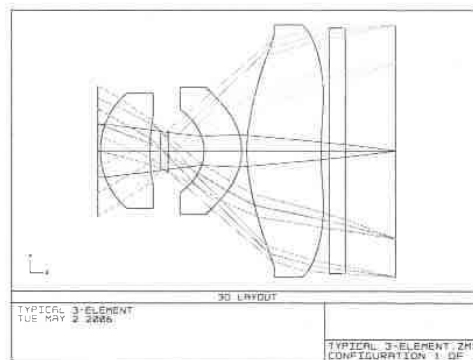


Fig.9: A typical 3-plastic element (3p) imaging system.

The three-element form is very common (fig.9), and a good place to start. Just about every camera module lens manufacturer has a lens of this form in their offerings. Designs tend not to be stop-symmetric. The aperture stop is usually towards the front of the lens, often before the first element, which helps CRA and TTL. The majority of these lenses are all-plastic although some incorporate one glass element (usually the front element) for the advantages of high-index refraction and color correction. Plastic elements are almost always bi-aspheric, and frequently the aspheres are not subtle! The shape of the last lens surface in the design above is typical. Four element systems provide high performance, but are only viable when the TTL is relatively large ($>6.0\text{mm}$), otherwise the performance degradation due to tolerances cancels out the nominal gain. Four element systems are mostly found in cameras with $1/4''$ sensor formats or larger, though they are becoming less common. Likewise, the effectiveness of a 3-element approach decreases to the point that a 2-element system becomes more practical when the TTL is less than 4 mm.

Part of the selection process, when considering materials, is the cost of satisfying the manufacturing constraints. Plastic injection molded optics have minimum edge thicknesses, minimum center thickness and a range of acceptability for their center to edge thickness ratio that must be met in order that they can be molded. Additionally, the maximum slope that can be diamond-turned in mold inserts and measured in either the lens or the mold is around 45 degrees. One big advantage of plastic is that flanges with mechanical details can be molded that eliminate the need for spacers and allow for mechanically driven centering of one element to another. One disadvantage is that there are very few plastic materials that lend themselves to precision optical molding with stability over large ranges of temperature and humidity, so the choices are limited.

Traditional glass lenses have similar types of requirements but with different values, based on their own manufacturing processes. The inability of lens manufacturers to accurately center the outer dimension of these elements on the optical axis, makes precise mounting very difficult. The benefits of traditional glass is reduced as the TTL requirements become shorter.

Another option becoming more readily available is molded glass, allowing the advantages of both high index and aspheric correction. Some current issues with molded glass are the small number of flint-type glasses available for molding, surfaces with inflections can only be used under very limited circumstances and flanges can only be formed in a restricted range of shapes, no sharp corners or abrupt changes in slope are allowed. Cost and manufacturing capacity also limit the use of molded glass elements today. Nevertheless molded glass can be the lens type of choice when the goal is stability over extreme ranges of conditions, or great lengths of time.

6. Performance Requirements

Lens performance for digital sensors is commonly expressed in terms of MTF at spatial frequencies between Nyquist/2 ($Ny/2$), and Nyquist/4 ($Ny/4$). The Nyquist frequency is $1/(2 \times (\text{pixel size}))$, so for 5.6 μm pixels $Ny/2$ is 45 lp/mm and $Ny/4$ is 22.5 lp/mm; for 1.75 pixels $Ny/2$ is 143 lp/mm, $Ny/4$ is 71.4 lp/mm.

Initially, when pixel sizes were relatively large (5.6 μm), cell phone manufacturers would specify MTF performance for $Ny/2$ and even Ny . This was because $Ny/2$ was still a relatively low frequency, so the requirements were possible to meet. As pixels became smaller (3.6-2.8 μm), the specifications gravitated to significant response at $Ny/4$ and $Ny/2$. These requirements were more challenging, but the size was allowed to grow to help satisfy the MTF requirements. At the same time the tooling capability of manufacturers was increasing so that build tolerances could be decreased, improving performance. The combination of these factors allowed delivery of high performance camera modules. And then the drive to reduce TTL began.

As cell phone manufacturers began demanding smaller and smaller camera modules to be able to offer extremely thin cell phones, image quality became secondary to size. Today most cell phone manufacturers understand that imposing severe size restrictions will significantly compromise image quality, and they are willing to accept worse performance based on $Ny/2$ and $Ny/4$ MTF response than with previous camera modules. This means that the image quality of 2MP camera modules are not all alike; as the pixels get smaller the image quality will be worse, and even newer, thinner

versions of cameras based on the same sensor will have worse performance. The opposing requirements of good image quality and short TTLs coupled with the shrinking size of pixels are rapidly running into the limitations of physics.

7. Tolerance-limited Design

The lens designer must consider manufacturing tolerances at the optimization stage, compromising nominal performance to achieve improved as-built performance. Nevertheless, manufacturing processes are not always available to achieve the necessary tolerances. One of the most challenging aspects of designing lenses for camera modules is desensitizing the system. If sensitivity to manufacturing tolerances is not built into the merit function, then the lens will not be manufacturable.

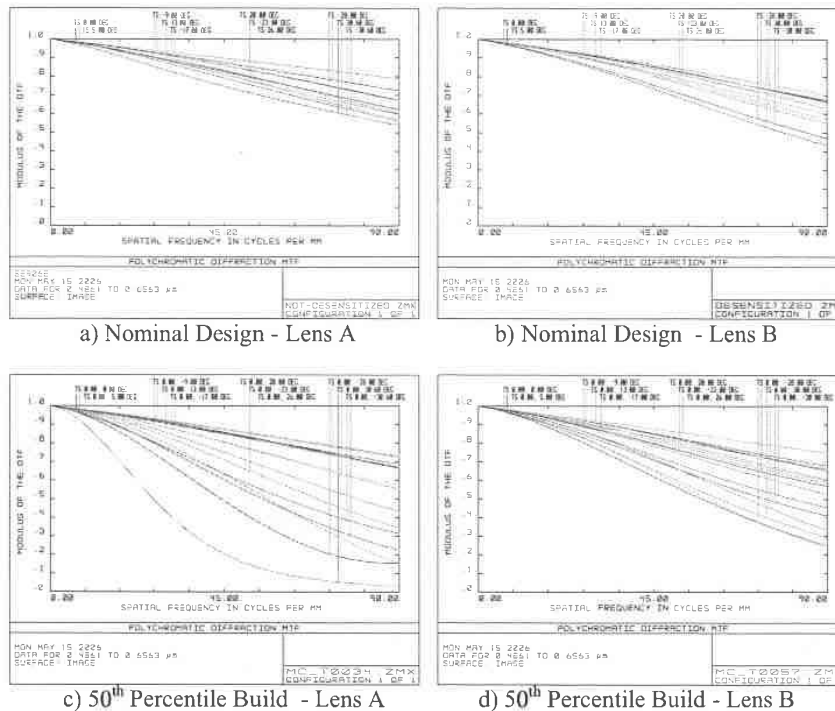


Fig.10: a) and b) Nominal MTF curves for two lens designs, lens B has been desensitized to the effects of manufacturing tolerances, lens A has not; c) and d) 50th percentile MTF curves representing a typical manufactured lens, based on simulated builds. The manufacturable MTF performance of lens A is greatly deteriorated from the nominal, the performance of lens B holds up much better when manufacturing tolerances are applied.

Fig.10 illustrates the impact of including desensitization in the optimization process. As the MTF curves clearly illustrate, a desensitized lens generally has slightly lower performance than a lens that has not been desensitized, but the benefit in the performance stability of manufactured systems more than offsets this difference, improving the overall performance of the manufactured lens population.

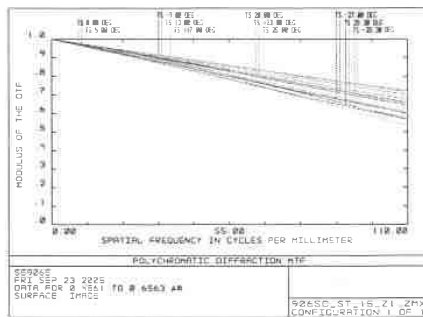
Due to the significant risk that an unfortunate combination of build tolerances will produce a lens with unacceptable performance, most lenses for miniature camera modules are 100% tested for image quality, usually with commercially available test systems that measure through-focus MTF. Performance is judged at representative points across the field, usually at one or two spatial frequencies. Evaluating MTF in two defocused planes can quickly expose field tilt or curvature problems.

The vast majority of systems are built in threaded barrels and focused at assembly, with no other alignments performed. Accurate, tight threads are difficult to produce, and they present measurement and contamination problems. Alternatives that allow alignments for lens to sensor centration and tilt are being implemented. As pixel counts get higher and sensor dimensions get smaller, these alignments are becoming more critical.

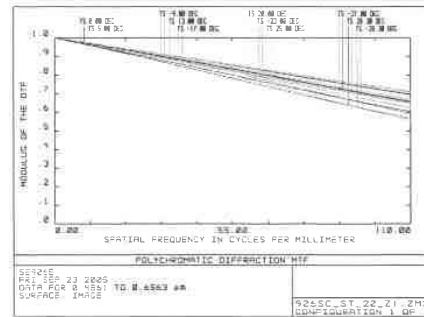
The problem of communication of quality between lens manufacturers and their customers is important. Manufacturers usually produce their own designs, and they are unwilling to share design data with customers. Also, actual manufacturing tolerance capability is not usually available, so it is not possible to verify the manufacturability of a new design. Standard methods of predicting production quality are needed to avoid unpleasant surprises during volume manufacturing.

8. TTL and Desensitization

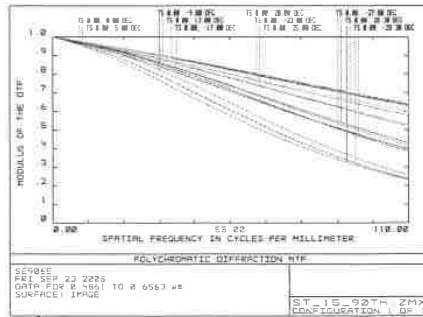
The ability of the designer to desensitize a lens is directly tied to the TTL and, for shorter forms, the BFL constraints. For instance, the 2MP 2.8um sensor required a lens with good performance over a large format. We were able to produce a lens that consistently delivers good image quality only because the TTL for this system was allowed to increase to as large as 7.8mm. The longer the TTL, the more modest the refraction needed at each surface, the weaker each lens can be and the less sensitive the performance of the system is to build tolerances. The more constrained the lens system in length, the more refractive power is needed at each surface, and the more sensitive the lens becomes to tolerance-induced image degradation.



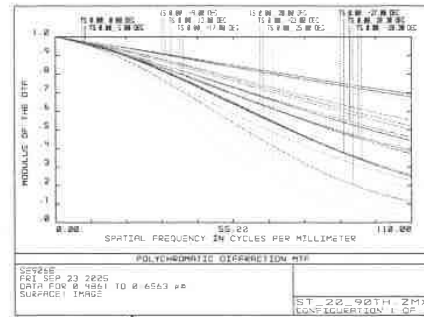
a) Nominal Design - Lens A (TTL=7.5 mm)



b) Nominal Design - Lens B (TTL=6.5 mm)



c) 90th Percentile Build - Lens A (TTL=7.5 mm)



d) 90th Percentile Build - Lens B (TTL=6.5 mm)

Fig.11: a) and b) Nominal MTF curves for two 4-element lens designs constrained by different TTLs, the performance is essentially identical; c) and d) MTF curves representing 90th percentile performance based on simulated builds. The longer TTL results in more consistently high performance.

The MTF curves in fig.11 illustrate the effect of TTL on desensitization. The additional constraint of conforming to a shorter TTL increases the difficulty of designing a manufacturable lens with acceptable performance and reasonable yields. Although this exercise was performed using a relatively long TTL lens (an older design), the same concept applies to today's shorter TTL designs for systems with three elements or more.

Two-element systems often naturally adopt forms with short TTL's, but desensitization to tolerances can require a relatively short BFL. Positioning the IR filter in such a system can be challenging. It is important for the back surface of the filter to be as far as possible from the sensor to ensure small surface defects and contamination are adequately out of focus. The closer to the sensor, the more restrictive the acceptability requirements on defect size. An IR filter positioned too close to the sensor could require such a tight scratch dig specification as to make it prohibitively costly or unmanufacturable.

The primary focus in recent camera module development has shifted from image quality to size and lens designers are being pressured to design lenses with shorter and shorter TTLs. Recent lenses for 1/4" formats are being held to TTLs < 5.0mm and there are plans for new lenses for the same format to be even shorter. Of course the pixels are smaller, so Ny/2 is higher (113.6 lp/mm for 2.2um pixels, 142.9 lp/mm for 1.75um pixels) making the problem even more difficult.

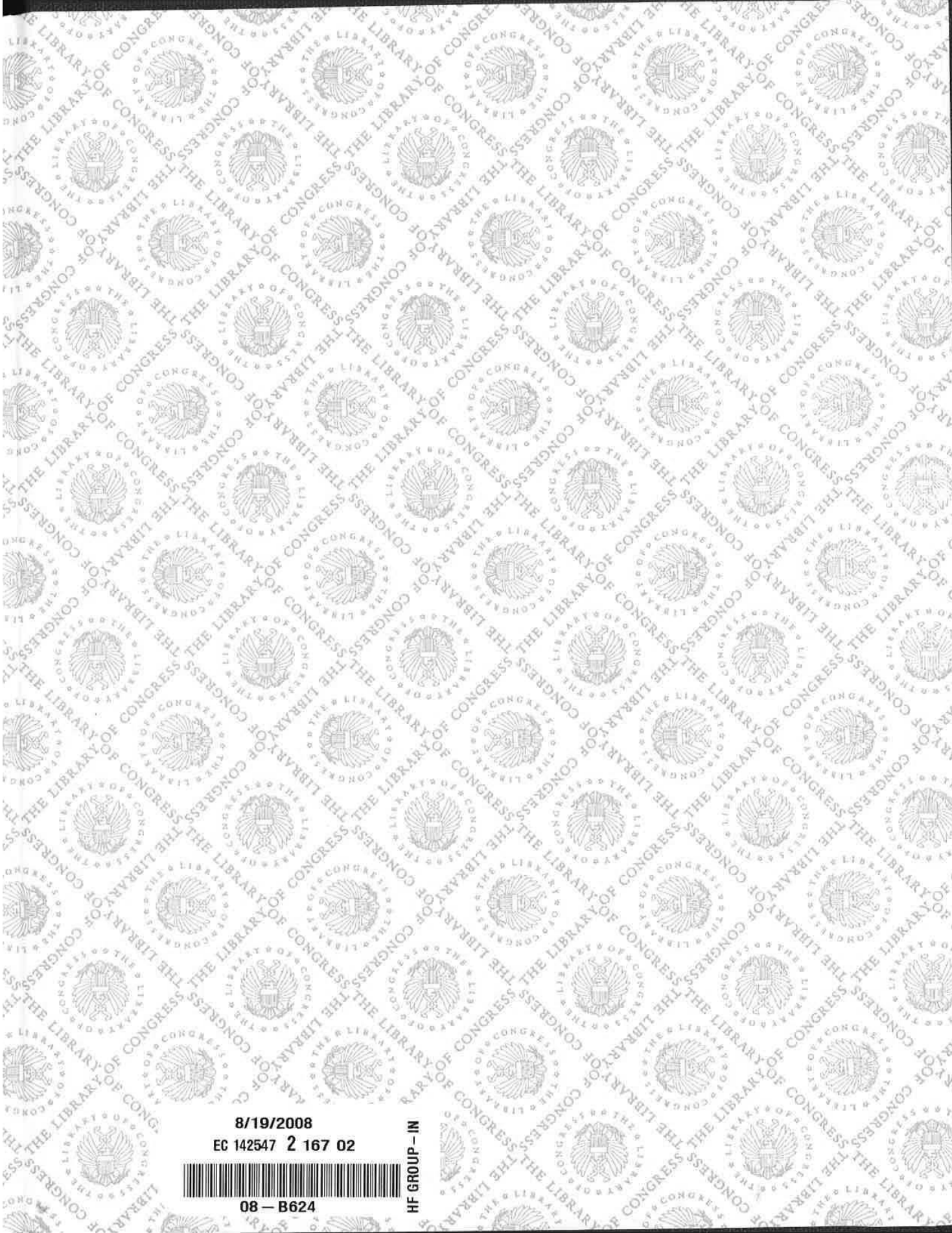
9. Future Prospects

We believe that the race for smaller pixels is slowing, because Moore's law cannot shorten the wavelength of visible light, or increase the brightness of photographic subjects. Pixels whose dimensions are under 2 um have limited light-collection ability, and much faster f/number lenses are unlikely to be developed. The continuing pressure to design with very short TTL's both for packaging and cost considerations suggests that in the near term the customer can expect worse image quality from camera modules using sensors with these very small pixels. Perhaps the market will split, to allow a choice between low cost/very small/modest quality cameras, and more costly/larger cameras that can rival today's digital still cameras.

The path to sharpness improvement most likely involves a hybrid solution incorporating a desensitized lens design combined with improved build tolerances, active alignment at lens and camera assembly, image processing for improved depth of field, or all three. There are companies currently developing image processing methods to improve image quality and depth of field in digital images. These methods may allow us to build simplified, desensitized lens systems whose performance is corrected by digital image processing. There are, of course, tradeoffs to be made between sharpness, noise levels and electronic complexity. In each case there will be added costs; it will be interesting to see what cost/image quality balance cell phone manufacturers finally select to offer their customers in the next generation of cell phone camera products.

LC COPYRIGHT
0 022 804 562 7

ISBN 0-8194-6427-9
ISSN 0277-786X



8/19/2008

EC 142547 2 167 02



08 - B624

HF GROUP - IN

INTERNATIONAL OPTICAL DESIGN CONFERENCE

TS 510
.155
2006
Pt 2
Copy 2



APPENDIX F

TS 517
5
P5 S33
009
Copy 1

The Design of
**Plastic
Optical
Systems**

Michael P. Schaub

The Design of
**Plastic
Optical
Systems**

Tutorial Texts Series

- *Optical Design: Applying the Fundamentals*, Max J. Riedl, Vol. TT84
- *Infrared Optics and Zoom Lenses, Second Edition*, Allen Mann, Vol. TT83
- *Optical Engineering Fundamentals, Second Edition*, Bruce H. Walker, Vol. TT82
- *Fundamentals of Polarimetric Remote Sensing*, John Schott, Vol. TT81
- *The Design of Plastic Optical Systems*, Michael P. Schaub, Vol. TT80
- *Radiation Thermometry: Fundamentals and Applications in the Petrochemical Industry*, Peter Saunders, Vol. TT78
- *Matrix Methods for Optical Layout*, Gerhard Kloos, Vol. TT77
- *Fundamentals of Infrared Detector Materials*, Michael A. Kinch, Vol. TT76
- *Practical Applications of Infrared Thermal Sensing and Imaging Equipment, Third Edition*, Herbert Kaplan, Vol. TT75
- *Bioluminescence for Food and Environmental Microbiological Safety*, Lubov Y. Brovko, Vol. TT74
- *Introduction to Image Stabilization*, Scott W. Teare, Sergio R. Restaino, Vol. TT73
- *Logic-based Nonlinear Image Processing*, Stephen Marshall, Vol. TT72
- *The Physics and Engineering of Solid State Lasers*, Yehoshua Kalisky, Vol. TT71
- *Thermal Infrared Characterization of Ground Targets and Backgrounds, Second Edition*, Pieter A. Jacobs, Vol. TT70
- *Introduction to Confocal Fluorescence Microscopy*, Michiel Müller, Vol. TT69
- *Artificial Neural Networks: An Introduction*, Kevin L. Priddy and Paul E. Keller, Vol. TT68
- *Basics of Code Division Multiple Access (CDMA)*, Raghuvveer Rao and Sohail Dianat, Vol. TT67
- *Optical Imaging in Projection Microlithography*, Alfred Kwok-Kit Wong, Vol. TT66
- *Metrics for High-Quality Specular Surfaces*, Lionel R. Baker, Vol. TT65
- *Field Mathematics for Electromagnetics, Photonics, and Materials Science*, Bernard Maxum, Vol. TT64
- *High-Fidelity Medical Imaging Displays*, Aldo Badano, Michael J. Flynn, and Jerzy Kanicki, Vol. TT63
- *Diffraction Optics—Design, Fabrication, and Test*, Donald C. O’Shea, Thomas J. Suleski, Alan D. Kathman, and Dennis W. Prather, Vol. TT62
- *Fourier-Transform Spectroscopy Instrumentation Engineering*, Vidi Saptari, Vol. TT61
- *The Power- and Energy-Handling Capability of Optical Materials, Components, and Systems*, Roger M. Wood, Vol. TT60
- *Hands-on Morphological Image Processing*, Edward R. Dougherty, Roberto A. Lotufo, Vol. TT59
- *Integrated Optomechanical Analysis*, Keith B. Doyle, Victor L. Genberg, Gregory J. Michels, Vol. TT58
- *Thin-Film Design: Modulated Thickness and Other Stopband Design Methods*, Bruce Perilloux, Vol. TT57
- *Optische Grundlagen für Infrarotsysteme*, Max J. Riedl, Vol. TT56
- *An Engineering Introduction to Biotechnology*, J. Patrick Fitch, Vol. TT55
- *Image Performance in CRT Displays*, Kenneth Compton, Vol. TT54
- *Introduction to Laser Diode-Pumped Solid State Lasers*, Richard Scheps, Vol. TT53
- *Modulation Transfer Function in Optical and Electro-Optical Systems*, Glenn D. Boreman, Vol. TT52
- *Uncooled Thermal Imaging Arrays, Systems, and Applications*, Paul W. Kruse, Vol. TT51
- *Fundamentals of Antennas*, Christos G. Christodoulou and Parveen Wahid, Vol. TT50
- *Basics of Spectroscopy*, David W. Ball, Vol. TT49
- *Optical Design Fundamentals for Infrared Systems, Second Edition*, Max J. Riedl, Vol. TT48
- *Resolution Enhancement Techniques in Optical Lithography*, Alfred Kwok-Kit Wong, Vol. TT47
- *Copper Interconnect Technology*, Christoph Steinbrüchel and Barry L. Chin, Vol. TT46

For a complete listing of Tutorial Texts, visit <http://spic.org/tutorialtexts.xml>

The Design of Plastic Optical Systems

Michael P. Schaub

Tutorial Texts in Optical Engineering
Volume TT80

SPIE
PRESS

Bellingham, Washington USA

stry, Peter Saunders, Vol.

Edition, Herbert Kaplan,

ovko, Vol. TT74

dition, Pieter A. Jacobs,

ol. TT68

at, Vol. TT67

66

d Maxum, Vol. TT64

y Kanicki, Vol. TT63

leski, Alan D. Kathman,

TT61

nd Systems, Roger M.

tufo, Vol. TT59

J. Michels, Vol. TT58

uce Perilloux, Vol. TT57

53

3oreman, Vol. TT52

pl. TT51

TT50

, Vol. TT48

'ong, Vol. TT47

, TT46

rialtexts.xml



Library of Congress Cataloging-in-Publication Data

Schaub, Michael P.

The design of plastic optical systems / Michael P. Schaub.

p. cm. -- (Tutorial texts series ; TT 80)

Includes bibliographical references and index.

ISBN 978-0-8194-7240-3

1. Plastic lenses. 2. Optical instruments--Design and construction. 3. Plastics--Optical properties. 4. Optical materials. I. Title.

TS517.5.P5S33 2009

681'.4--dc22

2009028012

Published by

SPIE

P.O. Box 10

Bellingham, Washington 98227-0010 USA

Phone: 360.676.3290

Fax: 360.647.1445

E-mail: Books@spie.org

www.spie.org

Copyright © 2009 Society of Photo-Optical Instrumentation Engineers

All rights reserved. No part of this publication may be reproduced or distributed in any form or by any means without written permission of the publisher.

The content of this book reflects the thought of the author(s). Every effort has been made to publish reliable and accurate information herein, but the publisher is not responsible for the validity of the information or for any outcomes resulting from reliance thereon.

Printed in the United States of America.



PROCEEDINGS
31 2003
SPE

3. Plastics--Optical

ers

r distributed
isher.

/ effort has been made
her is not responsible
m reliance thereon.

Introduction to the Series

Since its inception in 1989, the Tutorial Texts (TT) series has grown to more than 80 titles covering many diverse fields of science and engineering. The initial idea for the series was to make material presented in SPIE short courses available to those who could not attend and to provide a reference text for those who could. Thus, many of the texts in this series are generated by augmenting course notes with descriptive text that further illuminates the subject. In this way, the TT becomes an excellent stand-alone reference that finds a much wider audience than only short course attendees.

Tutorial Texts have grown in popularity and in the scope of material covered since 1989. They no longer necessarily stem from short courses; rather, they are often generated by experts in the field. They are popular because they provide a ready reference to those wishing to learn about emerging technologies or the latest information within their field. The topics within the series have grown from the initial areas of geometrical optics, optical detectors, and image processing to include the emerging fields of nanotechnology, biomedical optics, fiber optics, and laser technologies. Authors contributing to the TT series are instructed to provide introductory material so that those new to the field may use the book as a starting point to get a basic grasp of the material. It is hoped that some readers may develop sufficient interest to take a short course by the author or pursue further research in more advanced books to delve deeper into the subject.

The books in this series are distinguished from other technical monographs and textbooks in the way in which the material is presented. In keeping with the tutorial nature of the series, there is an emphasis on the use of graphical and illustrative material to better elucidate basic and advanced concepts. There is also heavy use of tabular reference data and numerous examples to further explain the concepts presented. The publishing time for the books is kept to a minimum so that the books will be as timely and up-to-date as possible. Furthermore, these introductory books are competitively priced compared to more traditional books on the same subject.

When a proposal for a text is received, each proposal is evaluated to determine the relevance of the proposed topic. This initial reviewing process has been very helpful to authors in identifying, early in the writing process, the need for additional material or other changes in approach that would serve to strengthen the text. Once a manuscript is completed, it is peer reviewed to ensure that chapters communicate accurately the essential ingredients of the science and technologies under discussion.

It is my goal to maintain the style and quality of books in the series and to further expand the topic areas to include new emerging fields as they become of interest to our reading audience.

*James A. Harrington
Rutgers University*

Contents

Preface	ix
Acknowledgments.....	xi
Chapter 1 Introduction.....	1
1.1 Background	1
1.2 When Are Plastic Optics Appropriate?	5
Chapter 2 Optical Plastics	15
2.1 Plastic Versus Glass Maps	15
2.2 Material Properties	19
2.3 Material Selection	28
2.4 Material Specification	29
Chapter 3 Manufacturing Methods	31
3.1 Casting.....	31
3.2 Embossing and Compression Molding.....	35
3.3 Machining.....	36
3.4 Injection Molding	39
Chapter 4 Design Guidelines	65
4.1 Design Basics	65
4.2 Tolerances	81
4.3 Plastic Versus Glass	87
4.4 Shape and Thickness	90
4.5 Aspheric Surfaces.....	94
4.6 Diffractive Surfaces.....	100
4.7 Athermalization	105
4.8 Coatings.....	110
4.9 Optomechanical Design	113
4.10 Stray Light.....	118
4.11 Special Considerations for Small and Large Parts	128
4.12 Drawings	132
4.13 Vendors and Vendor Interaction	140

Chapter 5	Design Examples	143
	5.1 Singlet Lens	143
	5.2 Webcams	151
	5.3 Cell Phone Camera	164
	5.4 Infrared Multiorder or Harmonic Diffractive Lens	167
Chapter 6	Testing	177
	6.1 Parameters, Equipment, and Techniques.....	177
	6.2 Making Testing Easier	189
Chapter 7	Prototyping.....	193
	7.1 Optics	193
	7.2 Mechanical Parts	197
	7.3 Assembly and Test	198
Chapter 8	Production	201
	8.1 Transition to Production	201
	8.2 Steady-State Production	206
	References	207
	Index	213

..... 143

..... 143

..... 151

..... 164

ve Lens 167

..... 177

..... 177

..... 189

..... 193

..... 193

..... 197

..... 198

..... 201

..... 201

..... 206

..... 207

..... 213

Preface

We routinely come into contact with and utilize plastic optical systems in our daily lives. As an illustration of this, consider the following events that may occur during a typical weekday. Traveling to work in our car, traffic signals change color to regulate the flow of vehicles. Arriving at work, as we enter the building, motion sensors turn on the hallway lights. At our desk, a fingerprint reader grants us access to our laptop computer. In the lab, we take and send pictures of the latest prototype, using the camera in our cell phone, enabling others to see the hardware. After work, stopping at the store, the bar code reader brings up the prices of our items. Back at home, we enjoy the latest movie released on DVD.

All of these devices—the traffic signals, motion sensors, fingerprint readers, cell phone cameras, bar code scanners, and DVD players—rely upon plastic optical systems to perform their function. As a result, there is a growing need for individuals who are knowledgeable in the design, development, and production of such systems. This tutorial text is written with this need in mind. The book is an elaboration upon the material covered in the SPIE short course “The Design of Plastic Optical Systems.” It is meant to provide an overview of the design of plastic optical systems and is structured along the lines of a typical development project. Following a brief background discussion, the advantages and disadvantages of plastic optics are considered. Next, the available materials and their properties are described, as well as the issues of material selection and specification. Various manufacturing methods are reviewed, followed by a chapter on design guidelines, leading into several design examples. Following the examples, the prototyping and testing of a design is covered. Finally, bringing the design to production is discussed.

There are several groups that should be able to benefit from the material presented. The first group is optical engineers, who often have received training in optical system design, particularly with glass optics, but who are unfamiliar with the special design characteristics of plastic optics. The second group is technical management, who need to understand the advantages and limitations of plastic optical systems. The third, and by far the largest group, is engineers of other disciplines who find they need to design and develop plastic optical systems but lack the knowledge or training to do so.

The text is written at an introductory level. No familiarity with plastic optical parts or their design is assumed. Any background knowledge of optics and optical design will be useful, but not required, to understand most of the subjects covered. Discussions of many of the subjects covered in this text can be found distributed amongst various publicly and/or commercially available sources. There is a wealth of information on plastic optics available in articles, conference proceedings, trade journals, books, the Internet, and various patent databases. We reference many of these throughout the text and encourage the reader to utilize

them as additional sources of information, knowledge, and possibly, creative inspiration.¹⁻⁸

The plastic optics industry tends to be somewhat secretive, with the details of many vendors' processes, techniques, and tooling methods considered proprietary. In spite of this, there are many well-established relationships amongst both individuals and companies in the field. It is a relatively small community, and it is not unusual for individuals to have worked for several plastic optics companies, repeatedly coming into contact with people throughout their career. Referral to and assistance from competing companies is not uncommon. While the proprietary aspects of the field may be frustrating for some readers, not knowing all the intimate details of a particular process will not prevent the successful design of a plastic optical system.

Having completed this book, readers should understand the benefits and limitations of plastic optical systems and be able to determine if this technology is appropriate for their applications. They will have the basic knowledge to undertake the design of these systems, should they choose to do so themselves, or they will be able to have the appropriate conversations with the individuals or companies they ask to perform the work.

possibly, creative

with the details of methods considered shed relationships a relatively small worked for several people throughout companies is not be frustrating for lar process will not

d the benefits and e if this technology asic knowledge to lo so themselves, or i the individuals or

Acknowledgments

As with most people in the field of plastic optics, I entered the profession somewhat by chance. During my time in graduate school, a local company (Donnelly Optics, which became Applied Image Group Optics, which later became Aurora Optical) announced a part-time position for an optical engineer. The work involved designing plastic optical systems, with an emphasis on diffractive optics. This was aligned with my dissertation research. After successfully interviewing for the position, I began my career in plastic optics. Part-time work turned to full-time work, to the annoyance of my advisor, Bob Shannon, whose retirement I probably delayed a few years. After graduation, I remained at the company for several more years before moving to my current position at Raytheon Missile Systems (RMS). I continue to be involved with the design of plastic optical systems at work, as a consultant, and through teaching my SPIE short course.

The irony is not lost on me that after an undergraduate optics degree from the University of Rochester, several years of work as a contractor at Kodak, an MSc from Oxford, graduate school at the Optical Sciences Center, resulting, finally, in a PhD with emphasis on optical design, the first design I had go into high volume production was a single-element, lens-in-barrel system that went into a version of the “Barbie Cam,” a silver plastic toy digital camera with a large pink flower surrounding the lens. Maybe not the greatest resume addition or claim to fame, but there must be some positive karma from, to quote my wife, “all those little girls you made happy.” In retrospect, in that simple design were many of the elements of successful plastic optical systems—appropriate material selection, design for molding and assembly, integral mounting features, toleranced performance, and testability. Regardless of the simplicity of the system, there is a certain joy in seeing thousands upon thousands (if not millions) of “my design” being produced.

I have had the opportunity to work with, and learn from, a large group of people throughout my career in plastic optics. I want to acknowledge the influence and work of the following individuals: Chris Bond, Jim Busche, John Daly, Ken Davis, Patricio Durazo, Jeff Fontaine, Rob Gallagher, Dan Joseph, Bill Kuhn, Bob Kuo, Judy Love, Paul McClellan, Paul Merems, Tom Miller, Bill Naylor, Jon Nisper, Rich Pfisterer, Tom Piedmont, Tom Rooney, Dave Strickland, Al Symmons, Jay Tome, Vince Vancho, and Zefy. The list is certainly incomplete. No slight is intended to anyone whose name does not appear.

Additional thanks go to John Schaefer for sharing his expertise in diamond turning, as well as information from some of his presentations on the subject. It is a little known fact that he worked at Donnelly Optics for a short period of time, setting up their entire diamond turning facility.

I thank all those who have taught me about optical design, particularly Bob Shannon, Jose Sasian, and George Lawrence, who are or were at the Optical Sciences Center. I also thank many of my Raytheon colleagues, particularly Dan

Brunton, Pat Coronato, Eric Fest, Greg Hanauska, Jim Hicks, Justin Jenia, Dave Jenkins, Rick Juergens, Dave Markason, Patrick McCarthy, Dan Melonis, Bill Reynolds, Ron Roncone, Wayne Sunne, Byron Taylor, and Dan Tolleson for useful discussions on a variety of optical, optomechanical, and nonoptical topics. Dr. Roncone supplied much of the background information on harmonic diffractive lenses, although any errors in the design example are mine alone.

I especially want to thank Barry Broome, whom I worked with during his time as an optics consultant at Donnelly Optics. He is well known in the plastic optics industry and has extensive experience in the design and production of plastic optical systems. He previously taught the SPIE plastic optics short course, referred me as his replacement in that role, and generously offered much of the material associated with the course.

I thank my parents, Charles and Dona Schaub, for raising me to value education and the possibilities that can come from it. My father never had the educational opportunities that he and my mother worked so hard to provide for their three children, and if he were still alive, I think he would be happy that a tutorial text I authored is being published.

Finally, I thank my wife Elsa, minha querida, for generally putting up with me, and our cat, Shadowzinha, for keeping me company during the writing of this text.

This tutorial text is dedicated in memory of Henry J. Kreis, better known to many of his Tucson friends and colleagues as "Uncle Henry." He was a good friend, a great man, and an extraordinary mold-process engineer. After many years at Polaroid, he moved to Arizona to take on the challenge of leading the mold-processing group at a newly formed plastic optics company. I had the good fortune of having the cubicle next to his, which allowed an easy, on-going discussion regarding manufacturability during the design process, as well as frequent brainstorming sessions. He taught me much of what I know about the design of robust, producible plastic optical systems. On the production floor, as lead process engineer, he taught the art of optical mold processing to the next generation of mold-process engineers and technicians. In addition, he was involved in the design, development, and evaluation of improved tooling methods.

Henry loved, among other things, his family, golf (which I sometimes think is the real reason he came to Tucson), a good meal, and tasty beverages. I am happy to be able to say that many times I had the pleasure of sharing the latter two with him. His passing not too long ago, besides leaving a void in the lives of his friends and family, reduced the already small number of highly skilled and experienced plastic optics mold-process engineers. It is safe to say that there are, and will be, very few people who know as much about processing a plastic optic injection mold as he did. Thankfully, due to his efforts, some of his knowledge lives on in the people he trained, the coworkers with whom he shared his experience, and hopefully, in this tutorial text.

*Michael Schaub
July 2008*

Chapter 1

Introduction

In this chapter, we provide some background information on plastic optics, including a brief history of their development, as well as recent advances in materials, machining, and manufacturing processes. We also discuss issues that may determine if plastic optics should be used for a particular application, as well as their potential advantages and disadvantages.

1.1 Background

Plastic optics have existed for longer than most currently practicing engineers. In 1936, after several years of development, the Rohm and Haas Company announced the commercial availability of polymethylmethacrylate (PMMA), now commonly referred to as acrylic, under the trade name Plexiglas.⁹ In the same year, DuPont began commercial production of its acrylic material, known as Lucite.¹⁰ In Britain, the Imperial Chemical Industries PLC introduced its version, which was called Perspex.¹¹ The following year, Dow Chemical introduced polystyrene in the United States under the name STYRON.¹²

Plastic lenses appeared around the same time, along with colorful marketing campaigns and disagreements over their invention. In London, on March 20, 1934, the KGK Syndicate Ltd. was formed between Peter Maurice Koch de Gooreynd and Arthur Kingston; just under four years later, in February 1938, the partnership was dissolved. The Wellcome Library, also in London, houses copies of documents concerning the partnership, as well as a copy of a letter from Kingston's lawyer regarding a dispute between the partners over who deserved credit for inventing the plastic optical lens.¹³ It seems that a BBC radio broadcast stated that Koch de Gooreynd was the inventor of the plastic lens, a claim that Kingston disagreed with.

In 1937, *TIME* magazine published an article describing competition between U.S., British, and German firms to substitute glass lenses with plastic lenses in cameras, eyeglasses, and binoculars. It is noted that shortly before the article's printing, Gooreynd (of the KGK Syndicate) appears in New York and bounces lenses on the table to show their fracture resistance. A few weeks later, in Los Angeles, a Rohm and Haas customer named E. G. Lloyd goes even further, putting on a dramatic exhibition for the press by taking a hammer to his lenses.¹⁴ Despite the impressive displays, these early lenses suffered from several problems, such as low scratch resistance and discoloration. Nevertheless, the field of plastic optics had begun in earnest.

With materials available, the manufacturers searched for markets to buy them. For instance, Rohm and Haas produced a few acrylic musical instruments, including a flute and a violin. The flute reportedly had good tone, while the violin

did not.⁹ Most early successful uses of optical plastic were either for eyeglasses or window applications. There were various attempts to create the equivalent of modern laminated windows, commonly known as "safety" glass, where a plastic film is sandwiched between glass plates to keep glass shards from flying when the window is broken.

The use of plastic windows in airplanes provided an initial market for the acrylic manufacturers and allowed them to continue development of the material. Acrylic initially was used for small windows, and as the material became more accepted and understood, larger windows; ultimately, even cockpit canopies were produced. With the beginning of World War II, the use of acrylic for military aircraft skyrocketed. Other war-time uses of plastic optics included antitank gun sights and experimental aerial cameras.¹⁵

Demand was high throughout the war period but abruptly declined with the end of the war and cancellation of government contracts. Manufacturers worked to replace the lost sales, putting acrylic into everyday items. Consumers, however, were not particularly interested in plastic products, due to the return of other materials that were not available during the war. In 1947, jukeboxes were the largest market for Plexiglas.⁹ Plastic optical elements began to appear in the auto industry, with acrylic replacing elements previously made of glass, such as tail lights. This association with the auto industry turned into a significant market for plastic optics and remains so today. Another application that developed shortly after the war, which remains with us today, is the illuminated sign.

Polycarbonate was introduced in the 1950s, with GE Plastics developing LEXAN¹⁶ and Bayer developing Makrolon.¹⁷ However, these early versions of polycarbonate were not suitable for most optical uses due to the "golden" tint of the material, as it was described by Bayer's advertising.¹⁷ Also in the 1950s, Kodak began producing cameras with acrylic viewfinders and objective lenses.¹⁸ Cameras continued to be a large market for plastic lenses in the 1960s, with over 50 million Kodak INSTAMATIC cameras made during the decade.¹⁹ Acrylic and polystyrene lenses were often used together to achieve color correction in these types of systems. Polycarbonate elements were still being used more often in nonimaging applications, such as car tail lights and traffic signals. In 1965, ICI developed polymethylpentene, often known by the trade name TPX. It is used today in some specialty plastic optical applications. In the 1970s, continued development of polycarbonate removed most of its tint, not necessarily enough for imaging applications, but enough to enable it to be used for automotive headlamps.

Significant progress in the use of polycarbonate elements occurred in the early 1980s with the introduction of optical-grade polycarbonate. The optical grade material was used for a variety of applications, such as eyeglass lenses and safety visors, as well as for canopies on fighter jets such as the F-14. Encouraged by the demand for optical data storage discs, optical-grade polycarbonate was used for CDs, first introduced in 1982, as well as for lenses to read them. This provided, in the view of the chemical companies producing the material, an optical application with significant plastic material usage. Having similar optical

either for eyeglasses or as the equivalent of glass, where a plastic lens is used instead of flying when

initial market for the material. The material became more common as cockpit canopies were made of acrylic for military aircraft. It also included antitank gun

which declined with the war. Manufacturers worked on other items. Consumers, however, due to the return of television sets, jukeboxes were made of plastic. They began to appear in the form of glass, such as in the case of a significant market for plastic. This led to the development of injection-molded signs.

Plastics developing in the early versions of the "golden" tint of the 1950s. Also in the 1950s, and objective lenses.¹⁸ In the 1960s, with over 50% of the market.¹⁹ Acrylic and polycarbonate correction in these lenses were used more often in eyeglasses. In 1965, ICI introduced the TPX. It is used in the 1970s, continued to be used, and necessarily enough used for automotive

lenses occurred in the polycarbonate. The optical properties of eyeglass lenses and the F-14. Encouraged by the use of polycarbonate was to read them. This led to the material, and having similar optical

properties to polystyrene, optical-grade polycarbonate could be used as an alternative in color-correcting optical systems.

The 1990s saw an increase in available optical plastics. Two newly developed materials to emerge were cyclic olefin copolymers (COCs), commonly known by the trade name Zeonex,ⁱ and cyclic olefin polymers (COPs), known by the names Apelⁱⁱ and Topas.ⁱⁱⁱ These materials are probably the first plastics designed specifically with optical products in mind. They have similar optical properties to acrylic but have higher thermal capability and lower water absorption. We will discuss these materials in more detail in the next chapter.

Besides these new polymers, optical grades of polyetherimide (PEI), best known by the trade name ULTEM,^{iv} and polyethersulfone (PES), known by the trade name RADEL,^v also became available. These materials have excellent temperature capability, beyond the other optical plastics, as well as relatively high refractive indices. Their potential downside is a deep amber color, which limits their use for many visible applications.

Another fairly recently introduced material is optical polyester. One example is OKP4,^{vi} which is produced by the Osaka Gas Chemicals Co., Ltd. This new material has a refractive index over 1.6, birefringence properties similar to acrylic, and a low Abbe number.

In addition to improvements in plastic optical materials, there have also been significant advances in areas that affect the production of plastic optics. In particular, there have been improvements in injection molding machines, as well as in machining technologies, such as single-point diamond turning. Improvements in molding machines have been driven by both product and process innovation.²⁰ Product innovation refers to changes such as reducing the number of components in a system by making the components perform multiple functions. This often results in more complex parts, pushing the capability of the molding machines and spurring their advance. Process innovation refers to optimizing a production process to make it as efficient and capable as possible.

There has been a big push for process control and improvement across many industries, driven by the acceptance of manufacturing philosophies such as statistical process control and "lean" and "just-in-time" manufacturing. These philosophies have created demand for injection molding machines with greater process control and feedback.

Probably the largest change in injection molding equipment, particularly for use in the production of plastic optics, has been the switch from hydraulic-operated machines to hybrid or electric machines. Hybrid machines, as the name suggests, use a combination of hydraulic and electrical drives. Electric machines, sometimes referred to as "all electric" machines, completely eliminate the use of

ⁱ ZEONEX is a registered trademark of ZEON Corporation.

ⁱⁱ Apel is a registered trademark of Mitsui Chemicals.

ⁱⁱⁱ Topas is a registered trademark of Topas Advanced Polymers.

^{iv} Ultem is a registered trademark of SABIC Innovative Plastics.

^v RADEL is a registered trademark of Solvay Advanced Polymers, LLC.

^{vi} OKP4 is a product of Osaka Gas Chemicals.

hydraulics, relying on electrical motors and drives. The transition to electric machines has occurred for several reasons. The primary reason is repeatability. The repeatability of an electric machine (or its potential for repeatability) is inherently higher than for a hydraulic machine.²¹ Given the precision required in optical elements, repeatability of a manufacturing process is a highly desired characteristic. In addition to this, moving from a hydraulic to an electric machine eliminates the use of hydraulic oil in the machine clamp mechanism. Hydraulic oil is associated with several problems. It can cause environmental issues, particularly ground contamination from leaking oil. It creates health and safety concerns such as oil vapors, falls, and fire hazards. There is also a cost associated with its storage and disposal. This argument can only be pressed so far though, for as we shall see, although switching to electric machines eliminates hydraulic oil in the molding machine, oil is still often required for temperature regulation of the mold itself. It can fairly be said that the use of electric machines does not completely remove the use of oil, but it does reduce the total quantity of oil used on the molding floor. In addition, electric machines tend to use less power than hydraulic machines, resulting in energy cost savings.

The general advances in processors and computing, which have also had great influence on the process of optical design, have influenced the development and use of injection molding machines. Most machines are now fully computer controlled, with a flat screen on the side of the machine displaying the current process parameters, as well as time-based graphs of pressure and other parameters for each injection cycle. Multiple sensors provide feedback, for display as well as for closed-loop control. The molding machine can be connected to a personal computer to continuously send process and sensor data for analysis and tracking, and the data can be stored for later download and further evaluation.

Besides the injection molding machines themselves, improvements have also taken place in the ancillary equipment associated with them. This includes improvements in material dryers, thermal conditioning equipment, and automated robotic pickers and degating systems. Improvements in automation have reduced the need for human intervention during steady-state production, which results in reduced cost, as well as less chance of human error or safety incidents. It is no longer necessary to have a person standing by each machine during production.

In addition to the advances in molding machine technology, there have also been significant advances in machining technologies. This affects the precision and complexity of molds that can be built and allows the direct machining of plastic optical parts, either as prototypes or for actual production. Advances in computing and computer control, as well as in other areas, have pushed machining capabilities to previously unthinkable levels. Nowhere is this more evident than in the process of single-point diamond turning, often simply referred to as diamond turning.

Diamond turning is a machining process combining the use of gem-quality diamond tools with precision computer numerically controlled (CNC) equipment. According to Schaefer, advances that have been made over the last 30 years

transition to electric
reason is repeatability.
(for repeatability) is
precision required in
is a highly desired
to an electric machine
mechanism. Hydraulic
environmental issues,
ites health and safety
also a cost associated
ressed so far though,
eliminates hydraulic
perature regulation of
ic machines does not
l quantity of oil used
use less power than

which have also had
aced the development
now fully computer
displaying the current
pressure and other
rovide feedback, for
ng machine can be
cess and sensor data
later download and

provements have also
them. This includes
ment, and automated
mation have reduced
tion, which results in
ety incidents. It is no
during production.
logy, there have also
affects the precision
direct machining of
duction. Advances in
areas, have pushed
lowhere is this more
often simply referred

the use of gem-quality
ed (CNC) equipment.
er the last 30 years

include going from air bearing to oil hydrostatic slide ways, changing from belt drive to direct brushless DC spindle drives, changing from laser positioning to glass scale positioning systems, using PC DSP instead of tape CNC controllers, using epoxy granite instead of granite machine bases, and switching from ball lead screws to linear motor drive axis drives.²²

The result of these advances has been a factor of eight improvement in surface finish and a factor of four improvement in surface form. In addition, the achievable spindle speeds have increased ten fold and the cost of the diamond-turning machines has dropped by about half. The machines are commercially available with a number of options, including machines with multiple axes.

These machining improvements have enabled the creation of high-precision complex parts. Off axis, nonsymmetric, and microfeatured surfaces can all be produced using modern diamond-turning equipment. For the optical designer, this allows additional freedom in selecting surface forms or in the integration of features such as multizonal surfaces. Proper machine setup, processing, and fixturing can eliminate the need for postpolishing. This means that plastic optical prototypes can be directly machined and that optical mold inserts can be built to high optical surface accuracy and surface roughness requirements. Combining this precision machining with advances in testing, mold compensation is readily performed.

Designers can, and should, take advantage of the improvements that have been made in plastic optical materials, injection molding machines, and machining technologies such as diamond turning. Conversations with vendors and/or suppliers, who need to stay current with these technologies, is usually the best way to be aware of the current state of capability, as well as ongoing development.

1.2 When Are Plastic Optics Appropriate?

As with all optical technologies, plastic optics are not the solution to every problem. When deciding whether to use plastic optics, the first question that needs to be answered is “Are plastic optics appropriate for my application?” There are a number of considerations in determining the answer to this question. Finances, project schedule, and supply chain issues can all play a role. Production volumes, along with cost and weight, are the top reasons that people decide to use plastic optics, while thermal issues such as storage temperature limits or temperature-dependant focus shift are the main reason that they are not chosen. Other considerations, such as the spectral band used, product lifetime, or even biological compatibility, may contribute to the decision whether or not they are appropriate. These issues, along with advantages, disadvantages, and application examples, are briefly discussed in the following paragraphs.

If there is a large anticipated production volume, that is, when many systems are expected to be manufactured, plastic optics may be appropriate. “What’s the volume?” is a question typically heard early in discussions with plastic optics

manufacturers. Certain plastic optics manufacturing methods are suitable for producing large quantities of parts. In certain consumer applications it is not unusual for millions of lenses and lens assemblies to be produced each month by a single manufacturer. As an example, in 2007 worldwide production of cell phone cameras topped one billion units, most of which contained plastic optics. Some manufacturing methods, such as injection molding, allow for the simultaneous production of multiple copies of a part. Molds can also be built with the ability to later increase the number of parts simultaneously produced to allow for additional production. Several plastic optics manufacturing methods will be discussed later in the text.

While large production volumes are often appropriate for plastic optics, low production volumes can also be appropriate, particularly in the case of highly complex parts. It is possible to make a wide variety of complex plastic optical components, some of which may challenge traditional glass fabrication methods, such as the part shown in Fig. 1.1. Multifaceted surfaces, multiple zone lenses, and lens arrays are examples of complex components that are routinely fabricated in plastic. That being said, the advantage of making complex parts from plastic rather than glass is diminishing somewhat. The advances in manufacturing technologies that have improved the quality and performance of plastic optics, particularly computer-controlled machining, can and are being applied to the fabrication of glass optics. Glass elements are regularly molded, although typically at lower rates than comparable plastic elements.²³⁻²⁵

Cost is often a factor in the decision to use plastic optics. In fact, it is typically the primary reason that they are considered. In general, and especially for large production volumes, plastic optics cost less than equivalent glass elements. This is mainly due to the time required to fabricate the element, but also partly due to material costs. The cost of a plastic optical element will be determined by a number of factors, including the fabrication method, the number of parts being made, the complexity of the part, the precision to which it must be made, its size and volume, and the material it is made of.



Figure 1.1 Complex molded plastic optical part. (Photograph courtesy of G-S Plastic Optics.)

s are suitable for applications it is not used each month by production of cell ned plastic optics. s, allow for the can also be built ously produced to facturing methods

plastic optics, low he case of highly lex plastic optical brication methods, ltpile zone lenses, outinely fabricated parts from plastic in manufacturing : of plastic optics, ng applied to the molded, although

tics. In fact, it is ral, and especially e equivalent glass e the element, but il element will be ethod, the number o which it must be

1 courtesy of G-S

Weight is another important reason to consider using plastic optics. For this particular characteristic, plastic optics have a significant advantage over traditional glass elements. Put simply, plastic is much less dense than glass, resulting in less weight for an equivalent volume of material. It can be argued that lenses of a given focal length, one made from glass and one made from plastic, do not necessarily require the same volume. High-index optical glasses allow longer radii of curvature, reducing lens volume, but the reduction does not typically make up the weight differential.

Head-mounted optical systems are an application where the weight advantage of plastic optics is often utilized. Heads-up displays for pilots, night vision goggles for soldiers, and microdisplays of technical manuals for mechanics or technicians are all examples of this. Studies have shown that wearing head-mounted displays can alter neck posture, increasing the stress on the musculoskeletal system of the neck and head.²⁶ Reducing the weight that must be borne will decrease the amount of stress imposed.

Other situations where weight can be a deciding factor for the use of plastic optics are those driven by battery lifetime or fuel limits. For instance, in a camcorder zoom lens, several elements typically move to change the magnification while maintaining focus. The number of times that these elements are capable of being driven before the battery must be recharged or replaced will depend upon the weight of the elements. In this case, replacing a glass element with a plastic element may increase the usage time the consumer experiences with a given battery charge. Another example would be an optical system meant to be carried by an airborne vehicle, such as a micro-UAV (unmanned aerial vehicle). The amount of time that the unit can remain aloft is in part a function of its weight, and plastic optics can be used to reduce overall system weight.

Plastic optics possess superior fracture resistance when compared to glass. Dropping a plastic lens may result in a scratch or dent to the element, but the lens will most likely remain in one piece. As an example of fracture resistance, consider that polycarbonate is often used in the production of "bulletproof glass" for vehicles or buildings. "Safety glasses," which are used for eye protection, are typically made from plastic, not glass. In this case, plastic can provide the fracture resistance necessary to meet the American National Standards Institute (ANSI) requirement that the lenses withstand the impact of a quarter-inch steel ball traveling at 150 feet per second.

Another potential advantage of plastic optics is part-to-part repeatability. Many plastic optics production methods rely upon replication processes. That is, the plastic part is formed by reproducing the shape of a master tool. An optical insert in an injection mold is one example of such a master. As mentioned above, it is possible to simultaneously produce multiple copies of a part. If a set of parts are simultaneously produced, each of the parts within the set may not be completely alike, since they may be formed from individually fabricated masters. However, the subsequent sets of parts will be very similar to the prior set. For a given part parameter, such as surface decentration, this can lead to a set of several narrow distributions. In contrast, traditional glass fabrication methods

typically produce continuous part characteristic distributions. The difference in distributions can play a role in the parameter probabilities used in tolerancing the designs, as well as in the final system performance.

Integration of features is yet another characteristic advantage of plastic optics. In addition to multiple optical surfaces, possibly for transmit and receive functions, or lens arrays for multiple beams, flanges and spacers can also be molded into an optical part. Molded-in flanges can allow multiple lenses to be stacked in a barrel, automatically setting the proper spacing of the elements. This can reduce overall part count and improve assembly, in both ease and time. Orientation marks can be added to parts, as can features such as keying or antirotation tabs. Snaps, bosses, through holes, or tapers can also be added for part retention or centration. Figure 1.2 shows a part, an automotive interior light cover, with a snap feature used for retention.

Surface form is an area where plastic optics can offer design advantages, as they are not limited to planar or spherical surfaces. It is quite common for plastic optic components to have highly aspheric, anamorphic, or freeform surface shapes. In addition to these continuous optical surfaces, it is also possible to create discrete or micro-optical features, such as Fresnel lenses, lens arrays, kinoform surfaces, fan-out patterns, diffraction gratings, or microlenses. Nonoptical features, such as channels for microfluidic or “lab-on-chip” applications, have also become common.

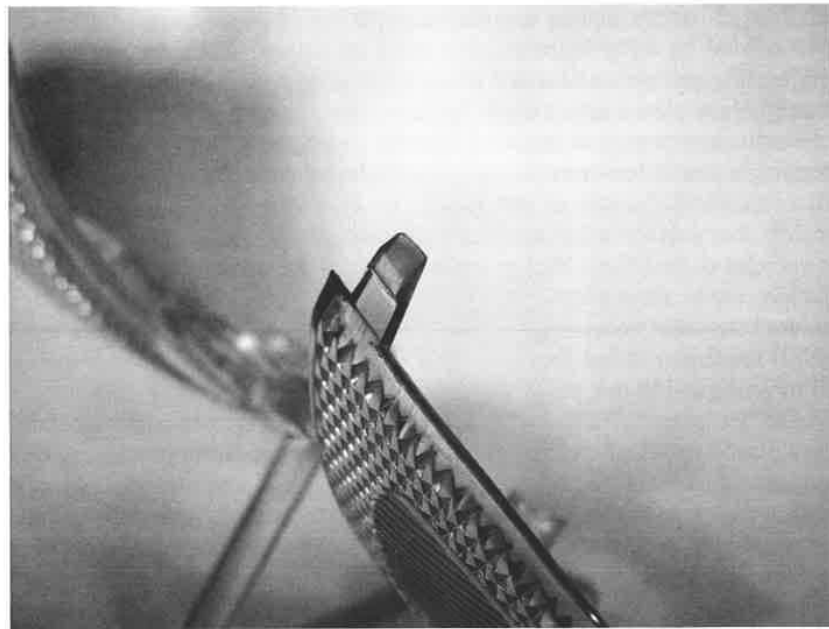


Figure 1.2 Plastic optical part using snap feature for retention. Note the complex, multizonal optical surface on the part. (Photograph courtesy of Alan Symmons.)

he difference in
tolerancing the

stage of plastic
mit and receive
ers can also be
ple lenses to be
elements. This
ease and time.
h as keying or
so be added for
ve interior light

t advantages, as
imon for plastic
eeform surface
also possible to
es, lens arrays,
r microlenses.
“lab-on-chip”



e the complex,
Symmons.)

One particular application that shows the continuing improvements and intriguing possibilities that plastic optics can offer is the intraocular lens. Modern intraocular lenses, or IOLs, as they are commonly called, take advantage of many of the positive characteristics of plastic optics. They are most commonly used to replace the crystalline lens of the human eye when cataracts (clouding of the lens) are impairing a patient's vision. Cataract surgery, with removal of the natural lens and implantation of an intraocular lens, is now the number one surgery performed in the United States of America.

Since they are implanted in the human body, the material the IOL is made from must be biocompatible; that is, it must not be rejected by the body. Sir Harold Ridley, a Royal Air Force (RAF) ophthalmologist, determined during World War II that acrylic was suitable for implantation into the eye. He noticed that airplane pilots who suffered eye injuries due to acrylic shrapnel, which came from their cockpit canopies, did not show rejection of the acrylic pieces. Knowing this, he had an IOL fashioned from acrylic and performed the first intraocular lens implant in 1949.²⁷

These early plastic IOLs were made from rigid material. Given their size, they required a large incision for implantation with a subsequent hospital stay, associated costs, and a significant recovery period. This is no longer the case, as the latest IOLs are implanted through a small, typically 2- to 3-mm incision, on an outpatient basis. This is possible because of available plastic material characteristics, in this case, flexibility. In order to achieve the desired small incision, flexible materials have been developed that allow the IOL to be folded or rolled up, then inserted into the eye through the incision using a syringe-like injector. Once inside the eye, the IOL is unfolded, at which point integrated features come into play. In order to be stably positioned within the eye, the lens must somehow be secured. In some cases an attachment structure, called a haptic, is inserted into the eye separately from the lens. The lens is then attached to the haptic, using integrated features such as loops or snaps. In other cases, the haptic is an integral part of the lens, and the entire lens and support structure is inserted. The haptic is lodged into the physical structure of the eye, securing the lens.

The optical power of standard IOLs are normally selected for far (distant) vision. The final axial position of the lens, along with correct power choice, determines the residual focus error. In some cases, the focus error is too large, and the lens must be replaced or repositioned. This is often done through a second surgical procedure. An alternative solution is to adjust the shape or position of the lens without performing invasive surgery. This can be accomplished by directing a laser onto the haptic to partially melt the structure.²⁸ In this case, we rely on the plastic material's ability to be melted and reshaped. An alternate method of adjusting power that can also be used to correct aberrations has recently been developed. It involves implanting a lens made of a material that is photosensitive, then illuminating it with a low-power light beam to adjust its shape.²⁹

Most patients suffering from cataracts are old enough to have presbyopia, the hardening of the eye lens, resulting in the loss of ability to focus on nearby

objects. Standard IOLs do not provide the focus adjustment of a nonpresbyopic eye. In this situation, reading glasses can be used for near-vision tasks such as reading a computer monitor or book. However, plastic optic characteristics have enabled the recent development of IOLs that provide both distant and near vision. This is typically accomplished in one of three ways. The first method relies upon the ability to create multizone surfaces. In this method, the IOL optical surface has multiple annular zones of different powers, the powers being selected for far, near, and sometimes midvision.³⁰ The second method relies on the ability to form diffractive structures. A diffractive surface is created on the lens that is designed to put light into multiple diffractive orders. The power and diffraction efficiency of the different orders are selected for the desired object distances.³¹ The third method relies on the same flexibility that allows the use of a small insertion incision. In this method, some form of (typically integral) bending structure is created. On insertion, the lens is placed in the correct position for far vision. To focus on nearby objects, the patient uses their eye muscles to bend the structure, moving the lens forward in the eye.³² Multiple element systems, where the lenses move relative to each other to produce a power change, have also been developed.³³

Another advance in IOL technology relies upon the ability to easily create aspheric surfaces on plastic optics. The average eye is not perfectly corrected, but it contains residual spherical aberration. This results from the spherical aberration contributions of the cornea and the natural lens not being perfectly balanced. The amount of spherical aberration in the eye normally changes with age, due to changes in the lens. When the natural lens is replaced with an IOL, it is possible to put in a lens with a desired amount of spherical aberration. The lens could have the correct amount of aberration to cancel that of the cornea, or it could be a lens that is itself corrected for spherical aberration.³⁴ This latter case allows the lens to be decentered upon insertion without introducing coma.

Since it is possible to correct vision when replacing the natural lens, it is a logical step to consider correcting vision not just by replacement, but by addition of an optical element to the eye. This next advance in IOLs, where an inserted lens eliminates or reduces the need for contact lenses or glasses, is underway. It is particularly appropriate for patients suffering from severe myopia. The large power and resulting eyeglass lens weight and thickness can be uncomfortable for patients with this condition. The inserted elements can theoretically be replaced throughout the patient's life to maintain optimum vision, or they can be removed if complications arise.

Intraocular lenses, while a relatively simple optical system, have made significant progress in recent years. It can be seen from this particular application that the judicious use of plastic optics, based on the understanding of their properties and capabilities, can enable advances in performance, reduce cost, and even improve quality of life.

Given all the characteristics discussed so far, plastic optics would appear to be an excellent choice for many applications, which is indeed the case. However, there are also a number of situations where the use of plastic optics may not be

a nonpresbyopic on tasks such as racteristics have t and near vision. method relies upon L optical surface g selected for far, re ability to form s that is designed action efficiency nces.³¹ The third a small insertion iding structure is for far vision. To end the structure, where the lenses have also been

to easily create tly corrected, but herical aberration tly balanced. The with age, due to OL, it is possible t. The lens could a, or it could be a r case allows the

tural lens, it is a t, but by addition where an inserted s, is underway. It yopia. The large uncomfortable for cally be replaced y can be removed

stem, have made icular application standing of their g, reduce cost, and

s would appear to e case. However, optics may not be

appropriate. One particular area of concern with plastic optics is thermal performance. This generally arises either in regard to storage and/or operating temperature, or focus shift with temperature change.

Optical plastics do not have as high a transition, or melting, temperature as optical glasses. This may rule out plastic optics, or at least certain types of plastic optics, for some thermal environments. In the simplest terms, under certain conditions plastic optics may melt. The various types of plastic optical materials have different service temperatures, so selection of the appropriate material from a thermal standpoint is very important. For instance, in several consumer applications we find that certain plastic optical materials will meet the thermal requirements, while others will not. This had led to specific plastic optical material combinations commonly being used for these applications. While the melting of plastic is often considered a negative characteristic, it is interesting to note that several plastic optics manufacturing methods specifically rely upon the melting, then hardening, of plastic materials.

Athermalization refers to maintaining the performance, most often focus, of an optical system over changes in temperature. Achieving an athermalized design using plastic optics over a large thermal range may be a challenge. This is due to the thermal material properties of optical plastics. Plastic optical materials have a larger coefficient of thermal expansion (CTE) and a much higher thermal change in refractive index (dn/dt) than optical glasses. Since the power of an optical element is determined by its radii of curvature and refractive index (and to a lesser extent its thickness), large changes in these parameters, unless balanced, will result in a large change in optical power. For a typical plastic optical element, the change in refractive index with temperature will dominate its thermal power change. This power change, its performance effect, and its potential compensation must be considered over the operating temperature range of the system. Some systems have either a manual or autofocus mechanism, which may reduce the need for the system to be completely athermalized. In these cases, the total amount of focus adjustment required must be evaluated and enough compensation range provided.

One method of athermalizing systems containing plastic elements is to use a combination of glass and plastic elements. Such designs are often referred to as "hybrid" systems, although this term is also sometimes used for systems that combine refractive and diffractive elements. In this athermalization method, the majority of the optical power is put into the glass elements, while the plastic elements, often aspherical, are used mainly for aberration correction. Since glass has a smaller change in optical power with temperature than plastic, and the majority of the power is in the glass elements, the total change in optical power with temperature is reduced. It is also possible to design systems using several plastic elements, some with positive power and some with negative power, so that their thermal power changes cancel each other.

Application spectral band can be another factor in the decision whether to use plastic optics. In general, plastic optical materials have high transmission between about 450 nm and 900 nm. The actual cutoffs will depend on the

particular material type and grade. Plastics also have absorption bands in the near infrared (NIR), due to their chemical structure, and do not transmit well in the midwave and long-wave infrared bands.³⁵

In general, optical plastics have less resistance to chemicals than do optical glasses. In some (typically nonoptical) cases, solvents are used for "solvent bonding," the joining of plastic pieces by using a solvent to melt them together. Certain solvents, such as toluene or acetone, as well as other chemicals, can seriously damage or degrade plastic optics. The selection of a specific optical plastic, or the decision not to use plastic optics in a particular application, may depend on the expected chemical environment.

While plastic optical elements are less prone to fracture than optical glass elements, the same cannot be said with regard to scratching. Plastic is softer than glass, and as such, is more susceptible to surface damage, be it due to particulates such as blowing sand or direct contact. Multiple methods are used to prevent scratching plastic optics. One is to coat the surface with an abrasion-resistant coating. A second method is to design housings such that the surface is sufficiently recessed to prevent fingers and other objects from being able to accidentally (or intentionally) touch the lens. This is often seen on camera lenses in the form of a sunshade or stray-light baffle. Another method is to protect the plastic surface with a window, or by having the front or any exposed optical elements made of glass.

Birefringence is another potential issue with plastic optical elements, particularly in applications where the optical system is highly polarization sensitive. Birefringence refers to the separation of an incident light beam into two beams, usually referred to as the ordinary and extraordinary beams, upon entering a material. This separation is due to a difference in refractive index of the material based upon the polarization states of the light. While not a fundamental property of the plastic material itself, the manufacturing method used to produce the plastic optical element may introduce birefringence. For instance, a part that is injection molded may show birefringence, particularly near the gate, (the region of the part where the plastic is injected), if subjected to significant injection or packing pressure.³⁶ In contrast, a part that is produced by diamond turning a cast piece of plastic will typically not show birefringence. Part design, material selection, and processing all play a large role in determining the birefringence of a plastic optic.

The final potential issue we discuss concerning the use of plastic optics is their environmental impact. There is a growing "green" movement that seeks to reduce the consumption of goods and the environmental effects of the goods that are consumed. Plastic items, such as plastic shopping bags, have received considerable attention. Optical plastics, like most plastics, biodegrade slowly (although more rapidly than glass). This can be a positive aspect from a product lifetime standpoint, but can be a negative if the plastic quickly ends up in a landfill, where it can remain intact for a very long time. It is possible to create plastic items that degrade fairly rapidly; for example, garbage bags such as the

tion bands in the near
t transmit well in the

micals than do optical
are used for “solvent
to melt them together.
other chemicals, can
of a specific optical
cular application, may

ure than optical glass
g. Plastic is softer than
e it due to particulates
s are used to prevent
an abrasion-resistant
t that the surface is
s from being able to
seen on camera lenses
ethod is to protect the
any exposed optical

tic optical elements,
s highly polarization
nt light beam into two
rdinary beams, upon
in refractive index of
light. While not a
manufacturing method
ce birefringence. For
nce, particularly near
cted), if subjected to
rt that is produced by
ow birefringence. Part
le in determining the

se of plastic optics is
ovement that seeks to
ects of the goods that
bags, have received
s, biodegrade slowly
spect from a product
quickly ends up in a
is possible to create
age bags such as the

BIOBAG,^{vii} use a corn-based polymer. However, currently available optical plastics do not exhibit this property.

Optical plastics and elements manufactured from them can and are being recycled and reused. It is a common practice in the (nonoptical) plastic industry to take excess material generated during injection molding of a part, grind it up, and reuse it. In optical molding, the excess material is typically not reused for optical elements, but it is often collected and sold to nonoptical molders or material distributors.

One example of large-scale recycling is seen in the “single-use” camera market. Single-use cameras, frequently referred to as “disposable” cameras, are quite popular at events such as weddings and parties, or on vacation where the traveler does not wish to bring an expensive personal camera. In the single-use model, the entire camera is turned into the processor, allowing the camera body and lens to be collected and reused. KODAK has set up a recycling program for their single-use cameras, claiming that between 77% and 90% (by weight) of the camera may be remanufactured, and that virtually no material ends up directly in a landfill, as the components that are not remanufactured are recycled elsewhere.³⁷

When considering the use of plastic optics, the issues discussed above, as well as any other pertinent application characteristics, need to be considered. In certain situations plastic optics may not be appropriate, but in many cases they are, and their use should at least be considered. Plastic optics are currently used in a broad range of fields, from consumer electronics and medical devices to defense and biosecurity applications. As advances in plastic optical materials, precision machining, manufacturing, and design techniques continue, the number of applications where plastic optical systems are used is expected to increase.

^{vii} BIOBAG is a registered trademark of BioBag International.

on the diamond-
on conventional
interface with the
h the blanks now
d tool is installed
tool is normally
e, then by cutting
that which will be
salignment of the
k are installed and
ion electronic dial
d fixture properly
s of varying and
dly removed from
lly performed on a
rocess before the
re setup or to the
ace is achieved, at
ce (or surfaces) is
to machine other

irfractive structure
ed. In the case of
the machine at the
instance, an older,
that must be taken
In the case of the
the base aspheric
ctive grooves into

rk in the center of
es to zero. With
l not noticeable to
nification, such as
aw into a feature,
enter mark can be
alignment of the
between multiple

ost often used to
evaluation before
. In some cases,
cause of the low
with building and

Diamond-turned plastic optical elements are by no means inexpensive. Hourly rates for time on a diamond-turning machine are typically over \$100 an hour, and it can take several hours, including setup, to produce a part. As a result, prices for a diamond-turned plastic part often range from a few hundred to several hundred (or more) dollars. There is normally a price break associated with larger quantities, as a portion of the cost is associated with setting up the machine and optimizing the process. When ordering diamond-turned parts, it is usually best to buy enough at one time, rather than pay for repeated setups.

Diamond-turned parts can be obtained in several weeks, with some vendors quoting as low as one week (rarely), and more likely four to eight weeks. The amount of time it takes to procure diamond-turned plastic optics can sometimes be a source of frustration for the designer. Many an employee at a plastic optics manufacturer has considered starting their own business, by purchasing a diamond-turning machine and capitalizing on their knowledge. However, after a more realistic look at the business model, most decide to stick with their day jobs. As a result, there are relatively few rapid-turn diamond-turning prototype options, though several may be found by searching the Internet.

As with other optics purchases, the time to obtain diamond-turned plastic optics will depend on a number of factors, such as vendor capacity and queue, the price the customer is willing to pay, the availability of the necessary blank material and diamond tools, and potentially how badly the vendor wants to win the customer's business. Most plastic optic molders also provide diamond-turning services, and performing a diamond-turning job may lead to future molding production for them.

3.4 Injection Molding

Injection molding is the most popular method of manufacturing plastic optical elements. While casting produces large quantities of eyeglass lenses, windows, and diffraction gratings, and embossing creates a huge number of holographic security film pieces, both of these methods tend to supply products for a fairly limited number of uses. Injection molding, on the other hand, creates parts for a widely varying number of fields and applications. These parts range from micro-optics to fairly large projection lenses, with all manner of part size and complexity in between.

From a flow-diagram viewpoint, the injection molding of plastic elements is a very simple process: molten plastic is injected into a mold, the plastic is allowed to cool, the mold is opened and the part (or parts) removed, the mold is closed, and the cycle repeated. In reality, the attention to detail required to successfully injection mold optical elements makes it a much more sophisticated process. Figure 3.2 shows a schematic view of a typical injection molding machine, which we refer to in our discussion of the injection-molding process. Most machines, as shown, are horizontally oriented.

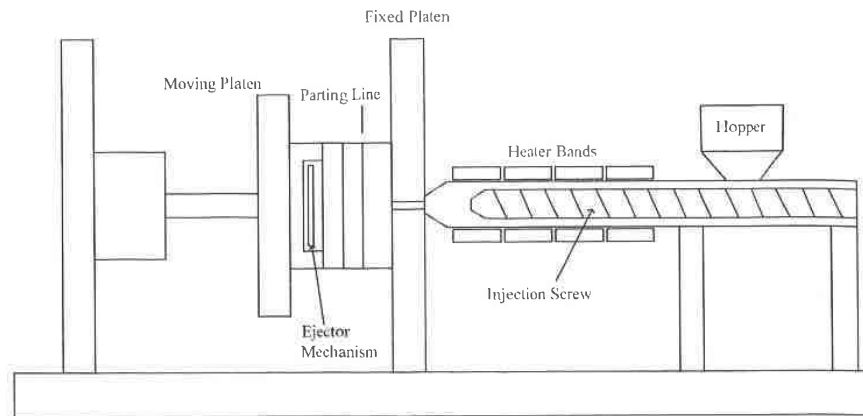
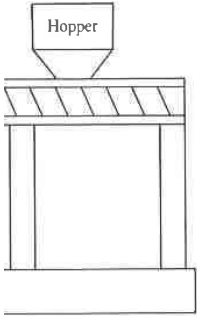


Figure 3.2 Schematic of an injection-molding machine.

An injection-molding machine is essentially a large clamping mechanism with a system for injecting plastic into a mold. Various ancillary pieces of equipment, such as robotic part pickers, are used to enable and improve the manufacturing process. The clamp itself consists of two platens (large, flat metal pieces), one of which moves. The platens, not surprisingly, are referred to as the “stationary” or “fixed” platen and the “moving” platen. The injection mold, divided into two halves, is attached to the platens, one half to each of them. The boundary between the two halves of the mold is known as the “parting line.” With the clamping mechanism (and mold) open, there is a gap between the two mold halves, which is used to remove the molded parts. The amount of motion that the moving platen has is referred to as the machine’s “stroke,” and “setting the stroke” means to adjust the platen motion such that the proper gap is created upon opening the mold, and proper closure is achieved upon closing the mold. To close the mold, the moving platen is driven forward, engaging the two mold halves and clamping them shut. The clamping mechanism itself can be hydraulic, although electric clamps have become more popular in recent years, particularly for plastic optics.

Injection-molding machines come in a wide range of sizes, from small table-top models to huge machines capable of molding parts as large as (or larger than) automobile bumpers. The machines are typically rated by their “tonnage,” which is the amount of clamping capability they have. Typical molding machines have clamp tonnage from 50 tons to 600 tons.²⁰ The machine size selected for a particular molding job depends on the part size and number of parts (which drives mold size), as well as the machine availability on the factory floor. The platen size generally increases with clamp capacity. For instance, a 55-ton ROBOSHOT^{viii} machine has a 500-mm × 470-mm platen, while the 110-ton ROBOSHOT machine has 660-mm × 610-mm platen.⁵⁴ Clamp capacity is

^{viii} ROBOSHOT is a registered trademark of FANUC.



chine.

amping mechanism
ancillary pieces of
e and improve the
is (large, flat metal
e referred to as the
he injection mold,
each of them. The
the "parting line."
up between the two
amount of motion
roke," and "setting
oper gap is created
losing the mold. To
ging the two mold
lf can be hydraulic,
years, particularly

s, from small table-
e as (or larger than)
r "tonnage," which
ling machines have
size selected for a
er of parts (which
actory floor. The
instance, a 55-ton
while the 110-ton
Clamp capacity is

important for the molding process because of the large forces that are at work during the injection-molding cycle. The plastic is injected into the mold at high pressure, and the clamp must be able to resist this pressure to keep the mold closed. When the pressure is too high for the clamp and the mold partially opens, it is known as "blowing the mold." This is a particularly bad situation to be in, as it can result in costly damage (both in terms of money and schedule) to the mold, or at least result in unacceptable parts, shutting down production. Most vendors have multiple machines, with a variety of sizes to handle the different jobs they are running. It is not unusual to see a series of 55, 110, 165, and even possibly 275-ton machines out on the production floor, often with decreasing numbers of the larger tonnage machines.

In plastic optic vendors' manufacturing areas, the machines are often arranged side by side according to size, with a suitable gap between them for personnel and equipment, such as mold carts, and with the injection side of the machine near the wall of the area. On the other side of the wall from the injection machines are the containers of plastic material that will be used in each machine, various equipment associated with the production process, room for fork lifts or other machinery used to distribute the plastic to the appropriate machines, and potential storage for additional or alternate material. This arrangement allows a separation between the somewhat "dirty" side of the operation and the "clean" side. Modern, high-end molding facilities often place their molding machines within an actual "clean room," a work area in which the air quality, humidity, and temperature are regulated and monitored. Air quality is maintained through the use of filters, proper air flow, and the control of materials and people entering the room. Clean rooms are more likely to be used for medical or micro-optic molding, where small amounts of contamination can ruin the product. In the manufacture of plastic optics, cleanliness is a definite plus. It is a characteristic to look for when evaluating an optics vendor. Contamination of the plastic material and/or the molding machine can result in optical parts with visible particles in them, while contamination of the optics after molding can ruin the coating process (if the parts are subjected to one) or result in products with undesirable cosmetic defects.

The optical plastic material typically comes in pellet form, in large cardboard boxes called Gaylords. Figure 3.3 shows a photo of some plastic pellets; the material shown is Zeonex. In special cases, such as in new material development, smaller material samples (e.g., 20-kg bags) may be used. Inside the Gaylord is typically a large plastic bag that was filled with plastic pellets by the material manufacturer. Clear plastic covers with access ports (for hoses) can be used over the top of the boxes to protect the material and allow for visual inspection of the amount of material remaining. The pellets are normally drawn from the Gaylord using a vacuum hose system. The pellets are first sent to a dryer, where they are dried to a specific dew point. It is important that the pellets do not contain too much moisture, which can result in cloudy optics. One of the first troubleshooting activities when cloudy optics are seen is to check that the dryer is working, or set, properly.

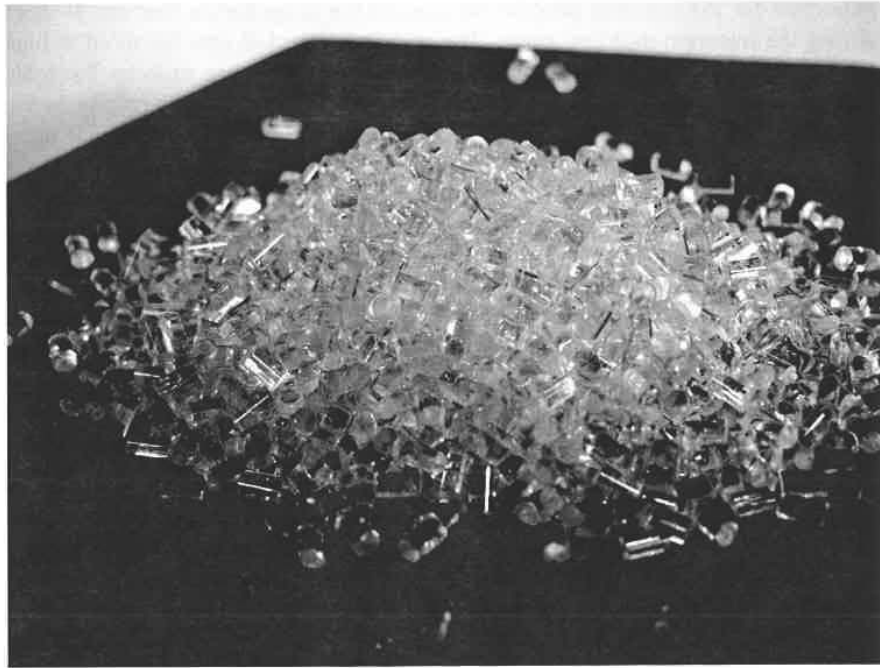
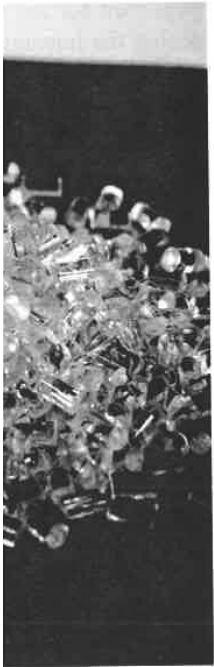


Figure 3.3 Plastic pellets used for injection molding of optical elements. (Photograph courtesy of Alan Symmons.)

After drying, the pellets are sent to a hopper on the molding machine where they drop into the barrel containing the injection screw. The injection screw is just that: a large screw that injects material into the mold. The screw actually serves two functions: first, it rotates to melt and move the plastic near the mold; second, it is used as a piston to inject the plastic. The amount of material that is injected is known as the “shot” or “shot size.” Injection screws are made from various materials, such as carbon or stainless steel, and are sized appropriately for the mold and/or molding machine. Normally, the threads on the screw are specifically designed to be used with one or several plastic materials. Some screw and plastic material combinations do not work well together, and as a result, an injection molder will typically have several types of screws available. The selection of the appropriate screw size is an important consideration. The screw must be able to hold a large enough shot to fill out the mold, but not hold so much material that the molten material stays in the barrel too long. The time that the plastic is in the barrel is known as the “residence time.” If the residence time is too long, the plastic is exposed to too much heat, which can burn, discolor, or alter the properties of the material. Small black specks in otherwise clear optics can be a result of exceeding the desired residence time. Normally, if the residence time is exceeded due to ancillary equipment issues or other delays, the screw and barrel will be pulled back from the mold, and the resident material



optical elements.

ling machine where
 e injection screw is
 The screw actually
 astic near the mold;
 it of material that is
 ews are made from
 sized appropriately
 is on the screw are
 tic materials. Some
 together, and as a
 of screws available.
 t consideration. The
 e mold, but not hold
 l too long. The time
 ne." If the residence
 it, which can burn,
 specks in otherwise
 e time. Normally, if
 sues or other delays,
 the resident material

purged. New material then enters the barrel, which is returned to the mold to continue production. Purge art, abstract sculptures formed by the cooling of the purged material on the ledge below the retracted barrel, can often be seen on mold processers' desks. Depending upon the vendor's machine capacity, queue of jobs, and delivery dates, the screw may need to be changed out when a different mold is hung in the machine. In this case the screw will be removed (and cleaned), and the barrel will be purged and cleaned to prevent cross-contamination of materials. It is not uncommon for vendors to have certain machines dedicated to specific materials, at least to the point that optical and nonoptical plastics do not run in the same machine.

As the injection screw rotates, the plastic pellets from the hopper move down the length of the barrel. By the time the plastic reaches the end of the barrel, it is meant to be molten. The friction from the screw turning provides some heat to the plastic as it moves the length of the barrel. In addition, the barrel is surrounded by a series of heater bands that provide controlled heat to the barrel. The heater bands are independently adjustable, so that a suitable temperature ramp or profile can be put into the barrel. Different types (or even grades) of optical materials require different temperatures and temperature profiles, and the independent control of the heater bands provides this adjustment. As a general rule, optical plastics are run at hotter temperatures than nonoptical plastics.

Once the plastic is molten and has traveled the length of the barrel, it is ready to be injected into the mold. To inject the material, the mold is closed, and the injection screw moves backward to allow molten plastic to accumulate in front of it. The screw is then driven forward, pushing a controlled amount of material through the nozzle on the end of the barrel into the mold. The movement of the injection screw is controlled such that the desired injection speed and pressure are achieved. Upon injection, the molten material flows into the mold, filling the spaces known as "cavities," where the parts are formed. During this "filling" stage, there is a sharp increase in the cavity pressure. Once the cavity is full of molten plastic, the pressure stabilizes and the material begins to cool. During this time the screw is typically held in position or pushed forward so that the material (or more material) is packed into the mold. This is called the "packing" stage of the injection cycle. Packing is necessary to achieve optical-quality surfaces, because material shrinks during cooling. At some point during the packing stage, the "gate," which is the area where the plastic enters the cavity, cools below the plastic transition temperature and hardens, or "freezes off." At this point, no more material can enter the part.

With the cavity full and the gate frozen off, the mold remains closed until the remaining material hardens enough to enable the mold to be opened and the part to be removed. This waiting period, from the time the cavity is filled until the time the mold can be opened, is known as the "cooling time." The amount of cooling time depends in part upon the size and thickness of the element. The situation is fundamentally a heat transfer problem. The molten plastic carried a certain amount of heat with it into the mold, and enough of that heat needs to be removed so that the temperature of the plastic material goes below its transition

temperature. Because the part has some finite thickness, there will be a temperature gradient through the material, and it will not harden all at once. The thicker the part, the longer that it will take for the heat to work its way from the center out, resulting in a longer cooling time.

The quality required of the optic plays into the cooling time as well. If the part is removed from the mold before it is fully hardened, the material may sag as it finishes cooling. This can result in surface irregularity being introduced. For lower-quality nonimaging lenses—for example, those used on the beam-break safety device receivers on garage door opener systems—the parts may be removed from the mold after a short cooling time, or they may even be quickly ejected and dropped into a container of water to finish cooling. Other low to midquality level parts, such as automotive turn signal lenses (which can be extremely thick), may be removed from the mold and placed on a “cooling tower” to finish their cooling. A cooling tower is a fairly simple belt-driven device that consists of a series of small shelves onto which the parts are placed. As the belt is turned, the shelves move up the tower at a prescribed speed. By the time the shelf reaches the top of the tower, the part has been properly cooled and can be removed from the shelf. Conveyor belts and other systems are also used to provide out-of-mold cooling time before handling. Parts requiring higher quality/tighter tolerances typically remain in the mold until they are cool enough (usually fully hardened) not to be affected by handling upon removal from the mold. This is the case for many imaging applications.

When the appropriate cooling time has passed, the mold is opened by pulling the moving platen back. As the mold opens, the parts typically remain with the half that is moving, which is referred to as “pulling” the parts. With the mold now open, the parts are removed from the “moving” mold through the use of an ejection system. There are a number of different ejection methods, which we will describe later during our discussion of molds. With the parts now removed, the mold can be closed again, more plastic is injected, and the cycle is repeated.

The mold itself is an important part of the injection-molding production process. The mold, and how it is built, will influence or determine several parameters of the production, such as how many parts can be made at a single time, the tolerances that they can be held to, the repeatability of the parts shot to shot, as well as over the production lifetime, and even the time required to make a part. Understanding the basics of a mold and the molding process is important for a designer of plastic optical systems. This knowledge enables the designer to appreciate how different optic parameters, such as center thickness, are adjusted or achieved, which in turn determine the tolerances that are easily held, held with difficulty, or not consistently achievable.

Molds, often referred to as tools, are typically divided into halves. In keeping with the platen naming convention, the mold halves may also be referred to as the “fixed” and “moving” halves. Alternate names that are used for the two halves are the “A” and “B,” the “hot” and “cold,” or the “cavity” and “core” halves. Regardless of the naming convention used, one half is attached to the fixed platen on the injection side of the machine and remains stationary

there will be a
en all at once. The
k its way from the

ime as well. If the
material may sag as
ng introduced. For
on the beam-break
the parts may be
y even be quickly
ling. Other low to
es (which can be
ed on a “cooling
simple belt-driven
e parts are placed.
ibed speed. By the
roperly cooled and
ms are also used to
requiring higher
y are cool enough
removal from the

opened by pulling
ly remain with the
ts. With the mold
ough the use of an
ods, which we will
now removed, the
e is repeated.

olding production
determine several
e made at a single
of the parts shot to
e required to make
ocess is important
les the designer to
ness, are adjusted
ily held, held with

halves. In keeping
o be referred to as
used for the two
avity” and “core”
is attached to the
emains stationary

throughout the molding process, while the other half is attached to the moving platen and moves back and forth with the platen as the mold is opened and closed. Figure 3.4 shows a photograph of a perspective view of a lens mold with the mold halves separated, while Fig 3.5 shows a photograph of a face-on view of a mold half.

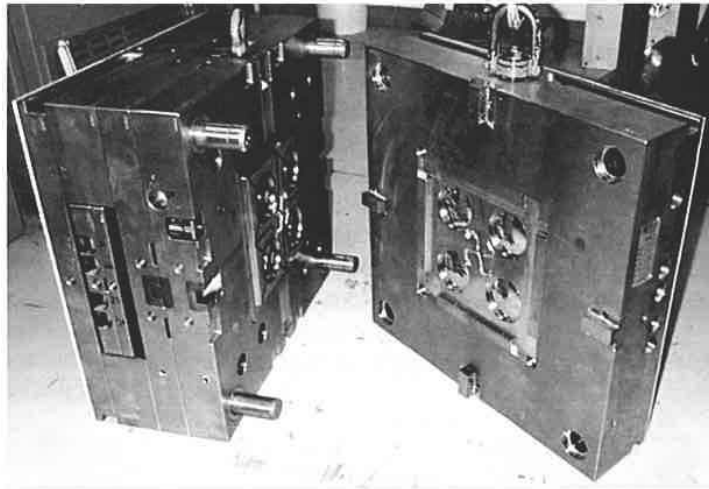


Figure 3.4 Photograph of a lens mold with halves separated.

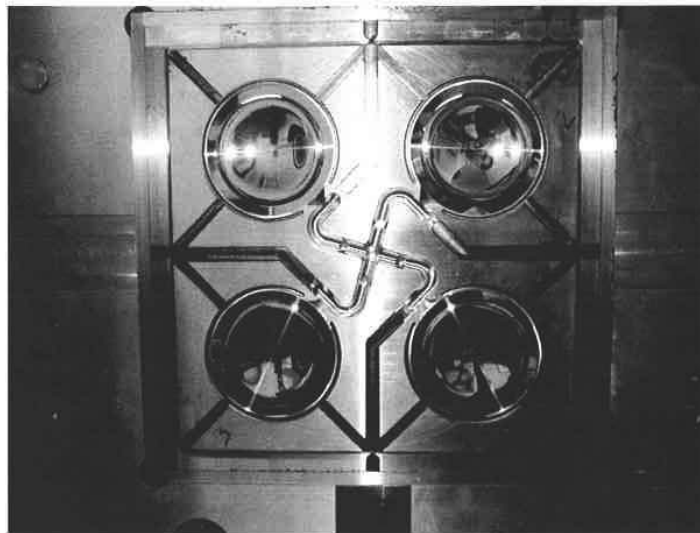


Figure 3.5 Face-on view of a four-cavity lens mold half.